ANALYSIS OF HYDROGEN METABOLISM IN *METHANOSARCINA BARKERI* FUSARO

BY

GARGI KULKARNI

DISSERTATION

Submitted in partial fulfillment of the requirements
for the degree of Doctor of Philosophy in Microbiology
in the Graduate College of the
University of Illinois at Urbana-Champaign, 2010

Urbana, Illinois

Doctoral Committee:

Professor William W. Metcalf, Chair
Associate Professor Brenda A. Wilson
Professor John E. Cronan, Jr.
Associate Professor Andrei Kuzminov

ABSTRACT

Methanogens utilize an unusual energy-conserving electron transport chain that involves reduction of a limited number of electron acceptors to methane (CH_4) gas. Previous biochemical studies suggest that the proton pumping $F_{420}H_2$ dehydrogenase (Fpo) plays a crucial role in this process during growth on methanol. However, *Methanosarcina barkeri* Δ*fpo* mutants investigated in Chapter 2 display no measurable phenotype on this substrate. In contrast, Δ*frh* mutants lacking the cytoplasmic F_{420}-dependent hydrogenase (Frh) are severely affected in their ability to grow and make methane from methanol, while double Δ*fpo* Δ*frh* mutants are completely unable to utilize this substrate. These data suggest that while *M. barkeri* has the flexibility to use the Fpo-dependent electron transport chain when needed, the preferred energy conservation pathway involves production of H_2 gas by Frh hydrogenase within the cytoplasm. The H_2 can then diffuse out of the cell, where it can be oxidized by the periplasmic methanophenazine-dependent hydrogenase (Vht), with transfer of electrons into the electron transport chain. Consistent with this "H_2-cycling" proposal, a conditional *vht* mutant isolated in Chapter 3, is unable to grow using any of the methanogenic substrates tested under non-permissive conditions, suggesting that Vht is essential for growth of *M. barkeri.* Moreover, repression of *vht* expression results in a rapid increase in H_2 partial pressure, which supports the hypothesis that Vht is required for H_2 uptake. H_2 accumulation in the culture headspace of conditional *vht* mutant is accompanied with cessation

of methanogenesis and growth, implying that H_2 uptake is essential for anaerobic respiration and viability. In contrast, Vht is not essential in mutants lacking the H_2-producing Frh hydrogenase. This is consistent with the hypothesis that Vht is required for H_2 uptake, only when Frh produces H_2, that is, Frh and Vht hydrogenases are functionally coupled in a "H_2-cycling" energy conservation mechanism. Because production of H_2 by Frh consumes protons within the cytoplasm and oxidation of H_2 by Vht releases protons outside the cell, this electron transport chain is capable of establishing a trans-membrane proton gradient that can be used to make ATP by the ATP synthase. Our study provides the first direct experimental evidence for H_2-cycling, since it was proposed to be involved in energy conservation in sulfate-reducing bacteria in 1981.

To further dissect the roles of these hydrogenases in *M. barkeri* physiology, I constructed a series of hydrogenase deletion mutants in various combinations in Chapter 4, including a mutant that is devoid of all three types of hydrogenases, ferredoxin-dependent Ech, Frh and Vht. My data show that each of the three types of hydrogenases is needed for growth via the CO_2 reduction pathway. In contrast, none of the hydrogenases is essential during methylotrophic growth, indicating the presence of H_2-independent electron transport chains, which are able to support wild-type growth yields. Either Vht or Ech hydrogenase alone can support growth using the methyl respiration pathway. However, both Ech and Vht hydrogenases are required for acetate utilization. The data presented in chapter 4 also suggest that Ech and/or Frh hydrogenases block the methyl oxidative pathway by catalyzing conversion of H_2

to Fd_{red} and $F_{420}H_2$, respectively. In addition, evidence is provided for involvement of Hyp proteins in maturation of Ech hydrogenase. This work highlights the similarities and differences between H_2-independent electron transport chains of the hydrogenotroph *M. barkeri* and the non-hydrogenotroph *Methanosarcina acetivorans.*

ACKNOWLEDGEMENTS

I would like to express my sincerest gratitude to the following people. Prof. Bill Metcalf, my advisor, for his support and guidance. I am eternally grateful to him for letting me be a part of his lab and mentoring me patiently throughout the course of this study. Members of my thesis committee: Prof. John Cronan, Prof. Andrei Kuzminov, Prof. Brenda Wilson and Prof. Gary Olsen, for their suggestions and help. Head, Staff and Faculty at the Department of Microbiology, for making this a smooth ride for me. All members of the Metcalf group, for their encouragement and companionship. Prof. Ralph Wolfe, for being an inspiration.

My friends, especially Lara Rajeev, Arpita Bose and Rina Opulencia. They were my family during the graduate school.

My parents, who instilled in me the importance of education and stood by my side through thick and thin. My brother, who always encourages me to be better and more confident. My husband, who believes in me and is always there for me.

This work is dedicated to:
my parents, Aai and Baba
my brother, Tushar
and my husband, Monik

TABLE OF CONTENTS

CHAPTER 1

INTRODUCTION

1.1 METHANOGENESIS: DEFINITION AND IMPORTANCE

Methanogenesis is defined as the production of methane (CH_4) gas. Under reducing hydrothermal conditions, typical of Earth's crust, metal-rich minerals catalyze abiogenic methane production from carbonates (geogenesis) (47, 109). However, majority of methane on earth is derived from organic matter through thermal decomposition (thermogenesis), microbial metabolism or combustion of biomass and fossil fuels (ignigenesis) (93, 109). Among these, microbially mediated methane production is the most prevalent, accounting for 2.4×10^{15} g of methane production annually from natural and anthropogenic sources (106). The former include marine and freshwater sediments, swamps and intestinal tracts of ruminants and termites (106), whereas landfills, animal husbandry, rice cultivation and waste management constitute man-made sources (2).

Over the last two hundred and fifty years, atmospheric concentration of methane has increased by about 143%, to reach 1,774 ppb in 2005 (2). Moreover, its concentration is rising further at an annual rate of 0.9% (59). This is of major concern as methane is a greenhouse gas that is 21 times more potent than carbon dioxide (CO_2) and has therefore been implicated in global warming. As more than half of the current methane flux to the atmosphere is estimated to

be anthropogenic, serious efforts are underway to mitigate methane emissions and harvest methane gas for use as an energy source (1, 2).

Methane is a clean, renewable energy source. It is the primary component of natural gas, which is extensively used for domestic and industrial purposes (1). Enormous amount of methane is also sequestered in the form of methane hydrates, which are cages of water molecules that enclose methane gas, most of which is produced biologically. These structures are stable at high pressures and low temperatures that occur in permafrost regions and within ocean floor sediments 500 m below sea level. Methane hydrates represent one of the largest hydrocarbon sources on Earth (>10^{19} g) and if tapped for methane, could potentially ensure long-term energy security. However, release of methane from the hydrates may also contribute to global warming (23, 59, 106).

Methanogenesis is a major player in the global carbon cycle as it represents the terminal step in biomass degradation in many anoxic habitats (Figure 1.1). In these environments, mineralization of organic matter is initiated by hydrolysis of biopolymers to monomers and lipids to glycerol and long chain fatty acids by bacteria, protozoa and fungi. In conjunction with syntrophic bacteria, these anaerobes further ferment the compounds to acetic acid, CO_2 and hydrogen (H_2), which are substrates for methane formation. Nearly half of the total methane produced by methanogenesis (10^{15} g) is oxidized by anaerobic archaea and bacteria to CO_2. The other half seeps into the aerobic zone, where aerobic bacteria oxidize about 60% of it. The rest of methane ends up in the atmosphere, where it is photo-oxidized to CO_2. The formation of CO_2 completes

the carbon cycle, as it can be once again fixed into organic matter by photosynthesis (106).

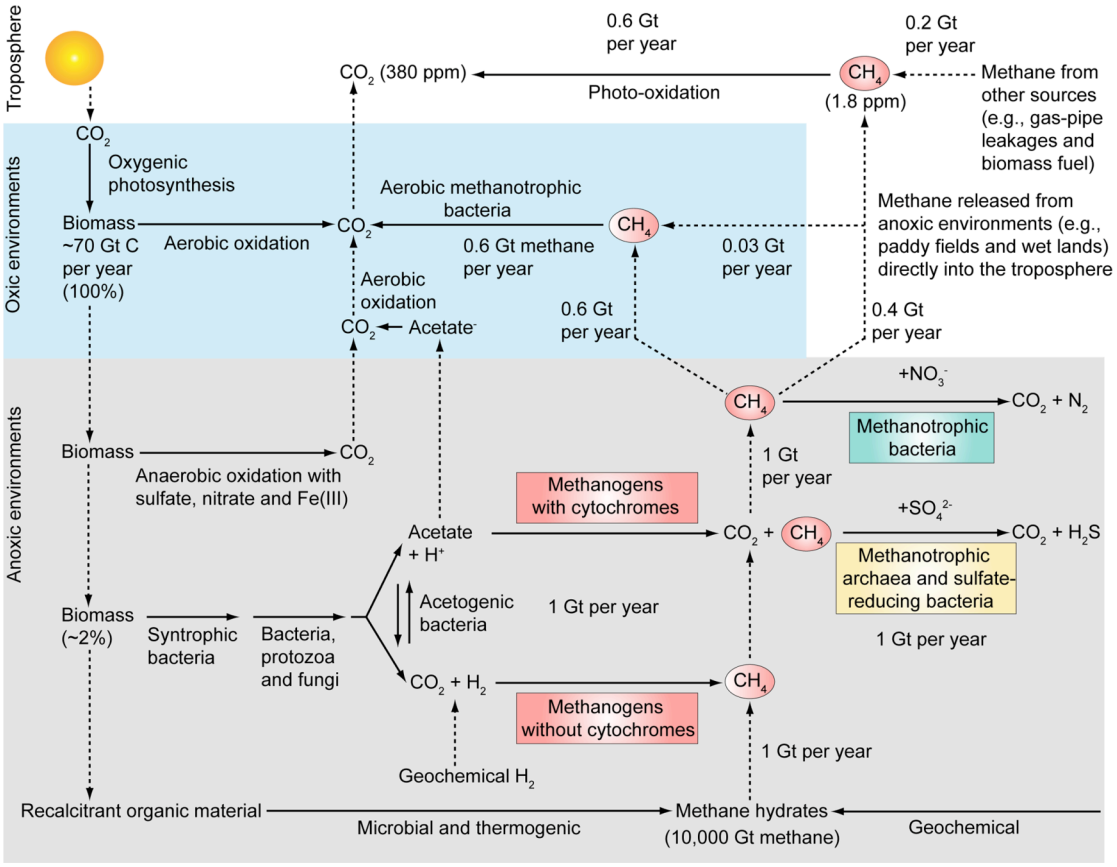

Figure 1.1 Methane (CH_4) as an intermediate in the global carbon cycle. Continuous arrows indicate a reaction and dashed arrows indicate diffusion and/or convection. In anoxic environments (for example, freshwater sediments, swamps, paddy fields, land fills and the intestinal tracts of ruminants and termites), approximately 1 giga ton (Gt) of methane (10^{15} g) is formed per year from acetate, carbon dioxide (CO_2) and hydrogen (H_2) through the metabolic activity of methanogenic archaea. Almost the same amount of methane is released into the environment from melting methane hydrates. From the 2 Gt of methane that is produced per year, ~0.6 Gt is oxidized to CO_2 by aerobic bacteria, ~1 Gt is oxidized by anaerobic archaea and ~0.4 Gt escapes into the atmosphere. Another 0.2 Gt per year is released into the atmosphere from other sources, such as gas-pipe leakages and the burning of biomass. In the atmosphere, most of the methane is photo-oxidized to CO_2. Only 0.03 Gt per year is removed from the atmosphere by aerobic bacteria that live in soils and water. Figure created from (106).

Operation of a similar food chain in anaerobic digesters allows treatment of organic wastes such as sewage sludge, animal manure, crop wastes and

municipal wastes (116). The methane thus produced provides sufficient energy to run a sewage treatment plant (94). Some methane-producing organisms that have the ability to degrade halogenated organic compounds can be potentially used in anaerobic digesters for bioremediation (75).

1.2 ECOLOGY OF METHANOGENS

Methane is produced as a byproduct of respiration by a group of strictly anaerobic organisms called methanogens (22). These organisms are abundant in anoxic habitats where electron acceptors such as NO_3^-, SO_4^{2+}, Fe^{3+} and Mn^{4+} are limiting. As reduction of these electron acceptors is thermodynamically more favorable than CO_2 reduction to methane, methanogens are usually out-competed by bacteria that utilize them (denitrifiers, sulfate-reducing bacteria, iron-reducing bacteria and manganese-reducers) (106). Common methanogenic habitats include wetlands, oceans, gastrointestinal tracts, anaerobic digestors, landfills and rice paddies (64).

Methanogens can be found in a range of salinities from freshwater to hypersaline (116). In marine sediments, where sulfate concentrations are 20-30 mM, sulfate-reducers out-compete methanogens for H_2 and acetate. Thus, methanogens resort to utilization of methylated compounds, which are not used efficiently by sulfate-reducing bacteria. Hydrogenotrophic methanogens isolated from marine environments are found below the sulfate-reducing zones and are possibly associated in syntrophic growth with H_2-producers. In marine sediments rich in organic matter, H_2 and acetate may become available for methanogenesis

once sulfate pools have been depleted. In freshwater environments, which have low sulfate concentrations (100-200 μM), methanogenesis can occur from both CO_2 and acetate. Nearly three-fourths of methane in these environments originates from acetate (64).

Methanogens are distributed over a wide range of temperatures. psychrophilic species like *Methanococcoides burtonii* and *Methanogenium frigidum* have been isolated from a frozen lake in Antarctica (1-2°C) (91). In contrast, extremely hot environments like hydrothermal vents (110°C) were the source of methanogens like *Methanopyrus kandleri* (99) and *Methanocaldococcus jannaschii* (37). Many methanogens are also mesophilic like *Methanosarcina barkeri* and *Methanococcus maripaludis* (91).

Most methanogens have pH optima near neutrality. However, methanogenesis has been detected in acidic peat bogs with a pH of 3 (116) and in alkaline lakes with a pH of 9.7 (14). A recent isolate from a minerotrophic fen, *Methanosphaerula palustris*, can grow at pH 4.8 – 6.4 (16). Other acidophilic species like *Methanobacterium espanolae* (86) and *Methanobrevibacter acidurans* (92) are capable of growth at pH 5.2 – 6.2. Alkaliphilic methanogens that can grow at pH 9.2, *Methanohalophilus oregonense* (14) and *Methanohalophilus zhilinae* (71), have also been isolated.

1.3 PHYLOGENY OF METHANOGENS

On the basis of their 16s rRNA sequences, methanogens were placed in a phylogenetic group distinct from Bacteria and Eukarya, called Archaea (114). Among the unique features that set Archaea apart are, lipids composed of

isoprenoid alcohols that are ether linked to glycerol, rather than ester linked fatty acids present in Bacteria and Eukarya; and cell walls that are made of pseudomurein, proteins or glycoproteins, instead of bacterial peptidoglycan. Although Archaea resemble Bacteria in their cellular and genomic organization, their transcription and translation machinery is similar to that from Eukarya. Thus Archaea exhibit Eukaryal-like RNA polymerase sensitivity and subunit structure, ribosomal proteins, initiator methionine for protein synthesis and elongation factor EF-2 (113).

Methanogens are a phylogenetically diverse group belonging to the kingdom Euryarchaeota. Based on their 16S rRNA sequence similarity, cell envelope structure, lipid composition, substrate range and other biological properties, they have been classified into five orders: *Methanobacteriales*, *Methanococcales*, *Methanomicrobiales*, *Methanosarcinales* and *Methanopyrales* (64).

Members of the order *Methanobacteriales* produce methane by reducing CO_2 with a variety of electron donors: H_2, formate, CO and secondary alcohols, of which H_2 is used most commonly. They are rod-shaped, often filamentous and non-motile with a pseudomurein-containing cell wall and caldarchaeol, archaeol and hydroxyarchaeol as core lipids (55). The order is divided into two families, Methanobacteriaceae and Methanothermaceae. The former contains three mesophilic genera, *Methanobacterium*, *Methanobrevibacter* and *Methanosphaera*, and one extremely thermophilic genus *Methanothermobacter*. Interestingly, *Methanosphaera* cannot use CO_2 as a terminal electron acceptor

and instead reduces methanol to methane using H_2. The hyperthermophilic genus *Methanothermus* is the sole member of Methanothermaceae and unlike other members of this order, is motile (64).

Methanogens within the order *Methanococcales* use H_2 or formate as electron donors for CO_2 reduction. They are cocci, motile and contain S-layer proteins in cell walls. Their lipids are composed of archaeol, caldarchaeol, hydroxyarchaeol and macrocyclic archaeal. This order comprises two families, the first of which is Methanocaldococcaceae that contains the hyperthermophilic genera, *Methanocaldococcus* and *Methanotorris.* The mesophilic genus *Methanococcus* and the extremely thermophilic genus *Methanothermococcus*, belong to the second family Methanococcaceae. All these genera have been isolated from marine habitats and require sea salts for optimal growth (64).

Although all *Methanomicrobiales* members are able to reduce CO_2 using H_2 gas as the electron donor, most of them can also use formate and many can employ secondary alcohols as reductants. Morphology (cocci, rods or sheathed rods) and motility varies between species. Their cell walls are made of proteins or glycoproteins, and lipids of archaeol and cardarchaeol. The order has three families, Methanomicrobiaceae, Methanocorpusculaceae and Methanospirillaceae. These families are further divided into nine genera (64).

The order *Methanopyrales* is represented by only one species, *Methanopyrus kandleri*, which belongs to the family Methanopyraceae. This hyperthermophilic species uses H_2 plus CO_2 to make methane. It is rod-shaped and motile, with pseudomurein-containing cell wall and archaeol as lipids (64).

Members of the order *Methanosarcinales* can use methylated compounds, acetate and/or CO_2 plus H_2 for methanogenesis. Thus, they are metabolically the most versatile methanogens. They are non-motile and occur as cocci, pseudosarcinae or sheathed rods. Most cells have a protein cell wall, whereas some are also surrounded by a sheath of acidic heteropolysaccharides. Their lipids contain archaeol, caldarchaeol and hydroxyarchaeol. The order is divided into two families, Methanosaetaceae and Methanosarcinaceae (64).

Methanosaetaceae is represented by only one genus, *Methanosaeta*, which uses only acetate for methane production. The family Methanosarcinaceae has 8 genera and is characterized by the ability of its members to use methylated compounds like methanol, methylamines and methylsulfides as methanogenic substrates (64). Although some species of the genus *Methanosarcina* like *M. barkeri* are able to reduce CO_2 with H_2, they are unable to compete with other hydrogenotrophic methanogens for H_2. This is because they have a 10-fold higher H_2 threshold concentration than hydrogenotrophic methanogens that are only able to use this substrate, i.e. hydrogenotrophic specialists like *Methanospirillum* or *Methanobacterium* (106). In contrast, generalists like *Methanosarcina* that have the ability to utilize a variety of substrates, exhibit faster growth rates and higher yields at high substrate concentrations, but are out-competed at lower concentrations due to lower affinities for the substrates. This case is further exemplified by the inability of *Methanosarcina* to compete with *Methanosaeta* for acetate, when the substrate is present at low concentrations. (116).

The work in this thesis focuses on *Methanosarcina* species, in particular *M. barkeri* Fusaro, which was isolated from a freshwater coastal lagoon called Lago Del Fusaro in Italy. Another freshwater species, *M. mazei* Gö1, was isolated form sewage sludge (69). Both these species have the widest substrate range among methanogens, being able to use CO_2 plus H_2, methylated compounds and acetate (48, 106). On the other hand, *M. acetivorans* C2A that was isolated from the sediment of a marine canyon in California is capable of using all these substrates except CO_2 plus H_2. Interestingly, *M. barkeri* and *M. acetivorans* can also utilize CO (64). Whole genome sequences are available for all species mentioned above (26, 33, 69). All *Methanosarcina* species are mesophilic and halotolerant, except *M. thermophila* that is moderately thermophilic (17) and *M siciliae* that is slightly halophilic (81). Also, *M. lacustris* isolated from lake sediment in Switzerland (97) and *M. baltica* isolated from the Baltic sea (112), are psychrotolerant. Other species include *M. semesiae*, which is a dimethylsulfide-utilizing methanogen from a mangrove sediment in Tanzania (68) and *M. vacuolata*, which is a gas vacuolated species isolated from an anaerobic digester in Moscow (115).

1.4 METHANOGENIC SUBSTRATES AND PATHWAYS

Although only two genera (*Methanosaeta* and *Methanosarcina*) are able to utilize acetate, these organisms account for nearly two-thirds of biological methane production (31, 64). The remaining one-third is derived primarily from reduction of CO_2 with H_2 or formate by most methanogens (31). All these

methanogenic substrates occur as major fermentation products in many anaerobic habitats (116). A fraction of methane also comes from the methyl groups of methylated compounds, which are formed from osmolytes of marine bacteria, algae, phytoplankton and plants. These compounds include methanol, methylated amines (tetramethylammonium, trimethylamine, dimethylamine and monomethylamine) and methylated sulfides (methanethiol and dimethylsulfide) (64). Methanol arises from the cleavage of methylated compounds such as pectin and liginin (98, 116). Anaerobic breakdown of methylated amino compounds such as choline and betaine gives rise to methylated amines (116). Methylated sulfides are derived from sulfur-containing amino acids like methionine or methylation of sulfide or methanethiol (65, 116). Production of these compounds has also been reported in methanogen cultures, including *M. acetivorans* (77).

Methanogenesis proceeds from the aforementioned substrates via four distinct but overlapping pathways (Table 1.1): 1) CO_2 reduction or hydrogenotrophic pathway, in which CO_2 is reduced to methane using electrons from H_2; 2) Aceticlastic pathway, wherein methyl group of acetate is reduced to methane using electrons derived from oxidation of its carbonyl group; 3) Methylotrophic pathway involves oxidation of a quarter of methyl groups of methylated compounds to provide electrons for reduction of the rest of the methyl groups to methane (29); and 4) Methyl respiration pathway, in which methyl group of methylated compounds is reduced to methane using electrons from H_2 (76).

Table 1.1 The overall reaction and energy yield from the four methanogenic pathways (11, 64, 105)

Pathway	**Reaction**	**$\Delta G^{\circ\prime}$ (kJ/mol)**	**$\Delta G^{\circ\prime}$ (kJ/molsubstrate)**
CO_2 reduction	$CO_2 + 4H_2 \rightarrow CH_4 + 2H_2O$	-131	-131
Aceticlastic	$CH_3COOH \rightarrow CH_4 + CO_2$	-33	-33
Methylotrophic	$4CH_3OH \rightarrow 3CH_4 + CO_2 + 2H_2O$	-106	-27
	$4(CH_3)_3N + 6H_2O \rightarrow 9CH_4 + 3CO_2 + 4NH_3$	-74	-19
	$2(CH_3)_2NH + 2H_2O \rightarrow 3CH_4 + CO_2 + 2NH_3$	-73	-18
	$4CH_3NH_2 + 2H_2O \rightarrow 3CH_4 + CO_2 + 4NH_3$	-75	-19
	$2(CH_3)_2S + 2H_2O \rightarrow 3CH_4 + CO_2 + 2H_2S$	-49	-25
Methyl respiration	$CH_3OH + H_2 \rightarrow CH_4 + H_2O$	-113	-113

1.4.1 CO_2 reduction pathway

In this pathway (reviewed in (64, 104)), CO_2 initially binds to the coenzyme methanofuran (MF) and is reduced to the formyl level by formyl-MF dehydrogenase (Fmd) using electrons from reduced ferredoxin (Fd_{red}) (Figure

1.2). In *M. barkeri*, the Ech hydrogenase has been proposed to catalyze the endergonic electron transfer from H_2 to ferredoxin (Fd_{ox}) by virtue of reverse

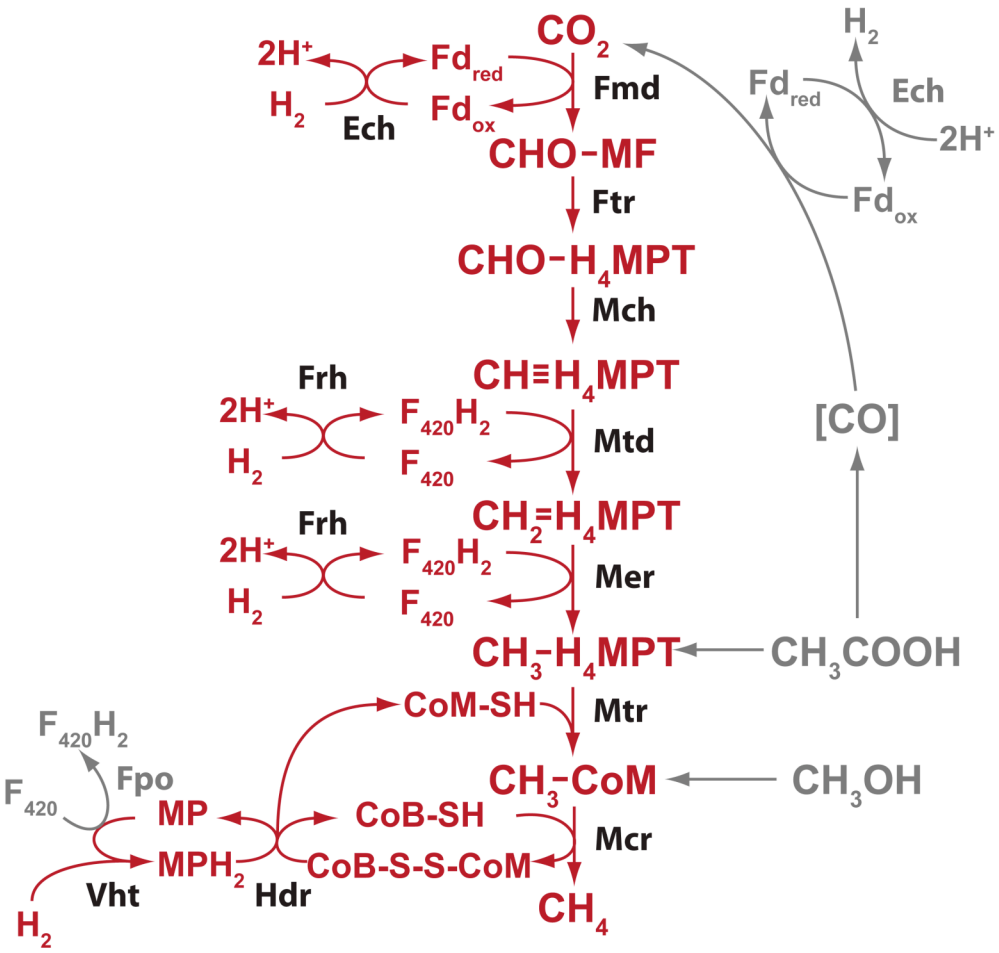

Figure 1.2 CO_2-reduction pathway. Many methanogens reduce CO_2 to methane using electrons derived from the oxidation of H_2. Steps not required in this pathway are shaded in gray. Abbreviations: CHO-MF. formyl-methanofuran; CHO-H_4MPT, formyl-tetrahydromethanopterin; CH≡H_4MPT, methenyl-tetrahydromethanopterin; CH_2=H_4MPT, methylene-tetrahydromethanopterin; CH_3-H_4MPT, methyl-tetrahydromethanopterin; CH_3-S-CoM, methyl-coenzyme M; CoM-SH, coenzyme M; CoB-SH, coenzyme B; CoM-S-S-CoB, heterodisulfide of CoM-SH and CoB-SH; MP/MPH_2, oxidized and reduced methanophenazine; F_{420}/$F_{420}H_2$, oxidized and reduced Factor 420; Fd_{ox}/Fd_{red}, oxidized and reduced ferredoxin; Ech, ferredoxin-dependent hydrogenase; Frh, F_{420}-dependent hydrogenase; Vht, methanophenazine-dependent hydrogenase; Fpo, $F_{420}H_2$ dehydrogenase; Hdr: heterodisulfide reductase; Fmd: formyl-MF dehydrogenase; Ftr: formyl-MF:H_4MPT formyltransferase; Mch: methenyl-H_4MPT cyclohydrolase; Mtd: methylene-H_4MPT dehydrogenase; Mer: methylene-H_4MPT reductase; Mtr, methyl-H_4MPT:CoM methyltransferase; Mcr: methyl-S-CoM reductase. Figure adapted from (39).

electron transport (72, 73). The formyl group is then transferred to the coenzyme tetrahydromethanopterin (H_4MPT) by formyl-MF:H_4MPT formyltransferase (Ftr). This is followed by dehydration of formyl-H_4MPT to methenyl-H_4MPT by methenyl-H_4MPT cyclohydrolase (Mch). Methenyl-H_4MPT is first reduced to methylene-H_4MPT by methylene-H_4MPT dehydrogenase (Mtd) and then to methyl-H_4MPT by methylene-H_4MPT reductase (Mer). Both reactions use reduced coenzyme F_{420} ($F_{420}H_2$) as the electron donor, which is produced from H_2 by the F_{420}-reducing hydrogenase (Frh) (32). In many methanogens like *Methanothermobacter marburgensis* and *M. maripaludis*, methenyl-group reduction can also be catalyzed with H_2 by a cytoplasmic iron-sulfur cluster-free hydrogenase, the H_2-forming methylene-H_4MPT dehydrogenase (Hmd) (96). The methyl group is then transferred to coenzyme M (CoM-SH) by methyl-H_4MPT:CoM methyltransferase (Mtr) in an exergonic reaction that generates an electrochemical sodium ion gradient (9). Methyl-CoM is subsequently reduced to methane by methyl-S-CoM reductase (Mcr) using coenzyme B (CoB-SH), to form a heterodisulfide of coenzyme M and coenzyme B (CoM-S-S-CoB). Finally, H_2 is used to reduce the heterodisulfide via a membrane-bound energy conserving electron transport chain, H_2:heterodisulfide oxidoreductase system, which is discussed in the next section (reviewed in (21, 22)).

Use of formate as an electron donor involves its initial oxidation to CO_2 and $F_{420}H_2$ by formate dehydrogenase (Fdh). CO_2 enters the hydrogenotrophic pathway and is reduced using four molecules of $F_{420}H_2$ (formed from the oxidation of four formate molecules). Although $F_{420}H_2$ can act as an electron

donor for methenyl and methylene group reduction, it is unclear how it is used to reduce CO_2 and methyl group (23). In *M. maripaludis*, it has been proposed that electrons from $F_{420}H_2$ are transferred to H_2 by Frh alone or via the concerted action of Mtd and Hmd (Figure 1.3) (67). The H_2 can be subsequently used for reduction steps that cannot utilize $F_{420}H_2$.

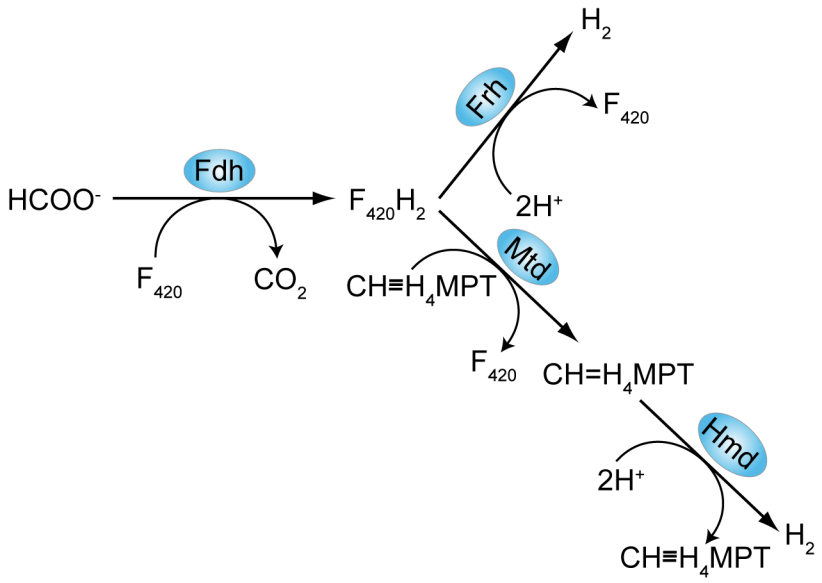

Figure 1.3 Potential pathways of H_2 production during formate utilization. Initially, Fdh reduces F_{420}. In the first pathway, $F_{420}H_2$ is oxidized by Frh to produce H_2. In the second pathway, $F_{420}H_2$ is oxidized by Mtd to reduce methenyl-H_4MPT to methylene-H_4MPT, which is then reoxidized by Hmd to produce H_2. Abbreviations are same as in Figure 1.2; $HCOO^-$, Formate; Fdh, formate dehydrogenase; Hmd, H_2-forming methylene-H_4MPT dehydrogenase. Figure created from (64).

Similarly, carbon monoxide (CO) can be utilized via the hydrogenotrophic pathway after being oxidized to CO_2 and H_2 by CO dehydrogenase (CODH) in *Methanothermobacter thermoautotrophicus* and *M. barkeri* (64).

1.4.2 Aceticlastic pathway

Acetate catabolism is initiated by its activation to acetyl-CoA (Figure 1.4) (reviewed in (30)). In *Methanosaeta* species, this is accomplished by acetyl-CoA

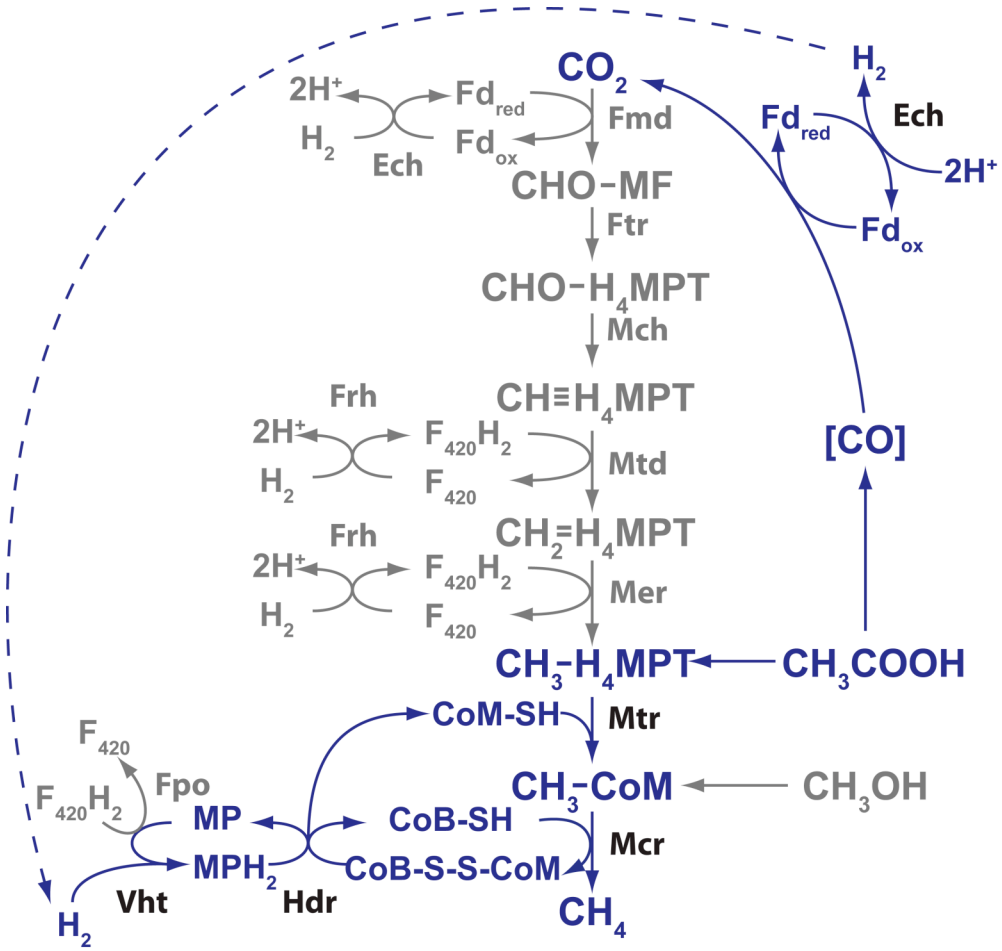

Figure 1.4 Aceticlastic pathway. Acetate (CH_3COOH) can be split into a methyl group and an enzyme-bound carbonyl moiety. The latter is oxidized to CO_2 to provide electrons required for reduction of the methyl group to methane. Steps not required by this pathway are shaded gray. Abbreviations are same as in Figure 1.2. Figure adapted from (39).

synthetase (ACS) in an AMP and PPi forming reaction. PPi is further cleaved by a pyrophosphatase (5). On the other hand, in *Methanosarcina* species, acetate is initially phosphorylated to acetyl-phosphate by acetate kinase (Ack) at the

expense of one ATP molecule. Phosphotransacetylase (Pta) then exchanges the phosphate group for coenzyme A (5, 50, 66). Acetyl-CoA is subsequently cleaved by the multifunctional enzyme complex, CO dehydrogenase (CODH)/ acetyl-CoA synthase (ACDS), into a methyl group that is transferred to H_4MPT and a carboxyl group that is oxidized to CO_2 with concomitant Fd_{red} production (3, 72, 73, 89). The methyl group is reduced to methane as in the hydrogenotrophic pathway, generating CoM-S-S-CoB. Regeneration of free coenzymes from the heterodisulfide occurs via different electron transport systems in *Methanosarcina* species. In *M. barkeri*, H_2 produced from Fd_{red} by the Ech hydrogenase has been proposed to reduce CoM-S-S-CoB via the H_2:heterodisulfide oxidoreductase system (72, 73). However, in *M. acetivorans*, a putative Fd oxidoreductase called Rnf (*Rhodobacter* nitrogen fixation) is responsible for channeling electrons from Fd_{red} to the heterodisulfide via MP (63).

1.4.3 Methylotrophic pathway

The entry of methylated compounds into this pathway (reviewed in (53)) is mediated by substrate-specific methyltransferases (MtaB for methanol) that transfer their methyl groups to a cognate corrinoid protein (MtaC for methanol). Together these two proteins constitute the methyltransferase 1 or MT1. The methyl group is then transferred to CoM-SH by methyltransferase 2 or MT2 (MtaA for methanol) (Figure 1.5). Methyl-CoM is subsequently reduced to methane as in the hydrogenotrophic pathway, generating CoM-S-S-CoB. Electrons needed for the regeneration of free coenzymes from the heterodisulfide

are derived from oxidizing one-fourth of methyl groups attached to CoM-SH to CO_2 via the reverse of the CO_2-reduction pathway. Thus, methyl and methylene

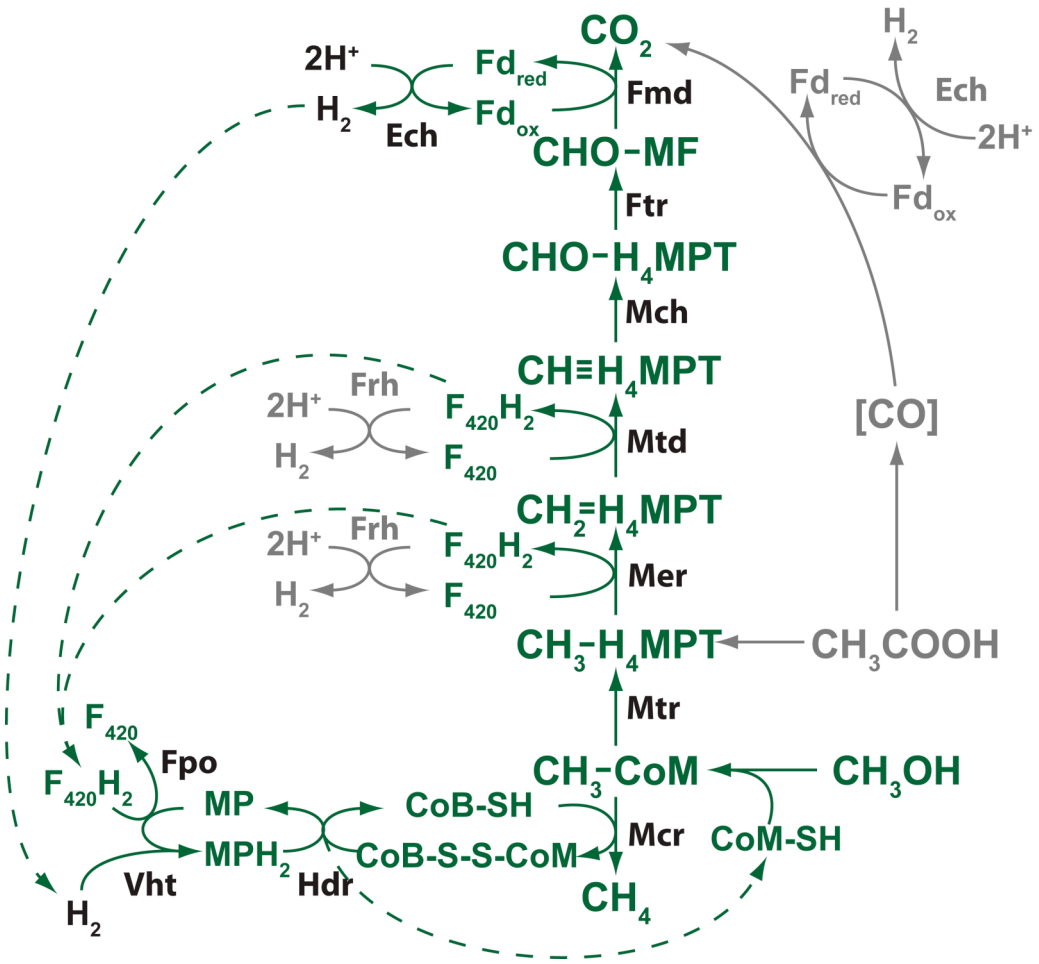

Figure 1.5 Methylotrophic pathway. C1-compounds, such as methanol (CH_3OH), can be disproportionated to CO_2 and methane. In the pathway shown, one molecule of methanol is oxidized to provide electrons for reduction of three additional molecules to methane. Steps not required by this pathway are shaded gray. Abbreviations are same as in Figure 1.2. Figure adapted from (39).

group oxidation produces two molecules of $F_{420}H_2$ (7, 8), whereas, Fd_{red} is generated from formyl group oxidation (72, 73). $F_{420}H_2$ enters the $F_{420}H_2$:heterodisulfide oxidoreductase system for reduction of the heterodisulfide (discussed below, (21, 22)). However, as in the aceticlastic pathway, depending

on the *Methanosarcina* species, reduction of CoM-S-S-CoB by Fd_{red} may involve H_2 (72, 73) as an intermediate or Rnf (63).

1.4.4 Methyl respiration pathway

The methyl groups of methylated compounds (Figure 1.6) enter at the level of methyl-CoM, as in the methylotrophic pathway. However, instead of

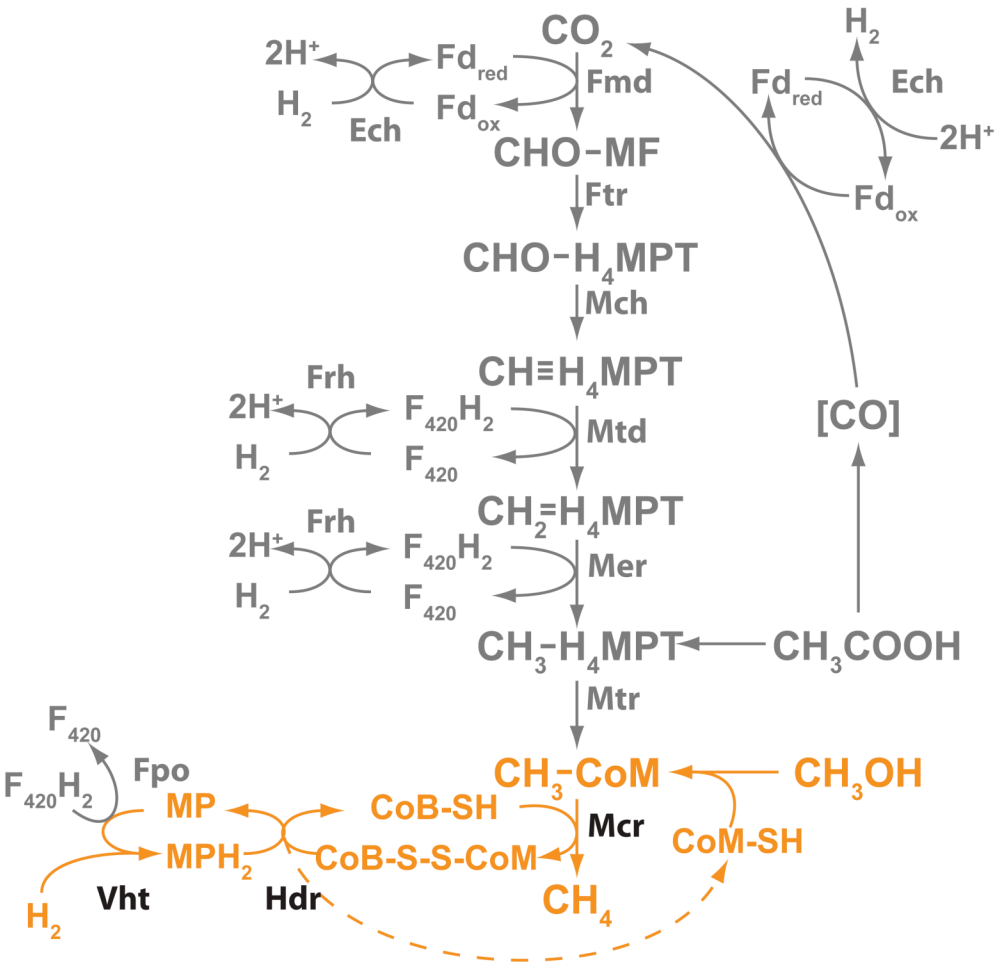

Figure 1.6 Methyl respiration pathway. C-1 compounds such as methanol or methylamines can be reduced directly using electrons derived from H_2 oxidation. Steps not required by this pathway are shaded gray. Abbreviations are same as in Figure 1.2. Figure adapted from (39).

being disproportionated into CO_2 and CH_4, they are entirely converted into methane. The heterodisulfide thus generated is reduced using H_2 via the H_2:heterodisulfide oxidoreductase system. Although this pathway was first discovered in *Methanosphaera stadtmaniae* (76), it was later reported in *M. barkeri* as well (39).

1.5 ENERGY CONSERVATION IN *METHANOSARCINA*

All methanogens are obligate methane producers as they conserve energy for growth and survival through methanogenesis. In each methanogenic pathway, formation of methane is accompanied by generation of the CoM-S-S-CoB heterodisulfide, which acts as the terminal electron acceptor in the respiratory chain. Regeneration of free coenzymes from the heterodisulfide is mediated by H_2, $F_{420}H_2$ or Fd_{red} via energy-conserving electron transport chains that have been characterized biochemically in *M. mazei* Gö1 (reviewed in (21, 22, 27-29)). These oxidoreductase systems are described below.

1.5.1 H_2:heterodisulfide oxidoreductase system

In this system, H_2 is used as an electron donor for heterodisulfide reduction (Figure 1.7) (20, 49). The membrane-bound F_{420}-nonreducing or methanophenazine-dependent hydrogenase, Vht, oxidizes H_2 in the periplasm to release two protons and two electrons. The electrons are transferred from the bimetallic [NiFe] catalytic center in the large subunit (VhtA), through the [Fe-S] clusters in the small subunit (VhtG), to the cytochrome *b* subunit (VhtC). VhtC

then accepts two protons from the cytoplasm and passes them along with the electrons to the membrane-bound electron carrier, methanophenazine (MP).

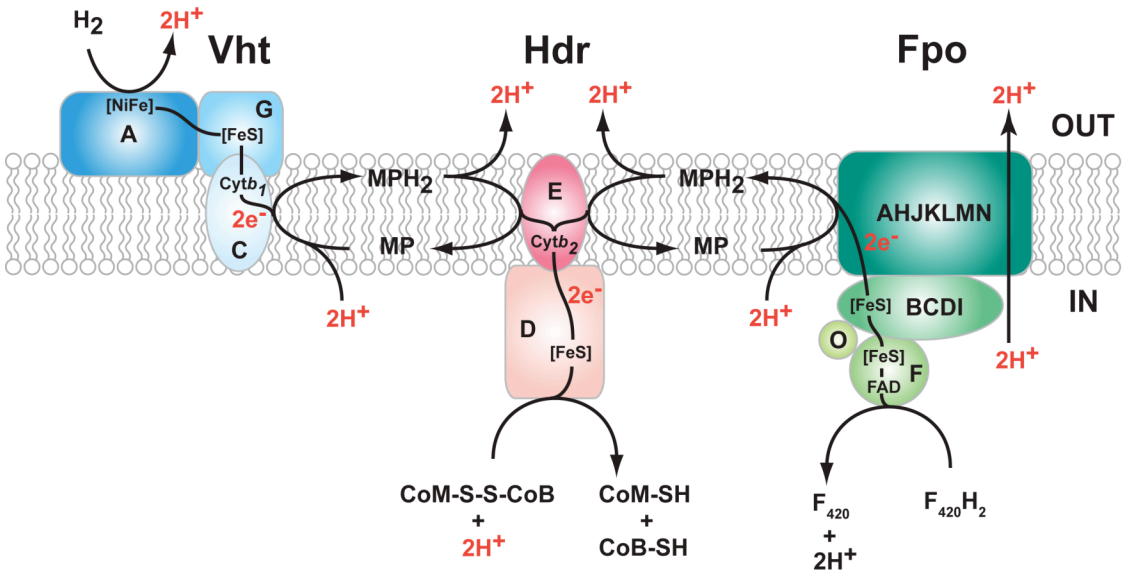

Figure 1.7 The electron transport chain of *Methanosarcina* has been proposed to comprise two energy-conserving systems, the H_2:heterodisulfide oxidoreductase and the $F_{420}H_2$:heterodisulfide oxidoreductase. In the former, H_2 is oxidized by Vht to produce two protons outside the cell and two electrons that are transferred to the membrane-soluble electron carrier MP. Reduction of MP consumes two protons from the cytoplasm, which are subsequently released outside the cell upon oxidation of MPH_2. The electrons are then transferred through HdrED to reduce CoM-S-S-CoB with two protons from the cytoplasm. Alternatively, in the $F_{420}H_2$:heterodisulfide oxidoreductase, $F_{420}H_2$ is oxidized by FpoF releasing two electrons that are transferred through FpoBCDI and then FpoAHJKLMN to MP. This reaction is coupled to pumping of two protons outside the cell. MPH_2 is then used to reduce CoM-S-S-CoB as in the H_2:heterodisulfide oxidoreductase. In both systems, the entire electron transport process leads to the net translocation of four protons (highlighted in red) outside the cell per two electrons transferred from $F_{420}H_2$ or H_2 to the CoM-S-S-CoB. Abbreviations are same as in Figure 1.2; FAD, flavin adenine dinucleotide; [FeS], iron-sulfur cluster; [NiFe], bimetallic catalytic center; Cyt*b*, cytochrome *b*; IN, inner face of the cytoplasmic membrane; OUT, outer face of the cytoplasmic membrane. Figure adapted from (56).

Thus, the net reaction leads to production of two scalar protons in the periplasm. Subsequently, oxidation of reduced MP (MPH_2) by the heterodisulfide reductase (Hdr) releases two protons in the periplasm and two electrons, which are transferred through the membrane-integral cytochrome *b* subunit (HdrE) to the

[Fe-S] clusters in the large subunit (HdrD). Finally, HdrD uses these electrons and two protons from the cytoplasm to reduce the CoM-S-S-CoB heterodisulfide. This leads to production of two additional scalar protons in the periplasm. Overall, four protons are translocated per one mole of heterodisulfide reduced. This proton-motive force can then be used for ATP production by the ATP synthase (21, 22).

M. barkeri has been proposed to use this electron transport chain during hydrogenotrophic and methyl-respiration pathways, as these involve use of H_2 as an electron donor (22). In the aceticlastic and methylotrophic pathways, Fd_{red} produced by carbonyl and formyl group oxidation, respectively, is postulated to give rise to H_2 by the action of Ech hydrogenase (72, 73). This H_2 can then be channeled into this oxidoreductase system as well. Although *M. mazei* has been shown to use this energy-conserving system *in vitro* while growing on H_2/CO_2 (49), *M. acetivorans* remains incapable of utilizing it due to its inability to express Vht and lack of the Ech hydrogenase (38, 39) .

1.5.2 $F_{420}H_2$:heterodisulfide oxidoreductase system

This system uses $F_{420}H_2$ to reduce the heterodisulfide (Figure 1.7) (7, 8). The membrane-bound $F_{420}H_2$ dehydrogenase (Fpo) oxidizes $F_{420}H_2$ via its input module (FpoF) to release two electrons that are channeled through FAD and [Fe-S] clusters in FpoF to the membrane-associated module of Fpo (FpoBCDI). Through the [Fe-S] clusters in FpoI and FpoB, the electrons are eventually transferred to the membrane-integral module of Fpo, FpoAHJKLMN, which uses

them to reduce MP. This reaction is coupled to the pumping of two protons outside the cell by Fpo. In addition, MP reduction consumes two protons from the cytoplasm, which are subsequently released in the periplasm on oxidation of MPH_2 by Hdr. This leads to production of two scalar protons in the periplasm. Hdr reduces the CoM-S-S-CoB heterodisulfide as in the H_2:heterodisulfide oxidoreductase system. Overall, this electron transport chain also leads to translocation of four protons outside the cell for one mole of heterodisulfide reduced. This proton-motive force can then be used for ATP production by the ATP synthase (22).

It has been proposed that *M. barkeri*, *M. mazei* and *M. acetivorans* use this electron transport chain during the methylotrophic pathway, in which $F_{420}H_2$ is produced from methyl and methylene group oxidation (22).

1.5.3 Fd_{red}:heterodisulfide oxidoreductase system

In *M. acetivorans,* Fd_{red} produced by the aceticlastic and methylotrophic pathways cannot be converted to H_2 for entry into the H_2:heterodisulfide oxidoreductase system. This is because *M. acetivorans* lacks the Ech hydrogenase and does not express the Vht hydrogenase (38, 39). Based on proteomic (63) and microarray analysis (62), it is postulated that during acetate utilization a membrane-bound complex called Rnf couples Fd_{red} oxidation to heterodisulfide reduction via MP, concomitantly pumping sodium ions outside the cell. The electrochemical sodium gradient can then be exchanged for a proton gradient via a Na^+/H^+ antiporter (Mrp) and used to make ATP by the ATP

synthase (31). Rnf and Mrp are absent in *M. barkeri* and *M. mazei* (26, 69). It is not known if Rnf or some other redox enzyme is responsible for Fd_{red} oxidation in the methylotrophic pathway. A putative Fd oxidoreductase capable of transferring electrons from Fd_{red} to CoM-S-S-CoB in a H_2-independent way has also been proposed in *M. barkeri* methylotrophic pathway. However, the identity of this protein is not known (73).

1.5.4 Mtr-catalyzed methyl group transfer from methyl-H_4MPT to CoM-SH

Mtr is a membrane-bound, eight-subunit enzyme that is encoded by the *mtrECDBAFGH* operon (Figure 1.8) (36). In the hydrogenotrophic and aceticlastic pathways, it catalyzes the exergonic transfer of methyl group from CH_3-H_4MPT to CoM-SH, concomitantly pumping two sodium ions outside the cell and conserving energy (9). On the other hand, during methanol utilization, Mtr catalyzes the reverse reaction (methyl transfer from CH_3-CoM to H_4MPT) by coupling it to the consumption of the sodium ion gradient (34, 41). The requirement of sodium ions by Mtr renders growth of methanogens Na^+ ion-dependent (36).

1.5.5 Ech-catalyzed H_2 production from Fd_{red}

Ech is a membrane-bound [NiFe] hydrogenase (Figure 1.8, described below in detail). In the hydrogenotrophic pathway, it couples the endergonic transfer of electrons from H_2 to Fd_{ox} with the consumption of an electrochemical proton gradient (72, 73). It has been postulated that this proton gradient is

created using the sodium ion gradient that is generated by the Mtr reaction in this pathway (51, 52, 106). This inter-conversion of ion gradients may be mediated by

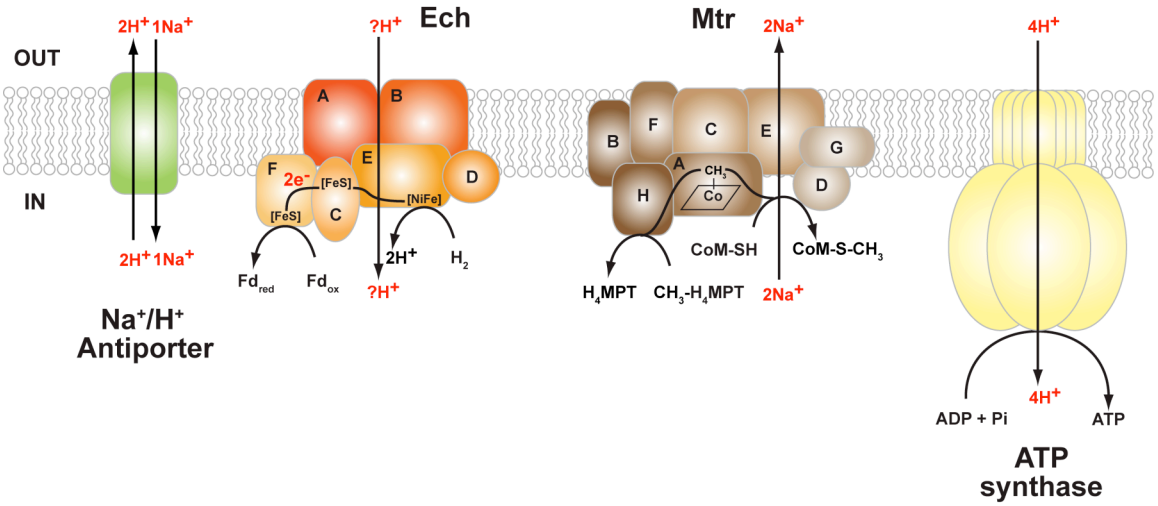

Figure 1.8 Ion-translocating protein complexes in *Methanosarcina*. Ech hydrogenase: H_2 is oxidized on the inner side of the membrane by EchE. The electrons thus released are passed through EchC and EchF to Fd_{ox}. This endergonic reaction is coupled to the import of an unknown number of protons inside the cell (42, 58, 72). **Methyl-H_4MPT:CoM methyltransferase (Mtr)**: The transfer of the methyl group from H_4MPT to CoM-SH involves a corrinoid group (CO) attached to the MtrA subunit. Initially, MtrH subunit catalyzes the methylation of the MtrA protein with methyl-H_4MPT. MtrE subunit then catalyzes the transfer of the methyl group from MtrA to CoM-SH, resulting in translocation of two sodium ions outside the cell (9, 36). **Na^+/H^+ antiporter** exchanges sodium ions for protons (106). **ATP synthase** couples import of protons into the cell with ATP synthesis (78). Abbreviations are same as in Figures 1.2 and 1.7.

the Na^+/H^+ antiporter, which is found in methanogens (Figure 1.8) (63, 79, 111). By analogy to its *Escherichia coli* homolog, the H^+/Na^+ stoichiometry of this antiporter is probably two (85, 102, 106). In the aceticlastic and methylotrophic pathways, Ech presumably catalyzes the exergonic production of H_2 from Fd_{red}, concomitantly pumping protons outside the cell (72, 73). Once converted into a sodium ion gradient, this proton gradient may be used to drive the endergonic

Mtr reaction in the methylotrophic pathway. It should be noted that *M. acetivorans* that lacks Ech cannot carry out these H_2-dependent reactions (38, 39).

1.5.6 A_1A_O ATPase

As outlined above, methanogenesis is coupled to the generation of electrochemical proton and sodium ion gradients that can be used to synthesize ATP using an ATPase (Figure 1.8). Archaea contain a unique class of ATPases, the A_1A_O ATPases that are structurally similar to eukaryal V_1V_O ATPases, but function as ATP synthases like the bacterial F_1F_O ATPases (78). The coupling ion for the ATPase is H^+ (87), however, the H^+ to ATP stoichiometry is uncertain, but is presumed to be 4 for most methanogens (80, 106). The genes encoding the ATPase from *M. mazei* Gö1 constitute one operon, *ahaHIKECFABD*, which is also present in the genomes of *M. barkeri* Fusaro and *M. acetivorans* C2A (80). Interestingly, the latter two species also contain a F_1F_O ATPase, but its functionality is not yet known (78).

1.6 ENERGY CONSERVATION IN OTHER METHANOGENS

Apart from members of the order *Methanosarcinales*, all methanogens are devoid of MP and cytochromes. In addition, they lack the membrane-bound Vht and HdrED enzymes. Therefore, these hydrogenotrophic methanogens cannot conserve energy via the H_2:heterodisulfide oxidoreductase system described above. Instead, they employ a cytoplasmic multi-enzyme complex that is

composed of [NiFe] hydrogenase MvhADG and heterodisulfide reductase (HdrABC) (Figure 1.9). This complex has been proposed to couple the exergonic reduction of heterodisulfide with H_2 to the endergonic reduction of Fd_{ox}, also by

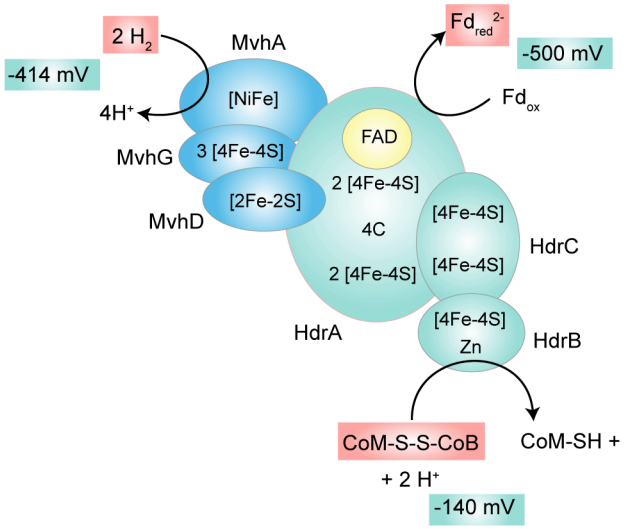

Figure 1.9 Proposed scheme for the reduction of CoM-S-S-CoB with H_2 that is catalyzed by the hydrogenase (MvhADG)-heterodisulfide reductase (HdrABC) complex in methanogens without cytochromes. The enzyme complex is proposed to couple the endergonic reduction of Fd_{ox} with H_2 to the exergonic reduction of CoM-S-S-CoB with H_2 by flavin-based electron dismutation that involves the FAD in HdrA. Abreviations are same as in Figures 1.2 and 1.7. Figure created from (106).

H_2 (106). The reaction proceeds via a flavin-based electron bifurcation mechanism that is similar to the one recently characterized during butyrate fermentation in *Clostridium kluyveri* (61). Thus, the Mvh hydrogenase oxidizes two molecules of H_2 to release electrons for reduction of the heterodisulfide at HdrC and Fd_{ox} at FAD-containing HdrA. The Fd_{red} can then be used for reduction of CO_2 to the formyl level in the first step of hydrogenotrophic methanogenesis. As aforementioned, *Methanosphaera stadtmanae* can only reduce methanol to methane. Hence, it utilizes the Fd_{red} generated by the Mvh-Hdr complex for H_2

production using an Ech-like hydrogenase called Ehb, which couples this reaction to the build-up of an ion-motive force. This electrochemical gradient can be subsequently used for ATP synthesis by the ATP synthase (106).

1.7 COMPONENTS OF ELECTRON TRANSPORT SYSTEMS IN *METHANOSARCINA*

The electron transport systems involve various redox enzymes that shuttle electrons between the four major electron carriers: H_2, F_{420}, Fd and MP. These enzymes include hydrogenases, Fpo and Hdr.

1.7.1 Ech: Fd_{ox}-dependent hydrogenase

Ech (***E****. coli* **c** [for three] **h**ydrogenase (58) or **E**nergy **c**onverting **h**ydrogenase (42)) is a multi-subunit membrane-bound [NiFe] hydrogenase that catalyzes the reversible reduction of Fd_{ox} with H_2 (Figure 1.8) (72). It belongs to a family of hydrogenases that are closely related to the proton-pumping NADH:quinone oxidoreductase (Nuo, complex I of *E. coli*). This family also includes *E. coli* hydrogenases 3 and 4, CO-induced hydrogenase from *Rhodospirillum rubrum* and Eha and Ehb from *Methanothermobacter* species (42).

Ech purified from *M. barkeri* (72) is composed of six subunits that are encoded by the *echABCDEF* operon (73). EchE and EchC are the large and small subunits of [NiFe] hydrogenases, respectively. Thus, EchE harbors the bimetallic [NiFe] catalytic center and EchC a [4Fe-4S] cluster. In addition to these subunits, EchF and EchD are also hydrophilic. Although the function of EchD is

unknown, EchF is an electron transfer protein containing two [4Fe-4S] clusters (58). The rest of the subunits, EchA and EchB, are membrane-bound and show homology to the proton-pumping subunits of Nuo (Nuo H and NuoL, respectively). Therefore, they may be involved in ion translocation during Ech activity (42, 58). It has been proposed that electrons released from H_2 oxidation at EchE are channeled through the [Fe-S] clusters in EchC and EchF to Fd_{ox} (72).

In *M. barkeri*, a soluble 2[4Fe-4S] Fd_{ox} ($E^{o'}$ = -420 mV) is the physiological electron acceptor of Ech. Reduction of this Fd_{ox} by H_2 ($E^{o'}$ = -414 mV) is endergonic, especially in methanogenic habitats with low H_2 partial pressure (E' = -286 mV at 5 Pa). There is evidence to suggest that Ech drives this unfavorable reaction by coupling it to the consumption of a proton gradient called reverse electron transport. The Fd_{red} thus generated is used to reduce CO_2 to the formyl level in the first step of hydrogenotrophic methanogenesis (Figure 1.2). Also, it is needed for biosynthesis of acetyl-CoA and pyruvate via the ACDS (Reaction 1) and pyruvate:ferredoxin oxidoreductase (POR, reaction 2) catalyzed reactions, in the hydrogenotrophic and methyl-respiration pathways. During acetate utilization, oxidation of carbonyl group to CO_2 produces Fd_{red} (Figure 1.4). Ech renders this reaction energy-conserving by coupling H_2 formation from Fd_{red} to generation of a proton-motive force. Subsequently, the H_2 presumably enters the H_2:heterodisulfide oxidoreducatse system for reduction of the heterodisulfide (Figure 1.7). A similar role of Ech has also been proposed in the methylotrophic pathway, in which Fd_{red} produced by formyl group oxidation may be converted

into H_2 by Ech (Figure 1.5). However, mutational analysis of *ech* revealed that electrons from Fd_{red} can be transferred to the heterodisulfide in an Ech- or H_2-independent manner (72, 73).

CH_3-H_4MPT + CO_2 + Fd_{red} + CoA-SH → CH_3-CO-SCoA + H_4MPT + Fd_{ox} (1)

CH_3-CO-SCoA + CO_2 + Fd_{red} → CH_3-CO-COOH + CoA-SH + Fd_{ox} (2)

Consistent with its role in each methanogenic pathway, *ech* is expressed on all substrates tested in *M. barkeri*. Notably, *ech* expression on acetate is *ca*. ten-fold more than on other substrates (38, 58). The *echABCDEF* operon is found in *M. barkeri* (69) and *M. mazei* (22), but is absent in *M. acetivorans* (33). Other hydrogenotrophic methanogens like *M. marburgensis* (103) and *M. maripaludis* (88) contain two Ech-like hydrogenases, Eha and Ehb. Although these belong to the same family as Ech, their subunit composition is different from Ech.

1.7.2 Frh: F_{420}-reducing hydrogenase

Frh (**F_{420}-r**educing **h**ydrogenase) is a soluble [NiFe] flavoprotein that catalyzes the reversible reduction of coenzyme F_{420} with H_2 (Figure 1.10) (74). F_{420} ($E^{o'}$ = -360 mV) is a deazaflavine derivative that carries hydride ions and is responsible for the characteristic blue auto-fluorescence of methanogens (23). Frh purified from *M. barkeri* is a three-subunit enzyme, encoded by the *frhADGB* operon (74, 110). FrhA is the large subunit of [NiFe] hydrogenases that harbors

the [NiFe] catalytic center, whereas FrhG is the small subunit containing at least 2 [4Fe-4S] clusters. FrhB is a flavoprotein that binds F_{420} and FrhD is a putative maturation peptidase needed for FrhA processing (6, 38, 74). A plausible route

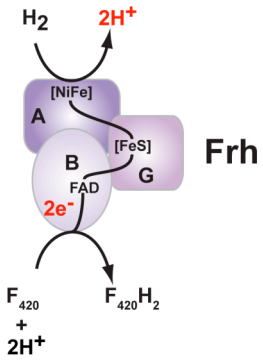

Figure 1.10 F_{420}-reducing hydrogenase. Frh catalyzes the reversible oxidation of $F_{420}H_2$ with H_2 in the cytoplasm (74). Abbreviations are same as in Figures 1.2 and 1.7.

for electron transfer to F_{420} involves oxidation of H_2 at the [NiFe] center in FrhA to release electrons that are channeled through the [Fe-S] clusters in FrhG to FAD in FrhB. Finally, FAD donates electrons to F_{420} via the $1e^-/2e^-$ redox switch (6).

$F_{420}H_2$ serves as an electron donor for reduction of methenyl and methylene groups in the hydrogenotrophic pathway (Figure 1.2) (6, 74, 104). This is consistent with *frh* expression on H_2/CO_2 in *M. barkeri*. However, it is unclear why *frh* is also expressed on methanol. On the other two substrates, methanol plus H_2/CO_2 and acetate, *frh* expression is down-regulated two to three-fold (38).

While *M. barkeri*, *M. mazei* and *M. acetivorans* each possess the *frhADGB* operon, *M. barkeri* also contains a second *freAEGB* operon that lacks the gene *D* (38, 110). Moreover, subunit E does not show homology to subunit D or any other protein in the database. The *fre* operon encodes a hydrogenase that is 85-

87% identical to Frh (110). In addition, Fre contains all the important structural and catalytic residues that are present in Frh. Thus, it has been proposed that Fre might be functional if it undergoes processing by FrhD. In *M. barkeri*, *fre* is expressed at very low levels on all methanogenic substrates. The expression of *frh* is undetectable in *M. acetivorans* under all tested conditions (38).

Some methanogens like *Methanococcus voltae* (40), *Methanococcus jannaschii* (15) and *M. maripaludis* (45), contain two isozymes of F_{420}-reducing hydrogenases. In one of these, an active-site cysteine residue is replaced by selenocysteine. The non-selenium containing hydrogenases are only synthesized in the absence of selenium in *M. voltae* (100).

1.7.3 Vht: F_{420}-nonreducing or MP-dependent hydrogenase

Vht (**V**iologen **h**ydrogenase **t**wo) is a membrane-bound [NiFe] hydrogenase that catalyzes the reversible reduction of MP (Figure 1.7) ($E^{o'}$ = -165 mV (108)) with H_2 (10, 24). Although Vht was purified from both *M. mazei* Gö1 (25) and *M. barkeri* MS (54), characterization of the enzyme was done using the *M. mazei* enzyme preparation. This preparation was found to contain two isozymes called Vho (**V**iologen **h**ydrogenase **o**ne) and Vht (**V**iologen **h**ydrogenase **t**wo) that are *ca*. 95% identical and are encoded by the *vhoGAC* and *vhtGACD* operons, respectively (19, 24). The A subunit is the hydrogenase large subunit with the [NiFe] catalytic center, whereas the G subunit is the small subunit containing [Fe-S] clusters and a Tat signal peptide, which probably localizes the enzyme to the periplasmic side of the membrane. Subunit C is a

cytochrome *b* and the D subunit, which is absent in *vho*, is a putative hydrogenase maturation protease needed for processing of the large hydrogenase subunit (24, 38). It has been proposed that electrons released from H_2 oxidation at Vht/VhoA are channeled through the [Fe-S] clusters in Vht/VhoG to Vht/VhoC, which then passes them on to MP (22). Washed membrane vesicles containing Vht/Vho and Hdr have been shown to catalyze H_2-dependent reduction of the CoM-S-S-CoB heterodisulfide, in the presence of 2-hydroxyphenazine (a soluble analog of MP). This reaction is coupled to the generation of a proton gradient ($4H^+/2e^-$), which is used to drive ATP synthesis (20, 49). Both Vho/Vht and Hdr can also function with chemically synthesized MP (10).

Thus, Vht channels electrons from H_2 oxidation to MP, which is then used as an electron donor by Hdr for heterodisulfide reduction in the terminal step of methanogenesis (49). The source of H_2 in the hydrogenotrophic pathway (Figure 1.2) is external (22, 104), whereas in the aceticlastic (Figure 1.4) and methylotrophic (Figure 1.5) pathways, H_2 is presumably produced from Fd_{red} by the Ech hydrogenase (72, 73).

In addition to *vho* and *vht*, *M. mazei* genome (26) harbors a third operon (*vhxGAC*) that encodes the methanophenazine-dependent hydrogenase Vhx (Vho-like hydrogenase with unknown [x] function) (38). Phylogenetic analysis indicates that Vho and Vht group together to the exclusion of Vhx (*ca*. 50% amino acid identity to the other two hydrogenases). Thus, *vho* could have arisen from a recent duplication in *M. mazei* genome (38). Both *M. barkeri* (69) and *M.*

acetivorans (33) possess one operon that is similar to *vhoGAC*/*vhtGACD* (designated as *vhtGACD*) and another to *vhxGAC*. The presence of *vhx* in all *Methanosarcina* species suggests that it was in their genomes before they diverged from each other. The deduced sequences of Vht/Vhx enzymes from *M. barkeri* and *M. acetivorans* possess all the important structural and catalytic residues that are present in *M. mazei* hydrogenases. However, the only exception is the VhxG subunits from *M. barkeri* and *M. mazei* that lack the first conserved cysteine residue in the motif CXXCXnGXCXXXGXmGCP, which is characteristic of the small hydrogenase subunits. Like *vho*, *vhx* lacks the maturation protease-encoding gene *D*. As methanophenazine-dependent hydrogenases are presumed to undergo post-translational modification using subunit D, it has been proposed that *vhtD* may provide this protease in *trans* for processing of Vho and Vhx enzymes (38).

The reason(s) for the existence of multiple methanophenazine-dependent hydrogenases in *Methanosarcina* species is unclear. A plausible explanation could be differential regulation of expression, as seen in *M. mazei*, in which *vho* is expressed constitutively on methanol, trimethylamine, H_2/CO_2 and acetate, whereas *vht* is not expressed on acetate (19). In *M. barkeri*, *vhx* is not expressed at detectable levels on any methanogenic substrate tested, whereas expression of *vht* is constitutive. Like *frh*, *vht* is also not expressed in *M. acetivorans*. However, *vhx* is expressed at very low levels on H_2/CO_2, methanol and methanol plus H_2/CO_2 and is up-regulated five-fold on acetate (38).

The F_{420}-nonreducing hydrogenases from other methanogens is cytoplasmic, lacks cytochrome and does not interact with MP (106). Therefore, it should be considered as distinct from Vht, despite their common name. For instance, the enzyme from *M. marburgensis* (95, 101) is composed of three subunits, MvhDGA, out of which MvhA and MvhG are the large and small subunits of [NiFe] hydrogenases, respectively. The MvhD subunit has been proposed to interact with Hdr and provide electrons for heterodisulfide reduction. Another subunit encoded by the *mvhDGAB* operon (MvhB) is a polyferredoxin with an unknown function. Similar enzymes are found in *M. jannaschii* (15), *M. kandleri* (99), *M. maripaludis* (45) and *M. voltae* (40). The latter two species contain two isozymes of F_{420}-nonreducing hydrogenases, a [NiFe] Vhc and another [NiFeSe] Vhu, encoded by *vhcDGAB* and *vhuDGAUB* operons, respectively.

1.7.4 Hyp: Hydrogenase maturation proteins

The synthesis and insertion of metal center in [NiFe] hydrogenases requires auxiliary proteins called Hyp, which have been well characterized in *E.coli*. The postulated pathway of maturation of hydrogenase 3 from *E. coli* involves six Hyp proteins that are encoded by the *hypABCDE* operon and *hypF* (Figure 1.11) (13). Firstly, the HypC and HypD proteins form a complex that binds an Fe atom. HypE and HypF then synthesize the CO and CN ligands of Fe atom from carbamoyl phosphate in an ATP-dependent reaction. HypD, which is an iron-sulfur protein, may provide electrons for attachment of these ligands to

the Fe atom (12, 13). Subsequently, HypC dissociates from HypD and binds the unmetallated large hydrogenase subunit (Pre-HycE) via one of its Ni-binding cysteine ligands (70). This helps maintain the protein in a conformation that is

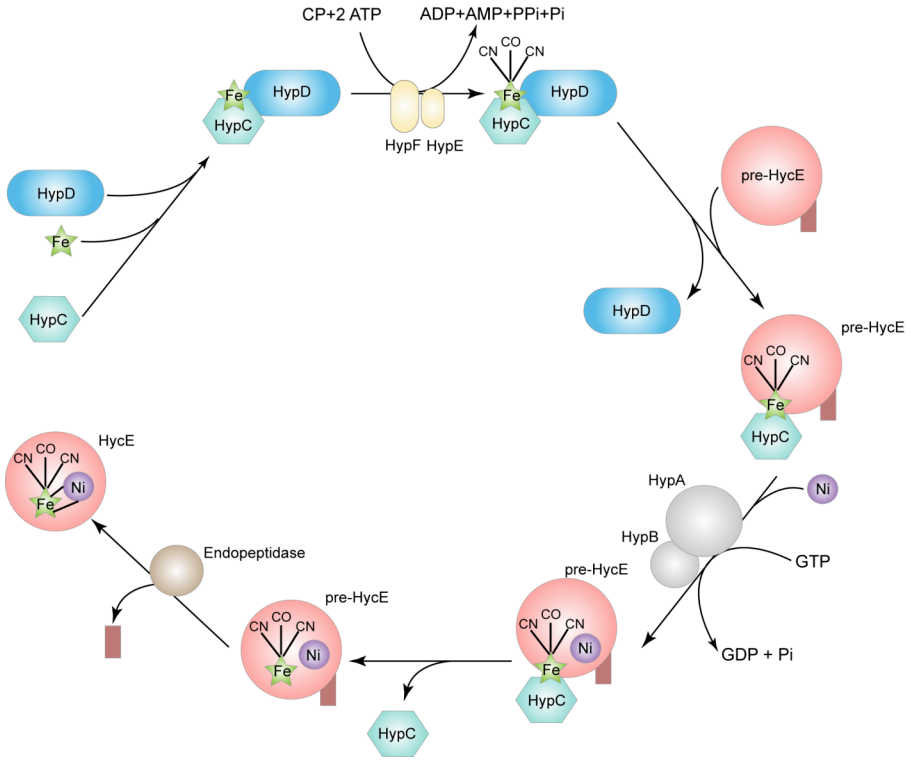

Figure 1.11 Postulated pathway of the maturation of hydrogenase 3 from *E.coli* (HycE). HypC and HypD form a complex with the Fe atom, which gets liganded to CO and CN groups that are synthesized from CP by HypE and HypF. HypC then dissociates from HypD and inserts the Fe atom into the precursor of HycE (pre-HycE). HypA and HypB subsequently catalyze coordination of the Ni atom into pre-HycE. HypC dissociates from the metallated pre-HycE, which is then acted upon by an endopeptidase that cleaves a carboxyl terminal peptide. This is followed by bridging of the two atoms via cysteine groups and closing of the metal center. Abbreviations, CP: carbamoyl phosphate; CO: carbon monoxide; CN: cyanide. Figure adapted from (12, 13).

accessible for metal insertion. Thus HypC acts as a chaperone. It then inserts the liganded Fe atom into the active site. This is followed by coordination of Ni atom into the large subunit precursor by HypA and HypB (GTPase), in concomitance with GTP hydrolysis (12, 13). Once HypC dissociates from the metallated

subunit, the Ni atom acts as a recoginition signal for an endopeptidase that is encoded *in cis* with the hydrogenase. It cleaves an oligopeptide from the C-terminus leading to a conformational change that allows bridging of the Ni and Fe atoms through cysteine residues. This closes the metal center of the large subunit and enables its interaction with the small subunit (13, 107).

All three *Methanosarcina* species (26, 33, 69) possess a *hypCDABE* operon and *hypF*. In addition, *M. mazei* has extra copies of *hypB* and *hypC*. These proteins presumably carry out the same reactions during maturation of Ech, Frh, Fre, Vho, Vht and Vhx hydrogenases. However, Ech may not undergo the terminal processing step involving the endopeptidase, as it lacks the carboxyl terminal oligopeptide (58).

1.7.5 Hmd: Iron-sulfur cluster-free hydrogenase

In addition to Fd-, F_{420}- and F_{420}-non reducing hydrogenases, members of *Methanobacteriales*, *Methanococcales* and *Methanopyrales* (35) also contain an iron-sulfur cluster-free hydrogenase that is phylogenetically unrelated to [FeFe] and [NiFe] hydrogenases (96). As mentioned above, this hydrogenase called H_2-forming methylene-H_4MPT dehydrogenase (Hmd) catalyzes the reversible reduction of methenyl-H_4MPT to methylene-H_4MPT with H_2 in the hydrogenotrophic pathway. Since this reaction can also be catalyzed by the concerted action of [NiFe] hydrogenase Frh and Mtd, Hmd is only essential under Ni-limiting conditions. Under such conditions, Hmd, in conjunction with Mtd, is also used for synthesis of $F_{420}H_2$ (Figure 1.3) (96). Together Hmd and Mtd also

catalyze the reverse reaction leading to H_2 production from $F_{420}H_2$ during formate utilization (46, 67).

The Hmd holoenzyme comprises of a homodimer, two pyridone derivative cofactor molecules and two Fe atoms (35). The protein is encoded by the *hmd* gene. Interestingly, methanogens with *hmd* also contain one or two *hmd* homologs that encode for proteins that are only *ca*. 20% identical to Hmd. The role of these proteins seems to be Hmd-related but is still unclear (96).

1.7.6 Fpo: $F_{420}H_2$ dehydrogenase

Fpo (**F**$_{420}$H$_2$ **p**henazine **o**xidoreductase) is a membrane-bound $F_{420}H_2$ dehydrogenase that catalyzes the transfer of electrons from $F_{420}H_2$ to MP, concomitantly pumping two protons outside the cell (Figure 1.7) (7). It was first purified from *M. mazei* Gö1 as a five-subunit complex (FpoBCDIF) capable of oxidizing $F_{420}H_2$ with a variety of artificial electron acceptors (4). Searching the genome for N-terminal amino acid sequences of these proteins resulted in the discovery of a 13-gene operon, *fpoABCDHIJJKLMNO* (*fpo*), containing *fpoBCDI*, with *fpoF* being located elsewhere on the genome (7). Fpo shares significant homology with NADH:quinone oxidoreductase (Nuo) of *E. coli* and the nomenclature reflects that similarity. Accordingly, both Fpo and Nuo are composed of similar membrane-integral (the A, H, J, K, L, M and N subunits) and membrane-associated (the B, C, D and I subunits) modules. However, the enzymes differ in their substrates and hence in their input modules, such that NuoEFG oxidizes NADH, whereas FpoF oxidizes $F_{420}H_2$. Another difference

between the enzymes is the presence of an additional hydrophilic iron-sulfur subunit of unknown function in Fpo, FpoO, which has no homolog in Nuo. Notably, the FpoF subunit shares homology with FrhB subunit of F_{420}-reducing hydrogenases (7, 21, 22).

It is postulated that electrons released from $F_{420}H_2$ oxidation at FpoF are channeled through the enzyme-bound FAD and [Fe-S] cluster to the [Fe-S] clusters in FpoI and FpoB. Subsequently, they are transferred via the membrane-bound module FpoAHJKLMN, which is predicted to be involved in proton extrusion, to MP (7, 21, 22). Washed membrane vesicles containing Fpo and Hdr have been shown to catalyze $F_{420}H_2$-dependent reduction of the CoM-S-S-CoB heterodisulfide, in the presence of 2-hydroxyphenazine. This reaction is coupled to the generation of a proton gradient ($4H^+/2e^-$), which is used to drive ATP synthesis (7, 8). Both Fpo and Hdr can also function with chemically synthesized MP (10).

Thus, Fpo couples oxidation of $F_{420}H_2$, generated during the methylotrophic pathway (Figure 1.5), to MP reduction and pumping of two protons outside the cell. MPH_2 is then used for reduction of the heterodisulfide by Hdr (7).

M. barkeri (69) and *M. acetivorans* (33) also contain the *fpo* operon and *fpoF.* Interestingly, when grown on CO as the growth substrate, *M. acetivorans* Fpo has been proposed to contain a small additional subunit, FpoP. However, there is no experimental evidence that FpoP protein is produced, nor is the gene

conserved in the other two *Methanosarcina* species. Thus it is still unknown if FpoP has a role in methanogenesis from any substrate (60).

1.7.7 Hdr: Heterodisulfide reductase

Hdr is a membrane-bound iron-sulfur hemoprotein that catalyzes the reversible reduction of the heterodisulfide of coenzyme M and coenzyme B, CoM-S-S-CoB ($E^{o'}$ = -143 mV (108)), with MPH_2 (Figure 1.7) (10, 57). Hdr purified from *M. barkeri* (44) is a two-subunit enzyme encoded by the *hdrED* operon. HdrE represents a membrane-integral cytochrome *b*, whereas HdrD is a hydrophilic subunit containing two [4Fe-4S] clusters (57). Electrons produced from the oxidation of MPH_2 are presumably transferred to cytochrome *b* and the protons are released at the outer phase of the cytoplasmic membrane. Subsequently, the electrons are channeled through the [4Fe-4S] clusters of HdrD to the heterodisulfide, which gets reduced by consumption of two protons from the cytoplasm (22). The scalar production of protons by HdrED has been demonstrated in washed membrane vesicles of *M. mazei* Gö1. This experimental system was also used to validate HdrED as a part of the H_2:heterodisulfide and $F_{420}H_2$:heterodisulfide oxidoreductase systems (7, 8, 20, 49).

As the CoM-S-S-CoB heterodisulfide is generated in all aforementioned methanogenic pathways, HdrED plays a key role in energy conservation in methanogenesis. Depending on the substrate utilized, it reduces the heterodisulfide using electrons from the oxidation of H_2, $F_{420}H_2$ or Fd_{red} via MP (21, 22).

All methanogens, except members of the order *Methanosarcinales*, lack the membrane-bound, cytochrome-containing Hdr (106). Instead, they possess a soluble Hdr that is composed of three different subunits, HdrABC (Figure 1.9) (reviewed in (43)). This enzyme has been purified and characterized from *M. marburgensis*. HdrA is a flavoprotein with four [4Fe-4S] clusters, whereas HdrC contains two [4Fe-4S] clusters. Although HdrB contains no characteristic cofactor-binding motif, it is probably the site of heterodisulfide reduction. Based on sequence similarity, HdrE is presumed to be a fusion protein of HdrB and HdrC subunits.

In addition to HdrED, these hydrogenotrophic methanogens also lack cytochromes, MP and a membrane-bound F_{420}-nonreducing hydrogenase (106). Thus, energy conservation using the cytoplasmic HdrABC enzyme is unclear. However, a recent review by Thauer *et al* (106) proposes that a soluble complex of the F_{420}-nonreducing hydrogenase (MvhDGA) and HdrABC, couples reduction of heterodisulfide to Fd_{ox} reduction with H_2, using a flavin-based bifurcation mechanism. The Fd_{red} is then used to catalyze the reduction of CO_2 to the formyl group in the first step of hydrogenotrophic methanogenesis.

Surprisingly, all sequenced *Methanosarcinales* genomes contain homologs of the *hdrABC* genes, in addition to *hdrED* (26, 33, 69). However, their function in methanogenesis in these organisms is unknown.

1.8 OUTLINE OF WORK PRESENTED IN THE THESIS

The energy-conserving electron transport chains of *Methanosarcina* have been modeled on the basis of *in vitro* biochemical studies (7, 20, 49). In this work, I employed a variety of genetic techniques that have been developed in the Metcalf lab (90) to investigate the *in vivo* roles of various components of these electron transfer systems. In Chapter 2, deletion analysis of the $F_{420}H_2$-metabolizing enzymes: Fpo, Frh and Fre (7, 110) revealed that *M. barkeri* uses a branched electron transport chain to conserve energy during methylotrophic growth. Thus, only a fraction of $F_{420}H_2$ generated during methyl group oxidation enters into the $F_{420}H_2$:heterodisulfide oxidoreductase system (7). Most of the $F_{420}H_2$, however, is oxidized by Frh to produce H_2, which is probably channeled into the H_2:heterodisulfide oxidoreductase system via Vht or Vhx (38, 49). In Chapter 3, deletion analysis of Vht and Vhx confirmed H_2 as a bona fide intermediate in the methylotrophic pathway, hence supporting "H_2-cycling" (83) as a mechanism of energy conservation in *M. barkeri* methylotrophic pathway. In this mechanism, H_2 produced from $F_{420}H_2$ oxidation by Frh in the cytoplasm diffuses out of the cell to the active site of Vht in the periplasm. Vht then oxidizes H_2 to regenerate protons, thus leading to the establishment of a trans-membrane proton gradient, which can be used for ATP synthesis by the ATP synthase. Due to the pivotal roles displayed by hydrogenases in *M. barkeri*, I characterized them further in Chapter 4. This was accomplished by constructing a series of single, double, triple, quadruple and quintuple hydrogenase gene deletion mutants. These mutants were then characterized in terms of growth, methane and CO_2

production, hydrogenase activity and expression of various genes. This analysis would also give us insight into the H_2-independent electron-transport chains of *M. barkeri*. In conclusion, the work presented here enhanced our understanding of energy conservation pathways in *Methanosarcina* species. Moreover, this knowledge could be possibly extrapolated to other anaerobic organisms, which possess hydrogenases and are hypothesized to utilize them during energy conservation (18, 82, 84).

1.9 LITERATURE CITED

1. 2009. Energy Sector Methane Recovery and Use. International Energy Agency.

2. 1999-2007. Inventory of U.S. greenhouse gas emissions and sinks. U.S. Environmental Protection Agency.

3. **Abbanat, D. R., and J. G. Ferry.** 1991. Resolution of component proteins in an enzyme complex from *Methanosarcina thermophila* catalyzing the synthesis or cleavage of acetyl-CoA. Proc Natl Acad Sci U S A **88:**3272-6.

4. **Abken, H. J., and U. Deppenmeier.** 1997. Purification and properties of an $F_{420}H_2$ dehydrogenase from *Methanosarcina mazei* Gö1. FEMS Microbiology Letters **154:**231-237.

5. **Aceti, D. J., and J. G. Ferry.** 1988. Purification and characterization of acetate kinase from acetate-grown *Methanosarcina thermophila*. Evidence for regulation of synthesis. J Biol Chem **263:**15444-8.

6. **Alex, L. A., J. N. Reeve, W. H. Orme-Johnson, and C. T. Walsh.** 1990. Cloning, sequence determination, and expression of the genes encoding the subunits of the nickel-containing 8-hydroxy-5-deazaflavin reducing hydrogenase from *Methanobacterium thermoautotrophicum* delta H. Biochemistry **29:**7237-44.

7. **Baumer, S., T. Ide, C. Jacobi, A. Johann, G. Gottschalk, and U. Deppenmeier.** 2000. The $F_{420}H_2$ dehydrogenase from *Methanosarcina mazei* is a redox-driven proton pump closely related to NADH dehydrogenases. J Biol Chem **275:**17968-73.

8. **Baumer, S., E. Murakami, J. Brodersen, G. Gottschalk, S. W. Ragsdale, and U. Deppenmeier.** 1998. The $F_{420}H_2$:heterodisulfide oxidoreductase system from *Methanosarcina* species. 2-Hydroxyphenazine mediates electron transfer from $F_{420}H_2$ dehydrogenase to heterodisulfide reductase. FEBS Lett **428:**295-8.

9. **Becher, B., V. Muller, and G. Gottschalk.** 1992. N5-methyl-tetrahydromethanopterin:coenzyme M methyltransferase of *Methanosarcina* strain Gö1 is an Na(+)-translocating membrane protein. J Bacteriol **174:**7656-60.

10. **Beifuss, U., M. Tietze, S. Baumer, and U. Deppenmeier.** 2000. Methanophenazine: Structure, Total Synthesis, and Function of a New Cofactor from Methanogenic Archaea. Angew Chem Int Ed Engl **39:**2470-2472.

11. **Blaut, M., V. Muller, and G. Gottschalk.** 1992. Energetics of methanogenesis studied in vesicular systems. J Bioenerg Biomembr **24:**529-46.

12. **Blokesch, M., and A. Bock.** 2002. Maturation of [NiFe]-hydrogenases in *Escherichia coli*: the HypC cycle. J Mol Biol **324:**287-96.

13. **Blokesch, M., A. Paschos, E. Theodoratou, A. Bauer, M. Hube, S. Huth, and A. Bock.** 2002. Metal insertion into NiFe-hydrogenases. Biochem Soc Trans **30:**674-80.

14. **Boone, D. R., S. Worakit, I. M. Mathrani, and R. A. Mah.** 1986. Alkaliphilic methanogens from high pH lake sediments. systematic and applied microbiology **7:**230-234.

15. **Bult, C. J., O. White, G. J. Olsen, L. Zhou, R. D. Fleischmann, G. G. Sutton, J. A. Blake, L. M. FitzGerald, R. A. Clayton, J. D. Gocayne, A. R. Kerlavage, B. A. Dougherty, J. F. Tomb, M. D. Adams, C. I. Reich, R. Overbeek, E. F. Kirkness, K. G. Weinstock, J. M. Merrick, A. Glodek, J. L. Scott, N. S. Geoghagen, and J. C. Venter.** 1996. Complete genome sequence of the methanogenic archaeon, *Methanococcus jannaschii*. Science **273:**1058-73.

16. **Cadillo-Quiroz, H., J. B. Yavitt, and S. H. Zinder.** 2009. *Methanosphaerula palustris* gen. nov., sp. nov., a hydrogenotrophic methanogen isolated from a minerotrophic fen peatland. Int J Syst Evol Microbiol **59:**928-35.

17. **Clements, A. P., and J. G. Ferry.** 1992. Cloning, nucleotide sequence, and transcriptional analyses of the gene encoding a ferredoxin from *Methanosarcina thermophila*. J Bacteriol **174:**5244-50.

18. **Coppi, M. V.** 2005. The hydrogenases of *Geobacter sulfurreducens*: a comparative genomic perspective. Microbiology **151:**1239-54.

19. **Deppenmeier, U.** 1995. Different structure and expression of the operons encoding the membrane-bound hydrogenases from *Methanosarcina mazei* Gö1. Arch Microbiol **164:**370-6.

20. **Deppenmeier, U.** 1991. H_2:heterodisulfide oxidoreductase, a second energy conserving system in the methnaogenic strain Gö1. Arch Microbiol **155:**272-277.

21. **Deppenmeier, U.** 2002. Redox-driven proton translocation in methanogenic Archaea. Cell Mol Life Sci **59:**1513-33.

22. **Deppenmeier, U.** 2004. The membrane-bound electron transport system of *Methanosarcina* species. J Bioenerg Biomembr **36:**55-64.

23. **Deppenmeier, U.** 2002. The unique biochemistry of methanogenesis. Prog Nucleic Acid Res Mol Biol **71:**223-83.

24. **Deppenmeier, U., M. Blaut, S. Lentes, C. Herzberg, and G. Gottschalk.** 1995. Analysis of the *vhoGAC* and *vhtGAC* operons from *Methanosarcina mazei* strain Gö1, both encoding a membrane-bound hydrogenase and a cytochrome b. Eur J Biochem **227:**261-9.

25. **Deppenmeier, U., M. Blaut, B. Schmidt, and G. Gottschalk.** 1992. Purification and properties of a F_{420}-nonreactive, membrane-bound hydrogenase from *Methanosarcina* strain Gö1. Arch Microbiol **157:**505-11.

26. **Deppenmeier, U., A. Johann, T. Hartsch, R. Merkl, R. A. Schmitz, R. Martinez-Arias, A. Henne, A. Wiezer, S. Baumer, C. Jacobi, H. Bruggemann, T. Lienard, A. Christmann, M. Bomeke, S. Steckel, A. Bhattacharyya, A. Lykidis, R. Overbeek, H. P. Klenk, R. P. Gunsalus, H. J. Fritz, and G. Gottschalk.** 2002. The genome of *Methanosarcina mazei*: evidence for lateral gene transfer between bacteria and archaea. J Mol Microbiol Biotechnol **4:**453-61.

27. **Deppenmeier, U., T. Lienard, and G. Gottschalk.** 1999. Novel reactions involved in energy conservation by methanogenic archaea. FEBS Lett **457:**291-7.

28. **Deppenmeier, U., and V. Muller.** 2008. Life close to the thermodynamic limit: how methanogenic archaea conserve energy. Results Probl Cell Differ **45:**123-52.

29. **Deppenmeier, U., V. Muller, and G. Gottschalk.** 1996. Pathways of energy conservation in methanogenic archaea. Arch Microbiol **165:**149-163.

30. **Ferry, J. G.** 1993. Fermentation of acetate. Chapman & Hall, New York, London.

31. **Ferry, J. G., and D. J. Lessner.** 2008. Methanogenesis in marine sediments. Ann N Y Acad Sci **1125:**147-57.

32. **Fiebig, K., and B. Friedrich.** 1989. Purification of the F_{420}-reducing hydrogenase from *Methanosarcina barkeri* (strain Fusaro). Eur J Biochem **184:**79-88.

33. **Galagan, J. E., C. Nusbaum, A. Roy, M. G. Endrizzi, P. Macdonald, W. FitzHugh, S. Calvo, R. Engels, S. Smirnov, D. Atnoor, A. Brown, N. Allen, J. Naylor, N. Stange-Thomann, K. DeArellano, R. Johnson, L. Linton, P. McEwan, K. McKernan, J. Talamas, A. Tirrell, W. Ye, A. Zimmer, R. D. Barber, I. Cann, D. E. Graham, D. A. Grahame, A. M. Guss, R. Hedderich, C. Ingram-Smith, H. C. Kuettner, J. A. Krzycki, J. A. Leigh, W. Li, J. Liu, B. Mukhopadhyay, J. N. Reeve, K. Smith, T. A. Springer, L. A. Umayam, O. White, R. H. White, E. Conway de Macario, J. G. Ferry, K. F. Jarrell, H. Jing, A. J. Macario, I. Paulsen, M. Pritchett, K. R. Sowers, R. V. Swanson, S. H. Zinder, E. Lander, W. W. Metcalf, and B. Birren.** 2002. The genome of *M. acetivorans* reveals extensive metabolic and physiological diversity. Genome Res **12:**532-42.

34. **Gartner, P., D. S. Weiss, U. Harms, and R. K. Thauer.** 1994. N5-methyltetrahydromethanopterin:coenzyme M methyltransferase from *Methanobacterium thermoautotrophicum*. Catalytic mechanism and sodium ion dependence. Eur J Biochem **226:**465-72.

35. **Goldman, A. D., J. A. Leigh, and R. Samudrala.** 2009. Comprehensive computational analysis of Hmd enzymes and paralogs in methanogenic Archaea. BMC Evol Biol **9:**199.

36. **Gottschalk, G., and R. K. Thauer.** 2001. The Na(+)-translocating methyltransferase complex from methanogenic archaea. Biochim Biophys Acta **1505:**28-36.

37. **Graham, D. E., N. Kyrpides, I. J. Anderson, R. Overbeek, and W. B. Whitman.** 2001. Genome of *Methanocaldococcus* (*Methanococcus*) *jannaschii*. Methods Enzymol **330:**40-123.

38. **Guss, A. M., G. Kulkarni, and W. W. Metcalf.** 2009. Differences in hydrogenase gene expression between *Methanosarcina acetivorans* and *Methanosarcina barkeri*. J Bacteriol **191:**2826-33.

39. **Guss, A. M., B. Mukhopadhyay, J. K. Zhang, and W. W. Metcalf.** 2005. Genetic analysis of *mch* mutants in two *Methanosarcina* species demonstrates multiple roles for the methanopterin-dependent C-1 oxidation/reduction pathway and differences in H(2) metabolism between closely related species. Mol Microbiol **55:**1671-80.

40. **Halboth, S., and A. Klein.** 1992. *Methanococcus voltae* harbors four gene clusters potentially encoding two [NiFe] and two [NiFeSe] hydrogenases, each of the cofactor F_{420}-reducing or F_{420}-non-reducing types. Mol Gen Genet **233:**217-24.

41. **Harms, U., D. S. Weiss, P. Gartner, D. Linder, and R. K. Thauer.** 1995. The energy conserving N5-methyltetrahydromethanopterin:coenzyme M methyltransferase complex from *Methanobacterium thermoautotrophicum* is composed of eight different subunits. Eur J Biochem **228:**640-8.

42. **Hedderich, R., and L. Forzi.** 2005. Energy-converting [NiFe] hydrogenases: more than just H_2 activation. J Mol Microbiol Biotechnol **10:**92-104.

43. **Hedderich, R., N. Hamann, and M. Bennati.** 2005. Heterodisulfide reductase from methanogenic archaea: a new catalytic role for an iron-sulfur cluster. Biol Chem **386:**961-70.

44. **Heiden, S., R. Hedderich, E. Setzke, and R. K. Thauer.** 1994. Purification of a two-subunit cytochrome-b-containing heterodisulfide reductase from methanol-grown *Methanosarcina barkeri*. Eur J Biochem **221:**855-61.

45. **Hendrickson, E. L., R. Kaul, Y. Zhou, D. Bovee, P. Chapman, J. Chung, E. Conway de Macario, J. A. Dodsworth, W. Gillett, D. E. Graham, M. Hackett, A. K. Haydock, A. Kang, M. L. Land, R. Levy, T. J. Lie, T. A. Major, B. C. Moore, I. Porat, A. Palmeiri, G. Rouse, C. Saenphimmachak, D. Soll, S. Van Dien, T. Wang, W. B. Whitman, Q. Xia, Y. Zhang, F. W. Larimer, M. V. Olson, and J. A. Leigh.** 2004. Complete genome sequence of the genetically tractable hydrogenotrophic methanogen *Methanococcus maripaludis*. J Bacteriol **186:**6956-69.

46. **Hendrickson, E. L., and J. A. Leigh.** 2008. Roles of coenzyme F_{420}-reducing hydrogenases and hydrogen- and F_{420}-dependent methylenetetrahydromethanopterin dehydrogenases in reduction of F_{420} and production of hydrogen during methanogenesis. J Bacteriol **190:**4818-21.

47. **Horita, J., and M. E. Berndt.** 1999. Abiogenic methane formation and isotopic fractionation under hydrothermal conditions. Science **285:**1055-7.

48. **Hovey, R., S. Lentes, A. Ehrenreich, K. Salmon, K. Saba, G. Gottschalk, R. P. Gunsalus, and U. Deppenmeier.** 2005. DNA microarray analysis of *Methanosarcina mazei* Gö1 reveals adaptation to different methanogenic substrates. Mol Genet Genomics **273:**225-39.

49. **Ide, T., S. Baumer, and U. Deppenmeier.** 1999. Energy conservation by the H_2:heterodisulfide oxidoreductase from *Methanosarcina mazei* Gö1: identification of two proton-translocating segments. J Bacteriol **181:**4076-80.

50. **Jetten, M. S. M., A. J. M. Stams, and A. J. B. Zehnder.** 1992. Methanogenesis from acetate: a comparison of the acetate metabolism in *Methanothrix soehngenii* and *Methanosarcina* spp. FEMS Microbiology Reviews **88:**181-198.

51. **Kaesler, B., and P. Schonheit.** 1989. The role of sodium ions in methanogenesis. Formaldehyde oxidation to CO_2 and $2H_2$ in methanogenic bacteria is coupled with primary electrogenic Na^+ translocation at a stoichiometry of 2-3 Na^+/CO_2. Eur J Biochem **184:**223-32.

52. **Kaesler, B., and P. Schonheit.** 1989. The sodium cycle in methanogenesis. CO_2 reduction to the formaldehyde level in methanogenic bacteria is driven by a primary electrochemical potential of Na^+ generated by formaldehyde reduction to CH_4. Eur J Biochem **186:**309-16.

53. **Keltjens, J. T., and G. D. Vogels.** 1993. Conversion of methanol and methylamines to methane and carbon dioxide. Chapman & Hall, New York, London.

54. **Kemner, J. M., and J. G. Zeikus.** 1994. Purification and characterization of membrane-bound hydrogenase from *Methanosarcina barkeri* MS. Arch Microbiol **161:**47-54.

55. **Koga, Y., M. Nishihara, H. Morii, and M. Akagawa-Matsushita.** 1993. Ether polar lipids of methanogenic bacteria: structures, comparative aspects, and biosyntheses. Microbiol Rev **57:**164-82.

56. **Kulkarni, G., D. M. Kriedelbaugh, A. M. Guss, and W. W. Metcalf.** 2009. H_2 is a preferred intermediate in the energy conserving electron transport chain of *Methanosarcina barkeri*. Proc Natl Acad Sci U S A **106:**15915-20.

57. **Kunkel, A., M. Vaupel, S. Heim, R. K. Thauer, and R. Hedderich.** 1997. Heterodisulfide reductase from methanol-grown cells of *Methanosarcina barkeri* is not a flavoenzyme. Eur J Biochem **244:**226-34.

58. **Kunkel, A., J. A. Vorholt, R. K. Thauer, and R. Hedderich.** 1998. An *Escherichia coli* hydrogenase-3-type hydrogenase in methanogenic archaea. Eur J Biochem **252:**467-76.

59. **Kvenvolden, K. A.** 1999. Potential effects of gas hydrate on human welfare. Proc Natl Acad Sci U S A **96:**3420-6.

60. **Lessner, D. J., L. Li, Q. Li, T. Rejtar, V. P. Andreev, M. Reichlen, K. Hill, J. J. Moran, B. L. Karger, and J. G. Ferry.** 2006. An unconventional pathway for reduction of CO_2 to methane in CO-grown *Methanosarcina acetivorans* revealed by proteomics. Proc Natl Acad Sci U S A **103:**17921-6.

61. **Li, F., J. Hinderberger, H. Seedorf, J. Zhang, W. Buckel, and R. K. Thauer.** 2008. Coupled ferredoxin and crotonyl coenzyme A (CoA) reduction with NADH catalyzed by the butyryl-CoA dehydrogenase/Etf complex from *Clostridium kluyveri*. J Bacteriol **190:**843-50.

62. **Li, L., Q. Li, L. Rohlin, U. Kim, K. Salmon, T. Rejtar, R. P. Gunsalus, B. L. Karger, and J. G. Ferry.** 2007. Quantitative proteomic and microarray analysis of the archaeon *Methanosarcina acetivorans* grown with acetate versus methanol. J Proteome Res **6:**759-71.

63. **Li, Q., L. Li, T. Rejtar, D. J. Lessner, B. L. Karger, and J. G. Ferry.** 2006. Electron transport in the pathway of acetate conversion to methane in the marine archaeon *Methanosarcina acetivorans*. J Bacteriol **188:**702-10.

64. **Liu, Y., and W. B. Whitman.** 2008. Metabolic, phylogenetic, and ecological diversity of the methanogenic archaea. Ann N Y Acad Sci **1125:**171-89.

65. **Lomans, B. P., A. Smolders, L. M. Intven, A. Pol, D. Op, and C. Van Der Drift.** 1997. Formation of Dimethyl Sulfide and Methanethiol in Anoxic Freshwater Sediments. Appl Environ Microbiol **63:**4741-4747.

66. **Lundie, Jr., L. L., and J. G. Ferry.** 1989. Activation of acetate by *Methanosarcina thermophila*. Purification and characterization of phosphotransacetylase. J Biol Chem **264:**18392-6.

67. **Lupa, B., E. L. Hendrickson, J. A. Leigh, and W. B. Whitman.** 2008. Formate-dependent H_2 production by the mesophilic methanogen *Methanococcus maripaludis*. Appl Environ Microbiol **74:**6584-90.

68. **Lyimo, T. J., A. Pol, H. J. Op den Camp, H. R. Harhangi, and G. D. Vogels.** 2000. *Methanosarcina semesiae* sp. nov., a dimethylsulfide-utilizing methanogen from mangrove sediment. Int J Syst Evol Microbiol **50 Pt 1:**171-8.

69. **Maeder, D. L., I. Anderson, T. S. Brettin, D. C. Bruce, P. Gilna, C. S. Han, A. Lapidus, W. W. Metcalf, E. Saunders, R. Tapia, and K. R. Sowers.** 2006. The *Methanosarcina barkeri* genome: comparative analysis with *Methanosarcina acetivorans* and *Methanosarcina mazei* reveals extensive rearrangement within methanosarcinal genomes. J Bacteriol **188:**7922-31.

70. **Magalon, A., and A. Bock.** 2000. Analysis of the HypC-hycE complex, a key intermediate in the assembly of the metal center of the *Escherichia coli* hydrogenase 3. J Biol Chem **275:**21114-20.

71. **Mathrani, I. M., D. R. Boone, R. A. Mah, G. E. Fox, and P. P. Lau.** 1988. *Methanohalophilus zhilinae* sp. nov., an alkaliphilic, halophilic, methylotrophic methanogen. Int J Syst Bacteriol **38:**139-42.

72. **Meuer, J., S. Bartoschek, J. Koch, A. Kunkel, and R. Hedderich.** 1999. Purification and catalytic properties of Ech hydrogenase from *Methanosarcina barkeri*. Eur J Biochem **265:**325-35.

73. **Meuer, J., H. C. Kuettner, J. K. Zhang, R. Hedderich, and W. W. Metcalf.** 2002. Genetic analysis of the archaeon *Methanosarcina barkeri* Fusaro reveals a central role for Ech hydrogenase and ferredoxin in methanogenesis and carbon fixation. Proc Natl Acad Sci U S A **99:**5632-7.

74. **Michel, R., C. Massanz, S. Kostka, M. Richter, and K. Fiebig.** 1995. Biochemical characterization of the 8-hydroxy-5-deazaflavin-reactive hydrogenase from *Methanosarcina barkeri* Fusaro. Eur J Biochem **233:**727-35.

75. **Mikesell, M. D., and S. A. Boyd.** 1990. Dechlorination of Chloroform by *Methanosarcina* Strains. Appl Environ Microbiol **56:**1198-1201.

76. **Miller, T. L., and M. J. Wolin.** 1985. *Methanosphaera stadtmaniae* gen. nov., sp. nov.: a species that forms methane by reducing methanol with hydrogen. Arch Microbiol **141:**116-22.

77. **Moran, J. J., C. H. House, J. M. Vrentas, and K. H. Freeman.** 2008. Methyl sulfide production by a novel carbon monoxide metabolism in *Methanosarcina acetivorans*. Appl Environ Microbiol **74:**540-2.

78. **Muller, V.** 2004. An exceptional variability in the motor of archael A1A0 ATPases: from multimeric to monomeric rotors comprising 6-13 ion binding sites. J Bioenerg Biomembr **36:**115-25.

79. **Muller, V., M. Blaut, and G. Gottschalk.** 1987. Generation of a transmembrane gradient of Na^+ in *Methanosarcina barkeri*. Eur J Biochem **162:**461-6.

80. **Muller, V., T. Lemker, A. Lingl, C. Weidner, U. Coskun, and G. Gruber.** 2005. Bioenergetics of archaea: ATP synthesis under harsh environmental conditions. J Mol Microbiol Biotechnol **10:**167-80.

81. **Ni, S., C. R. Woese, H. C. Aldrich, and D. R. Boone.** 1994. Transfer of *Methanolobus siciliae* to the genus *Methanosarcina*, naming it *Methanosarcina siciliae*, and emendation of the genus *Methanosarcina*. Int J Syst Bacteriol **44:**357-9.

82. **Noguera, D. R., G. A. Brusseau, B. E. Rittmann, and D. A. Stahl.** 1998. A unified model describing the role of hydrogen in the growth of *Desulfovibrio vulgaris* under different environmental conditions. Biotechnol Bioeng **59:**732-46.

83. **Odom, J. M., and H. D. Peck, Jr.** 1981. Hydrogen cycling as a general mechanism for energy coupling in the sulfate-reducing bacteria, *Desulfovibrio* sp. FEMS Microbiology Letters **12:**47-50.

84. **Odom, J. M., and H. D. Peck, Jr.** 1984. Hydrogenase, electron-transfer proteins, and energy coupling in the sulfate-reducing bacteria *Desulfovibrio*. Annu Rev Microbiol **38:**551-92.

85. **Padan, E., and S. Schuldiner.** 1994. Molecular physiology of Na^+/H^+ antiporters, key transporters in circulation of Na^+ and H^+ in cells. Biochim Biophys Acta **1185:**129-51.

86. **Patel, G. B., D. Sprott, and I. Ekiel.** 1993. Production of Specifically Labeled Compounds by *Methanobacterium espanolae* Grown on H(2)-CO(2) plus [C]Acetate. Appl Environ Microbiol **59:**1099-1103.

87. **Pisa, K. Y., C. Weidner, H. Maischak, H. Kavermann, and V. Muller.** 2007. The coupling ion in the methanoarchaeal ATP synthases: H(+) vs. Na(+) in the A(1)A(o) ATP synthase from the archaeon *Methanosarcina mazei* Gö1. FEMS Microbiol Lett **277:**56-63.

88. **Porat, I., W. Kim, E. L. Hendrickson, Q. Xia, Y. Zhang, T. Wang, F. Taub, B. C. Moore, I. J. Anderson, M. Hackett, J. A. Leigh, and W. B. Whitman.** 2006. Disruption of the operon encoding Ehb hydrogenase limits anabolic CO_2 assimilation in the archaeon *Methanococcus maripaludis*. J Bacteriol **188:**1373-80.

89. **Raybuck, S. A., S. E. Ramer, D. R. Abbanat, J. W. Peters, W. H. Orme-Johnson, J. G. Ferry, and C. T. Walsh.** 1991. Demonstration of carbon-carbon bond cleavage of acetyl coenzyme A by using isotopic exchange catalyzed by the CO dehydrogenase complex from acetate-grown *Methanosarcina thermophila*. J Bacteriol **173:**929-32.

90. **Rother, M., and W. W. Metcalf.** 2005. Genetic technologies for Archaea. Curr Opin Microbiol **8:**745-51.

91. **Saunders, N. F., T. Thomas, P. M. Curmi, J. S. Mattick, E. Kuczek, R. Slade, J. Davis, P. D. Franzmann, D. Boone, K. Rusterholtz, R. Feldman, C. Gates, S. Bench, K. Sowers, K. Kadner, A. Aerts, P. Dehal, C. Detter, T. Glavina, S. Lucas, P. Richardson, F. Larimer, L. Hauser, M. Land, and R. Cavicchioli.** 2003. Mechanisms of thermal adaptation revealed from the genomes of the Antarctic Archaea *Methanogenium frigidum* and *Methanococcoides burtonii*. Genome Res **13:**1580-8.

92. **Savant, D. V., Y. S. Shouche, S. Prakash, and D. R. Ranade.** 2002. *Methanobrevibacter acididurans* sp. nov., a novel methanogen from a sour anaerobic digester. Int J Syst Evol Microbiol **52:**1081-7.

93. **Schoell, M.** 1988. Multiple origins of methane in the earth. Chemical Biology **71:**1-10.

94. **Schwarzenback, N., E. Bomball, and W. Pfeiffer.** 2008. Can a wastewater treatment plant be a powerplant? A case study. water science & technology **57:**1555-1561.

95. **Setzke, E., R. Hedderich, S. Heiden, and R. K. Thauer.** 1994. H_2: heterodisulfide oxidoreductase complex from *Methanobacterium thermoautotrophicum*. Composition and properties. Eur J Biochem **220:**139-48.

96. **Shima, S., and R. K. Thauer.** 2007. A third type of hydrogenase catalyzing H_2 activation. Chem Rec **7:**37-46.

97. **Simankova, M. V., S. N. Parshina, T. P. Tourova, T. V. Kolganova, A. J. Zehnder, and A. N. Nozhevnikova.** 2001. *Methanosarcina lacustris* sp. nov., a new psychrotolerant methanogenic archaeon from anoxic lake sediments. Syst Appl Microbiol **24:**362-7.

98. **Siragusa, R. J., J. J. Cerda, M. M. Baig, C. W. Burgin, and F. L. Robbins.** 1988. Methanol production from the degradation of pectin by human colonic bacteria. Am J Clin Nutr **47:**848-51.

99. **Slesarev, A. I., K. V. Mezhevaya, K. S. Makarova, N. N. Polushin, O. V. Shcherbinina, V. V. Shakhova, G. I. Belova, L. Aravind, D. A. Natale, I. B. Rogozin, R. L. Tatusov, Y. I. Wolf, K. O. Stetter, A. G. Malykh, E. V. Koonin, and S. A. Kozyavkin.** 2002. The complete genome of hyperthermophile *Methanopyrus kandleri* AV19 and monophyly of archaeal methanogens. Proc Natl Acad Sci U S A **99:**4644-9.

100. **Sorgenfrei, O., S. Muller, M. Pfeiffer, I. Sniezko, and A. Klein.** 1997. The [NiFe] hydrogenases of *Methanococcus voltae*: genes, enzymes and regulation. Arch Microbiol **167:**189-95.

101. **Stojanowic, A., G. J. Mander, E. C. Duin, and R. Hedderich.** 2003. Physiological role of the F_{420}-non-reducing hydrogenase (Mvh) from *Methanothermobacter marburgensis*. Arch Microbiol **180:**194-203.

102. **Taglicht, D., E. Padan, and S. Schuldiner.** 1993. Proton-sodium stoichiometry of NhaA, an electrogenic antiporter from *Escherichia coli*. J Biol Chem **268:**5382-7.

103. **Tersteegen, A., and R. Hedderich.** 1999. *Methanobacterium thermoautotrophicum* encodes two multisubunit membrane-bound [NiFe] hydrogenases. Transcription of the operons and sequence analysis of the deduced proteins. Eur J Biochem **264:**930-43.

104. **Thauer, R. K., R. Hedderich, and R. Fischer.** 1993. Reactions and Enzymes involved in methanogenesis from CO_2 and H_2. Chapman & Hall, New York, London.

105. **Thauer, R. K., K. Jungermann, and K. Decker.** 1977. Energy conservation in chemotrophic anaerobic bacteria. Bacteriol Rev **41:**100-80.

106. **Thauer, R. K., A. K. Kaster, H. Seedorf, W. Buckel, and R. Hedderich.** 2008. Methanogenic archaea: ecologically relevant differences in energy conservation. Nat Rev Microbiol **6:**579-91.

107. **Theodoratou, E., R. Huber, and A. Bock.** 2005. [NiFe]-Hydrogenase maturation endopeptidase: structure and function. Biochem Soc Trans **33:**108-11.

108. **Tietze, M., A. Beuchle, I. Lamla, N. Orth, M. Dehler, G. Greiner, and U. Beifuss.** 2003. Redox potentials of methanophenazine and CoB-S-S-CoM, factors involved in electron transport in Methanogenic archaea. Chembiochem **4:**333-5.

109. **Valentine, D. L., A. Chidthaisong, A. Rice, W. S. Reeburgh, and S. C. Tyler.** 2004. Carbon and hydrogen isotope fractionation by moderately thermophilic methanogens. Geochimica et Cosmochimica Acta **68:**1571-1590.

110. **Vaupel, M., and R. K. Thauer.** 1998. Two F_{420}-reducing hydrogenases in *Methanosarcina barkeri*. Arch Microbiol **169:**201-5.

111. **Vinothkumar, K. R., S. H. Smits, and W. Kuhlbrandt.** 2005. pH-induced structural change in a sodium/proton antiporter from *Methanococcus jannaschii*. Embo J **24:**2720-9.

112. **von Klein, D., H. Arab, H. Volker, and M. Thomm.** 2002. *Methanosarcina baltica*, sp. nov., a novel methanogen isolated from the Gotland Deep of the Baltic Sea. Extremophiles **6:**103-10.

113. **White, D.** 2000. The Physiology and Biochemistry of Prokaryotes., Second ed. Oxford University Press, Oxford, New York.

114. **Wolfe, R. S.** 2006. The Archaea: A personal overview of the formative years. Prokaryotes **3:**3-9.

115. **Zhilina, T. N., and G. A. Zavarzin.** 1987. *Methanosarcina vacuolata* sp. nov., a vacuolated *Methanosarcina*. International Journal of Systematic Bacteriology **37:**281-283.

116. **Zinder, S. H.** 1993. Physiological Ecology of Methanogens Chapman & Hall, New York, London.

CHAPTER 2

HYDROGEN IS A PREFERRED INTERMEDIATE IN THE ENERGY CONSERVING ELECTRON TRANSPORT CHAIN OF *METHANOSARCINA BARKERI*

2.1 ABSTRACT

Methanogens utilize an unusual energy-conserving electron transport chain that involves reduction of a limited number of electron acceptors to methane (CH_4) gas. Previous biochemical studies suggested that the proton pumping $F_{420}H_2$ dehydrogenase (Fpo) plays a crucial role in this process during growth on methanol. However, *Methanosarcina barkeri* Δ*fpo* mutants investigated in this study display no measurable phenotype on this substrate, indicating that Fpo plays a minor role, if any. In contrast, Δ*frh* mutants lacking the cytoplasmic F_{420}-reducing hydrogenase (Frh) are severely affected in their ability to grow and make methane from methanol, while double Δ*fpo* Δ*frh* mutants are completely unable to utilize this substrate. These data suggest that the preferred electron transport chain involves production of H_2 in the cytoplasm, which then diffuses out of the cell where it is reoxidized with transfer of electrons into the energy conserving electron transport chain. This "hydrogen cycling" metabolism leads directly to production of a proton motive force that can be used by the cell for ATP synthesis. Nevertheless, *M. barkeri* does have the flexibility to utilize the Fpo-dependent electron transport chain when needed, as shown by the poor growth of the Δ*frh* mutant. Our data support a model in which the rapid enzymatic turnover of hydrogenases may allow a competitive advantage via faster growth rates in this freshwater organism. The mutant analysis also confirms the

proposed role of Frh in growth on hydrogen (H_2)/carbon dioxide (CO_2) and suggests that either Frh or Fpo is needed for aceticlastic growth of *M. barkeri*.

2.2 INTRODUCTION

Methanogenesis is the terminal step in biomass degradation in many anaerobic environments and plays a central role in the global carbon cycle. Although most of the CH_4 produced is oxidized to CO_2 by methane consuming organisms, substantial quantities (*ca*. 10^{14} g/year) escape into the atmosphere where it acts as a potent greenhouse gas (49). Most methanogens produce CH_4 by reducing CO_2 with H_2 (11). However, some *Methanosarcina* species like *M. barkeri* and *M. mazei* are also capable of utilizing a variety of other substrates, including acetate, which accounts for *ca*. two-thirds of global CH_4 production (16), and C-1 compounds like methanol, methylsulfides and methylamines (10). Four distinct, but overlapping, methanogenic pathways are involved in the use of these diverse substrates (Figure 2.1).

Methanogenic organisms produce CH_4 as a byproduct of anaerobic respiration involving a unique energy-conserving electron transport chain found only in Archaea. At least two distinct types of methanogenic respiration exist: one found in methanogens, including *Methanosarcina* species, that synthesize cytochromes and the other in those that lack cytochromes (49). The penultimate step of both respiratory pathways involves the reduction of methyl-Coenzyme M (CoM-SH, mercaptoethanesulfonic acid) to CH_4 using coenzyme B (CoB-SH, *N*-7-mercaptoheptanoyl-*O*-phospho-L-threonine) as the electron donor. The other

product of this reaction is the heterodisulfide of CoM-SH and CoB-SH (CoM-S-S-CoB), which serves as the terminal electron acceptor in the energy-conserving

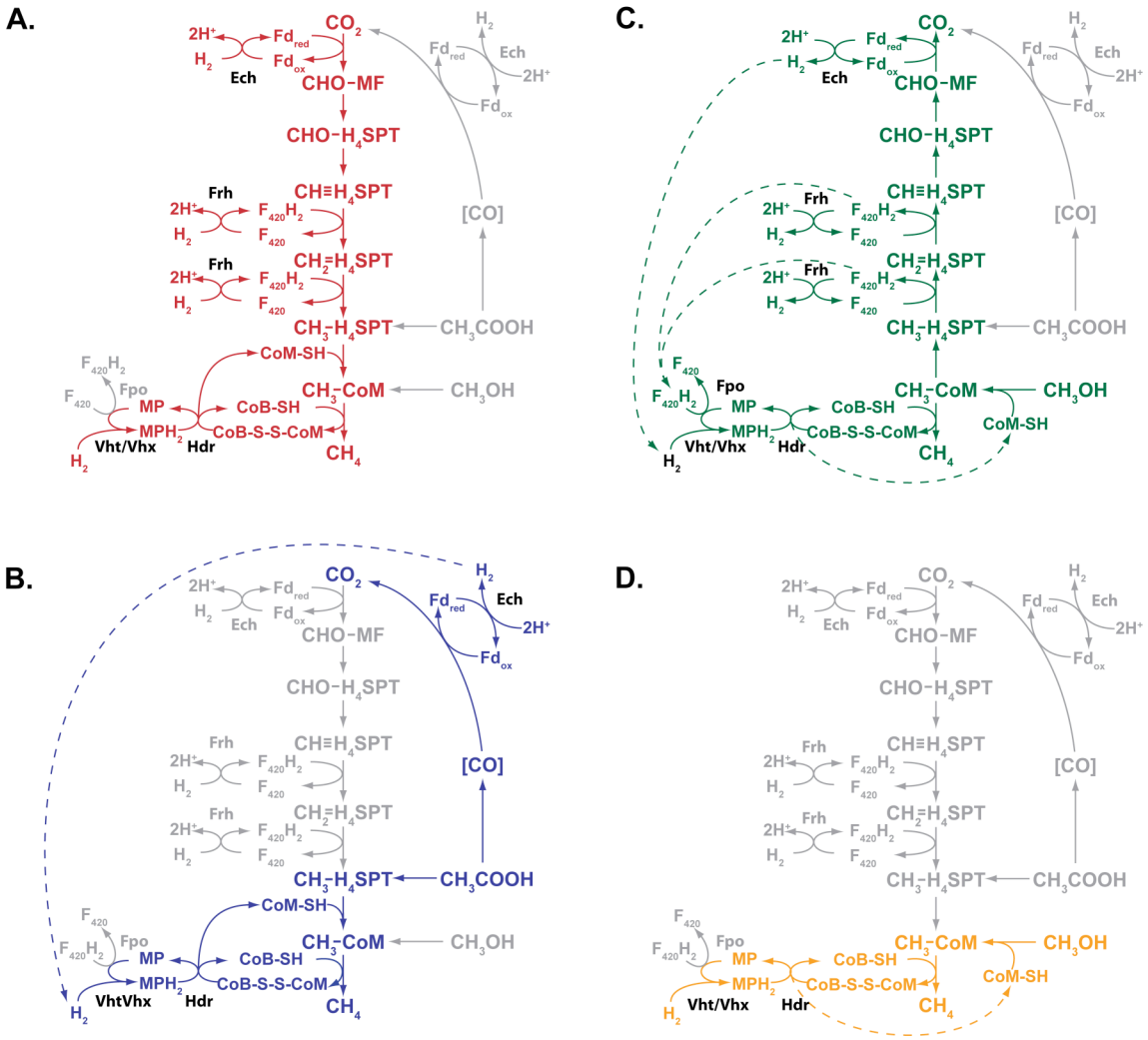

Figure 2.1 Four overlapping methanogenic pathways found in *Methanosarcina barkeri* (adapted from (19)). Each pathway shares a common step in the reduction of methyl-CoM to methane; however, they differ in the route used to form methyl-CoM and in the source of electrons used for its reduction to methane. Many methanogens reduce CO_2 to methane using electrons derived from the oxidation of H_2 (hydrogenotrophic pathway, A) Alternatively, acetate can be split into a methyl group and an enzyme-bound carbonyl moiety. The latter is oxidized to CO_2 to provide electrons required for reduction of methyl group to methane (aceticlastic pathway, B) C-1 compounds like methanol or methylamines can be disproportionated to CO_2 and methane via the methylotrophic pathway, C) In this pathway, one molecule of the C-1 compound is oxidized to provide electrons for reduction of three additional molecules to methane. Finally, C-1 compounds can also be reduced using electrons derived from H_2 oxidation (methyl respiration

Figure 2.1 (cont.)

pathway, D) Steps not required by each pathway are shown in gray. The steps catalyzed by Fpo, Frh, Vht/Vhx, Ech and Hdr proteins are indicated: note that Fpo is predicted to be required in the methylotrophic pathway and Frh in the hydrogenotrophic pathway. Abbreviations; Ech, Fd_{ox}-dependent hydrogenase; Frh, F_{420}-reducing hydrogenase; Fpo, $F_{420}H_2$:phenazine oxidoreductase; Vht/Vhx, methanophenazine-dependent hydrogenase; Hdr, heterodisulfide reductase; CoM-SH, coenzyme M; CoB-SH, coenzyme B; CoM-S-S-CoB, mixed disulfide of CoM-SH and CoB-SH; MP/MPH_2, oxidized and reduced methanophenazine; $F_{420}/F_{420}H_2$, oxidized and reduced Factor 420; Fd_{ox}/Fd_{red}, oxidized and reduced ferredoxin; CHO-MF, formyl-methanofuran; CHO-H_4SPT, formyl-tetrahydrosarcinapterin; CH≡H_4SPT, methenyl-tetrahydrosarcinapterin; CH=H_4SPT, methylene-tetrahydrosarcinapterin; CH_3- H_4SPT, methyl-tetrahydrosarcinapterin; CH_3-CoM, methyl-coenzyme M.

electron transport chain. In methanogenic archaea that lack cytochromes, the means by which energy is conserved is poorly understood, but probably involves a cytoplasmic electron bifurcation pathway similar to one recently characterized in *Clostridium* (25, 49). In contrast, the energy-conserving electron transport chain of cytochrome-containing methanogens, exemplified by *Methanosarcina* species, has been studied in detail, including the reconstitution of two distinct proton-translocating electron transport systems *in vitro* (4, 5, 12, 22).

In *Methanosarcina* species, a membrane-bound electron transport chain that terminates with the reduction of the CoM-S-S-CoB heterodisulfide generates ion-motive force that can be used by ATP synthase to form ATP (Figure 2.2). Either H_2 or reduced coenzyme F_{420} ($F_{420}H_2$) can donate electrons for reduction of CoM-S-S-CoB (10, 11). In the H_2:heterodisulfide oxidoreductase system, a methanophenazine-dependent hydrogenase (Vht or Vhx (18)) oxidizes H_2 in the periplasm with transfer of two electrons to the membrane soluble electron carrier methanophenazine (MP). The reduced MP (MPH_2) is subsequently oxidized by the enzyme heterodisulfide reductase (Hdr) with concomitant reduction of CoM-S-S-CoB. In the $F_{420}H_2$:heterodisulfide oxidoreductase system, the $F_{420}H_2$

dehydrogenase (Fpo) catalyzes electron transfer from $F_{420}H_2$ to MP, concomitantly pumping two protons out of the cell. As in the H_2:heterodisulfide

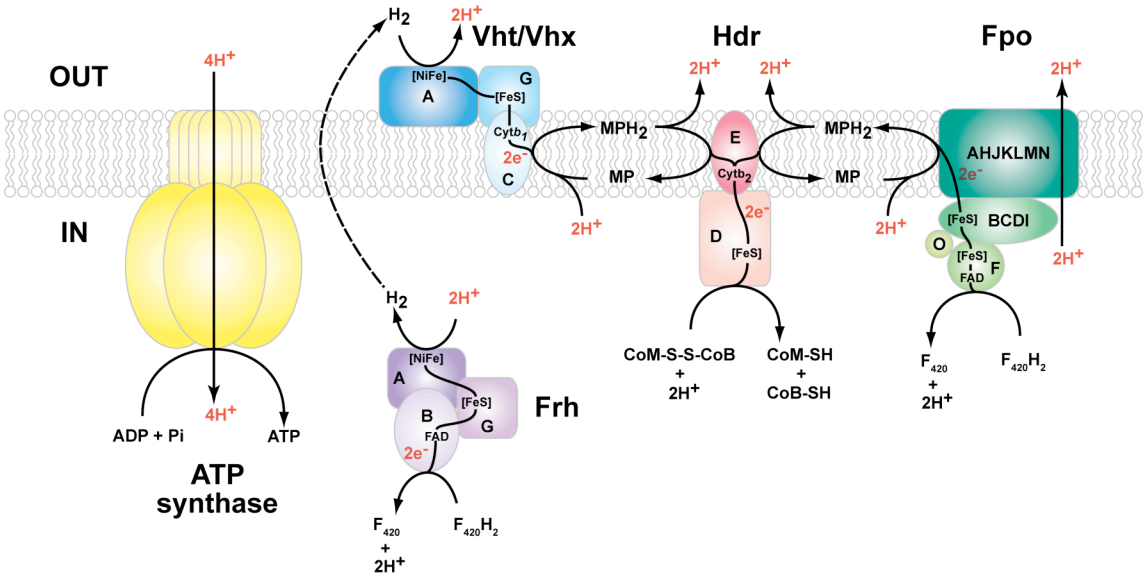

Figure 2.2 The electron transport chain of *M. barkeri* has been proposed to comprise two energy-conserving systems, the $F_{420}H_2$:heterodisulfide oxidoreductase and the H_2:heterodisulfide oxidoreductase. In the former, $F_{420}H_2$ is oxidized by FpoF releasing two electrons that are transferred through FpoBCDI and then FpoAHJKLMN to membrane-soluble MP. This reaction is coupled to pumping of two protons outside the cell. Reduction of MP consumes two protons from the cytoplasm, which are subsequently released outside the cell upon oxidation of MPH_2. The electrons are then transferred through HdrED to reduce CoM-S-S-CoB with two protons from the cytoplasm. Alternatively, in the H_2:heterodisulfide oxidoreductase, H_2 is oxidized by Vht/Vhx to produce two protons outside the cell and two electrons that are transferred to MPH_2, which is then used to reduce CoM-S-S-CoB. The dashed arrow represents a third possible energy-conserving mechanism that is proposed in this study. In this pathway, $F_{420}H_2$ is oxidized by the cytoplasmic hydrogenase Frh to generate H_2. The H_2 then diffuses outside the cell to the active site of membrane-bound hydrogenase Vht/Vhx, where it is oxidized, resulting in the translocation of two protons via a "H_2-cycling" mechanism. The electrons are passed through MP to CoM-S-S-CoB as in the other two systems. In all three systems, the entire electron transport process leads to the net translocation of four protons (highlighted in red) outside the cell per two electrons transferred from $F_{420}H_2$ or H_2 to the CoM-S-S-CoB. The electrochemical gradient generated is coupled to ATP synthesis via an A-type ATPase. Abbreviations are same as in Figure 1; FAD, flavin adenine dinucleotide; [FeS], iron-sulfur cluster; [NiFe], bimetallic catalytic center; Cytb_2, cytochrome b_2.

oxidoreductase system, MPH_2 passes electrons to CoM-S-S-CoB, leading to translocation of two additional protons. *In vitro* measurements suggest that the

magnitude of proton motive force generated is the same for both oxidoreductase systems, probably $4H^+/2\ e^-$ (3, 22).

The $F_{420}H_2$:heterodisulfide oxidoreductase system shares features with the aerobic electron transport chain found in many bacteria. Fpo was purified from *M. mazei* Gö1 as a five subunit complex (FpoBCDIF) capable of oxidizing $F_{420}H_2$ with a variety of artificial electron acceptors (1). Most of these proteins were later shown to be encoded by a 13-gene operon, *fpoABCDHIJJKLMNO* (*fpo*), with *fpoF* being located elsewhere on the genome (Figure 2.3) (3). Fpo

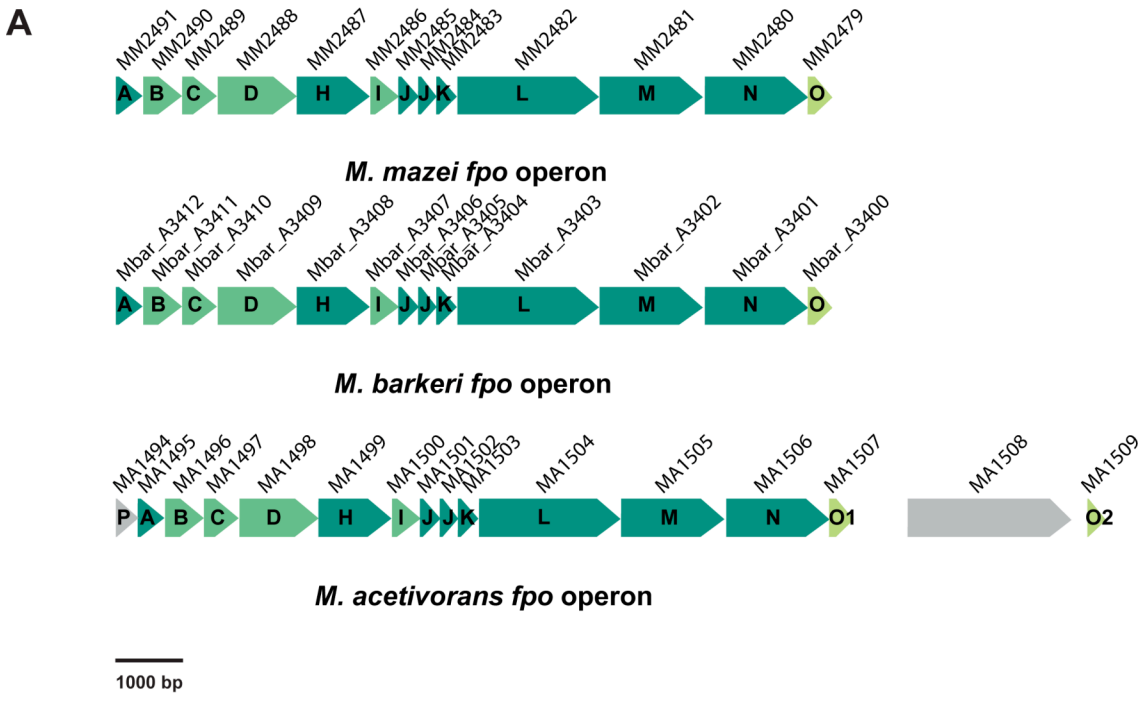

Figure 2.3 (cont.)

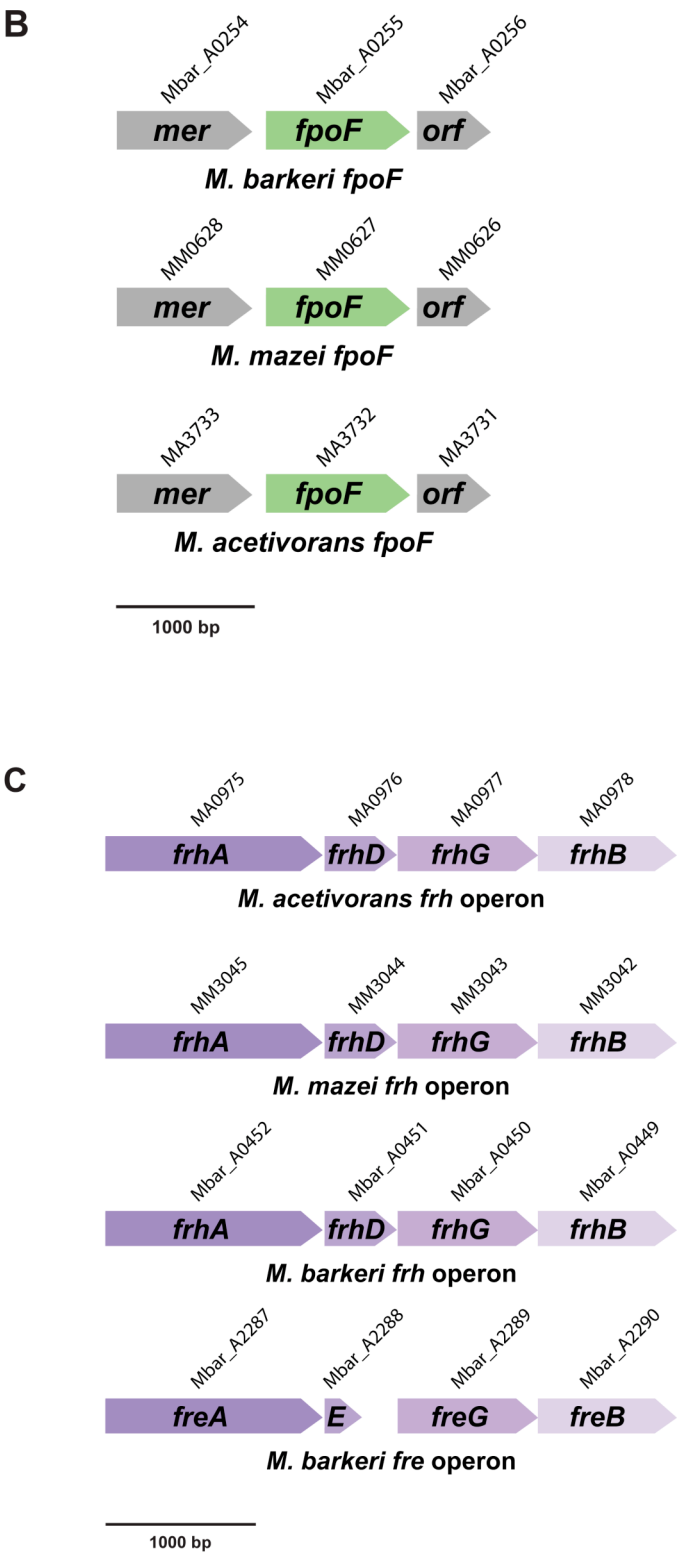

Figure 2.3 (cont.)

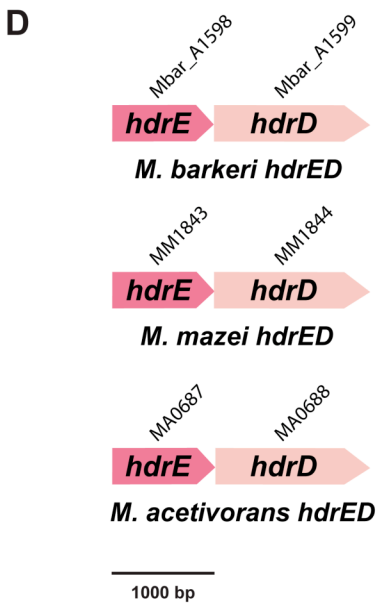

Figure 2.3 Genomic organization of operons encoding F_{420}-phenazine oxidoreductase (Fpo), F_{420}-reducing hydrogenase (Frh) and heterodisulfide reductase (Hdr) in *Methanosarcina* species. Panel A depicts the 13-gene operon (*fpoABCDHIJJKLMNO*) that encodes the hydrophilic (FpoO), membrane-associated (FpoBCDI) and membrane-integral modules (FpoAHIJKLMN) of Fpo in the three species. As is evident, *M. acetivorans* harbors two copies of *fpoO*, *fpoO1* and *fpoO2*, and *fpoP* that is not present in the other two *Methanosarcina* species. Panel B depicts the gene (*fpoF*) that encodes the input module of Fpo (FpoF). In all three species, *fpoF* is located between genes encoding methylene-tertrahydrosarcinapterin reductase (*mer*) and a putative cytidylyltransferase (28). These genes may constitute an operon. Panel C depicts the F_{420}-reducing hydrogenase operons (*frhADGB*) in the three species. *M. barkeri* has two of these operons, *frhADGB* and *freAEGB*. The *freAEGB* operon lacks gene D that encodes a putative hydrogenase maturation protein presumed to be essential for post-translational modification of the *cis*-encoded hydrogenase. Panel D depicts the operons encoding heterodisulfide reductase (HdrED) in the three species. Other open reading frames (ORFs) are shown as gray arrows.

shares significant homology with NADH dehydrogenase I (Nuo) of *Escherichia coli* and the nomenclature reflects that similarity. Accordingly, both Fpo and Nuo are composed of similar membrane-integral (the A, H, J, K, L, M and N subunits) and membrane-associated (the B, C, D and I subunits) modules. However, the enzymes differ in their substrates and hence in their input modules, such that

NuoEFG oxidizes NADH, whereas FpoF oxidizes $F_{420}H_2$, which is a hydride carrier analogous to NADH (11).

The source of electrons for the two disparate *Methanosarcina* electron transport chains varies with the growth substrate (Figure 2.1). During growth on H_2/CO_2 (the hydrogenotrophic pathway), or on H_2 in combination with a C-1 electron acceptor (the methyl-espiration pathway), electrons are derived from H_2 oxidation and are utilized via the H_2:heterodisulfide oxidoreductase system (11). Genetic and biochemical experiments in *M. barkeri* suggest that use of acetate (the aceticlastic pathway) also involves the obligate intermediacy of H_2 and the H_2:heterodisulfide oxidoreductase system (31, 32). In contrast, metabolism of compounds such as methanol or methylamines (the methylotrophic pathway) produces two equivalents of $F_{420}H_2$ per C-1 molecule oxidized. Thus, it has been suggested that $F_{420}H_2$:heterodisulfide oxidoreductase system plays a central, perhaps essential, role in the energy-conserving electron transport chain of the methylotrophic pathway in all *Methanosarcina* species (reviewed in (10, 11, 14, 15, 22)).

Surprisingly, the *in vivo* genetic data presented here tell a different story. Contrary to expectations, Fpo is not required for growth under any condition tested, including during growth on methanol. Instead, reducing equivalents from methanol oxidation appear to be preferentially passed to molecular H_2 by the cytoplasmic F_{420}-reducing hydrogenase (Frh). Subsequently, H_2 may enter into the electron transport chain via the H_2:heterodisulfide oxidoreductase system (Figure 2.2). These data are reminiscent of the “hydrogen-cycling” model for

electron transport first proposed by Odom and Peck for sulfate-reducing bacteria (37) and suggest that a reanalysis of energy conservation mechanisms in freshwater *Methanosarcina* species is warranted.

2.3 MATERIALS AND METHODS

2.3.1 Sequence analysis

All sequence data are from publicly available genomes (3, 11, 17, 27). The Integrated Microbial Genome (IMG) system was used to identify orthologs and assess the genomic context of genes (28). Protein sequences were aligned using ClustalW (http://www.ebi.ac.uk/Tools/clustalw2).

2.3.2 Media and growth conditions

Methanosarcina strains were grown as single cells (47) at 37^{o}C in high salt (HS) broth medium (30) or on agar-solidified medium as described (6). Growth substrates provided were methanol (125 mM) or sodium acetate (120 mM) under a headspace of either N_2/CO_2 (80/20%) mix at 50 kPa over ambient pressure or H_2/CO_2 (80/20%) mix at 300 kPa over ambient pressure. Puromycin (CalBioChem, San Diego, CA) was added at 2 μg/ml for selection of the puromycin transacetylase (*pac*) gene (42, 43). 8-Aza-2,6-diaminopurine (8-ADP) (Sigma, St Louis, MO) was added at 20 μg/ml for selection against the presence of *hpt* (43). Standard conditions were used for growth of *E. coli* strains (53) DH5α/λ-*pir* (34) and DH10B (Stratagene, La Jolla, CA), which were used as hosts for plasmid constructions.

2.3.3 DNA methods and plasmid constructions

Standard methods were used for plasmid DNA isolation and manipulation in *E. coli* (2). Liposome mediated transformation was used for *Methanosarcina* as described (29). Genomic DNA isolation and DNA hybridization were as described (6, 30, 56). DNA sequences were determined from double-stranded templates by the W.M. Keck Center for Comparative and Functional Genomics, University of Illinois. Plasmid constructions are described in Tables 2.1 and 2.2.

2.3.4 Construction of *M. barkeri* Fusaro deletion mutants

The construction and genotype of all *Methanosarcina* strains is presented in Table 2.3. The markerless genetic exchange method (43) was employed to delete *fpoA-O* operon (*fpo*), *fpoF* and *freAEGB* operon (*fre*) in the Δ*hpt* (WWM85 or WWM86) (20) background of *M. barkeri* Fusaro. DNA sequences immediately flanking the deleted genes were left intact to exclude loss of regulatory elements needed for expression of adjacent genes. The plasmids, pDK4, pDK13 and pGK6 were used to delete *fpoA-O* in WWM86, *fpoF* in WWM85 and *fre* in WWM85, respectively on methanol plus H_2/CO_2 as the growth substrate. The *frhADGB* operon (*frh*) was deleted in the Δ*hpt* (WWM86), Δ*fpo* (WWM71) and Δ*fpoF* (WWM123) backgrounds of *M. barkeri* Fusaro by the homologous recombination-mediated gene replacement method (56). In this method, ApaI/NotI-cut 5.5 kb region of pAMG81 was transformed into Δ*hpt*, Δ*fpo* and Δ*fpoF* mutants and the transformants were selected on methanol plus H_2/CO_2 and puromycin to obtain Δ*frh* (WWM122), Δ*fpo* Δ*frh* (WWM108), Δ*fpoF* Δ*frh*

Table 2.1 Plasmids used in this study

Plasmid	Description and/or construction	Reference
pMP44	Vector, containing a *pac-hpt* cassette, used to delete genes from *M. barkeri Fusaro* chromosome using the markerless exchange method	(43)
pDK4	SpeI/XmaI-digested *fpo* upstream PCR product amplified using primers LfpoA and RfpoA1 and NotI/XmaI-digested *fpo* downstream PCR product amplified using primers LfpoO and RfpoO were ligated to SpeI/NotI-digested pMP44	(23)
pDK13	SpeI/XmaI-digested *fpoF* upstream PCR product amplified using primers FusfpoF(us)for and FusfpoF(us)rev and NotI/XmaI-digested *fpoF* downstream PCR product amplified using primers FusfpoF(ds)for and FusfpoF(ds)rev were ligated to SpeI/NotI-digested pMP44	(23)
pGK6	AscI/PstI-digested *fre* upstream and downstream fusion PCR product amplified using primers freupfor, freuprev, frednfor and frednrev and ligated to MluI/NsiI-digested pMP44	This study
pJK301	Vector, containing a *pac-hpt* cassette, used to delete genes from *M. barkeri Fusaro* chromosome using double homologous recombination-mediated gene replacement method	(55)

Table 2.1 (cont.)

Plasmid	Description and/or construction	Reference
pAMG78	ApaI/XhoI-digested *frh* upstream PCR product amplified using primers Fusfrhupfor and Fusfrhuprev and ligated to ApaI/XhoI-digested pJK301	(23)
pAMG81	SpeI/NotI-digested *frh* downstream PCR product amplified using primers Fusfrhdnfor and Fusfrhdnrev and ligated to Spe/NotI-digested pAMG78	(23)

Table 2.2 Primers used in this study

Primer	Sequence[a]	Added sites
LfpoA	ACTAGTGAAGTGAACCCTCGCCTCTT	SpeI
RfpoA1	GGATCCCCCGGGCATATGTATCACCTATTAAAGTGCAGC	BamHI/XmaI/NdeI
LfpoO	AAGCTTCCCGGGTGAATTTGAGTAAAGCTGCATTTTG	HindIII/XmaI
RfpoO	CTCGAGGCGGCCGCCCTACTAATGTTGGCATTGACG	XhoI/NotI
FusfpoF(us)for	GGCGCGCCACTAGTGAATCGAATTTGTGCCGAGCGA	AscI/SpeI
FusfpoF(us)rev	GGCGCGCCCCCGGGTTAGTTACCTCCAACACCTT	AscI/XmaI
FusfpoF(ds)for	GGCGCGCCCCCGGGAATCAGAATATATCGAGAATAA	AscI/XmaI
FusfpoF(ds)rev	GGCGCGCCGCGGCCGCTTTTTAAATCCGATTTTCAC	AscI/NotI
freupfor	GGCGCGCCAAATCCGATGCATTCTCTGC	AscI
freuprev	CAGTGTAAATAACAAAATAGTTTTTCGCTGCCTCGTTTTCTATTTGGTG	None
frednfor	CACCAAATAGAAAACGAGGCAGCGAAAAACTATTTTGTTATTTACACTG	None
frednrev	GGCGCGCCCTGCAGCCCGTAAACCATCCAACATC	AscI/PstI
Fusfrhupfor	GGCGCGCCCTTAAGGGGCCCTCCGTTGTCCTTCTTTCCAC	AscI/AflII/ApaI

Table 2.2 (cont.)

Primer	Sequence[a]	Added sites
Fusfrhuprev	GGCGCGCCACTAGTCTCGAGCAATTGTATGCCTCGTTTTCGATTT	AscI/SpeI/XhoI/MfeI
Fusfrhdnfor	GGCGCGCCACTAGTTAAAACTCCTCTTTTTTTGTCAGCG	AscI/SpeI
Fusfrhdnfor	GGCGCGCCGCGGCCGCTGTTGCGAGTTGTTCAATCC	AscI/NotI
QPCRrpoA1for	GGCTTCGCTGCAAGACATG	None
QPCRrpoA1rev	CCCGAAGTGTCCAGGACATT	None
QPCRfpofor	CCTTCTCCGAAATGGGTCATC	None
QPCRfporev	AAACGGGCCGCCACTAA	None

[a]The added restriction sites are underlined.

Table 2.3 *M. barkeri* Fusaro strains used in this study

Strain	Genotype	Source or construction
WWM85	Δ*hpt*::P*mcrB*-ϕ*C31int-attP*	(20)
WWM86	Δ*hpt*::P*mcrB*-ϕ*C31int-attB*	(20)
WWM71	Δ*hpt*::P*mcrB*-ϕ*C31int-attB*, Δ*fpoA-O*	Deletion of *fpo* by markerless exchange with pDK4 in WWM86 (23)
WWM123	Δ*hpt*::P*mcrB*-ϕ*C31int-attP*, Δ*fpoF*	Deletion of *fpoF* by markerless exchange with pDK13 in WWM85 (23)
WWM116	Δ*hpt*::P*mcrB*-ϕ*C31int-attP*, Δ*freAEGB*	Deletion of *fre* by markerless exchange with pGK6 in WWM85
WWM122	Δ*hpt*::P*mcrB*-ϕ*C31int-attB*, Δ*frhADGB*::*pac-hpt*	Deletion of *frh* with ApaI/NotI-digested pAMG81 in WWM86 (23)
WWM108	Δ*hpt*::P*mcrB*-ϕ*C31int-attB*, Δ*fpoA-O*, Δ*frhADGB*::*pac-hpt*	Deletion of *frh* with ApaI/NotI-digested pAMG81 in WWM71 (23)

Table 2.3 (cont.)

Strain	Genotype	Source or construction
WWM145	Δ*hpt*::P*mcrB*-ϕ*C31int-attP*, Δ*fpoF*, Δ*frhADGB*::*pac-hpt*	Deletion of *frh* with ApaI/NotI-digested pAMG81 in WWM123 (23)

(WWM145) mutants, respectively. The Δ*fpo*, Δ*fpoF*, Δ*frh*, Δ*fpo* Δ*frh* and Δ*fpoF* Δ*frh* mutants were isolated and verified with DNA hybridization by Kridelbaugh *et al* (23). The Southern hybridization blot confirming Δ*fre* mutant, which was isolated in this study, is shown in Figure 2.4. All genetic manipulations were carried out using methanol plus H_2/CO_2 as the growth substrate because the $F_{420}H_2$:heterodisulfide oxidoreductase system was not expected to be required for growth via the methyl-respiration pathway.

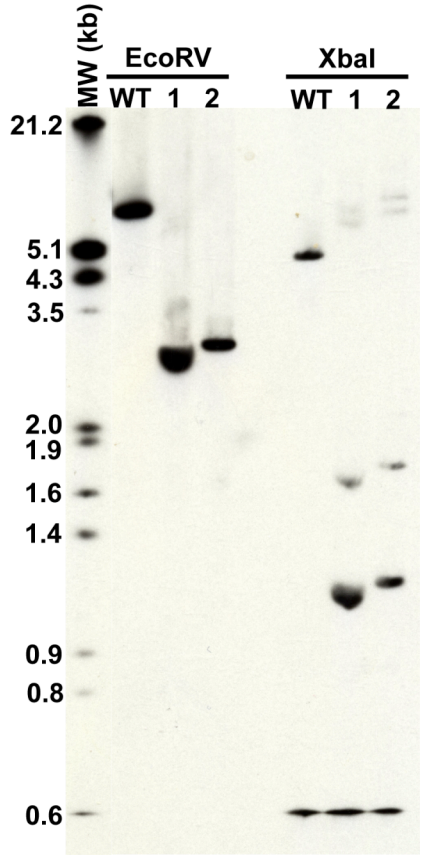

Figure 2.4 Verification of Δ*fre* by Southern hybridization. Predicted bands (kb): **EcoRV**: WT (WWM85) = 6.3, mutants (1 and 2) = 2.9; **XbaI**: WT = 4.6 and 0.5**,** mutants = 1.1 and 0.5. MW: DIG-labeled DNA molecular weight marker III (Roche, Indianapolis, IN). 520 bp fragment of NdeI-digested *fre* deletion plasmid (pGK6, Table 2.1) was used as probe.

2.3.5 Determination of growth characteristics

Growth rate determination of Δ*fpo*, Δ*fpoF*, Δ*frh*, Δ*fpo* Δ*frh* and Δ*fpoF* Δ*frh* mutants was done by Kridelbaugh *et al* (23), whereas, Δ*fre* growth was quantified in this study. The mutant was initially adapted to all substrates for at least 15 generations till mid-log phase (optical density at 600 nm [OD_{600}] *ca.* 0.5 for methanol and methanol/H_2/CO_2 and *ca*. 0.25 for H_2/CO_2 and acetate). Subsequently, approximately 3% inoculum (or 10%, in case of H_2/CO_2 and acetate) of the culture was transferred to fresh medium in quadruplets and incubated at 37^{o}C. Growth was quantified by measuring OD_{600}. Generation times were calculated during exponential growth phase, growth yield was determined by measuring the maximal OD_{600} of the culture and lag phase was defined as the time required to achieve half-maximal OD_{600}.

2.3.6 Cell suspension experiments

Cells grown on methanol plus H_2/CO_2 were collected in late exponential phase (OD_{600}= 0.6-0.7) by centrifugation at 5000 x g for 15 minutes at 4^{o}C. They were then washed with anaerobic HS PIPES buffer, 50 mM PIPES (pH 6.8), 400 mM NaCl, 13 mM KCl, 54 mM $MgCl_2$, 2 mM $CaCl_2$, 2.8 mM cysteine, 0.4 mM Na_2S, and resuspended in the same buffer to a final concentration of 10^9 cells/ml. Cells were counted visually using the Petroff-Hausser counting chamber (Hausser Scientific, PA). Assay mixtures contained 2 ml of the suspension and were incubated under strictly anaerobic conditions in 25 ml Balch tubes sealed with butyl rubber stoppers. Puromycin (20 μg/ml) or Mupirocin (pseudomonic

acid, 105 μg/ml, Sigma-Aldrich, St Louis, MO) (6) was added to prevent protein synthesis and, as indicated, the assay mixture contained 250 mM methanol under a headspace of N_2, H_2 or H_2/CO_2 (80/20%) at 250 kPa over the ambient pressure. Cells were held on ice until use and assays were started by transferring to 37^{o}C. For rate determination, gas phase samples were withdrawn at various time points and assayed for CH_4 by gas chromatography at 225^{o}C in a Hewlett Packard gas chromatograph (5890 Series II) equipped with a flame ionization detector. The column was of stainless steel filled with 80/120 Carbopack^{TM} B/3% SP^{TM}-1500 (Supelco, Bellefonte, PA) with helium as the carrier gas. For total CH_4 and CO_2 production, assays were incubated at 37^{o}C for 36 hours and then gas phase samples were withdrawn and analyzed by GC at 225^{o}C in a Hewlett Packard gas chromatograph (5890 Series II) equipped with a thermal conductivity detector. A stainless steel 60/80 Carboxen-1000 column (Supelco, Bellefonte, PA) with helium as the carrier gas was used. Total cell protein was determined using the Bradford (7) method after 1 ml of the cells was lysed by resuspending it in dd$H_2$0 with 1 μg/ml RNase and DNase.

2.3.7 RNA isolation and quantitative RT-PCR

Cultures grown to mid-exponential phase (OD_{600} *ca*. 0.28 for Δ*frh* and *ca*. 0.4 for other strains) on methanol were lysed using three volumes of TRIzol LS Reagent (Invitrogen, Carlsbad, CA), followed by phase separation using chloroform as per manufacturer's instructions. Subsequently, RNA was precipitated using one volume of 70% ethanol and purified using RNeasy mini

spin columns (Qiagen, Valencia, CA) according to manufacturer's protocol. Contaminating DNA was removed by treatment with TURBO DNA-*free* DNase (Ambion, Austin, TX). The concentration and purity of RNA were evaluated using a NanoDrop spectrophotometer (NanoDrop, Wilmington, DE).

Gene-specific primers (Table 2.2) were designed using Primer Express Software v2.0 (Applied Biosystems, Foster City, CA). A one-step qRT-PCR reaction was performed using SuperScript III Platinum SYBR Green One-Step qRT-PCR Kit with ROX (Invitrogen, Carlsbad, CA) in the ABI PRISM 7900HT Sequence Detection System (Applied Biosystems). All reactions (20 µl) contained 1X SYBR Green Reaction Mix with ROX, 0.4 µl SuperScript III RT/Platinum Taq mix, 100 ng RNA and 10pmol each of primers. Synthesis of cDNA from RNA and subsequent amplification were performed as follows: 50°C for 5 min and 95°C for 2 min, followed by 40 cycles of 95°C for 15 s and 60°C for 1 min. Two negative controls, one without reverse transcriptase and another without template RNA, were run to check for DNA or RNA contamination.

The relative standard curve method was used to quantify expression of *fpo* (ABI PRISM 7700 Sequence Detection System User Bulletin #2) using *rpoA1* as the reference gene. In this, standard curves relating C_T values versus log amount of RNA were constructed for *fpo* and *rpoA1* using RNA isolated from methanol-grown WWM85 (Table 2.3). The *fpo* RNA amount in each sample was calculated using linear regression of the standard curve and averaged across triplicates of three biological samples for each culture. The average *fpo* amount was normalized to average *rpoA1* amount to obtain the relative *fpo* amount. This

value was divided by the calibrator value (WWM85) to obtain *fpo* fold regulation from wild-type.

2.4 RESULTS

2.4.1 The $F_{420}H_2$:heterodisulfide oxidoreductase is conserved in all sequenced *Methanosarcina* genomes

The genomes of *M. barkeri* Fusaro (27) and *M. acetivorans* C2A (17) encode *fpoABCDHIJJKLMNO* and *fpoF* operons that are nearly identical to those found in *M. mazei* Gö1 (Figure 2.3) (28). To test *in silico* if the operons from *M. barkeri* and *M. acetivorans* encode a functional Fpo, the predicted protein sequences of Fpo subunits from all three *Methanosarcina* species were aligned and analyzed for presence of conserved structural and catalytic amino acid residues that are present in *M. mazei* Fpo subunits (Figure 2.5).

The input module of Fpo, FpoF, has been proposed to oxidize $F_{420}H_2$ and transfer electrons via enzyme-bound FAD to two [4Fe-4S] clusters that are bound to FpoF by cysteine-containing motifs, $C^{14}XXC^{17}XXC^{20}XXXC^{24}P$ and $C^{55}XXC^{58}XXC^{61}XXXC^{65}P$, which are conserved in all three *Methanosarcina* FpoF subunits (3) (Figure 2.5). These subunits show 86-89% amino acid identity among each other (Table 2.4). Interestingly, the genomic location of *fpoF* is conserved in all three species, such that it is located between genes encoding methylenetetrahydrosarcinapterin reductase (*mer*) and a putative cytidylyltransferase (28) (Figure 2.6). Although it is unknown if the three genes constitute an operon, the *mer-fpoF* intergenic region in all three *Methanosarcina*

species includes multiple poly-T tracts, which are known to signal transcription termination in Archaea (44).

1. FpoF

```
Mm FpoF         MPPKIAEVIQHDVCAACGACEAVCPIGAVTVKKAAEIRDPNDLSLYEKGAAFQVCEGCLT 60
Ma FpoF         MPPKIAEVIDYDVCAACGACEAVCPIGAVTVKKAAGIRDPNDLSLYEKGGGYQVCEGCLT 60
Mb FpoF         MPPKIAEVIEHDVCAACGACEAVCPIGAVTVRKAAEIRDPNDPNLYQKGAGYLVCEGCLT 60

Mm FpoF         CSRICPVVDGFIENELLNVRKFFGAKSKDNAGSQDGGVTSGILKALFNKGEIDCAVGITR 120
Ma FpoF         CSRVCPVVDGFIQDELTNVRKFFGARSKDNVGSQDGGVASGILKSLFKQGKIDCAVGITR 120
Mb FpoF         CSRICPVVDGFIENELANVRKFFAARSKENAGSQDGGVTSGILKSLFKQGKIDCAVGITR 120

Mm FpoF         NENWEPEVVLLTSAEDVERTRGTKYTSDPVVAALREAFEKYDRIAVVGVPCQAHAARLIR 180
Ma FpoF         NEKWEPEVVLLTSAEDVERTRGTKYTSDPVLAALREAFEKYDRIAVIGVPCQAHAAHLIR 180
Mb FpoF         DEKWESKVVLLTSAEDVEKVRGTKYTSDPVVAALREAFEKYDRIAVVGVPCQAHSARLIR 180

Mm FpoF         ENVNEKIVLIIGLLCMESFHHDVMLDKIIPEIMKVNVRDIVKMEFTKGKFWVYTKDGEVH 240
Ma FpoF         ENVNEKIVLIIGLLCMESFHHDVMLEKIIPEILKVKLEDIRKMEFTKGKFWVYTKDGEVH 240
Mb FpoF         ENVSEKIVLIIGLLCMESFHHDVMLDKIIPEIMKVKIEDVRKMEFTKGKFWVYTSDGEVH 240

Mm FpoF         SVPIKDIAKYARNPCHHCCDYTSVFADISVGSVGAPDGWNSVFIRTEIGEKYFDMVRDEM 300
Ma FpoF         SVPIKDVAKFARNPCHHCCDYTSVFADISVGSVGAPDGWNSVFIRTEIGEKYFDMVREDM 300
Mb FpoF         SVPIKDVAKYARNPCHHCCDYTSVFADISVGSVGAPDGWNSVFIRTDAGEEYFEMVREEM 300

Mm FpoF         EIMEDPKPGLELVGKLIEMKRKGNAEHFQEVCKEFSFETGIRSETV 346
Ma FpoF         EIMEDPKPGLELVEKLIGMKRKGNAEHFLEVCEKFSFETGIRNETI 346
Mb FpoF         EIMEDPKPGLELVKKLIDMKRKNNAEHFKEVCKEFSFETGIRDETV 346
```

2. FpoA

```
Ma FpoA         -----MSGIIDSYIPVAIFLAVGLIMPPMTMFMVKQLSPRSKAASKYTTYESGSIPTGTA 55
Mm FpoA         MIGDTMSGIIDSYIPVAIFLAVGLIMPPMTMFMVKQLSPRSKAASKYTTYESGSVPTGTA 60
Mb FpoA         -----MSEIIDSYIPVAIFLVVALIMPPMTMFMVKQLSPRSKAAGKYTTYESGSVPTGTA 55

Ma FpoA         RIQFNVEYYLYAIAFVLFDIEVLFLYPWATVYKGHGITSIAVVEMFVFIFILLFGYVYLW 115
Mm FpoA         RIQFNVEYYLYAIAFVLFDIEVLFLYPWATVYKGHGITSIAVVEMFVFIFILLFGYVYLW 120
Mb FpoA         RIQFNVEYYLYAIAFVLFDIEVLFLYPWVTVYKGHGITSLAVVEMFAFIFILLFGYIYLW 115

Ma FpoA         KKEALTWVK 124
Mm FpoA         KKEALTWVK 129
Mb FpoA         KKGALTWVK 124
```

3. FpoB

```
Ma FpoB         MGEVKETKTNNTTGTPEEEIPGVITTTTNAISDFLKKTKAQDLINWGRKNSLWFMTQPMG 60
Mm FpoB         MGEVKETKTNNSKENPEEEVPGVITTTTSAIHNFLKKTKAQDIINWGRKNSLWFMTQPMG 60
Mb FpoB         MGEVKEKKTSKPYETSEEEIPGVITTTSNAISEFLKKTKVQDIINWGRKNSLWFMTQPMG 60
```

Figure 2.5 (cont.)

```
Ma FpoB         CCGVEMIATGCAHYDTDRFGIIPRNSPRHADVMIISGYVTKKYLPALKRLWEQMPAPKWV 120
Mm FpoB         CCGVEMIATGCAHYDTDRFGIIPRNSPRHADVMIISGYVTKKYLPALKRLWDQMPAPKWV 120
Mb FpoB         CCGVEMIAMGCAHYDTDRFGIIPRNSPRQADVMLISGYVTKKYLPALKRLWEQMPSPKWV 120

Ma FpoB         IAMGDCSISGGPFYESYSTVQNIDELFPIDVFIPGCPPRPEALIQGFVELQEKIKAKKDR 180
Mm FpoB         IAMGDCAISGGPFYESYSTVQNIDEIFPIDVYIPGCPPRPEALIQGFVELQEKIKARKDR 180
Mb FpoB         IAFGDCSISGGPFYESYSTVQNIDEIFPIDVFVPGCPPRPEAMLQGFVELQEKIKAKKDL 180

Ma FpoB         GTEY 184
Mm FpoB         GTEY 184
Mb FpoB         GSEY 184
```

4. FpoC

```
Ma FpoC         MDAMTIIESLTGKFPEAISEAEVESPIRIRAYADKEKAKEVCQYLKDSLQFDHLCSVCGV 60
Mm FpoC         MDARTIIESLTGKFPEAISEAGIESPIRIRAYVDKDKAKEVCEYLKGSLQFDHLCSVSGV 60
Mb FpoC         MDVTEILKSLTGAFPEAISETTAESEIRARAYVEKEKTKEVCQYLKDSLQFDHLCSVCGV 60

Ma FpoC         DYPQRNEQEVVYHIASYDHPVVLMLKARLPRDSPEIESIVPVYWNANWYERETYELFGIF 120
Mm FpoC         DYPQRDELEAVYHIASYDHPVVLMLKARLPRDSPEIESVVSVYWNANWYERETYELYGIF 120
Mb FpoC         DYIKRNELEVVYHIASYNHPVVLTLKAKLPRENPEIESIVSVYWNANWYERETYELFGIL 120

Ma FpoC         FKNHPNLKALVLPEDMLGEWPLRKDYEGFPNRTARNLV 158
Mm FpoC         FKNHPELKPLVLPDDMLGEWPLRKDYEGFPNRTARNLV 158
Mb FpoC         FKNHPNLKPLILPEDMLGEWPLRKDYEGFPNKTARNLV 158
```

5. FpoD

```
Mb FpoD         MEEKLEPNEMIVHLGPQHPMQPGPFRLNLRLKGETVVDADIELGFIHKGIEKILENKTYL 60
Ma FpoD         MEEMLEPNEMIVHLGPQHPMQPGPFRLNLRLKGETVMDAEVELGFIHKGIEKILENKTYL 60
Mm FpoD         MEEMLESNEMIVHLGPQHPMQPGPFRLNLKLKGETIMDAEVEMGYIHKGIEKILENRTYL 60

Mb FpoD         QGITIVDRICYLVALVNEECFVGCTEKLLGIEPPERSQYIRVILDELTRIQSHLLGMGEF 120
Ma FpoD         QGITIVDRICYLVALTNEECFVGCTEKLLGIEPPERAQYIRVILEELSRLQSHLLGMGEF 120
Mm FpoD         QGITIVDRICYLVALTNEECYVGCVEKLLDIEPPERAQYIRVILEELSRLQSHLLGLGEY 120

Mb FpoD         GEFIGFVSMFMYTIREREEVLSLIDMITGARITHSYLKFGGVRDDLPDGFKEKALSVLNN 180
Ma FpoD         GEFIGFVSMFMYTIKEREDILTLIDMVTGARVTHSYLKFGGVRDDLPEGFKEKALPVLNN 180
Mm FpoD         GEFIGFVSMFMYTIKEREDILTLIDMVTGARVTHSYLRFGGVRDDLPEGFKEKTIPVLNK 180

Mb FpoD         LKKSVDDFEEMFHTDRIYRERTVGVGVLTADVAKNLGVSGPPLRATGVPFDIRKNEPYLV 240
Ma FpoD         LKKVISDYEEMFNSDRIYRERTVGVGVLTADVAKNLGVSGPPLRATGVPFDIRKNEPYLV 240
Mm FpoD         LKKVIRDYEEMFYSDTIYRERTIGIGVLTADEAKSLGVSGPVLRATGVPFDIRKNEPYLV 240


Mb FpoD         YKDLDFKVCTETAGDCFARVQVRINEIRESIYILEQCFDQIPSGPLFPEGSLYGRRTPVM 300
Ma FpoD         YKDLDFKVCTETAGDCFARVQVRLNEMRESIYILEQCLDQIPNGPLFPEGTPYGRRTPVM 300
Mm FpoD         YRDLDFKVCTETAGDCFARVQVRLNEMRESIYIIEQCLDMIPNGPIFPEGTPYGKRTPVM 300
```

Figure 2.5 (cont.)

```
Mb FpoD         RVPAGEVFYRVEDPRGEMGMYMISDGSDKPYRVKIRGPYYPTLQALPPLIIGTTVADVAA 360
Ma FpoD         RVPAGEVFHRVEDPRGEMGMYMISDGSDKPYRVKVRGPYYPTLQALPPLIKGTTVADVAA 360
Mm FpoD         RVPAGEVFHRVEDPRGEMGMYMVSDGSDRPYRVKVRGPYYPTLQALPPLIIGTTVADMVS 360

Mb FpoD         ISGSMDGCTSEADR 374
Ma FpoD         ISGSMDGCTSEADR 374
Mm FpoD         ISGSMDGCTSEVDR 374
```

6. FpoH

```
Ma FpoH         -MNIMIEIPEFIIPLIPWIRGVVGLVLVGAIFLGAMGAVWLERKLSADIQFRYGPSRVGK 59
Mm FpoH         MTFMAIEIPEFIVPFVPWIRGTVGLVLVGAIFLGGMAAVWIERKLSADIQLRYGPSRVGK 60
Mb FpoH         ---MTVVIPEYITPLIPWVRGIVGLVLIGVIFMGAMGAVWLERKLSADIQTRMGPCRVGK 57

Ma FpoH         FGLLQLVADAIKLFTKEDMRPRNADRLLFDNAPIFMMSSVFLMLVAIPVGAVFINGVEYP 119
Mm FpoH         FGLLQLVADAIKLFTKEDVRPGNADRFLYDNAPVFMLTSLFLMLVAIPVGAVFIDGNLYP 120
Mb FpoH         YGLLQLVADAIKLFTKEDLKPLNADSLLFNNANIFMLGSVFLMLVALPVGAVFINGVEYP 117

Ma FpoH         LAVTEMDISVLYIEAMSAITIFGIFMIAYGSNNKYSLLGAFRNFARMVGYEVPLGITVVS 179
Mm FpoH         LAVTEMDISILFIEAVSAINIFGIFMAAYGSNNKYSLLGAFRNFARMIGYEVPLGIAIVS 180
Mb FpoH         LAVTQMDISVLYIEAVSALSIFGIFMVAYGSNNKYSLLGAFRNFARMVGYEVPLGITVIS 177

Ma FpoH         VAIMTGSLNIVEIASAQG-LLWNIFLQPIGFIVFFIALMADMGRLPFDQNESEEELVAGW 238
Mm FpoH         VAVMTGSLNIIDITSAQGSFVWNIFLQPIGFVVFFIALMADLGRLPFDQNESEEELVAGW 240
Mb FpoH         VAAMTGSLNIVDISTAQG-LHWNIFLQPLGCFVFFVSLMADMGRLPFDQNESEEELIAGW 236

Ma FpoH         ITEYTGMRFGLGFFAEYIHMILGSFLVALLFLGGWNVPAFVANNPVLGLIAPTGFFLLKT 298
Mm FpoH         VTEYTGMRFGLVFFAEYMHMILGSFLVALLFLGGWNVPAFVANNAVLGLIAPTGILLLKT 300
Mb FpoH         ITEYCGMRFGLGFFAEYIHMILGSFLVALLFLGGWNVPGFIANNSFFGIIVPTGFLIVKV 296

Ma FpoH         VLVLMTIIGMRWAVPRFRIDQVVDLSWKRLLPLSLLNLVWAVGLGLYLGA 348
Mm FpoH         VLVLMTIIGMRWAVPRFRIDQVVDMSWKKLLPLSLLNLAWAVGLGLYLGA 350
Mb FpoH         VFVLMVIIGLRWAVPRFRIDQVVDLSWKKLLPLALLNLVWAVGLGLYLGA 346
```

7. FpoI

```
Ma FpoI         MVLKNIKYAVKNIPKKRVTRLCPEVESPLSDRFRGLQILDKSKCIGCGICANTCPNNAIK 60
Mm FpoI         MVLKNIKYALKNIPKERVTRLCPEVESPLSERFRGLQTLDKSKCIGCGICANTCPNSAIK 60
Mb FpoI         MVLKNIKYAIRNITRPPVTRMYPEKQSELSDRFRGLQILDKSKCIGCGICANTCPNAAIK 60

Ma FpoI         IVKAPIAPGSSKQRWFPEIDIGHCLFCGLCIDQCPKGALSSGKEYTKGMVKWAHKDLLMT 120
Mm FpoI         IVKAPIAPGSEKKRWFPQIDIGHCLFCGLCIDQCPKGALSSGKEYCKGMVKWAHKDLLMT 120
Mb FpoI         IVKAPIAPGSTKQRWFPQIDIGHCLFCGLCIDQCPKGALSSGKEYAKGLVKWKHKDLLIT 120

Ma FpoI         PEKLAREVDIKEGDEK 136
Mm FpoI         PEKLAREVDIQEGDER 136
Mb FpoI         PEKLAREVDLEEGDEK 136
```

Figure 2.5 (cont.)

8. FpoJ

```
Ma FpoJ1        MIGLETVGAALEMAVFGLLAFVTVFFAIFVVIAKDVVRAGLALIMCMFGVAALYILLNAQ 60
Mm FpoJ1        MIDPGTVGAALETAVFGLLALVTVFFAIFVVIAKDVVRAGLALIMCMFGVAGLYILLNAQ 60
Mb FpoJ1        MIELETIGEALKMAVFWVLAISTVFFAVFVVTAKDIVRAGLALIMCMFGIAALYILLNAQ 60

Ma FpoJ1        FLGIIQVLVYIGAIGVLILFAVMLTKRHLGGGSRAD 96
Mm FpoJ1        FLGVIQVLVYIGAIGVLILFAVMLTKREIGGGPRAN 96
Mb FpoJ1        FLGIIQVLVYIGAIGVLILFAVMLTKHEIGGEPGED 96
```

9. FpoJ

```
Ma FpoJ2        MGPVRINRPLALLVSLLFVAVIVTGVFGTSWHTVSELPENPADPSNIQGIGMLIFTQYVV 60
Mm FpoJ2        ---MQINRPLAFLVCLLFVAVVVTGAFGTSWNTVSELPENPADPSNIEGIGMLIFTHFVA 57
Mb FpoJ2        ---MRINRPLAFLVVLLFTAIVVIGAFGTSWNTVSELPQSPADQSNIEGIGMLIFTQYVA 57

Ma FpoJ2        PFEVLSIVLLASLIGAIYMAKGEGNR 86
Mm FpoJ2        PFEVLSIVLLASLIGAIYMAKGEGNR 83
Mb FpoJ2        PFEVLSIVLLASLIGAIYLAKGEGNR 83
```

10. FpoK

```
Ma FpoK         MTAIPLTFYLGLAALLFSIGLYGVMTHKSGIRMIMCIELMLNSANLNLVAFSSYTDTLNG 60
Mm FpoK         MTAIPLTFYLGLAALLFSIGLYGVMTHKSGIRLIMCIELMLNSANLNLVAFSSYTDTLHG 60
Mb FpoK         --MIPLIFYLGLAALLFSIGLYGVMTHKNGIRMIMCIELMLNSANLNLVAFSSYTDTLNG 58

Ma FpoK         QVFAIFSIALAAAEAAVGFAIFMAIYRMHDKINLDELNILRW 102
Mm FpoK         QVFAMFSIALAAAEAAVGFAIFMAIYRMHDKINLDELNILRW 102
Mb FpoK         QVFAVFSIALAAAEAAVGFAILMAIYRMHDKINLNELKSLRW 100
```

11. FpoL

```
Ma FpoL         MVKTALEEFAFLIPLLPALAFAITFFFGKKMPSGGAIVPILAIAASFVISFAITLGLLAN 60
Mm FpoL         MVKTALEEFAFLIPLLPALAFAITFFFGRKMPSGGAIVPILAIAASFVISFAITLGLLAN 60
Mb FpoL         -----MEEFAFLIPLLPALAFVITFFFGRKMPSGGAIVPILAIAASFVISLMITLRLLAN 55

Ma FpoL         PGEVVSQSYSWFAVLDIGILIDPLAAVMLSMVSFVSLLIHIYAVSYMSHDAGKARYFAET 120
Mm FpoL         PEEVISQSYSWFAVLNIGILIDPLAAVMLSMVSFVSLLIHIYAVSYMSHDAGKARYFAET 120
Mb FpoL         PDEVISQSYPWFAVLNIGVLIDPLAAVMLSMVSFVSLLIHIYAVSYMSGDPGEARYFAET 115

Ma FpoL         ALFTAAMLSLVLSDNILQLFVSWELVGLCSYLLIGFWFEKPSAAAAAKKAFLTTRVGDVM 180
Mm FpoL         ALFTAAMLSLVLSDNILQLFVSWELVGLCSYLLIGFWFEKPSAAAAAKKAFLTTRIGDVM 180
Mb FpoL         ALFTAAMLSLVLSDNILQLFVSWELVGLCSYLLIGFWFERPSAAAAAKKAFLTTRIGDVM 175
```

Figure 2.5 (cont.)

```
Ma FpoL         FLTGIIVLTSDLLKLAGGFQEGVYLLRFDEIFSYIPQLSALQANIFGFEVSHLTIITLLF 240
Mm FpoL         FLTGIIVLTSDLLKVSGGFQDGVYLLRFDEIFSYIPELAALQINILGFEISHLTIITLLF 240
Mb FpoL         FLTGIIVLTSDILKLAGGFQDGTYLLRFDEIFSYIPQLSALQTNIFGFEVSHLTIITLLF 235

Ma FpoL         FGGAVGKSGQFPLHVWLPDAMEGPTTVSALIHAATMVTAGVYLVARTFPMFIAAPGTLMV 300
Mm FpoL         FGGAVGKSGQFPLHVWLPDAMEGPTTVSALIHAATMVTAGVYLVARTFPMFIAAPDSLMV 300
Mb FpoL         FGGAVGKSGQFPLHVWLPDAMEGPTTVSALIHAATMVTAGVYLVARTFPMFIAAPDSLMV 295

Ma FpoL         IAYLGGFTALFAGTMGIVMNDLKRVLAYSTISQLGYMMLALGLGATVGLEAVGVSLFHLI 360
Mm FpoL         VAYFGGFTALFAGTMGIVMNDLKRVLAFSTISQLGYMMLGLGLGTAIGLEAVGISLFHLI 360
Mb FpoL         VAYLGGFTALFAGTMGIVMNDLKRVLAYSTISQLGYMMLGLGLGSAIGLEAIGISLFHLI 355

Ma FpoL         NHAFFKALLFLCAGSVIHAVGTQDMRELGGVGKVMPITAGTMAIAALSLAGFGIPGTSIG 420
Mm FpoL         NHAFFKALLFLCAGSVIHAVGTQDMRELGGVGKVMPITAATMTIAALALAGFGIPGTSIG 420
Mb FpoL         NHAFFKALLFLCAGSVIHAVGTQDMRELGGVRKVMPVTAATMAIAALALAGFGIPGTSIG 415

Ma FpoL         TSGFMSKDPIIENAYLFAEHSGNWIPYIFAIAAALLTSIYIFRLIFMTFAGKPRSDYHGH 480
Mm FpoL         TSGFMSKDPIIEAAYLFGEHSSNWIPYVFSILAALLTSIYIFRLIFMTFTGKPRSNYHGH 480
Mb FpoL         TSGFFSKDAIIEAAYLFGENSNNWIPYAFSIAAALLTSIYIFRLIFMTFTGKPRSDYHGH 475

Ma FpoL         ESPSIMTVPLSILALFALVFGSLTRTGFMNFLEETFTNSFVDLNIGNLAGIGGYELVEAA 540
Mm FpoL         ESPAIMTIPLSILAIFALAFGALTRTGFMEFLEETFTNSFVNLDIGALAGIGENELVAAA 540
Mb FpoL         ESPAIMTIPLSILAIFSLVFGGLTKTGFMNFLEETFANGFVNLNIGGLAALGRNELVGTA 535

Ma FpoL         GHEPVLILWLPLIMAVAGLAIAFVIYYLRVFSLGPIASMKNPIYRLLYKRYYQHEIYTEF 600
Mm FpoL         GHEPLAVLWPPVIVALAGFAIAFVIYYLRAFSLGPLASMKNPIYRLLYNRYYQHQIYTEF 600
Mb FpoL         GSESLFVQWLPMIVAVAGLAVAFVIYYLRIIKLGPLASMKNPVYRLLYKRYYQHKIYTEF 595

Ma FpoL         FSIGIVYGVIAFLTQVVDVIVDSIVEGIGILTVGVGEELRKVQTGVVQTYATVIIAGVSL 660
Mm FpoL         FSIGIVYGIIAFLTQVVDVIIDSVVEGIGIVTVFVGEELRKIQTGVVQTYATALIAGVSL 660
Mb FpoL         FSLGIVYGVIALLSQVLDVIIDSIVEGIGILTVGVSEELRRVQTGVVQTYAIVVIAGVSL 655

Ma FpoL         LIILIKLITEVL 672
Mm FpoL         LIILVKLIMEVL 672
Mb FpoL         LIILVKLIMEVL 667
```

12. FpoM

```
Ma FpoM         MLPVASLLILVPLIFAAVTFFFTKTKDQAAGLGLIGSLVTLGLTLYAYLNFDSSTAAMQFY 60
Mm FpoM         MLPVASLLILVPLIFAVVTFFFTKTKQLAAGFGFLGSLATLGLTLYAYLNFDSSTAAMQFY 60
Mb FpoM         MLPVASLLILVPLIFAAVTFFFTKTKEQAAGLAFLGSLATLGLTLYAYLNFDSSTAAMQFF 60

Ma FpoM         ESVPWVPFLGINYSVGIDGISMPLILLNAIVIPLLILFSWKEDREAPNRFYGLILTMQAA 120
Mm FpoM         ESVSWIPFLGVNYSVGIDGVSMPLILLNAIVIPFMILFTWKEEMESPNRFYGLILTMQAA 120
Mb FpoM         ESIDWIPLLGVKYSVGIDGISMPLILLNAIVIPFLILYSWKEEREDSNRFYGLILTMQAA 120

Ma FpoM         VIGVFVALDFVVFYIFWELTLVPLFFIVNIWGGEKRAHASYKFFIYTHVASLVMLLGIFG 180
Mm FpoM         VIGVFVALDFVVFYIFWELTLVPLFFIVNLWGGANRAHASYKFFIYTHVASLVMLLGIFG 180
Mb FpoM         VIGVFVALDFVVFYIFWELTLIPLFFMVNIWGGEKRAHASYKFFIYTHVASLVMLLGIFG 180
```

Figure 2.5 (cont.)

```
Ma FpoM         LFYTALHQTGIPTFDIRELIAQFQFFESGLMRDAIFLAILFGFLAKLPTFPFHSWLPDAY 240
Mm FpoM         LFYTALNQTGVPTFDIRELIAQFQFFEPGLMKDGIFLAILFGFLAKLPAFPFHSWLPDAY 240
Mb FpoM         LFYASWQQTGVPTFDIRELVGQFQFLGSGLLRNAIFLSIIFGFLAKLPTFPFHSWLPDAY 240

Ma FpoM         TEAPTAGSVLFILLKIGGYGLFRISLPMLPNTGNPNLMIMMLGLLGSFSIVYGALLALRQ 300
Mm FpoM         SEAPTAGSILFILLKIGGYGLFRISLPMLPNTGSPQLMIMILGLLGSVSILYGALLALRQ 300
Mb FpoM         TEAPTAGSVLFILLKIGGYGLFRISLPMLPNTGNPELMITILGLLGAFSILYGALLALRQ 300

Ma FpoM         KDLKRMIAYSSLSHMGFVTLGSAGLVALSVSGAMFQQFSHGLIMSIMFMSAGAIQTTTGT 360
Mm FpoM         KDLKRMIAYSSLSHMGYVILGSAGLVTLSVSGAMFQQFSHGLIMSIMFMSAGAIQTAAGT 360
Mb FpoM         KDLKRMIAYSSLSHMGYVLLGSAGFVALSVSGAMFQQFSHGLIMSIMFMSAGAIQTSTGT 360

Ma FpoM         RIINDLGGLARKMPMLAVLMMVGFMASLGLPGLTGFIAEFLVLTFSFVNLPGFVLLALLA 420
Mm FpoM         RIINELGGLAKKMPMLTVAMMVGFMASLGLPGLTGFIAEFLVLTFTFTNLPVFVVIALLA 420
Mb FpoM         RIINNLGGLAKKMPTLAVLMMLGFMASLGLPGLTGFIAEFLVLAFSYVNLPGFVLLALLA 420

Ma FpoM         IVITAGYHLWAMQRAMFGVYNEKLGSIRDINSMQVFSMGVIALLVLYFGLNPSPVLNMMI 480
Mm FpoM         IVVTAGYHLWAMQRAMFGVYNEKLGDVRDINSIQVFSMAVIALLVLYFGLNPSPVLDMMI 480
Mb FpoM         IVITAGYHLWAMQRAMFGVYNEKLGDVRDINSLQVFSMAVIALLVVYFGWNPNPVLNMMI 480

Ma FpoM         KNSEAIVSLAAVMGV 495
Mm FpoM         NNSEAIVSLAAGMGV 495
Mb FpoM         TNSEAIVSLAAALGV 495
```

13. FpoN

```
Ma FpoN         MDELMYLAPEIVVVATGLVVLLAGVFLSPRAKNILGYLATLGILAALFLTVKSFGLLTMQ 60
Mm FpoN         MQEIMYLAPELVLVATGLVILLTGVFLSPQSKNILGYLATLGTLAAIFLTVKSFGLLTME 60
Mb FpoN         MENLMFLAPEIAIAATGLIILFIGVFMSSRTKNVLGYLATLGILAALVLTIQSFG----- 55

Ma FpoN         GFQVGYSIFSEALNIDALSQFFKLVFLVVALIVSIAAIKYNENSDHTEEFYTLMLFATFG 120
Mm FpoN         GFSVQYTIFSETLSIDALSQFFKLVFLAVALIVSIASIKYTENSDHTEEFYTLVLFATFG 120
Mb FpoN         ---TEATMFYGTVSIDALSQFFKLVFLVVALIVSIASIKYNENSDHTEEFYSLVLFATLG 112

Ma FpoN         MMIVASANDLVVLFVAFELASLATYALAGYEKQNPRSLEGAMKYFVIGSVSAALMLFGLS 180
Mm FpoN         MMIVASANDLILLFCAFELASLATFALAGFEKQNARSLEGAMKYFVIGSVSAALMLFGLS 180
Mb FpoN         MMVVASSNDFILLFCAFELASFATYALAGFEKQNPRSLEGAMKYFMMGAVSSALMLFGIS 172

Ma FpoN         FVYGATGTTSIPLIAANPGLLIENPIGLVAVVLLIAGFGFKMALVPFHMWAPDTYQGSPS 240
Mm FpoN         FVYGATGTTSIPLIAQNPGLLTGNPIGIVAIVLLTAGFGFKMALVPFHMWAPDTYQGSPS 240
Mb FpoN         FVYGATGTTSIPMIAENVSLLAENPIGLVAVVLLIAGFGFKMALVPFHMWAPDTYQGSPS 232

Ma FpoN         VVSALLAAGSKKMGFVAAFRIFIVALVALQPDWQFIFTILAVATMTFGNIVAVAQTSVKR 300
Mm FpoN         VVSALLAAGSKKMGFVAAFRVFIIALAALQPDWQFMFTLLAVVTMTFGNVVAVAQTSVKR 300
Mb FpoN         VVSSLLAAGSKKMGFVAAFRVFILALAALQPDWQFAFTILAVVTMTFGNVVAVSQTSVKR 292

Ma FpoN         MLAYSSVAQAGYIAMAFAVMTPVALGGGIMYALAHAFMKAGAFIAAGVVVWMVSQEKTGN 360
Mm FpoN         MLAYSSLAQAGYIAMAFAVMTPVALAGGIMYTLAHAFMKAGAFIAAAAVVWMITSEKTGN 360
Mb FpoN         MLAYSSLAQAGYIAMAFVVMTPMALTGGIFYTLAHAFMKGGAFIAAGAVVWMITTQRTGD 352
```

Figure 2.5 (cont.)

```
Ma FpoN          LDVPDHLDSFKGLGKRMPLAALSMTVFVFALAGIPPTAGFMAKFVLFSSTIQAGMAWLAV 420
Mm FpoN          LDIPDHLDSFRGLGKRMPLAALCMTVFVFALAGIPPTAGFMAKFVLFSSTIQAGMTWLAV 420
Mb FpoN          LQVPDHLDNFRGLGKRMPLVALCMTVFVFALAGIPLTSGFMAKFVLFSSTIQAGMTWLAV 412

Ma FpoN          IAILNSALSLFYYARLVRYMYFLPPEGK--SVSVPFPYAAALLVAVAGVLVMGIWPEPFV 478
Mm FpoN          IAILNSALSLFYYARLVKYMYFMPPEGKTEKVSIPFPYAAALLVAVAGVLVMGLWPEPFV 480
Mb FpoN          IAILNSALSLFYYARLVRYMYFLPPKGK--KIGLPFPYAAALLLATAGVLVMGLWPEPFL 470

Ma FpoN          ELAMKAAMVLV-- 489
Mm FpoN          ELAMKAAMVLVPF 493
Mb FpoN          QWAMEAAKVLI-- 481
```

14. FpoO

```
Ma FpoO1         MTDCDLCGKAIPTVIPVRVIRPLLKFAYPNGVWKGLCETCLDSAQKTYLEVNKNQPSCRK 60
Mm FpoO          MTDCDLCGKGIPTVIPVRTYPPLLRFAYPEGVWKGLCETCLDSAQKTYLEVNRNHTSCRR 60
Mb FpoO          MTDCDLCGRALPSVIPVRVFRSRLKFAYPEGIWKGLCEACLDSAQETYLSINKDEISCRR 60

Ma FpoO1         GKCALCGDKTGVFPVELQVPDFSKGIVKKDVDLCYRCLKGVDEAYIRHKKEQIEMEH--- 117
Mm FpoO          GKCSLCGSKTGVFSVELQIPDFSKGIVRKDVDVCYRCLKLVDEAYIRYKREQIEQDHEQG 120
Mb FpoO          NKCVLCGKKGRVYPVEIQIPDFSKGVVIKKVNVCTKCLDSINETYIRFKREQIEGSVCE- 119

Ma FpoO1         ---GYH----- 120
Mm FpoO          RIHGHEHVHPH 131
Mb FpoO          --HGHGNVPEH 128
```

15. FpoO1/O2

```
Ma FpoO1         MTDCDLCGKAIPTVIPVRVIRPLLKFAYPNGVWKGLCETCLDSAQKTYLEVNKNQPSCRK 60
Ma FpoO2         MSLLNPK----PDCILVRVVRPLLKFAYPNGVWKDLCETCLDSAQKTYLEANKNQPSCRK 56

Ma FpoO1         GKCALCGDKTGVFPVELQVPDFSKGIVKKDVDLCYRCLKGVDEAYIRHKKEQIEMEHGYH 120
Ma FpoO2         GKCALCGDKTGVFSVELQVPDFVLF---------------------------------- 81
```

Figure 2.5 F_{420}:phenazine oxidoreductase (Fpo) subunit alignments. Inferred protein sequences were aligned using ClustalW for each Fpo subunit from *M. barkeri* (Mb), *M. mazei* (Mm) and *M. acetivorans* (Ma). Green bases denote conserved amino acid residues. Red bases highlighted in yellow are proposed to coordinate iron-sulfur centers or bind the substrate methanophenazine (MP). Refer to text for Fpo sequence analysis.

Table 2.4 Pairwise percent identities[a] of *M. barkeri* (Mb) Fpo, *M. acetivorans* (Ma) Fpo, *M. mazei* (Mm) Fpo[b] and *E. coli* (Ec) Nuo predicted protein sequences

	Mb FpoF	Ma FpoF	Mm FpoF	Ec NuoF
Mb FpoF	-	86	88	Absent
Ma FpoF		-	89	
Mm FpoF			-	

	Mb FpoA	Ma FpoA	Mm FpoA	Ec NuoA
Mb FpoA	-	91	92	36
Ma FpoA		-	99	35
Mm FpoA			-	34

	Mb FpoB	Ma FpoB	Mm FpoB	Ec NuoB
Mb FpoB	-	88	85	37
Ma FpoB		-	92	38
Mm FpoB			-	40

	Mb FpoC	Ma FpoC	Mm FpoC	Ec NuoC
Mb FpoC	-	82	79	24
Ma FpoC		-	89	30
Mm FpoC			-	20

Table 2.4 (cont.)

	Mb FpoD	Ma FpoD	Mm FpoD	Ec NuoD
Mb FpoD	-	91	83	35
Ma FpoD		-	90	36
Mm FpoD			-	37

	Mb FpoH	Ma FpoH	Mm FpoH	Ec NuoH
Mb FpoH	-	83	77	38
Ma FpoH		-	86	39
Mm FpoH			-	39

	Mb FpoI	Ma FpoI	Mm FpoI	Ec NuoI
Mb FpoI	-	85	83	29
Ma FpoI		-	91	29
Mm FpoI			-	20

	Mb FpoJ	Ma FpoJ	Mm FpoJ	EcNuoJ
Mb FpoJ	-	81	81	21
Ma FpoJ		-	88	23
Mm FpoJ			-	21

Table 2.4 (cont.)

	Mb FpoK	Ma FpoK	Mm FpoK	Ec NuoK
Mb FpoK	-	92	90	38
Ma FpoK		-	97	37
Mm FpoK			-	35

	Mb FpoL	Ma FpoL	Mm FpoL	Ec NuoL
Mb FpoL	-	87	88	34
Ma FpoL		-	89	33
Mm FpoL			-	34

	Mb FpoM	Ma FpoM	Mm FpoM	Ec NuoM
Mb FpoM	-	88	85	30
Ma FpoM		-	88	31
Mm FpoM			-	30

	Mb FpoN	Ma FpoN	Mm FpoN	Ec NuoN
Mb FpoN	-	80	81	31
Ma FpoN		-	88	31
Mm FpoN			-	32

Table 2.4 (cont.)

	Mb FpoO	Ma FpoO1	Ma FpoO2	Mm FpoO
Mb FpoO	-	63	55	58
Ma FpoO1		-	79	80
Ma FpoO2			-	66
Mm FpoO				-

[a]ClustalW was used for determination of percent identity.
[b]Locus tags for genes encoding Fpo subunits are given in Figure 2.3.

Electrons from FpoF are probably channeled through the membrane-associated module of Fpo, Fpo BCDI, via three tetranuclear iron-sulfur clusters in FpoI and FpoB. Two of these [4Fe-4S] clusters are bound to FpoI by motifs, $C^{44}XXC^{47}XXC^{50}XXXC^{54}P$ and $C^{84}XXC^{87}XXC^{90}XXXC^{94}P$ (Figure 2.5), and are presumed to be analogous to the N6a and N6b clusters of Nuo of *Escheichia coli*. On the other hand, the third [4Fe-4S] cluster has been compared to the N2 cluster of Nuo of *E.coli* and probably binds FpoB via the motif, $C^{61}C^{62}XXEX_{60}C^{126}X_{29}C^{156}P$. All three [4Fe-4S] cluster binding motifs are well-conserved in the three *Methanosarcina* FpoI and FpoB subunits (3, 10, 11). These subunits show a high degree of amino acid sequence identity (>83%) among each other (Table 2.4). Although the amphipathic subunits FpoC and FpoD do not have well-defined functions, FpoD has been implicated in binding MP aromatic rings via the conserved glycine^{367} residue. FpoD also contains two conserved cysteines, C^{70} and C^{368}, which are reminiscent of its ancestral protein, the large subunit of [NiFe] hydrogenases that harbors these cysteines as Ni-

binding ligands (11) (Figure 2.5). Both the FpoC and FpoD subunits from the three *Methanosarcina* species show significant amino acid sequence identity of 80-90% (Table 2.4). Another Fpo subunit that has eluded characterization is the hydrophilic FpoO subunit. In *M. mazei*, FpoO contains a [2Fe-2S] binding motif,

A. *mer*/*fpoF* intergenic region

```
MmfpoFup        TAATTTTTATTACATCTTGCATAATCATTTTTTTTACGTTATATTTTTAAAA-------- 52
MafpoFup        TAATTTTTATTACATCTTGCATAATCATTTTTTTTACGTTATATTTTTAAAA-------- 52
MbfpoFup        TAAGTTT-ATTACATCCTGCATAAATTTTTTAATTTCATTGATTTTTTAATTTTTTATTT 59

MmfpoFup        -ACTTTTAAAAAAACATCTTGCCGTTAAGGCAAGCTTATCGAGGCATTGGAGGTAACTGAT 118
MafpoFup        -ACTTTTAAAAAAACATCTTGCCGTTAAGGCAAGCTTATCGAGGCATTGGAGGTAACTGAT 118
MbfpoFup        TATTTTTAAAAAAACATCTTGCCGTTAAGGCAAGCTTATCGAGGCATTGGAGGTAACTGAT 119

MmfpoFup        TG 120
MafpoFup        TG 120
MbfpoFup        TG 121
```

B. *fpoF*/downstream ORF intergenic region

```
Mmfpofdn        TGAAGTCCGAAACTTAATTTAAATTCAAAACTTAATTTAAATCCGAAACTTAATTCAAAA 60
MafpoFdn        TGAGACCAGAAGATATATCCAGAT--------------ATATCCAAAA-----------A 35
MbfpoFdn        TGAAATCAGAA--TATATCGAGAAT-------------AAAT----AA------------ 29

Mmfpofdn        AAGAAATATGGTACATTCGAGGTTGGA-TAC--GATG 94
MafpoFdn        GATAACCAGTACAAATTCGAGGTGGAA-TCCGGGATG 71
MbfpoFdn        --TAAATGTATT--GTTGGAGGTTGAAATACGGGATG 62
```

Figure 2.6 Alignment of regions flanking *fpoF*. ClustalW was used to align the intergenic region between methylenetetrahydrosarcinapterin reductase gene (*mer*) and *fpoF* (fpoFup, panel A) and between *fpoF* and putative cytidylyltransferase gene (fpoFdn, panel B). Green bases denote conserved amino acid residues. The annotated start and stop codons of genes are in red. The putative ribosome binding sites are in blue. Mb, *M. barkeri*; Mm, *M. mazei*; Ma, *M.acetivorans*.

$SC^{58}RXGXC^{63}SXC^{66}XXKX_{24}C^{94}$ (3) (Figure 2.5). The four cysteines of the motif that coordinate the iron-sulfur center are conserved in the other two *Methanosarcina* species. However, *M. acetivorans* is missing the serine[64] residue and *M. barkeri* the glycine[61] and serine[64] residues. *M. acetivorans* has an

additional copy of *fpoO* (*fpoO2*) that is *ca*. 3 kb downstream of the first copy in the *fpo* operon (*fpoO1*) (28) (Figure 2.3). Both FpoO subunits show 79% amino acid identity, however, FpoO2 is missing one of the cysteines (C^{94}) that coordinates the putative iron-sulfur cluster. The FpoO subunits from *M. mazei* and *M. acetivorans* show 80% amino acid identity, however, *M. barkeri* FpoO shows only *ca.* 60% identity to the other two FpoO subunits.

Electrons from FpoF through FpoI and then FpoB are thought to be transferred to the membrane-integral module of Fpo, FpoAHJKLMN, which uses them to reduce MP by a yet unknown mechanism (10). All hydrophobic Fpo subunits possess 77-99% amino acid sequence identity among the three *Methanosarcina* species (Table 2.4). Also, in all the species, FpoJ is encoded by two contiguous *fpoJ* genes, such that the first gene encodes a protein that is homologous to the amino terminus of NuoJ, while the second one encodes a protein that is homologous to the carboxyl-terminus of NuoJ (28). Interestingly, *M. acetivorans* Fpo has been proposed to contain a small additional subunit, FpoP, when grown on CO as the growth substrate (24). However, there is no experimental evidence that FpoP protein is produced, nor is the gene conserved in the other two *Methanosarcina* species (28). Thus it is still unknown if FpoP has a role in methanogenesis from any substrate.

In conclusion, the *in silico* analysis of Fpo predicted protein sequences from the three *Methanosarcina* species shows conservation of all important catalytic and structural residues in the proteins suggesting that like *M. mazei* Fpo, Fpo enzymes from *M. barkeri* and *M. acetivorans* might also be functional.

Further, each sequenced genome carries homologs of the *hdrDE* operon, which encodes the methanophenazine-linked heterodisulfide reductase (Figure 2.3) (13, 17, 27, 28). Thus, although biochemical activity has only been examined in *M. mazei*, functional $F_{420}H_2$:heterodisulfide oxidoreductase systems are probably present in each of the *Methanosarcina* species examined to date.

2.4.2 $F_{420}H_2$ dehydrogenase is not required for methanogenesis or growth in *M. barkeri*

As described above**,** *in vitro* biochemical experiments led to the suggestion that the $F_{420}H_2$:heterodisulfide oxidoreductase system should be essential for growth on C-1 compounds via the methylotrophic pathway. To test this *in vivo*, we constructed *M. barkeri* mutants lacking $F_{420}H_2$ dehydrogenase by deleting the *fpoA-O* operon or the *fpoF* gene (Table 2.3).

The Δ*fpoA-O* and Δ*fpoF* mutants were tested for their ability to grow on various methanogenic substrates (Table 2.5). As expected, both mutants grow on H_2/CO_2, methanol plus H_2/CO_2 and acetate with growth rates and yields similar to the isogenic parental strain. However, we were surprised to discover that growth of the mutants on methanol was also unaffected. Further, CH_4 and CO_2 were produced by the Δ*fpoA-O* and Δ*fpoF* mutants in the expected 3:1 stoichiometry in amounts and at rates similar to the parent on all substrates (Tables 2.6 & 2.7). Thus, loss of $F_{420}H_2$ dehydrogenase, and therefore of the $F_{420}H_2$:heterodisulfide oxidoreductase system, does not measurably affect methanogenesis or growth of *M. barkeri*.

Table 2.5 Generation time (h) and relative growth yield (%)[a] of *M. barkeri* Fusaro strains[b] in various media

Strain	Substrates			
	CH_3OH	CH_3OH + H_2/CO_2	H_2/CO_2	CH_3COOH
Δ***hpt***[c]	7.3±0.3 (100%)	5.7±0.1 (100%)	13.7±2.5 (100%)	37±3.4 (100%)
Δ***fpo***	7.3±0.2 (101%)	6.1±0.5 (100%)	11.9±0.9 (100%)	36±2.6 (100%)
Δ***fpoF***	7.3±0.2 (96%)	5.8±0.5 (96%)	12.4±1.2 (90%)	39±1.9 (84%)
Δ***fre***	7.7±0.3 (116%)	5.5±0.4 (125%)	8.8±0.8 (95%)	41±3.1 (84%)
Δ***frh***	13.7±0.6 (52%)	6.5±0.3 (80%)	NG (NA)	55±7.0 (84%)
Δ***fpo*** Δ***frh***	NG (NA)	5.0±0.3 (80%)	NG (NA)	NG (NA)
Δ***fpoF*** Δ***frh***	NG (NA)	6.4±0.4 (73%)	NG (NA)	76±0.8 (66%)

[a]Growth rate and yield were measured as described in Materials and Methods; growth yield is relative to the parental strain on the same substrate. Values represent the average and standard deviation of at least triplicate measurements.
[b]Strains used were WWM85 (Δ*hpt*), WWM71 (Δ*fpo*), WWM123 (Δ*fpoF*), WWM122 (Δ*frh*), WWM108 (Δ*fpo* Δ*frh*) and WWM145 (Δ*fpoF* Δ*frh*).
[c]*M. barkeri* Fusaro parent strain in which all deletions were constructed.
NG, no growth for at least 6 months of incubation.
NA, not applicable.

Table 2.6 Methane (μmol) and carbon dioxide (μmol) production[a] from resting cell suspensions of *M. barkeri* Fusaro strains[b]

	Substrates[c]							
	N_2		CH_3OH		CH_3OH /H_2		H_2/CO_2	
Strain	CH_4	CO_2	CH_4	CO_2	CH_4	CO_2	CH_4	CO_2
Δ***hpt***[d]	<1	2±0.1	343±4	108±2	465±17	<1	298±21	NA
Δ***fpo***	<1	1±0.1	365±3	115±1	494±11	<1	356±6	NA
Δ***fpoF***	<1	1±0.1	332±7	106±2	439±27	<1	359±9	NA
Δ***fre***	<1	1±0.1	399±14	133±4	508±66	<1	381±21	NA
Δ***frh***	<1	2±0.9	149±3	42±1	481±14	<1	7±2	NA
Δ***fpo*** Δ***frh***	<1	2±0.7	47±2	9±1	480±59	<1	10±1	NA
Δ***fpoF*** Δ***frh***	<1	4±0.1	54±3	16±1	465±9	<1	11±5	NA

[a]Values are the average and standard deviation of at least three trials.
[b]Strains used were WWM85 (Δ*hpt*), WWM71 (Δ*fpo*), WWM123 (Δ*fpoF*), WWM122 (Δ*frh*), WWM108 (Δ*fpo* Δ*frh*) and WWM145 (Δ*fpoF* Δ*frh*).
[c]Assays were conducted as described in Materials and Methods.
[d]*M. barkeri* Fusaro parent strain in which all deletions were constructed.
NA, not applicable (CO_2 produced could not be measured because it was added to headspace).

Table 2.7 Rate (nmol min^{-1} mg^{-1}) of methane production[a] from resting cell suspensions of *M. barkeri* Fusaro strains[b]

Strain	Substrate[c]		
	N_2	CH_3OH	CH_3OH /H_2
Δ***hpt***[d]	<1	70±6	121±35
Δ***fpo***	<1	93±13	127±29
Δ***fpoF***	<1	82±2	143±7
Δ***fre***	<1	95±13	134±32
Δ***frh***	<1	14±0.5	97±3
Δ***fpo*** Δ***frh***	<1	4±0.5	151±3
Δ***fpoF*** Δ***frh***	<1	4±0.1	135±15

[a]Values are the average and standard deviation of at least three trials.
[b]Strains used were WWM85 (Δ*hpt*), WWM71 (Δ*fpo*), WWM123 (Δ*fpoF*), WWM122 (Δ*frh*), WWM108 (Δ*fpo* Δ*frh*) and WWM145 (Δ*fpoF* Δ*frh*).
[c]Assays were conducted as described in Materials and Methods.
[d]*M. barkeri* Fusaro parent strain in which all deletions were constructed.

2.4.3 Frh is essential for growth of *M. barkeri* on H_2/CO_2 and plays an important role in the methylotrophic pathway

The dispensability of Fpo raises the question of which enzyme(s) transfers electrons from $F_{420}H_2$ to MP in the methylotrophic pathway. Because *M. barkeri* possesses a highly active F_{420}-reducing hydrogenase (Frh) (33), we considered the possibility of electrons being channeled from $F_{420}H_2$ into the H_2:heterodisulfide oxidoreductase system via production of H_2 by Frh (Figure 2.2).

The F_{420}-reducing hydrogenase couples oxidation of H_2 to F_{420} reduction *in vitro* and is fully reversible (9, 33, 52). *M. barkeri* has two operons, *frhADGB*

and *freAEGB*, with the potential to encode F_{420}-reducing hydrogenases (Figure 2.3) (51). It is unclear whether *freAEGB* encodes an active hydrogenase, because it lacks the required maturation protease, encoded by *frhD* in the homologous operon. Nevertheless, the putative *fre*-encoded hydrogenase shares all important catalytic and structural amino acid residues with the *frh*-encoded enzyme. Thus, *freAEGB* could encode a functional F_{420}-reducing hydrogenase if the FrhD protease can function *in trans* (18). The F_{420}-reducing hydrogenase is proposed to provide $F_{420}H_2$, which is needed for CO_2 reduction in the hydrogenotrophic pathway (Figure 2.1) (33); however, *frhADGB* and *freAEGB* are expressed during growth on both H_2/CO_2 and methanol (18, 51). Thus, it seems possible that these genes play a role in both the hydrogenotrophic and methylotrophic pathways.

To test this, the *freAEGB* or *frhADGB* operons were deleted from the chromosome of *M. barkeri* (Table 2.3) and the resulting mutants characterized. The Δ*fre* mutant is indistinguishable from its parent with respect to growth rate and yield on all substrates tested (Table 2.5). Further, deletion of *fre* from *M. barkeri* does not affect amount and rate of CH_4 produced in resting cell suspensions from the various substrates, nor does the mutation change the expected 3:1 ratio of CH_4 to CO_2 on methanol (Tables 2.6 & 2.7). These data indicate that Fre is not required for growth of *M. barkeri* on any of the substrates tested.

In contrast, the Δ*frh* mutation has severe phenotypic consequences on several of the growth media examined (Tables 2.5, 2.6 & 2.7). While the Δ*frh*

mutant is indistinguishable from its parent when grown on methanol plus H_2/CO_2 and acetate, it is unable to grow on H_2/CO_2. Moreover, the Δ*frh* mutant has a two-fold slower growth rate and a 50% reduction in growth yield when methanol alone is used as a substrate. The Δ*frh* mutant exhibits a very long lag phase of 911±21 hours (h) as compared to 31±0.4 h for wild-type *M. barkeri* on methanol. The growth defects of the Δ*frh* mutant are further reflected in CH_4 production. Resting cell suspensions of the Δ*frh* mutant produce negligible amounts of CH_4 from H_2/CO_2, and while they disproportionate methanol in the expected 3:1 ratio, they consistently produce only half as much CH_4 and CO_2 as the parent. Finally, the Δ*frh* mutation lowers rate of CH_4 production from methanol in resting cells *ca.* four-fold relative to the parent.

Taken together, these data indicate that Frh is essential for growth by the hydrogenotrophic pathway and plays an important, but dispensable, role in the methylotrophic pathway; the latter potentially being the delivery of electrons from $F_{420}H_2$ into the H_2:heterodisulfide oxidoreductase system. Importantly, Fre is not able to substitute for the role of Frh under the conditions tested, suggesting that it does not encode a functional F_{420}-reducing hydrogenase in the absence of *frhADGB*.

2.4.4 *M. barkeri* possesses two functional pathways for electron transfer from $F_{420}H_2$ to MP

The fact that the Δ*frh* mutant retains the ability to grow and produce CH_4 from methanol, although at reduced rates, suggests that the cell has an alternative, less efficient route to deliver electrons from $F_{420}H_2$ to the CoM-S-S-

CoB heterodisulfide. The most obvious candidate for this electron transfer pathway is the $F_{420}H_2$:heterodisulfide oxidoreductase system. To test this hypothesis, we constructed and characterized double mutants lacking *frhADGB* and either *fpoA-O* or *fpoF* (Tables 2.3, 2.5, 2.6 & 2.7).

Like the single Δ*frh* mutant, the Δ*fpoA-O* Δ*frh* and Δ*fpoF* Δ*frh* double mutants are unable to grow on H_2/CO_2 and produce negligible amounts of CH_4 in resting cell suspensions from this substrate. Both mutants are able to grow and produce CH_4 at levels and rates comparable to the parent on methanol plus H_2/CO_2. However, in contrast to the Δ*frh,* Δ*fpoA-O* and Δ*fpoF* single mutants, the double mutants are incapable of growth on methanol. Thus, Frh and Fpo fulfill a similar role during growth on this substrate that is lost in the absence of both enzymes. Quantitative RT-PCR experiments show that although *fpoA-O* transcripts levels are slightly higher in the Δ*frh* mutant (3.9±1.5 fold), they are easily detectable in the parental strain (Δ*hpt*, WWM85), Δ*fpoF* and Δ*fre* (Table 2.8). Therefore, Fpo is expressed and has the potential to contribute to the methylotrophic electron transport chain in wild-type *M. barkeri* as well. Interestingly, the Δ*fpoA-O* Δ*frh* and Δ*fpoF* Δ*frh* mutants still produce small amounts of CH_4 and CO_2 from methanol despite their inability to grow on this substrate. Hence, an additional minor electron transport pathway(s) exists in *M. barkeri* that is incapable of supporting growth.

Surprisingly, the double mutants display different phenotypes when grown on acetate. The Δ*fpoF* Δ*frh* mutant grows slowly on acetate, whereas the Δ*fpoA-O* Δ*frh* mutant is unable to utilize acetate. It is unclear how absence of both Fpo

and Frh affects growth on acetate because neither the Δ*fpoA-O* nor the Δ*frh* single mutant exhibits a growth defect on this substrate. These data seem to suggest that the input module of Fpo (FpoF) can be dispensable under conditions in which the proton-pumping methanophenazine oxidoreductase (FpoABCDHIJKLMNO) is not.

Table 2.8 Relative abundance of *fpoA-O* transcript[a] in methanol grown *M. barkeri* Fusaro mutants[b] as compared to the parent strain

Strain	Fold-expression[c]
Δ***fpo***	0
Δ***fpoF***	1.7±0.6
Δ***fre***	1.4±0.4
Δ***frh***	3.9±1.5
Δ***fpo*** Δ***frh***	NG
Δ***fpoF*** Δ***frh***	NG

[a] Values are expressed as mRNA in the given strain/mRNA in the parent strain (WWM85) and represent average and standard error of three independent biological replicates measured in triplicates.
[b]Strains used were WWM85 (Δ*hpt*), WWM71 (Δ*fpo*), WWM123 (Δ*fpoF*), WWM122 (Δ*frh*), WWM108 (Δ*fpo* Δ*frh*) and WWM145 (Δ*fpoF* Δ*frh*).
[C]Experiment was conducted and calculations were done as described in Materials and Methods. NG, no growth.

2.5 DISCUSSION

Methanosarcina species have proven to be exceptional model organisms for genetic analysis of methanogenesis (19, 32, 54, 55), an approach that modified our concept of energy conservation in *M. barkeri*. The data presented here indicate that *M. barkeri* has two distinct energy-conserving electron

transport pathways during growth via the methylotrophic methanogenic pathway (Figure 2.2). Contrary to expectations, *M. barkeri* apparently prefers to transfer electrons obtained from C-1 compound oxidation to the H_2:heterodisulfide oxidoreductase system via H_2, rather than to transfer them directly into the $F_{420}H_2$:heterodisulfide oxidoreductase system. Our results suggest that the cytoplasmic F_{420}-reducing hydrogenase (Frh) mediates electron transfer to H_2 via oxidation of $F_{420}H_2$, which, along with Fd_{red}, is the direct product of C-1 compound oxidation (33, 52). When the cells lose the ability to produce H_2 via this route, growth on methanol is severely affected, with reduction in the rates of growth and CH_4 production, as well as reduction in total growth yield and amount of CH_4 produced. We suggest that the H_2 diffuses out of the cell where it enters the H_2:heterodisulfide oxidoreductase system via methanophenazine-dependent hydrogenase (Vht or Vhx (18)), whose active site is known to be in the periplasm (10). Because production of H_2 by Frh consumes protons within the cytoplasm, while oxidation of H_2 by Vht/Vhx releases protons outside the cell, this electron transport chain is capable of establishing a proton gradient across the membrane that can be used to generate ATP by the ATP synthase (35), thus conserving energy via a H_2-cycling mechanism (37). *M. barkeri* genome harbors two operons, *vhtGACD* and *vhxGAC*, that can potentially encode methanophenazine–dependent hydrogenases. Analogous to the *fre* operon, the *vhx* operon lacks gene D that encodes the hydrogenase maturation protease and therefore may not encode a functional hydrogenase. However, Vhx shares all important catalytic and structural amino acid residues with Vht and could encode

an active methanophenazine-dependent hydrogenase if the VhtD protease can function *in trans* (18).

H_2-cycling, as a mechanism of energy conservation, was first proposed in sulfate-reducing bacteria (37). Later, it was also proposed in other anaerobic organisms like *Acetobacterium woodii* (38) and *Geobacter sulfurreducens* (8). Based on the production of H_2 during growth of *Methanosarcina* species on methylated substrates like methanol, trimethylamine and acetate, H_2-cycling was also suggested to occur in *Methanosarcina* (26). Experimental support for H_2-cycling has been provided in *Desulfovibrio vulgaris*, wherein simultaneous production and consumption of H_2 were detected during metabolism of pyruvate and sulfate (41). Also, suppression of a *D. vulgaris* H_2-evolving hydrogenase led to reduced growth rates on lactate and sulfate, suggesting the importance of H_2 production in growth (50). Nevertheless, the H_2-cycling theory is not universally accepted and several lines of evidence have been used to argue that this mechanism is unlikely (reviewed in (36)). For example, high concentrations of H_2 do not inhibit lactate oxidation in sulfate-reducing bacteria (40), nor does a mutation that blocks use of H_2 prevent growth on lactate (39). Further, the idea that the cell would preferentially transfer electrons to a molecule that can freely diffuse away from the cell seems highly problematic.

The data presented here suggest a way to reconcile these conflicting views. While *M. barkeri* apparently prefers to transfer electrons via H_2, they remain capable of using the $F_{420}H_2$:heterodisulfide oxidoreductase system when the ability to produce cytoplasmic H_2 is lost. Thus, *M. barkeri* employs a

branched electron transport chain with most electrons flowing from $F_{420}H_2$ into the H_2:heterodisulfide oxidoreductase system via H_2, but with some fraction flowing directly into the $F_{420}H_2$:heterodisulfide oxidoreductase system. A similar branched electron transport chain in sulfate reducers would explain the results cited above as arguing against H_2-cycling without invalidating the model. It should be noted that a recently proposed metabolic model for *D. vulgaris* suggests just such a branched electron transport chain (36).

Why then is H_2-cycling pathway the preferred electron transport chain in *M. barkeri*? Because the initial electron donor ($F_{420}H_2$) and final electron acceptor (MP) are the same, the amount of energy available from the two electron transport schemes must be identical. Experimental measurements suggest that electron transfer from $F_{420}H_2$ to CoM-S-S-CoB via Fpo and Hdr is accompanied by translocation of four protons across the membrane (3). Similarly, flow of electrons from $F_{420}H_2$ to MP via Frh and Vht/Vhx leads to translocation of two protons across the membrane by virtue of the H_2-cycling mechanism, while electron transfer from MPH_2 to CoM-S-S-CoB translocates another two protons (22). Thus, the magnitude of proton motive force generated should be identical via either route, Figure 2.2. In contrast, the rate of CH_4 production from methanol in resting cell suspensions of Δ*frh* mutant is *ca*. four times slower than that of Δ*fpoA-O* and Δ*fpoF* mutants. This indicates that H_2-cycling is a much faster mechanism of energy conservation and, as observed in our mutant strains, allows correspondingly faster growth rates. The biochemical properties of the enzymes involved are remarkably consistent with our *in vivo* data. Thus,

FpoBCDIF (Molecular weight, MW = 135.1 kDa (3)) purified from *M. mazei* catalyzes $F_{420}H_2$ oxidation with a turnover number (K_{cat}) of 38 s^{-1} and catalytic efficiency (K_{cat}/K_m) of 5.4 x 10^6 M^{-1} s^{-1} (1). Whereas, FrhAGB (MW = 194.4 kDa (51)) purified from *M. barkeri* catalyzes H_2 oxidation using F_{420} as the electron acceptor with a K_{cat} of 134 s^{-1} and K_{cat}/K_m of 4.4 x 10^7 M^{-1} s^{-1} (33). Because methanol-metabolizing *M. barkeri* cells have been shown to maintain ratios of $F_{420}H_2$ and F_{420} in thermodynamic equilibrium with the H_2 partial pressure (9), it is reasonable to assume that Frh catalyzes the reverse reaction ($F_{420}H_2$ oxidation) with similar efficiency as the forward reaction (H_2 oxidation). Therefore the turnover number of Frh is *ca.* four times higher than Fpo for $F_{420}H_2$ oxidation, implying that Frh is faster in catalyzing this reaction than Fpo.

A variety of data indicate that H_2-cycling is important to many, but not all *Methanosarcina* species. Growth of *M. barkeri* on acetate involves the obligate intermediacy of H_2 (32). Thus, in combination with the data presented here, it seems likely that this species prefers to use H_2 cycling for all soluble substrates. The situation is probably similar in *M. mazei* as it has functional Frh, Vht and Fpo enzymes as well (3). However, methylotrophic species like *M. acetivorans* (17-19), *Methanolobus tindarius* (21, 46) and *Methanococcoides burtonii* (45) do not encode functional hydrogenases (28). Hence, these organisms probably rely exclusively on the $F_{420}H_2$:heterodisulfide oxidoreductase system for energy conservation. It has previously been suggested that these organisms forego H_2-dependent electron transport pathways due to their high-salt marine habitat, wherein they exist as disaggregated single cells and would be prone to lose the

freely diffusible H_2 gas to competing organisms. In contrast, freshwater organisms like *M. barkeri* that exist as large multicellular aggregates, have a higher chance of retaining H_2 gas within the aggregates, enabling them to use it as an electron carrier (19).

Lastly, the phenotypes of the mutants constructed here also provide insight into the metabolism of H_2/CO_2 and acetate by *M. barkeri*. Due to its ability to catalyze F_{420} reduction with H_2, F_{420}-reducing hydrogenase was proposed to provide $F_{420}H_2$ for reduction of methenyl-H_4SPT (tetrahydrosarcinapterin) and methylene-H_4SPT in the hydrogenotrophic pathway (Figure 2.1) (33, 48). The inability of the *frh* mutants to grow on H_2/CO_2 provides direct experimental support for this proposal. Interestingly, the putative *fre*-encoded hydrogenase cannot substitute for the *frh*-encoded hydrogenase. This may be due to low expression of *fre*, absence of post-translational processing, mutations in structural or catalytic residues, or some combination of these (18). Nevertheless, the dispensability of *fre* in *M. barkeri* is not surprising because *M. mazei* lacks the *fre* opeon and is able to grow via all four methanogenic pathways (10, 18). Thus, the role of Fre in *M. barkeri* remains mysterious.

Methanogenesis from acetate does not require either Frh or Fpo; however, our results show that one of the two enzymes, but not both, is needed for growth on this substrate. We previously showed that mutations in the C-1 oxidation pathway prevent growth on acetate, presumably by blocking the production of reducing equivalents needed for biosynthetic reactions (55). The lack of growth of the Δ*frh* Δ*fpo* double mutant on acetate medium suggests that

these reducing equivalents must flow through either Frh or Fpo to allow growth. Interestingly, the Δ*frh* Δ*fpoF* double mutant is able to grow on acetate. This clearly suggests that the membrane-bound proton-pumping module has the ability to accept electrons from input modules other than FpoF. In this regard, FpoF is homologous to the β-subunit (B) of F_{420}-reducing hydrogenases, and shares a common substrate: coenzyme F_{420} (3, 51). It is conceivable that in the absence of FpoF and FrhB, FreB serves as the input module, thus channeling electrons from $F_{420}H_2$ to Fpo and allowing growth of Δ*frh* Δ*fpoF* double mutant on acetate; however, this remains to be tested.

2.6 LITERATURE CITED

1. **Abken, H. J., and U. Deppenmeier.** 1997. Purification and properties of an $F_{420}H_2$ dehydrogenase from *Methanosarcina mazei* Gö1. FEMS Microbiology Letters **154:**231-237.

2. **Ausubel, F. M., R. Brent, R. E. Kingston, D. D. Moore, J. G. Seidman, J. A. Smith, and K. Strhul.** 1992. Current protocols in molecular biology. John Wiley & Sons, New York.

3. **Baumer, S., T. Ide, C. Jacobi, A. Johann, G. Gottschalk, and U. Deppenmeier.** 2000. The $F_{420}H_2$ dehydrogenase from *Methanosarcina mazei* is a Redox-driven proton pump closely related to NADH dehydrogenases. J Biol Chem **275:**17968-73.

4. **Baumer, S., S. Lentes, G. Gottschalk, and U. Deppenmeier.** 2002. Identification and analysis of proton-translocating pyrophosphatases in the methanogenic archaeon *Methansarcina mazei*. Archaea **1:**1-7.

5. **Baumer, S., E. Murakami, J. Brodersen, G. Gottschalk, S. W. Ragsdale, and U. Deppenmeier.** 1998. The $F_{420}H_2$:heterodisulfide oxidoreductase system from *Methanosarcina* species. 2-Hydroxyphenazine mediates electron transfer from $F_{420}H_2$ dehydrogenase to heterodisulfide reductase. FEBS Lett **428:**295-8.

6. **Boccazzi, P., J. K. Zhang, and W. W. Metcalf.** 2000. Generation of dominant selectable markers for resistance to pseudomonic acid by cloning and mutagenesis of the *ileS* gene from the archaeon *Methanosarcina barkeri* Fusaro. J Bacteriol **182:**2611-8.

7. **Bradford, M. M.** 1976. A rapid and sensitive method for the quantitation of microgram quantities of protein utilizing the principle of protein-dye binding. Anal Biochem **72:**248-54.

8. **Coppi, M. V.** 2005. The hydrogenases of *Geobacter sulfurreducens*: a comparative genomic perspective. Microbiology **151:**1239-54.

9. **de Poorter, L. M., W. J. Geerts, and J. T. Keltjens.** 2005. Hydrogen concentrations in methane-forming cells probed by the ratios of reduced and oxidized coenzyme F_{420}. Microbiology **151:**1697-705.

10. **Deppenmeier, U.** 2004. The membrane-bound electron transport system of *Methanosarcina* species. J Bioenerg Biomembr **36:**55-64.

11. **Deppenmeier, U.** 2002. The unique biochemistry of methanogenesis. Prog Nucleic Acid Res Mol Biol **71:**223-83.

12. **Deppenmeier, U., M. Blaut, A. Mahlmann, and G. Gottschalk.** 1990. Reduced coenzyme F_{420}: heterodisulfide oxidoreductase, a proton-translocating redox system in methanogenic bacteria. Proc Natl Acad Sci U S A **87:**9449-53.

13. **Deppenmeier, U., A. Johann, T. Hartsch, R. Merkl, R. A. Schmitz, R. Martinez-Arias, A. Henne, A. Wiezer, S. Baumer, C. Jacobi, H. Bruggemann, T. Lienard, A. Christmann, M. Bomeke, S. Steckel, A. Bhattacharyya, A. Lykidis, R. Overbeek, H. P. Klenk, R. P. Gunsalus, H. J. Fritz, and G. Gottschalk.** 2002. The genome of *Methanosarcina mazei*: evidence for lateral gene transfer between bacteria and archaea. J Mol Microbiol Biotechnol **4:**453-61.

14. **Deppenmeier, U., and V. Muller.** 2008. Life close to the thermodynamic limit: how methanogenic archaea conserve energy. Results Probl Cell Differ **45:**123-52.

15. **Deppenmeier, U., V. Muller, and G. Gottschalk.** 1996. Pathways of energy conservation in methanogenic archaea. Arch Microbiol **165:**149-163.

16. **Ferry, J. G.** 1992. Methane from acetate. J Bacteriol **174:**5489-95.

17. **Galagan, J. E., C. Nusbaum, A. Roy, M. G. Endrizzi, P. Macdonald, W. FitzHugh, S. Calvo, R. Engels, S. Smirnov, D. Atnoor, A. Brown, N. Allen, J. Naylor, N. Stange-Thomann, K. DeArellano, R. Johnson, L. Linton, P. McEwan, K. McKernan, J. Talamas, A. Tirrell, W. Ye, A. Zimmer, R. D. Barber, I. Cann, D. E. Graham, D. A. Grahame, A. M. Guss, R. Hedderich, C. Ingram-Smith, H. C. Kuettner, J. A. Krzycki, J. A. Leigh, W. Li, J. Liu, B. Mukhopadhyay, J. N. Reeve, K. Smith, T. A. Springer, L. A. Umayam, O. White, R. H. White, E. Conway de Macario, J. G. Ferry, K. F. Jarrell, H. Jing, A. J. Macario, I. Paulsen, M. Pritchett, K. R. Sowers, R. V. Swanson, S. H. Zinder, E. Lander, W. W. Metcalf, and B. Birren.** 2002. The genome of *M. acetivorans* reveals extensive metabolic and physiological diversity. Genome Res **12:**532-42.

18. **Guss, A. M., G. Kulkarni, and W. W. Metcalf.** 2009. Differences in hydrogenase gene expression between *Methanosarcina acetivorans* and *Methanosarcina barkeri*. J Bacteriol **191:**2826-33.

19. **Guss, A. M., B. Mukhopadhyay, J. K. Zhang, and W. W. Metcalf.** 2005. Genetic analysis of *mch* mutants in two *Methanosarcina* species demonstrates multiple roles for the methanopterin-dependent C-1 oxidation/reduction pathway and differences in H(2) metabolism between closely related species. Mol Microbiol **55:**1671-80.

20. **Guss, A. M., M. Rother, J. K. Zhang, G. Kulkarni, and W. W. Metcalf.** 2008. New methods for tightly regulated gene expression and highly efficient chromosomal integration of cloned genes for *Methanosarcina* species. Archaea **2:**193-203.

21. **Haase, P., U. Deppenmeier, M. Blaut, and G. Gottschalk.** 1992. Purification and characterization of $F_{420}H_2$-dehydrogenase from *Methanolobus tindarius*. Eur J Biochem **203:**527-31.

22. **Ide, T., S. Baumer, and U. Deppenmeier.** 1999. Energy conservation by the H2:heterodisulfide oxidoreductase from Methanosarcina mazei Go1: identification of two proton-translocating segments. J Bacteriol **181:**4076-80.

23. **Kridelbaugh, D. M., and W. W. Metcalf.** Unpublished data.

24. **Lessner, D. J., L. Li, Q. Li, T. Rejtar, V. P. Andreev, M. Reichlen, K. Hill, J. J. Moran, B. L. Karger, and J. G. Ferry.** 2006. An unconventional pathway for reduction of CO_2 to methane in CO-grown *Methanosarcina acetivorans* revealed by proteomics. Proc Natl Acad Sci U S A **103:**17921-6.

25. **Li, F., J. Hinderberger, H. Seedorf, J. Zhang, W. Buckel, and R. K. Thauer.** 2008. Coupled ferredoxin and crotonyl coenzyme A (CoA) reduction with NADH catalyzed by the butyryl-CoA dehydrogenase/Etf complex from *Clostridium kluyveri*. J Bacteriol **190:**843-50.

26. **Lovley, D. R., and J. G. Ferry.** 1985. Production and Consumption of H(2) during Growth of *Methanosarcina* spp. on Acetate. Appl Environ Microbiol **49:**247-249.

27. **Maeder, D. L., I. Anderson, T. S. Brettin, D. C. Bruce, P. Gilna, C. S. Han, A. Lapidus, W. W. Metcalf, E. Saunders, R. Tapia, and K. R. Sowers.** 2006. The *Methanosarcina barkeri* genome: comparative analysis with *Methanosarcina acetivorans* and *Methanosarcina mazei* reveals extensive rearrangement within methanosarcinal genomes. J Bacteriol **188:**7922-31.

28. **Markowitz, V. M., E. Szeto, K. Palaniappan, Y. Grechkin, K. Chu, I. M. Chen, I. Dubchak, I. Anderson, A. Lykidis, K. Mavromatis, N. N. Ivanova, and N. C. Kyrpides.** 2008. The integrated microbial genomes (IMG) system in 2007: data content and analysis tool extensions. Nucleic Acids Res **36:**D528-33.

29. **Metcalf, W. W., J. K. Zhang, E. Apolinario, K. R. Sowers, and R. S. Wolfe.** 1997. A genetic system for Archaea of the genus *Methanosarcina*: liposome-mediated transformation and construction of shuttle vectors. Proc Natl Acad Sci U S A **94:**2626-31.

30. **Metcalf, W. W., J. K. Zhang, X. Shi, and R. S. Wolfe.** 1996. Molecular, genetic, and biochemical characterization of the *serC* gene of *Methanosarcina barkeri* Fusaro. J Bacteriol **178:**5797-802.

31. **Meuer, J., S. Bartoschek, J. Koch, A. Kunkel, and R. Hedderich.** 1999. Purification and catalytic properties of Ech hydrogenase from *Methanosarcina barkeri*. Eur J Biochem **265:**325-35.

32. **Meuer, J., H. C. Kuettner, J. K. Zhang, R. Hedderich, and W. W. Metcalf.** 2002. Genetic analysis of the archaeon *Methanosarcina barkeri* Fusaro reveals a central role for Ech hydrogenase and ferredoxin in methanogenesis and carbon fixation. Proc Natl Acad Sci U S A **99:**5632-7.

33. **Michel, R., C. Massanz, S. Kostka, M. Richter, and K. Fiebig.** 1995. Biochemical characterization of the 8-hydroxy-5-deazaflavin-reactive hydrogenase from *Methanosarcina barkeri* Fusaro. Eur J Biochem **233:**727-35.

34. **Miller, V. L., and J. J. Mekalanos.** 1988. A novel suicide vector and its use in construction of insertion mutations: osmoregulation of outer membrane proteins and virulence determinants in *Vibrio cholerae* requires toxR. J Bacteriol **170:**2575-83.

35. **Muller, V.** 2004. An exceptional variability in the motor of archael A_1A_O ATPases: from multimeric to monomeric rotors comprising 6-13 ion binding sites. J Bioenerg Biomembr **36:**115-25.

36. **Noguera, D. R., G. A. Brusseau, B. E. Rittmann, and D. A. Stahl.** 1998. A unified model describing the role of hydrogen in the growth of *Desulfovibrio vulgaris* under different environmental conditions. Biotechnol Bioeng **59:**732-46.

37. **Odom, J. M., and H. D. Peck, Jr.** 1981. Hydrogen cycling as a general mechanism for energy coupling in the sulfate-reducing bacteria, *Desulfovibrio* sp. FEMS Microbiology Letters **12:**47-50.

38. **Odom, J. M., and H. D. Peck, Jr.** 1984. Hydrogenase, electron-transfer proteins, and energy coupling in the sulfate-reducing bacteria *Desulfovibrio*. Annu Rev Microbiol **38:**551-92.

39. **Odom, J. M., and J. D. Wall.** 1987. Properties of a hydrogen-inhibited mutant of *Desulfovibrio desulfuricans* ATCC 27774. J Bacteriol **169:**1335-7.

40. **Pankhania, I. P., L. A. Gow, and W. A. Hamilton.** 1986. The effect of hydrogen on the growth of *Desulfovibrio vulgaris* (Hildenborough) on lactate. Journal of General Microbiology **132:**3349-3356.

41. **Peck, Jr., H. D., J. LeGall, P. A. Lespinat, Y. Berlier, and G. Fauque.** 1987. A direct demonstration of hydrogen cycling by *Desulfovibrio vulgaris* employing membrane-inlet mass spectrometry. FEMS Microbiol Lett **40:**295-299.

42. **Possot, O., P. Gernhardt, A. Klein, and L. Sibold.** 1988. Analysis of drug resistance in the archaebacterium *Methanococcus voltae* with respect to potential use in genetic engineering. Appl Environ Microbiol **54:**734-40.

43. **Pritchett, M. A., J. K. Zhang, and W. W. Metcalf.** 2004. Development of a markerless genetic exchange method for *Methanosarcina acetivorans* C2A and its use in construction of new genetic tools for methanogenic archaea. Appl Environ Microbiol **70:**1425-33.

44. **Reeve, J. N.** 1992. Molecular biology of methanogens. Annu Rev Microbiol **46:**165-91.

45. **Saunders, N. F., T. Thomas, P. M. Curmi, J. S. Mattick, E. Kuczek, R. Slade, J. Davis, P. D. Franzmann, D. Boone, K. Rusterholtz, R. Feldman, C. Gates, S. Bench, K. Sowers, K. Kadner, A. Aerts, P. Dehal, C. Detter, T. Glavina, S. Lucas, P. Richardson, F. Larimer, L. Hauser, M. Land, and R. Cavicchioli.** 2003. Mechanisms of thermal adaptation revealed from the genomes of the Antarctic Archaea *Methanogenium frigidum* and *Methanococcoides burtonii*. Genome Res **13:**1580-8.

46. **Scheel, E., and G. Schafer.** 1990. Chemiosmotic energy conversion and the membrane ATPase of *Methanolobus tindarius*. Eur J Biochem **187:**727-35.

47. **Sowers, K. R., J. E. Boone, and R. P. Gunsalus.** 1993. Disaggregation of *Methanosarcina* spp. and Growth as Single Cells at Elevated Osmolarity. Appl Environ Microbiol **59:**3832-3839.

48. **Thauer, R. K., R. Hedderich, and R. Fischer.** 1993. Methanogenesis. Chapman and Hall, New York.

49. **Thauer, R. K., A. K. Kaster, H. Seedorf, W. Buckel, and R. Hedderich.** 2008. Methanogenic archaea: ecologically relevant differences in energy conservation. Nat Rev Microbiol **6:**579-91.

50. **van den Berg, W. A., W. M. van Dongen, and C. Veeger.** 1991. Reduction of the amount of periplasmic hydrogenase in *Desulfovibrio vulgaris* (Hildenborough) with antisense RNA: direct evidence for an important role of this hydrogenase in lactate metabolism. J Bacteriol **173:**3688-94.

51. **Vaupel, M., and R. K. Thauer.** 1998. Two F_{420}-reducing hydrogenases in *Methanosarcina barkeri*. Arch Microbiol **169:**201-5.

52. **Vignais, P. M., B. Billoud, and J. Meyer.** 2001. Classification and phylogeny of hydrogenases. FEMS Microbiol Rev **25:**455-501.

53. **Wanner, B. L.** 1986. Novel regulatory mutants of the phosphate regulon in *Escherichia coli* K-12. J Mol Biol **191:**39-58.

54. **Welander, P. V., and W. W. Metcalf.** 2005. Loss of the *mtr* operon in *Methanosarcina* blocks growth on methanol, but not methanogenesis, and reveals an unknown methanogenic pathway. Proc Natl Acad Sci U S A **102:**10664-9.

55. **Welander, P. V., and W. W. Metcalf.** 2008. Mutagenesis of the C1 oxidation pathway in *Methanosarcina barkeri*: new insights into the Mtr/Mer bypass pathway. J Bacteriol **190:**1928-36.

56. **Zhang, J. K., A. K. White, H. C. Kuettner, P. Boccazzi, and W. W. Metcalf.** 2002. Directed mutagenesis and plasmid-based complementation in the methanogenic archaeon *Methanosarcina acetivorans* C2A demonstrated by genetic analysis of proline biosynthesis. J Bacteriol **184:**1449-54.

CHAPTER 3

DEMONSTRATION OF HYDROGEN CYCLING DURING ELECTRON TRANSPORT IN *METHANOSARCINA BARKERI*

3.1 ABSTRACT

In the preceding Chapter, *M. barkeri* was proposed to utilize the "H_2-cycling" mechanism for energy conservation during methylotrophic growth. Here, we provide direct experimental evidence for this proposal. The H_2-cycling pathway presumably involves two hydrogenases, the cytoplasmic F_{420}-dependent hydrogenase (Frh) that produces H_2 from reduced coenzyme F_{420} ($F_{420}H_2$) within the cytosol, and the periplasmic methanophenazine-dependent hydrogenase (Vht) that consumes this H_2 within the periplasm to feed it into *M. barkeri* electron transport chain. Consistent with this role of Vht, we were unable to isolate a deletion mutant of the *vht* operon. Furthermore, a tetracycline-regulated conditional *vht* mutant is not able to grow using any of the methanogenic substrates tested, under non-permissive conditions. This suggests that Vht is essential for growth of wild-type *M. barkeri.* Repression of *vht* expression led to a rapid increase in H_2 partial pressure, which is consistent with a requirement for Vht in H_2 uptake. Moreover, H_2 accumulation also coincided with cessation of methanogenesis and growth, suggesting that H_2 uptake is essential for anaerobic respiration and viability. In contrast, Vht is not essential in mutants lacking the H_2-producing, cytoplasmic Frh. This is consistent with functional coupling of Frh and Vht hydrogenases in the H_2-cycling mechanism. Because production of H_2 by Frh consumes protons within the cytoplasm, whereas, oxidation of H_2 by Vht

releases protons outside the cell, this electron transport chain is capable of establishing a trans-membrane proton gradient that can be used to make ATP by the ATP synthase.

3.2 INTRODUCTION

Adenosine triphosphate (ATP) is the universal energy currency of cells. It is synthesized in two ways, substrate-level or electron-transport mediated phosphorylation of adenosine diphosphate (ADP). In the former, ATP is made in the cytosol using molecules with a high group transfer potential like acetyl-phosphate (51). The latter involves generation of a trans-membrane electrochemical ion (usually proton) gradient that can be used directly as a source of energy or indirectly by conversion to ATP using an ATP synthase. A proton gradient is created during electron transfer in either of the two ways: vectorial pumping of protons outside the cell or their scalar movement across the membrane due to consumption of protons within the cell and production outside it, as in a quinone-loop (52).

In 1981, Odom and Peck proposed a novel method of energy conservation, called H_2-cycling (36). In this, H_2 is produced by a cytoplasmic hydrogenase using protons within the cytosol. Subsequently, the H_2 diffuses to a periplasmic hydrogenase, where it is oxidized to regenerate protons. This creates a trans-membrane proton gradient that can be used to make ATP. Although H_2-cycling has been suggested to occur in a number of anaerobic organisms (8, 24, 36, 37), evidence in favor of the theory is limited and indirect. It includes

demonstration of simultaneous production and consumption of H_2 using membrane-inlet mass spectrometry during metabolism of pyruvate and sulfate by *Desulfovibrio vulgaris* (40). Also, reduction in growth rate of *D. vulgaris* on lactate and sulfate, due to reduced expression of the H_2-evolving hydrogenase, has been observed (49). However, these supporting data have been clouded by conflicting reports, wherein, neither high concentrations of H_2 (39), nor a block in H_2 utilization inhibits lactate oxidation in sulfate-reducing bacteria (38). Thus, till date there is no direct experimental evidence for H_2-cycling. Moreover, energy conservation using a diffusible molecule as an essential intermediate is considered highly implausible.

The methanogen, *Methanosarcina*, conserves energy via electron-transport mediated phosphorylation. Two electron transport chains have been identified in *Methanosarcina* species, H_2:heterodisulfide and $F_{420}H_2$:heterodisulfide oxidoreductase systems (Figure 3.1). These involve electron transfer from H_2 or $F_{420}H_2$ to a heterodisulfide (CoM-S-S-CoB) of coenzyme M (CoM-SH) and coenzyme B (CoB-SH) (reviewed in (10, 11)). On the basis of biochemical evidence, $F_{420}H_2$:heterodisulfide oxidoreductase system was presumed to be utilized in the methylotrophic electron transport chain (3, 4, 13). However, evidence presented in Chapter 2 suggested that *M. barkeri* preferentially employs H_2-cycling during methylotrophic growth (22). In the $F_{420}H_2$:heterodisulfide system, the $F_{420}H_2$ dehydrogenase (Fpo) is used for $F_{420}H_2$ oxidation, whereas, in the H_2:heterodisulfide system, methanophenazine (MP)-dependent hydrogenase is used to oxidize H_2. The deletion of *fpo* in *M. barkeri*

has no phenotypic consequences on any methanogenic substrate tested. Instead, a knockout of *frh* that is unable to synthesize the F_{420}-reducing hydrogenase (Frh), displays severe growth defect on methanol. The Frh

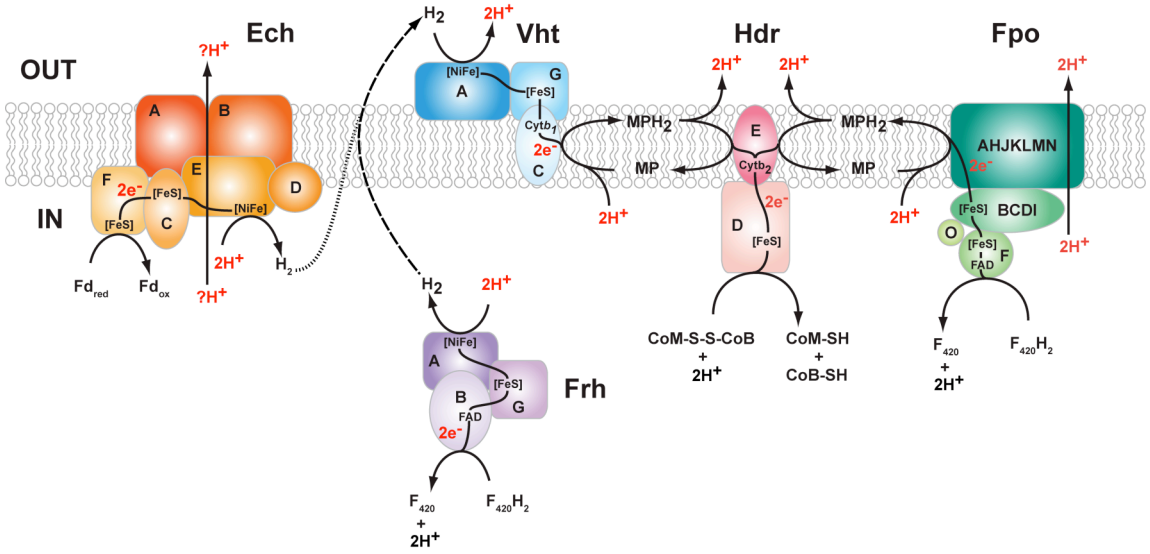

Figure 3.1 The electron transport chain of *Methanosarcina barkeri* (adapted from (24)) has been proposed to comprise two energy-conservation systems, the $F_{420}H_2$:heterodisulfide oxidoreductase and the H_2:heterodisulfide oxidoreductase. In the former, $F_{420}H_2$ is oxidized by FpoF releasing two electrons that are transferred through FpoBCDI and then FpoAHJKLMN to membrane-soluble MP. This reaction is coupled to pumping of two protons outside the cell. Reduction of MP consumes two protons from the cytoplasm, which are subsequently released outside the cell upon oxidation of MPH_2. The electrons are then transferred through HdrED to reduce CoM-S-S-CoB with two protons from the cytoplasm. Alternatively, in the H_2:heterodisulfide oxidoreductase, H_2 is oxidized by Vht to produce two protons outside the cell and two electrons that are transferred to MP, which is then used to reduce CoM-S-S-CoB. The dashed arrow represents a third energy-conservation mechanism that is proved in this study. In this pathway, $F_{420}H_2$ is oxidized by the cytoplasmic hydrogenase Frh to generate H_2. The H_2 then diffuses outside the cell to the active site of membrane-bound hydrogenase Vht, where it is reoxidized, resulting in the translocation of two protons via a H_2-cycling mechanism. The electrons are passed through MP to CoM-S-S-CoB as in the other two systems. In all three systems, the entire electron transport process leads to the net translocation of four protons outside the cell per two electrons transferred from $F_{420}H_2$ or H_2 to CoM-S-S-CoB. The electrochemical gradient generated is coupled to ATP synthesis via an A-type ATPase. This study also presents evidence for involvement of the Ech hydrogenase in H_2-cycling (dotted line). Ech presumably couples the exergonic oxidation of Fd_{red} to H_2 formation, concomitantly pumping an unknown number of protons outside the cell. The proton-motive force is likely used for the transfer of methyl group from methyl-CoM to tetrahydrosarcinapterin. However, the H_2 may diffuse out to Vht and enter the H_2:heterodisulfide oxidoreductase system for energy conservation. Scalar or vectorial protons translocated across the cell membrane are highlighted in red. Abbreviations; Ech, Fd-dependent hydrogenase; Frh, F_{420}-reducing hydrogenase; Fpo, $F_{420}H_2$:phenazine oxidoreductase; Vht, methanophenazine-dependent hydrogenase; Hdr, heterodisulfide reductase; CoM-SH, coenzyme M; CoB-SH, coenzyme B; CoM-S-S-CoB, mixed disulfide of CoM-SH and CoB-SH; MP/MPH_2,

Figure 3.1 (cont.)

oxidized and reduced methanophenazine; Fd_{ox}/Fd_{red}, oxidized and reduced ferredoxin; $F_{420}/F_{420}H_2$, oxidized and reduced Factor 420; FAD, flavin adenine dinucleotide; [FeS], iron-sulfur cluster; [NiFe], bimetallic catalytic center; Cytb_2, cytochrome b_2.

hydrogenase catalyzes the reversible reduction of F_{420} with H_2 (32). Therefore, Frh was proposed to oxidize $F_{420}H_2$ to H_2 during methylotrophic growth. The H_2 could be subsequently channeled via the MP-dependent hydrogenase into the H_2:heterodisulfide oxidoreductase system . This also suggested that the cytoplasmic Frh hydrogenase and periplasmic MP-dependent hydrogenase might conserve energy via the H_2-cycling mechanism. Nevertheless, it was shown that Fpo remains capable of directing electrons from $F_{420}H_2$ into the $F_{420}H_2$:heterodisulfide oxidoreductase system in the Δ*frh* mutant. Hence, *M. barkeri* was proposed to possess a branched electron transport chain on methanol, with one branch involving H_2 as an intermediate and another, the proton-pumping Fpo oxidoreductase (22).

The MP-dependent hydrogenase of *Methanosarcina* was characterized as part of the H_2:heterodisulfide oxidoreductase system in *Methanosarcina mazei* Gö1 (9, 12, 20). This membrane-bound hydrogenase reduces the membrane soluble electron carrier MP using H_2 (5) and has therefore been proposed to provide reduced MP (MPH_2) for reduction of CoM-S-S-CoB heterodisulfide, in the hydrogenotrophic , methyl-respiration and aceticlastic pathways (10, 11, 31). *M. barkeri* contains two operons, *vhtGACD* and *vhxGAC*, encoding the two MP-dependent hydrogenases, Vht and Vhx, respectively (Figure 3.2). The deduced amino acid sequences of Vht and Vhx have all the important structural and

catalytic residues that are present in *M. mazei* hydrogenases, suggesting that these enzymes might also be functional as part of the H_2:heterodisulfide system.

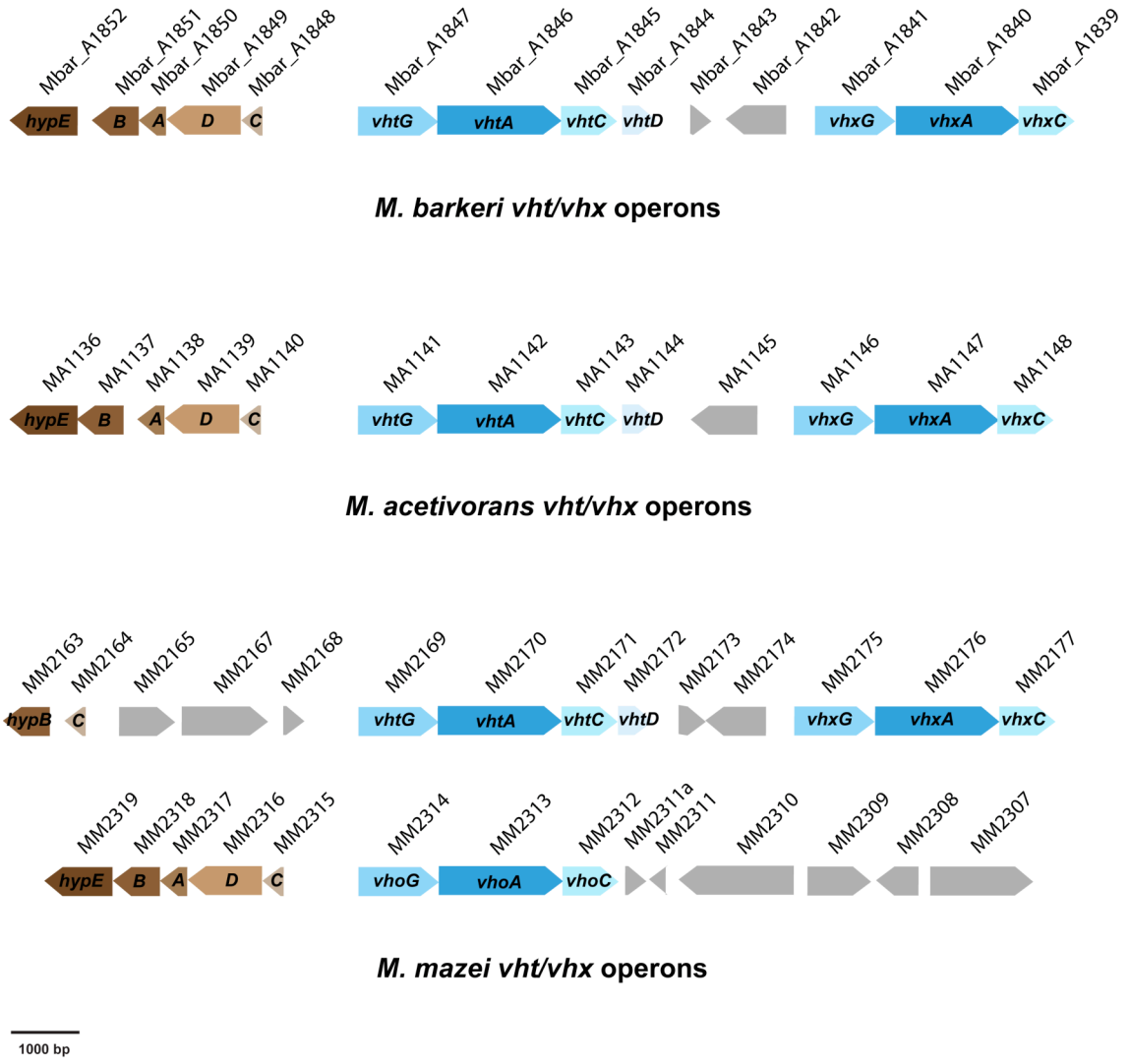

Figure 3.2 Genomic organization of operons encoding methanophenazine-dependent hydrogenases in *Methanosarcina* species. Vho and Vht encoded by the *vhoGAC* and *vhtGACD* operons, respectively, of *M. mazei* are *ca*. 95% identical, however, Vhx encoded by *vhxGAC* shares only *ca*. 50% amino acid sequence identity to each of them. Both *M. barkeri* and *M. acetivorans* posses an operon similar to *vhtGACD* and another to *vhxGAC*. The *vho* and *vhx* operons lack gene D that encodes a putative hydrogenase maturation protein presumed to be essential for post-translational modification of the *cis*-encoded hydrogenase. All the three species also possess a *hypCDABE* operon that encodes proteins presumed to be required for synthesis and insertion of the [NiFe] bimetallic catalytic center in the hydrogenases of *M. barkeri*. Notably, *M. mazei* contains duplicate copies of *hypB* and *hypC* genes. Other open reading frames (ORFs) are shown as gray arrows.

Unlike the *vht* operon, the *vhx* operon is missing gene D that encodes a putative maturation protease. It has been proposed that *vhx*-encoded hydrogenase might be functional, if the protein encoded by *vhtD* can process it. However, the *vhx* operon is not expressed at detectable levels on any methanogenic substrate, whereas expression of *vht* is constitutive (16).

To test the role of Vht in H_2-cycling, we attempted deletion of the *vht* operon in *M. barkeri*. However, we discovered that Vht is essential for growth of wild-type *M. barkeri* under all conditions tested. Furthermore, repression of *vht* expression led to an increase in H_2 partial pressure in a conditional *vht* mutant. These results are consistent with a requirement for Vht in H_2 uptake. The accumulation of H_2 was also accompanied by growth inhibition, suggesting that H_2 uptake is essential for viability. However, Vht is not essential in mutants lacking the H_2-producing, Frh hydrogenase. This is consistent with the functional coupling of Frh and Vht in the H_2-cycling mechanism.

3.3 MATERIALS AND METHODS

3.3.1 Media and growth conditions

Methanosarcina strains were grown as single cells (46) at 37^{o} C in high salt (HS) broth medium (28) or on agar-solidified medium as described (6). Growth substrates provided were methanol (125 mM in broth medium and 50 mM in agar-solidified medium) or sodium acetate (120 mM) under a headspace of either N_2/CO_2 (80/20%) mix at 50 kPa over ambient pressure or H_2/CO_2 (80/20%) mix at 300 kPa over ambient pressure. Cultures were supplemented as

indicated with 0.1% yeast extract, 0.1% casamino acids, 10 mM sodium acetate or 10 mM pyruvate. Puromycin (CalBioChem, San Diego, CA) was added at 2 μg/ml for selection of the puromycin transacetylase (*pac*) gene (42). 8-Aza-2,6-diaminopurine (8-ADP) (Sigma, St Louis, MO) was added at 20 μg/ml for selection against the presence of *hpt* (42). Tetracycline (Tc) was added at 100 μg/ml to induce the tetracycline-regulated P*mcrB*(*tet*O) promoter (18). Standard conditions were used for growth of *Escherichia coli* strains (50) DH5α/λ-*pir* (33) and DH10B (Stratagene, La Jolla, CA), which were used as hosts for plasmid constructions.

3.3.2 DNA methods and plasmid constructions

Standard methods were used for plasmid DNA isolation and manipulation in *E. coli* (2). Liposome mediated transformation was used for *Methanosarcina* as described (27). Genomic DNA isolation and DNA hybridization were as described (6, 28, 53). DNA sequences were determined from double-stranded templates by the W.M. Keck Center for comparative and functional genomics, University of Illinois. Plasmid constructions are described in Tables 3.1 and 3.2.

3.3.3 Construction of Δ*vhx*, Δ*frh* and Δ*vht* Δ*frh* deletion mutants

The construction and genotype of all *Methanosarcina* strains is presented in Table 3.3. The markerless genetic exchange method (42) was employed to delete *vhx* and *frh* in the Δ*hpt* (WWM85 or WWM86) background of *M. barkeri*

Table 3.1 Plasmids used in this study

Plasmid	Description and/or construction	Reference
pMP44	Vector, containing a *pac-hpt* cassette, used to delete genes from *M. barkeri* Fusaro chromosome using the markerless exchange method	(43)
pGK4	AscI/KpnI-digested *frh* upstream and downstream fusion PCR product amplified using primers frhupfor, frhuprev, frhdnfor and frhdnrev and ligated to MluI/KpnI-digested pMP44	This study
pGK5	AscI/NotI-digested *vht* upstream and downstream fusion PCR product amplified using primers vhtupfor, vhtuprev, vhtdnfor and vhtdnrev and ligated to MluI/NotI-digested pMP44	This study
pGK7	AscI/NotI-digested *vhx* upstream and downstream fusion PCR product amplified using primers vh3upfor, vh3uprev, vh3dnfor and vh3dnrev and ligated to MluI/NotI-digested pMP44	This study
pMR55	Non-replicating plasmid that contains the Flp recombinase gene under control of the *mcrB* promoter	(45)
pJK301	Vector, containing a *pac-hpt* cassette, used to delete genes from *M. barkeri* Fusaro chromosome using double homologous recombination-mediated gene replacement method	(54)

Table 3.1 (cont.)

Plasmid	Description and/or construction	Reference
pGK82A	XhoI/HindIII-digested *vht* upstream region amplified using primers vhtdoubleupfor and vhtdoubleuprev and ligated to XhoI/HindIII-digested pJK301	This study
pGK82B	SpeI/NotI-digested *vht* downstream region amplified using primers vhtdoublednfor and vhtdoublednrev and ligated to SpeI/NotI-digested pGK82A	This study
pGK1	Vector, containing a *pac-hpt* cassette, used for markerless insertion of P*mcrB-tetR-*ϕ*C31int-attB* into the *M. barkeri* Fusaro *hpt* locus	This study
pGK2	Vector, containing a *pac-hpt* cassette, used for markerless insertion of P*mcrB-tetR-*ϕ*C31int-attP* into the *M. barkeri* Fusaro *hpt* locus	This study
pGK50A	Vector, containing a *pac-hpt* cassette flanked by FRT5 sites and P*mcrB-tetR*, used to express genes from the tetracycline-regulated promoter P*mcrB*(*tet*O1) in *M*. *barkeri* Fusaro	This study
pGK51A	Vector, containing a *pac-hpt* cassette flanked by FRT5 sites and P*mcrB-tetR*, used to express genes from the tetracycline-regulated promoter P*mcrB*(*tet*O3) in *M*. *barkeri* Fusaro	This study

Table 3.1 (cont.)

Plasmid	Description and/or construction	Reference
pGK52A	Vector, containing a *pac-hpt* cassette flanked by FRT5 sites and P*mcrB-tetR*, used to express genes from the tetracycline-regulated promoter P*mcrB*(*tet*O4) in *M*. *barkeri* Fusaro	This study
pGK50B	Vector, containing a *pac-hpt* cassette flanked by FRT5 sites and P*mcrB-tetR*, used to express genes from the tetracycline-regulated promoter P*mcrB*(*tet*O1) in *M*. *barkeri* Fusaro (*tetR* is in opposite orientation to pGK50A)	This study
pGK51B	Vector, containing a *pac-hpt* cassette flanked by FRT5 sites and P*mcrB-tetR*, used to express genes from the tetracycline-regulated promoter P*mcrB*(*tet*O3) in *M*. *barkeri* Fusaro (*tetR* is in opposite orientation to pGK51A)	This study
pGK52B	Vector, containing a *pac-hpt* cassette flanked by FRT5 sites and P*mcrB-tetR*, used to express genes from the tetracycline-regulated promoter P*mcrB*(*tet*O4) in *M*. *barkeri* Fusaro (*tetR* is in opposite orientation to pGK52A)	This study
pGK87	NdeI/SpeI-digested *mcr* coding region amplified using primers Tcmcrcodfor and Tcmcrcodrev and ligated to NdeI/SpeI-digested pGK50A (modified GTG start codon of *mcr* to ATG)	This study

Table 3.1 (cont.)

Plasmid	Description and/or construction	Reference
pGK88	ApaI-digested *mcr* upstream region amplified using primers Tcmcrupfor and Tcmcruprev and ligated to ApaI-digested pGK87	This study
pGK89	NdeI/SpeI-digested *mcr* coding region amplified using primers Tcmcrcodfor and Tcmcrcodrev and ligated to NdeI/SpeI-digested pGK50B (modified GTG start codon of *mcr* to ATG)	This study
pGK90	ApaI-digested *mcr* upstream region amplified using primers Tcmcrupfor and Tcmcruprev and ligated to ApaI-digested pGK89	This study
pGK53	ApaI/NcoI-digested *vht* upstream region amplified using primers Tcvhtupfor and Tcvhtuprev and ligated to ApaI/NcoI-digested pGK50A	This study
pGK59A	NdeI/SpeI-digested *vht* coding region amplified using primers Tcvhtcodfor and Tcvhtcodrev and ligated to NdeI/SpeI-digested pGK53	This study
pGK54	ApaI/NcoI-digested *vht* upstream region amplified using primers Tcvhtupfor and Tcvhtuprev and ligated to ApaI/NcoI-digested pGK50B	This study

Table 3.1 (cont.)

Plasmid	Description and/or construction	Reference
pGK60A	NdeI/SpeI-digested *vht* coding region amplified using primers Tcvhtcodfor and Tcvhtcodrev and ligated to NdeI/SpeI-digested pGK54	This study
pGK55	ApaI/NcoI-digested *vht* upstream region amplified using primers Tcvhtupfor and Tcvhtuprev and ligated to ApaI/NcoI-digested pGK51A	This study
pGK61A	NdeI/SpeI-digested *vht* coding region amplified using primers Tcvhtcodfor and Tcvhtcodrev and ligated to NdeI/SpeI-digested pGK55	This study
pGK56	ApaI/NcoI-digested *vht* upstream region amplified using primers Tcvhtupfor and Tcvhtuprev and ligated to ApaI/NcoI-digested pGK51B	This study
pGK62A	NdeI/SpeI-digested *vht* coding region amplified using primers Tcvhtcodfor and Tcvhtcodrev and ligated to NdeI/SpeI-digested pGK56	This study
pGK57	ApaI/NcoI-digested *vht* upstream region amplified using primers Tcvhtupfor and Tcvhtuprev and ligated to ApaI/NcoI-digested pGK52A	This study

Table 3.1 (cont.)

Plasmid	Description and/or construction	Reference
pGK63A	NdeI/SpeI-digested *vht* coding region amplified using primers Tcvhtcodfor and Tcvhtcodrev and ligated to NdeI/SpeI-digested pGK55	This study
pGK58	ApaI/NcoI-digested *vht* upstream region amplified using primers Tcvhtupfor and Tcvhtuprev and ligated to ApaI/NcoI-digested pGK52B	This study
pGK64A	NdeI/SpeI-digested *vht* coding region amplified using primers Tcvhtcodfor and Tcvhtcodrev and ligated to NdeI/SpeI-digested pGK58	This study
pGK25	Vector, containing a *pac-hpt* cassette flanked by FRT sites and P*mcrB-tetR*-terminator*mcr*, used to express genes from the tetracycline-regulated promoter P*mcrB*(*tet*O1) in *M*. *barkeri* Fusaro	This study
pGK26	Vector, containing a *pac-hpt* cassette flanked by FRT sites and P*mcrB-tetR*-terminator*mcr*, used to express genes from the tetracycline-regulated promoter P*mcrB*(*tet*O3) in *M*. *barkeri* Fusaro	This study

Table 3.1 (cont.)

Plasmid	Description and/or construction	Reference
pGK27	Vector, containing a *pac*-*hpt* cassette flanked by FRT sites and P*mcrB*-*tetR*-terminator*mcr*, used to express genes from the tetracycline-regulated promoter P*mcrB*(*tet*O4) in *M*. *barkeri* Fusaro	This study
pGK34	NdeI/SpeI-digested *vht* coding region amplified using primers Tcvhtcodfor and Tcvhtcodrev and ligated to NdeI/SpeI-digested pGK25	This study
pGK35	ApaI/NcoI-digested *vht* upstream region amplified using primers Tcvhtupfor and Tcvhtuprev and ligated to ApaI/NcoI-digested pGK34	This study
pGK30	NdeI/SpeI-digested *vht* coding region amplified using primers Tcvhtcodfor and Tcvhtcodrev and ligated to NdeI/SpeI-digested pGK26	This study
pGK31	ApaI/NcoI-digested *vht* upstream region amplified using primers Tcvhtupfor and Tcvhtuprev and ligated to ApaI/NcoI-digested pGK30	This study
pGK36	NdeI/SpeI-digested *vht* coding region amplified using primers Tcvhtcodfor and Tcvhtcodrev and ligated to NdeI/SpeI-digested pGK27	This study

Table 3.1 (cont.)

Plasmid	Description and/or construction	Reference
pGK37	ApaI/NcoI-digested *vht* upstream region amplified using primers Tcvhtupfor and Tcvhtuprev and ligated to ApaI/NcoI-digested pGK36	This study

Table 3.2 Primers used in this study

Primer	Sequence[a]	Added sites
frhupfor	GGCGCGCCTCCGTTGTCCTTCTTTCCAC	AscI
frhuprev	CATCCCCGTATTCAGCGTAGAGGCTGTACCGTGGTTAAGG	None
frhdnfor	CCTTAACCACGGTACAGCCTCTACGCTGAATACGGGGATG	None
frhdnrev	GGCGCGCCGGTACCTGTTGCGAGTTGTTCAATCC	AscI/KpnI
vhtupfor	GGCGCGCCAAGGTGAATTCCCGTTTTCC	AscI
vhtuprev	GTGAAGAAAATAATTGAACAAAACAAATCTTGATTTTACCCAAATTATACATACG	None
vhtdnfor	CGTATGTATAATTTGGGTAAAATCAAGATTTGTTTTGTTCAATTATTTTCTTCAC	None
vhtdnrev	GGCGCGCCGCGGCCGCTTTGGACTTTCCCGTACCTG	AscI/NotI
vh3upfor	GGCGCGCCCCGTGAGGTGACAGGAGTTT	AscI
vh3uprev	TTCTTCTTCGAACTTCCCCATTTGCAACAGTAGGAGATTGTTT	None
vh3dnfor	AAACAATCTCCTACTGTTGCAAATGGGGAAGTTCGAAGAAGAA	None
vh3dnrev	GGCGCGCCGCGGCCGCGCTTGGAAGCTGTTTTGGAG	AscI/NotI
vhtdoubleupfor	GGCGCGCCCTCGAGAAGGTGAATTCCCGTTTTCC	AscI/XhoI

Table 3.2 (cont.)

Primer	Sequence[a]	Added sites
vhtdoubleuprev	GGCGCGCCAAGCTTTCTTGATTTTACCCAAATTATACATACG	AscI/HindIII
vhtdoubleupfor	GGCGCGCCACTAGTTTTGTTTTGTTCAATTATTTTCTTCAC	AscI/SpeI
vhtdoubleupfor	GGCGCGCCGCGGCCGCTTTGGACTTTCCCGTACCTG	AscI/NotI
Tcmcrupfor	GGCGCGCCGGGCCCCCCCGGGATAAAAACAGTCT	AscI/ApaI
Tcmcruprev	GGCGCGCCGGGCCCGTGTTCTCCGATAAATGAATTTATG	AscI/ApaI
Tcmcrcodfor	GGCGCGCCCATATGTCTGACACAGTAGACATCTACGAC	AscI/NdeI
Tcmcrcodrev	GGCGCGCCACTAGTTTACCCCGTCCACCTTGTAG	AscI/SpeI
Tcvhtupfor	GGCGCGCCCCATGGGAAGTTTTCGGGGGTCTTTC	AscI/NcoI
Tcvhtuprev	GGCGCGCCGGGCCCTGCATGAAAAGAAAATAAAATGC	AscI/ApaI
Tcvhtcodfor	GGCGCGCCCATATGAGTACTGGAATAAAAAATCTTGTC	AscI/NdeI
Tcvhtcodrev	GGCGCGCCACTAGTCCTGCGTCTTTGGAGAAATC	AscI/SpeI
vho3southernfor	AGACATTCAACGGGCTTTTG	None
vho3southernrev	GAAGCACCGATAGCAGAACC	None

Table 3.2 (cont.)

Primer	Sequence[a]	Added sites
tetRsouthernfor	CGAGAAAGGTGTGGAGATCAA	None
tetRsouthernrev	GTCACTGGATGCGGAGATTT	None

[a]The addes sites are underlined.

Table 3.3 *M. barkeri* Fusaro strains used in this study

Strain	Genotype	Source or construction
M. barkeri Fusaro	Wild-type	DSM804
WWM85	Δ*hpt*::P*mcrB*-ϕ*C31int-attP*	Guss *et al*, 2008
WWM86	Δ*hpt*::P*mcrB*-ϕ*C31int-attB*	Guss *et al*, 2008
WWM115	Δ*frh* Δ*hpt*::P*mcrB*-ϕ*C31int-attB*	Deletion of *frh* in WWM86 with pGK4
WWM237	Δ*vhx* Δ*hpt*::P*mcrB*-ϕ*C31int-attP*	Deletion of *vhx* in WWM85 with pGK7
WWM146	Δ*vht*::*pac-hpt* Δ*frh* Δ*hpt*::P*mcrB*-ϕ*C31int-attB*	Deletion of *vht* in WWM115 with XhoI/NotI-digested 5.6 kb pGK82B
WWM351	Δ*vht*::FRT Δ*frh* Δ*hpt*::P*mcrB*-ϕ*C31int-attB*	Removal of *pac-hpt* cassette in WWM146 using pMR55
WWM154	Δ*hpt*::P*mcrB-tetR*-ϕ*C31int-attB*	Markerless insertion of *tetR*, ϕ*C31int* and *attB at hpt* locus using pGK1

Table 3.3 (cont.)

Strain	Genotype	Source or construction
WWM155	Δ*hpt*::P*mcrB-tetR*-ϕ*C31int-attP*	Markerless insertion of *tetR*, ϕ*C31int* and *attP at hpt* locus using pGK2
WWM235	*mcr*ΩP*mcrB-tetR pac-hpt* P*mcrB*(*tet*O1) Δ*hpt*::P*mcrB-tetR*-ϕ*C31int-attP*	Expression of *mcr* from P*mcrB*(*tet*O1) in WWM155 using SpeI-digested pGK90
WWM156	*vht*ΩP*mcrB-tetR pac-hpt* P*mcrB*(*tet*O1) Δ*hpt*::P*mcrB-tetR*-ϕ*C31int-attB*	Expression of *vht* from P*mcrB*(*tet*O1) in WWM154 using NcoI/SpeI-digested 7.0 kb pGK59A
WWM157	*vht*ΩP*mcrB-tetR pac-hpt* P*mcrB*(*tet*O3) Δ*hpt*::P*mcrB-tetR*-ϕ*C31int-attB*	Expression of *vht* from P*mcrB*(*tet*O3) in WWM154 using NcoI/SpeI-digested 7.0 kb pGK61A
WWM158	*vht*ΩP*mcrB-tetR pac-hpt* P*mcrB*(*tet*O4) Δ*hpt*::P*mcrB-tetR*-ϕ*C31int-attB*	Expression of *vht* from P*mcrB*(*tet*O4) in WWM154 using NcoI/SpeI-digested 7.0 kb pGK63A
WWM162	*vht*ΩP*mcrB-tetR pac-hpt* P*mcrB*(*tet*O1) Δ*hpt*::P*mcrB-tetR*-ϕ*C31int-attB*	Expression of *vht* from P*mcrB*(*tet*O1) in WWM155 using NcoI/SpeI-digested 7.0 kb pGK35

Table 3.3 (cont.)

Strain	Genotype	Source or construction
WWM163	*vht*ΩP*mcrB-tetR pac-hpt* P*mcrB*(*tet*O3) Δ*hpt*::P*mcrB-tetR*-ϕ*C31int-attB*	Expression of *vht* from P*mcrB*(*tet*O3) in WWM155 using NcoI/SpeI-digested 7.0 kb pGK31
WWM164	*vht*ΩP*mcrB-tetR pac-hpt* P*mcrB*(*tet*O4) Δ*hpt*::P*mcrB-tetR*-ϕ*C31int-attB*	Expression of *vht* from P*mcrB*(*tet*O4) in WWM155 using NcoI/SpeI-digested 7.0 kb pGK37

Fusaro. The plasmids, pGK4 and pGK7 were used to delete *frh* in WWM86 and *vhx* in WWM85, respectively, using methanol plus H_2/CO_2 as the growth substrate. The Δ*vht* Δ*frh* mutant was constructed by deleting *vht* in the Δ*frh* markerless mutant by the homologous recombination-mediated gene replacement method (53). In this method, XhoI/NotI cut 5.6 kb region of pGK82B was transformed into the Δ*frh* mutant and the transformants were selected using methanol and puromycin. All the mutants were confirmed by DNA hybridization (Figures 3.3, 3.4 and 3.5).

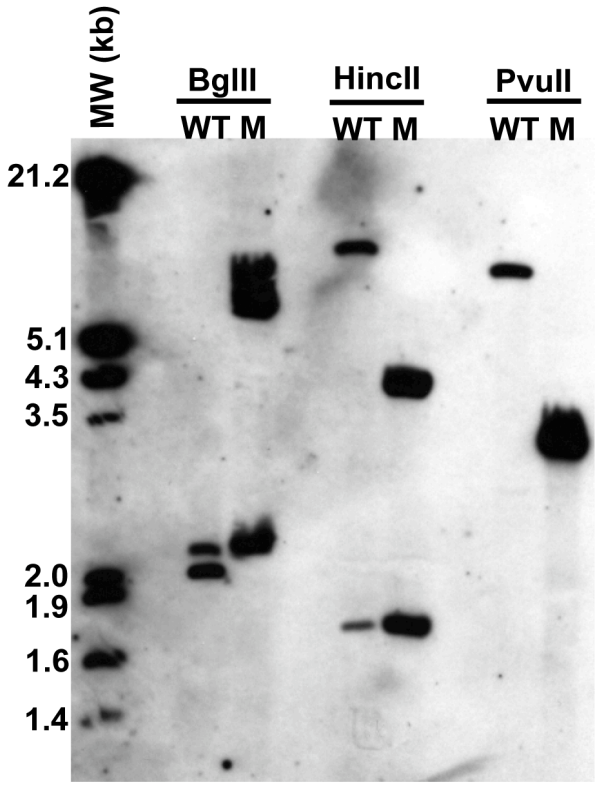

Figure 3.3 Verification of Δ*vhx* by Southern hybridization. Predicted bands (kb): **BglII**: WT (WWM85) = 2.1 and 2, mutant (M) = 5.6 and 2.1; **HincII**: WT = 8 and 1.7**,** mutant = 3.9 and 1.7; **PvuII**: WT = 7.1, mutant = 3. MW: DIG-labeled DNA molecular weight marker III (Roche, Indianapolis, IN). 750-bp PCR product of pGK7 amplified with primers vho3southernfor and vho3southernrev was used as probe (Tables 3.1 and 3.2).

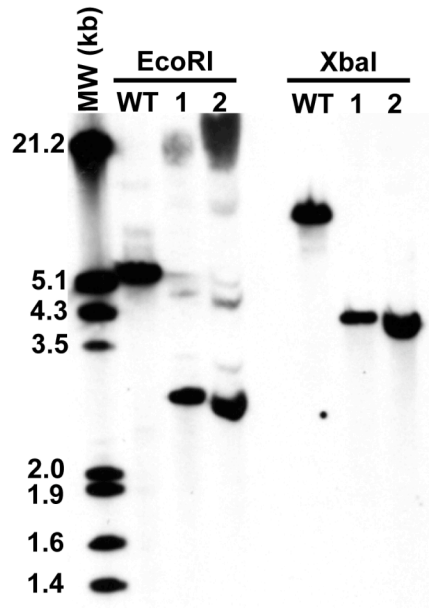

Figure 3.4 Verification of Δ*frh* by Southern hybridization. Predicted bands (kb): **EcoRI**: WT (WWM86) = 5.4, mutants (1 and 2) = 2.8; **XbaI**: WT = 7.8**,** mutants = 4.1. MW: DIG-labeled DNA molecular weight marker III (Roche, Indianapolis, IN). 872 bp fragment of Sau3AI-digested *frh* deletion plasmid (pGK4, Table 3.1) was used as probe.

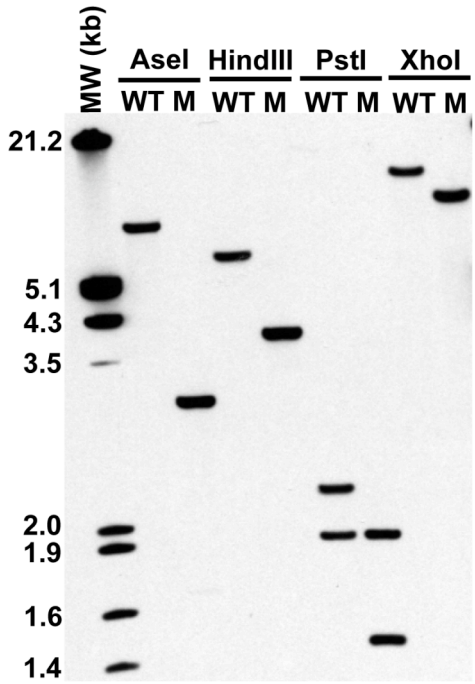

Figure 3.5 Verification of Δ*vht* in Δ*vht* Δ*frh* by Southern hybridization. Predicted bands (kb): **AseI**: WT (WWM85) = 7.4, mutant (M) = 3.1; **HindIII**: WT = 5.9**,** mutant = 3.9; **PstI**: WT = 2.2 and 2**,** mutant = 2 and 1.4; **XhoI**: WT = 10.7**,** mutant = 8.5. MW: DIG-labeled DNA molecular weight marker III (Roche, Indianapolis, IN). 831 bp fragment of KpnI-digested *vht* deletion plasmid (pGK5, Table 3.1) was used as probe.

3.3.4 Construction of tetracycline-regulated *vht* and *mcr* mutants

In a previous study (18), the P*mcrB* promoter of *M. barkeri* was modified to include binding sites for the TetR protein (*tet*O). Three promoters with variable placement of *tet*O were constructed, designated P*mcrB*(*tet*O1), P*mcrB*(*tet*O3) and P*mcrB*(*tet*O4), to allow expression of the desired gene at different levels. Thus, the P*mcrB*(*tet*O1) promoter is expressed at the highest level, whereas, expression of P*mcrB*(*tet*O3) is lowest. To render expression of hybrid P*mcrB*(*tet*O) promoters (18) tetracycline-dependent, *M. barkeri* Fusaro strains containing a *tetR* gene were constructed. To accomplish this, plasmids harboring P*mcrB-tetR*-ϕ*C31int-attB* (pGK1) or P*mcrB-tetR*-ϕ*C31int-attP* (pGK2) were inserted into the *hpt* locus using the markerless method of genetic exchange (42) to obtain WWM154 or WWM155, respectively (Table 3.3). These strains were then confirmed by DNA hybridization (Figure 3.6). To enable expression of *M. barkeri* genes from the hybrid promoters, each one of these P*mcrB*(*tet*O) promoter was cloned into a vector containing selectable (*pac*) & counter-selectable (*hpt*) markers and a copy of P*mcrB* driven *tetR* to give rise to a series of plasmids. This includes pGK50A/B & pGK25 with P*mcrB*(*tet*O1), pGK51A/B & pGK26 with P*mcrB*(*tet*O3) and pGK52A/B and pGK27 with P*mcrB*(*tet*O4) (Table 3.1). Subsequently, in each of these vectors, the upstream and coding regions of *vht* were cloned using the NcoI/ApaI and NdeI/SpeI sites, respectively. The resulting plasmids were then digested with NcoI/SpeI to give a 7 kb fragment that was transformed into WWM154 or WWM155 (Table 3.3). The transformants were selected using methanol plus H_2/CO_2 in the presence of puromycin and Tc.

To ensure that the native promoter of *vht* does not interfere with P*mcrB*(*tet*O) in *vht* expression, 382 bp upstream of *vht* were deleted in the Tc-regulated *vht*

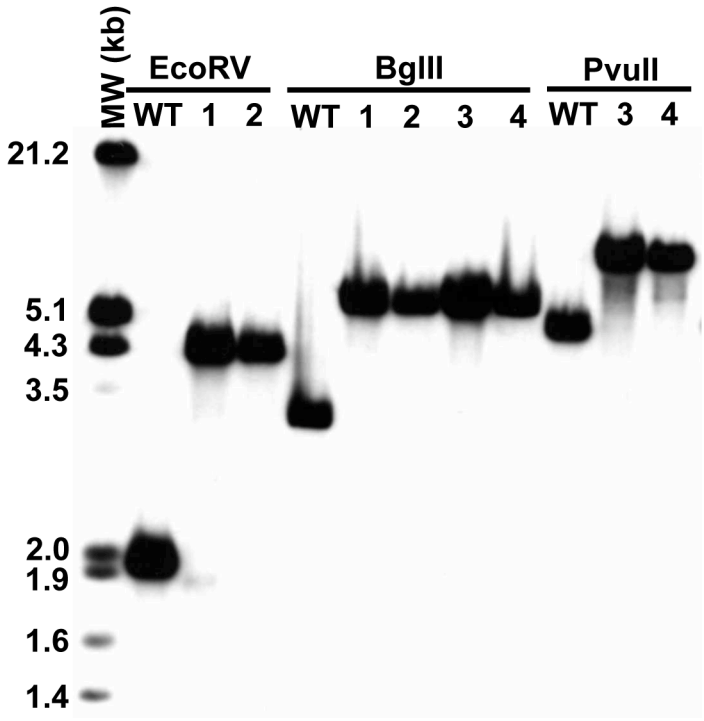

Figure 3.6 Verification of P*mcrB-tetR-ϕC31int-attB* insertion at *hpt* locus in WWM154 and WWM155 by Southern hybridization. Predicted bands (kb): **EcoRV**: WT (*M. barkeri* Fusaro) = 2, WWM154 (1 and 2) = 4.2; **BglII**: WT = 3.2, WWM154 and WWM155 (3 and 4) = 5.4; **PvuII**: WT = 4.9**,** WWM155 = 7.1. MW: DIG-labeled DNA molecular weight marker III (Roche, Indianapolis, IN). 700 bp PCR-product of pGK1 amplified with primers tetRsouthernfor and tetRsouthernrev was used as probe (Tables 3.1 and 3.2).

strains, still keeping intact 1038 bp for the expression of *hyp* operon (Figure 3.2). Based on sequence homology to *M. mazei vht* promoter (16), the *M. barkeri vht* promoter is presumed to be located within 140 bp upstream of *vht* (12) and thus, the Tc-regulated *vht* strains are probably deleted of the native *vht* promoter. Further studies were perfomed using the strain obtained from transformation with the pGK51A derivative, which contains P*mcrB*(*tet*O3) (P_{tet}*vht*, WWM157). This strain was confirmed by sequencing the PCR amplified *vht* promoter of WWM157

and using DNA hybridization (Figure 3.7). The *mcr* upstream and coding regions were cloned in P*mcrB*(*tet*O1)-containing pGK50A/B, using ApaI and NdeI/SpeI sites, respectively (Table 3.1). The translational start site of *mcr* was modified

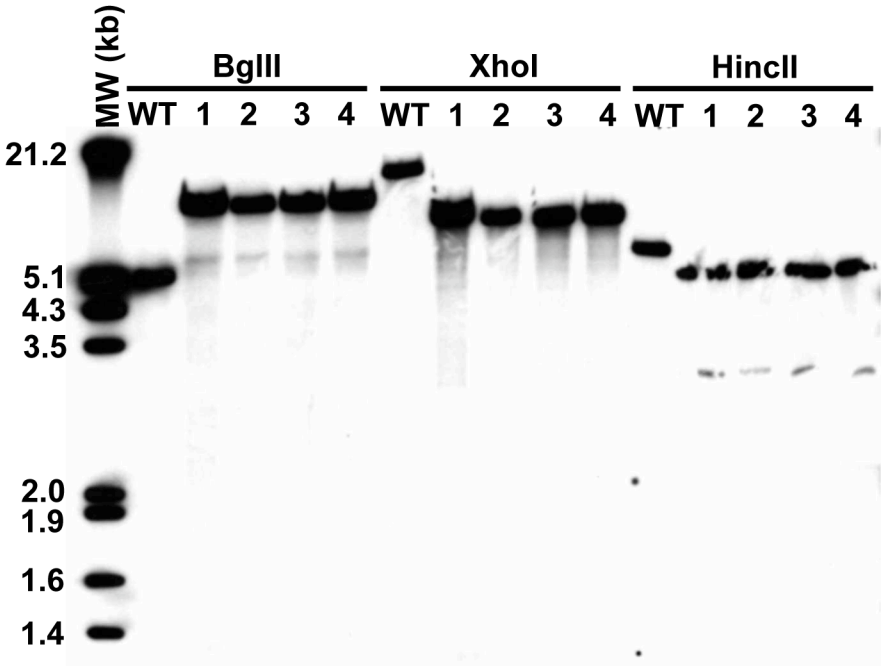

Figure 3.7 Verification of P_{tet}*vht* by Southern hybridization. Predicted bands (kb): **BglII**: WT (WWM154) = 5.1, P_{tet}*vht* (1, 2, 3 and 4) = 7.9; **XhoI**: WT = 10.7**,** P_{tet}*vht* = 6.8; **HincII**: WT = 5.7**,** P_{tet}*vht* = 4.9. MW: DIG-labeled DNA molecular weight marker III (Roche, Indianapolis, IN). 481-bp fragment of EcoRI-digested pGK60A (Table 3.1) was used as probe.

from GTG to ATG for cloning purposes. The SpeI-digested pGK50B derivative (pGK90) was then used to obtain the Tc-regulated *mcr* strain (P_{tet}*mcr*, WWM235). This strain was confirmed by sequencing the PCR amplified *mcr* promoter of WWM235. Surprisingly, the modified ATG start codon of *mcr* was mutated back to its native GTG in each of the three clones sequenced. As in case of P_{tet}*vht* strain, 149 bp upstream of *mcr* were deleted to remove the native *mcr* promoter in P_{tet}*mcr* strain (18).

3.3.5 Determination of growth characteristics

For growth rate determinations, cultures were grown using methanol (Δ*hpt*, Δ*vhx* and Δ*vht* Δ*frh*) or methanol plus H_2/CO_2 (Δ*frh*) to mid-log phase (optical density at 600 nm [OD_{600}] *ca.* 0.5). Approximately 3% inoculum of the culture (or 10%, in case of acetate) was then transferred to fresh medium in four replicates and incubated at 37^{o} C. Growth was quantified by measuring OD_{600}. Generation times were calculated during exponential growth phase and lag phase was defined as the time required to achieve half-maximal OD_{600}. For growth curve experiments with and without Tc, strains were adapted to methanol and methanol plus H_2/CO_2 for 30 generations, and H_2/CO_2 and acetate for 15 generations in the presence of Tc. The adapted cultures were grown till mid-log phase (OD_{600} *ca.* 0.5 for methanol and methanol plus H_2/CO_2 and OD_{600} *ca.* 0.25 for H_2/CO_2 and acetate) and then serially diluted to 10^{-5} (methanol and methanol plus H_2/CO_2) or 10^{-4} (H_2/CO_2 and acetate) with and without Tc in four replicates. Growth was then monitored at OD_{600}.

3.3.6 Cell suspension experiments

Cells grown on methanol (Δ*hpt*, Δ*vhx* and Δ*vht* Δ*frh*) or methanol plus H_2/CO_2 (Δ*frh*) were collected in late exponential phase (OD_{600}= 0.6-0.7) by centrifugation at 5,000 x g for 15 minutes at 4 ^{o}C. They were then washed once with anaerobic HS PIPES buffer, 50 mM PIPES (pH 6.8), 400 mM NaCl, 13 mM KCl, 54 mM $MgCl_2$, 2 mM $CaCl_2$, 2.8 mM cysteine, 0.4 mM Na_2S and resuspended in the same buffer to a final concentration of 10^9 cells/ml. Cells

were counted visually using the Petroff-Hausser counting chamber (Hausser Scientific, PA). All assay mixtures contained 2 ml of the suspension and were conducted under strictly anaerobic conditions in 25 ml Balch tubes sealed with butyl rubber stoppers. Puromycin (20 μg/ml) was added to prevent protein synthesis and as indicated, the assay mixture contained 250 mM methanol under a headspace of N_2, H_2 or H_2/CO_2 (80/20%) at 250 kPa over the ambient pressure. Cells were held on ice until use and assays were started by transferring tubes to 37°C. For rate determination, gas phase samples were withdrawn at various time points and assayed for CH_4 by gas chromatography at 225°C in a Hewlett Packard gas chromatograph (5890 Series II) equipped with a flame ionization detector. The column used was of stainless steel filled with 80/120 Carbopack™ B/3% SP™-1500 (Supelco, Bellefonte, PA) with helium as the carrier gas. For total CH_4 and CO_2 production, assays were incubated at 37°C for 36 hours and then gas phase samples were withdrawn. These samples were analyzed by GC at 225°C in a Hewlett Packard gas chromatograph (5890 Series II) equipped with a thermal conductivity detector. A stainless steel 60/80 Carboxen-1000 column (Supelco, Bellefonte, PA) with helium as the carrier gas was used. Total cell protein was determined using the Bradford method (7) after 1 ml of the cells was lysed by resuspending it in ddH_20 with 1 μg/ml RNase and DNase.

3.3.7 Measurement of H_2, CH_4 and OD_{600} during methylotrophic growth

WWM154, P_{tet}*vht* (grown in presence of Tc), Δ*frh* and Δ*vht* Δ*frh* strains were grown using methanol till mid-log phase (OD_{600} *c.* 0.5) and then 1 ml (WWM154 and P_{tet}*vht*) or 5ml (Δ*frh* and Δ*vht* Δ*frh*) were inoculated into 100 ml HS-methanol in a 500 ml serum bottle. For P_{tet}*vht* strain, the culture was washed once prior to inoculation into media with or without Tc. To measure H_2 and CH_4, *ca*. 1 ml or 2 ml headspace samples were withdrawn aseptically from the culture at various time points with a syringe that had been flushed with sterile, anaerobic N_2. The gas samples were then diluted into 70 ml helium. A gas-tight syringe flushed with helium was subsequently used to withdraw 3 ml of the diluted sample, which was then injected into an SRI gas chromatograph, equipped with a reduction gas detector (RGD) and a thermal conductivity detector (TCD) at 52^{o}C. The RGD column was a three feet long 13X molecule sieve, whereas the TCD column was six feet HayeSep D. RGD was used to detect H_2 by peak height and TCD for CH_4 by peak area. Helium was used as the carrier gas. OD_{600} was also measured during the growth curve.

3.4 RESULTS

3.4.1 Vhx is dispensable whereas Vht is essential for growth of *M. barkeri*

As described above, Frh preferentially channels electrons from $F_{420}H_2$ to H_2 during methylotrophic growth of *M. barkeri* (Figure 3.1). The H_2 is then presumably taken up by MP-dependent hydrogenase and fed into the H_2:heterodisulfide oxidoreductase system for reduction of CoM-S-S-CoB (22).

Thus, we predicted that deletion of MP-dependent hydrogenase from the organism should affect its growth using methanol. To test this *in vivo*, we attempted to delete the operons encoding MP-dependent hydrogenases in *M. barkeri*, *vhxGAC* and *vhtGACD*.

The *vhxGAC* operon (Figure 3.2) was deleted from the chromosome of *M. barkeri* Fusaro using methanol plus H_2/CO_2 as the growth substrate (Table 3.3). The phenotype exhibited by the Δ*vhx* mutant, in terms of growth characteristics and CH_4 and CO_2 production in resting cell suspensions, is similar to the isogenic parental strain on all substrates (Tables 3.4, 3.5 & 3.6). Therefore, Vhx is not required for growth of *M. barkeri* under the conditions tested; however, this does not rule out the possibility that it may still encode a functional hydrogenase.

We tried to delete the *vhtGACD* operon (Figure 3.2) numerous times from the chromosome of *M. barkeri* Fusaro by the homologous gene replacement method (53) using methanol or methanol plus H_2/CO_2 as growth substrates, with and without media supplementation (yeast extract, casamino acids, pyruvate and acetate). However, no puromycin-resistant *vht* mutant colonies were obtained, implying that loss of Vht might be deleterious to the cell under the tested conditions. As an alternative strategy, we also employed the markerless method of genetic exchange (42) to delete *vht*. In this selection/counterselection method, if there is no selective pressure for or against the mutant allele, then 50% of the segregants are expected to be mutant strains. However, in case the mutant strain has a growth defect, the wild-type strain would outgrow it, thereby reducing the probability of obtaining segregants with the mutant allele. All the

Table 3.4 Growth[a] of *M. barkeri* Fusaro strains[b] in various media

Substrate	Strain	Growth Rate (h)	Maximum OD_{600}	Lag Phase (h)
CH_3OH	Δ***hpt***[c]	7.4±0.9	0.67±0.03	39±0.2
	Δ***frh***	13.9±0.9	0.55±0.02	493±29
	Δ***vhx***	7±0.2	0.79±0.01	43±1
	Δ***vht*** Δ***frh***	9.9±0.3	0.83±0.00	54±2
$CH_3OH/H_2/CO_2$	Δ***hpt***[c]	6.2±0.1	0.60±0.04	52±6
	Δ***frh***	8.8±0.8	0.59±0.04	70±6
	Δ***vhx***	6.2±0.2	0.69±0.08	49±4
	Δ***vht*** Δ***frh***	37±4	0.31±0.05	141±19
H_2/CO_2	Δ***hpt***[c]	8.3±1.3	0.38±0.04	67±8
	Δ***frh***	NG	NA	NA
	Δ***vhx***	9.1±0.5	0.43±0.03	54±4
	Δ***vht*** Δ***frh***	NG	NA	NA
CH_3COOH	Δ***hpt***[c]	79±13	0.35±0.02	641±43
	Δ***frh***	54±3	0.44±0.00	199±8
	Δ***vhx***	78±11	0.31±0.04	466±83
	Δ***vht*** Δ***frh***	NG	NA	NA

[a]Growth was measured as indicated in Materials and Methods; lag time represents the time required to reach one half of the maximum optical density at 600 nm (OD_{600}). Values represent the average and standard deviation of at least triplicate measurements.
[b]Strains used were WWM85 (Δ*hpt*), WWM115 (Δ*frh*), WWM237 (Δ*vhx*) and WWM351 (Δ*vht* Δ*frh*).
[c]*M. barkeri* Fusaro parent strain in which all deletions were constructed.
NG, no growth for at least 6 months of incubation.
NA, not applicable.

Table 3.5 Methane (μmol) and carbon dioxide (μmol) production by resting cell suspensions[a] of *M. barkeri* Fusaro strains[b]

	Substrates							
	N_2		CH_3OH		CH_3OH /H_2		H_2/CO_2	
Strain	CH_4	CO_2	CH_4	CO_2	CH_4	CO_2	CH_4	CO_2
Δ***hpt***[c]	<1	1±0.2	328±12	130±04	433±10	<1	255±50	NA
Δ***frh***	<1	2±0.2	232±15	80±04	374±19	<1	9±1	NA
Δ***vhx***	<1	<1	332±8	135±03	420±62	<1	300±20	NA
Δ***vht*** Δ***frh***	<1	1±0.2	289±26	95±08	119±15	<1	1±0.4	NA

[a]Assays were conducted as described in Materials and Methods. Values are the average and standard deviation of at least three trials.
[b]Strains used were WWM85 (Δ*hpt*), WWM115 (Δ*frh*), WWM237 (Δ*vhx*) and WWM351 (Δ*vht* Δ*frh*).
[c]*M. barkeri* Fusaro parent strain in which all deletions were constructed.
NA, not applicable (CO_2 produced could not be measured because it was added to headspace).

Table 3.6 Rate (nmol min^{-1} mg^{-1}) of methane production from resting cell suspensions[a] of *M. barkeri* Fusaro strains[b]

	***M. barkeri* Fusaro strains**			
Substrate	**Δ*hpt*[c]**	**Δ*frh***	**Δ*vhx***	**Δ*vht* Δ*frh***
N_2	<1	<1	<1	<1
CH_3OH	71±12	12±2	92±6	27±6
CH_3OH/H_2	190±34	176±19	178±10	27±1

[a]Assays were conducted as described in Materials and Methods. Values are the average and standard deviation of at least three trials.
[b]Strains used were WWM85 (Δ*hpt*), WWM115 (Δ*frh*), WWM237 (Δ*vhx*) and WWM351 (Δ*vht* Δ*frh*).
[c]*M. barkeri* Fusaro parent strain in which all deletions were constructed.

101 8-ADP-resistant segregant colonies screened for *vht* deletion were wild-type, which is consistent with the idea that *vht* might be essential for growth of *M. barkeri* under the conditions examined.

3.4.2 Validation of the tetracycline-regulated system used to test gene essentiality

To test this system, the expression of an essential gene in *M. barkeri* encoding the methyl-CoM reductase, *mcr* (43), was rendered Tc-dependent in the P_{tet}*mcr* strain (WWM235, Table 3.3). Expression of native *mcr* promoter is closest to that of P*mcrB*(*tet*O1), thus, this promoter was used to express *mcr* in P_{tet}*mcr* strain. This strain grew well on solid medium with methanol as a growth substrate, so long as tetracycline was included. However, no growth was observed in the absence of tetracycline (Figure 3.8). Similar results were obtained in liquid media containing methanol, methanol plus H_2/CO_2, H_2/CO_2 or

acetate as growth substrates, indicates that Mcr is essential for growth on all methanogenic substrates tested (Figure 3.9). This validates the Tc-regulated gene essentiality system.

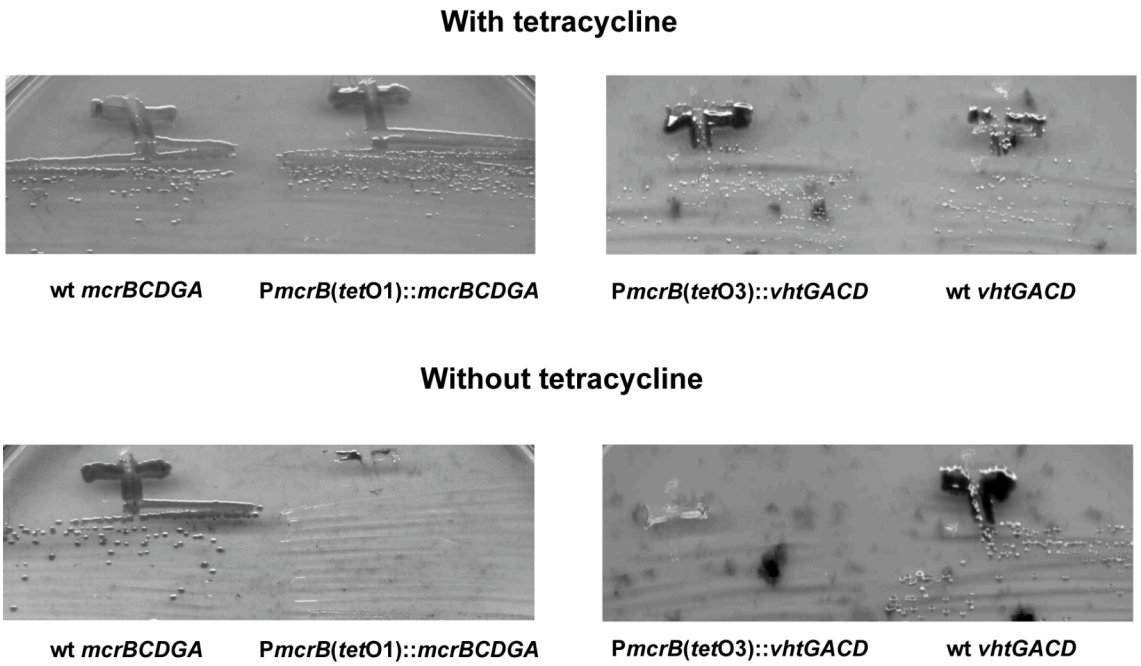

Figure 3.8 Growth of tetracycline-regulated *mcr* (P_{tet}*mcr*) and *vht* (P_{tet}*vht*) mutants of *M. barkeri* on plates containing methanol. WWM154 (parent strain, Table 3.3), P_{tet}*mcr* and P_{tet}*vht* strains were streaked on methanol plates with and without tetracycline (Tc). Unlike WWM154, which was able to grow in the presence and absence of Tc, P_{tet}*mcr* and P_{tet}*vht* strains could grow only in the presence of Tc.

3.4.3 Isolation of an *M. barkeri* conditional *vht* mutant

Due to our inability to isolate a *vht* deletion mutant, a Tc-regulated *vht* conditional mutant, hereafter referred to as P_{tet}*vht* (WWM157), was constructed (Table 3.3) (18). The native promoter of *vht* is expressed at levels similar to P*mcrB*(*tet*O3) (16, 18), therefore, this promoter was used to drive *vht* expression in P_{tet}*vht*. To check if Vht is essential for growth using methanol, the P_{tet}*vht* strain

was streaked on this substrate with and without Tc (Figure 3.8). Unlike the parental strain that grew under both conditions, the P_{tet}*vht* strain could only grow

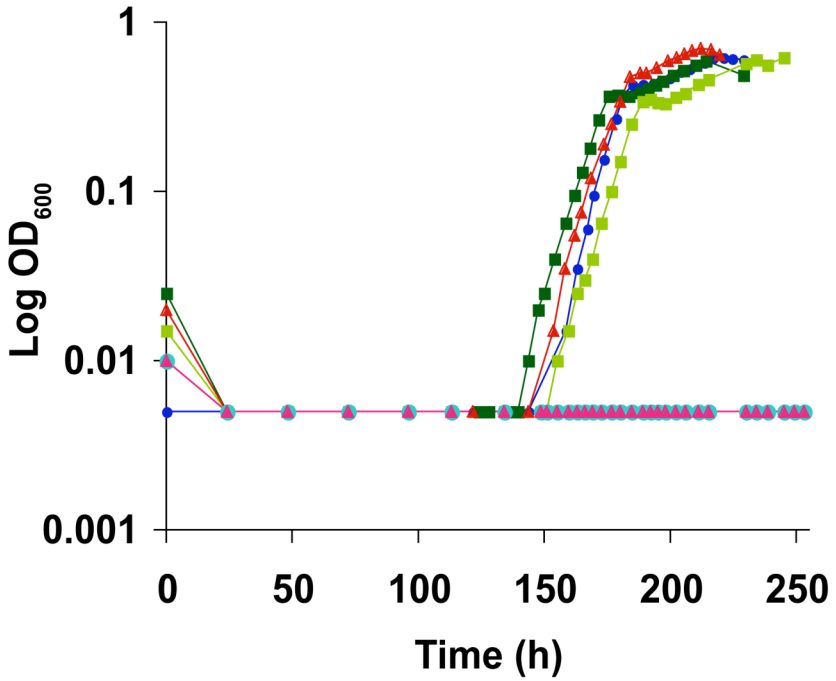

Figure 3.9 Growth of tetracycline-regulated *mcr* (P_{tet}*mcr*) and *vht* (P_{tet}*vht*) mutants of *M. barkeri* on methanol plus H_2/CO_2. WWM154 (parent strain, Table 3.3), P_{tet}*mcr* and P_{tet}*vht* strains were grown on methanol plus H_2/CO_2 with and without tetracycline (Tc) as described in Materials and Methods. Growth was monitored in triplicate cultures at OD_{600}. Unlike WWM154, which was able to grow in the presence and absence of Tc, P_{tet}*mcr* and P_{tet}*vht* could grow only in the presence of Tc. Similar growth curve experiments were also performed on methanol, H_2/CO_2 and acetate. Growth was tested at 10^{-5} dilution on methanol and methanol plus H_2/CO_2, and at a dilution of 10^{-4} on H_2/CO_2 and acetate. At these dilutions, the concentration of residual Tc contributed by the inoculum is less than that required for induction of the P*mcrB*(*tet*O) promoter (1 μg/ml) (18) and there are *ca*. 1000 cells present in the inoculum. On each of the methanogenic substrate tested, both the Tc-dependent strains, P_{tet}*mcr* and P_{tet}*vht*, could not grow without tetracycline for more than six months. This proves their essentiality on the substrates tested. Cultures, WWM154 with Tc (dark green squares), WWM154 without Tc (lime sqaures), P_{tet}*mcr* with Tc (red triangles), P_{tet}*mcr* without Tc (pink triangles), P_{tet}*vht* with Tc(dark blue circles), P_{tet}*vht* without Tc (turquoise circles).

when Tc was present in the medium. Similar results were obtained in liquid media containing methanol, methanol plus H_2/CO_2, H_2/CO_2 or acetate as growth substrates (Figure 3.9). This proves that Vht is essential for growth of wild-type

M. barkeri on all methanogenic substrates tested. Vhx is present in the P_{tet}*vht* strain; however, it is not able to substitute for the role of Vht in growth of *M. barkeri*, indicating that Vhx is non-functional under the conditions tested.

3.4.4 Hydrogen accumulation in the tetracycline-regulated *vht* mutant inhibits methylotrophic growth

If Frh and Vht mediate electron transfer from $F_{420}H_2$ to MP via H_2 during growth on methanol, then absence of Vht from the cell should result in H_2 accumulation (Figure 3.1). To test this, H_2 production was measured as a function of growth and amount of CH_4 production in cultures of wild-type (WWM154), Δ*frh* and P_{tet}*vht* strains. The P_{tet}*vht* strain was grown with and without Tc. In the presence of Tc, *vht* is expressed, enabling P_{tet}*vht* strain to grow like the parental strain. However, *vht* is not expressed in the absence of Tc. Nevertheless, growth occurs to a level of *ca*. 50% of wild-type, which we believe is due to dilution of existing Vht protein in the cells of the inoculum. The parental strain showed a gradual increase in H_2 concentration as CH_4 production and growth ensued (Figure 3.10). Once CH_4 production ceased (*ca*. 26 kPa), the culture entered stationary phase and the concentration of H_2 reached an equilibrium value of *ca*. 18 Pa. When inoculated into HS-methanol medium with Tc, growth of P_{tet}*vht* strain was indistinguishable from the parental strain. However, when inoculated into the same medium without Tc, the P_{tet}*vht* strain accumulated H_2 to a level six times higher than the parental strain. CH_4 production ceased and the P_{tet}*vht* culture began to lyse, as H_2 concentration

increased to *ca*. 40 Pa. H_2 accumulation continued further with no growth and a considerable decrease in rate of CH_4 production. Thus, absence of Vht from the

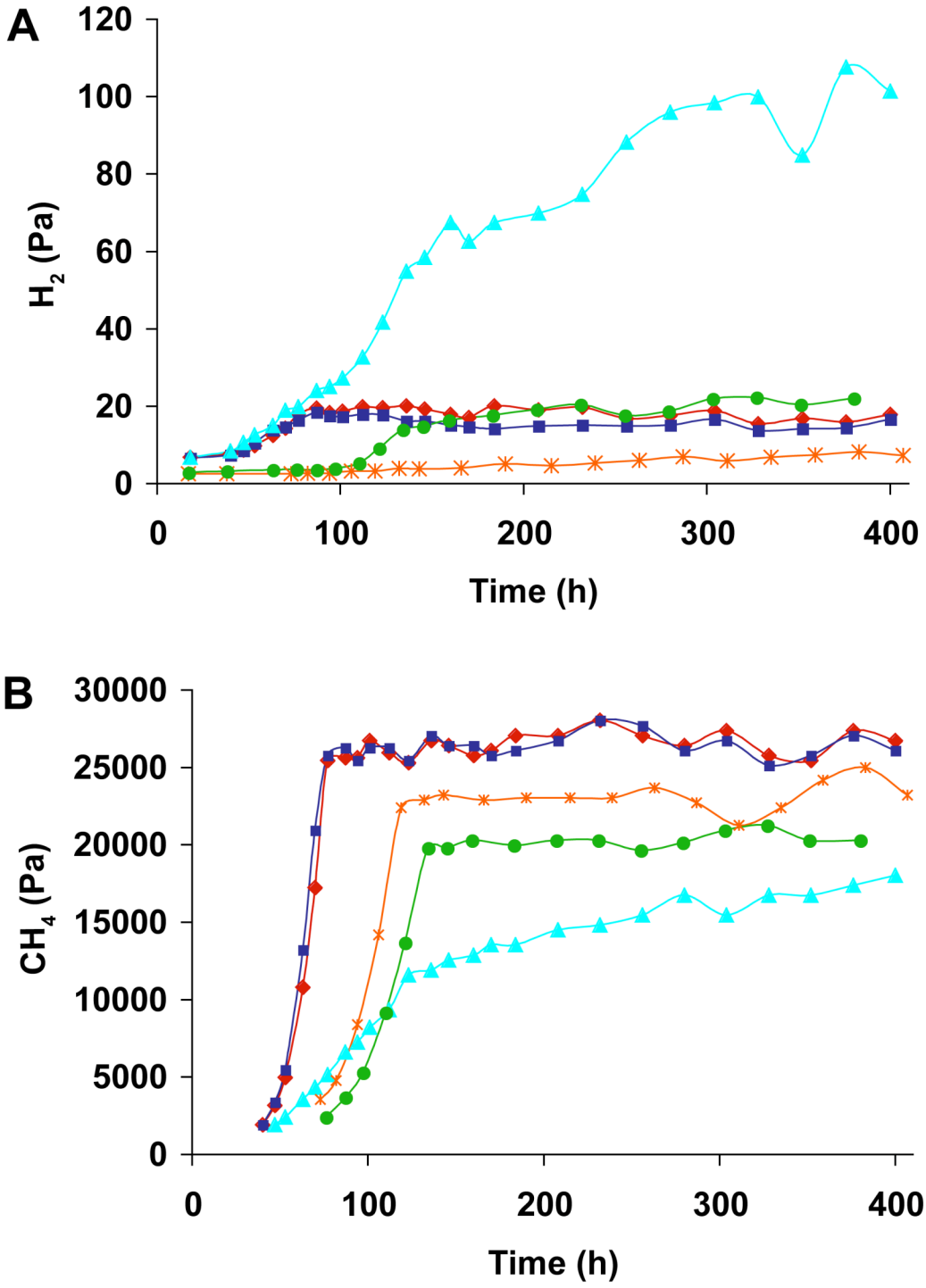

Figure 3.10 (cont.)

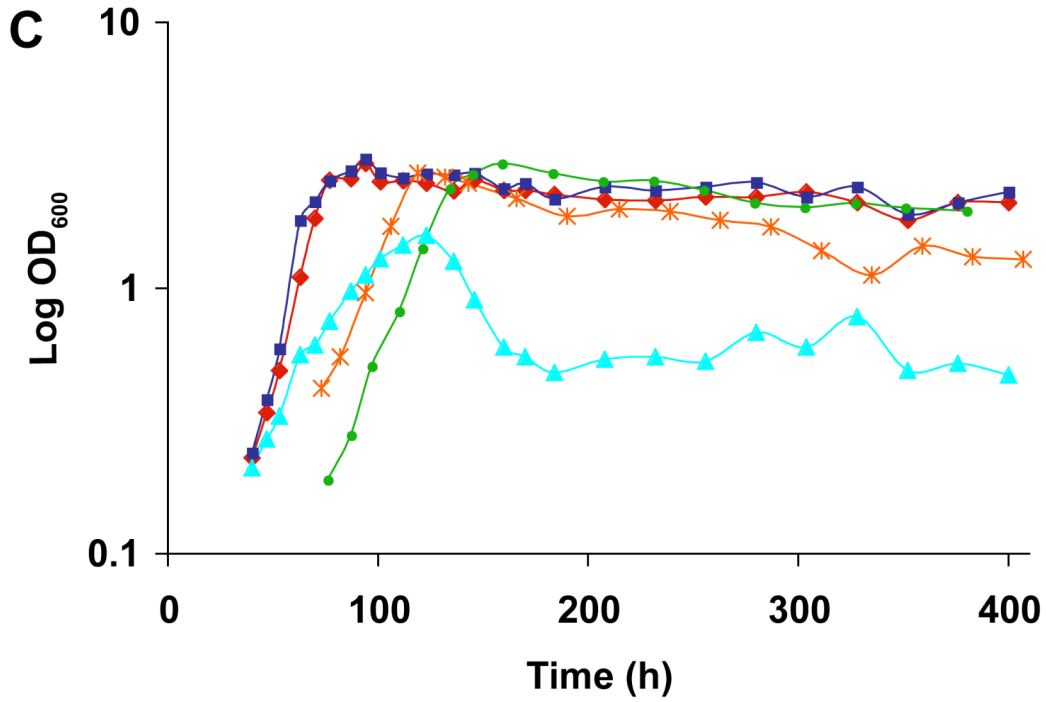

Figure 3.10 Hydrogen, methane and growth production in methanol-growing *M. barkeri* cultures. In Panel A, H_2 production was measured as a function of time in methanol-growing cultures of, WWM85 (red diamonds, *M. barkeri* Fusaro parent strain used to construct mutants, Table 3.3), tetracycline-regulated *vht* mutant (P_{tet}*vht*) with tetracycline (dark blue squares), P_{tet}*vht* without tetracycline (turquoise triangles), Δ*frh* mutant (orange stars), Δ*vht* Δ*frh* (lime circles) double mutant. The P_{tet}*vht* strain accumulated H_2 to 107 Pa as opposed to the parent strain that produced only 18 Pa H_2. For each time point in the experiment, corresponding measurements were also made for methane production (Panel B) and growth (Panel C). Growth was measured by monitoring optical density at 600 nm (OD_{600}). Measurements were done in triplicates as described in Materials and Methods. H_2 accumulation causes cessation of CH_4 production and cell lysis in the P_{tet}*vht* strain.

cell leads to H_2 accumulation, which is consistent with our prediction that Vht consumes H_2 produced during methylotrophic growth. In contrast to the isogenic parental strain, the Δ*frh* mutant did not produce H_2 as CH_4 production and growth ensued. The H_2 concentration barely increased from 2 Pa to a final value of *ca*. 8 Pa, as opposed to 18 Pa in the parental strain. This suggests that Frh might be one of the sources of H_2 in the parental strain.

3.4.5 Vht is dispensable in an *M. barkeri frh* mutant background

As discussed in the previous section, H_2 accumulation in P_{tet}*vht* strain is accompanied by growth inhibition. Also, the Frh hydrogenase produces H_2 during methylotrophic growth. Therefore, we predicted that a Δ*vht* mutant would be viable in a Δ*frh* markerless mutant background (42). While multiple attempts to isolate the single Δ*vht* mutant had failed, the Δ*vht* Δ*frh* double mutant was isolated in the first attempt, using methanol as the growth substrate (Table 3.3). Like the single Δ*frh* mutant, the Δ*vht* Δ*frh* double mutant is unable to grow using H_2/CO_2 (Tables 3.4, 3.5 & 3.6). The double mutant grows slower using methanol relative to the parental strain, with a *ca*. 34% increase in doubling time and 50% reduction in rate of CH_4 production in resting cell suspensions. However, the ratio of CO_2 to CH_4 produced in resting cell suspensions on methanol is 1:3, which is identical to that of the parental strain. The single Δ*frh* mutant exhibits a similar phenotype on methanol. The Δ*vht* Δ*frh* double mutant has a five-fold slower growth rate, *ca*. 50% reduction in growth yield, and a longer lag phase than the parental strain on methanol plus H_2/CO_2. The rate of CH_4 production and the total CH_4 produced in resting cell suspensions are also *ca*. six-times and three-times lower, respectively, relative to the parental strain on this substrate. The Δ*vht* Δ*frh* double mutant does not produce CO_2 in resting cell suspensions on methanol plus H_2/CO_2. In contrast to the single Δ*frh* mutant, the Δ*vht* Δ*frh* double mutant fails to grow on acetate. H_2 production was also measured in methanol-growing cultures of Δ*vht* Δ*frh* double mutant (Figure 3.10). Unlike the single Δ*frh* mutant that produces only 8 Pa of H_2, the Δ*vht* Δ*frh* double mutant accumulates H_2 to

about 22 Pa, indicating an alternate source of hydrogen production apart from Frh.

3.5 DISCUSSION

H_2-cycling, as a mechanism of energy conservation, has been controversial since its proposal by Odom and Peck in 1981 (36). However, our results suggest that H_2 accumulates when cycling is disrupted genetically in *M. barkeri*. The cycling apparently involves Frh hydrogenase that produces H_2 from $F_{420}H_2$, and Vht hydrogenase that consumes this H_2 (Figure 3.1). Consistent with this idea, our data show that Vht is essential for growth of *M. barkeri* on all substrates, including methanol. Furthermore, a tetracycline-regulated conditional *vht* mutant is shown to accumulate H_2 to a six-times higher level than the parental strain on methanol as the growth substrate, confirming involvement of Vht in H_2 consumption. In contrast, our results suggest that the Δ*frh* mutant produces negligible amount of H_2 on methanol, which is consistent with the role of Frh as the H_2-evolving hydrogenase. Based on these results, we propose a model of energy conservation, in which, Frh couples $F_{420}H_2$ oxidation to H_2 production using two protons from the cytoplasm. Subsequently, the H_2 diffuses to the active site of Vht in the periplasm, where it is oxidized to release two protons. Thus, this H_2-cycling mechanism creates a trans-membrane proton gradient that can be used to form ATP by the ATP synthase (34).

In Chapter 2 (22), I demonstrated that *M. barkeri* uses the H_2-cycling pathway preferentially, but not exclusively, because Δ*frh* mutants grow on

methanol, using Fpo. It was postulated that the H_2-dependent route is preferred due to kinetic advantage of Frh over Fpo. This is consistent with the observation that Fpo is unable to compete with Frh to prevent loss of electrons from $F_{420}H_2$ in the form of H_2 gas, when the H_2-uptake hydrogenase, Vht, is absent. The H_2 escapes from the cell, because it is detected in H_2 measurements with the conditional *vht* mutant. This is probably the reason for the inabilty of this mutant to grow on methanol. Consistent with this idea, deletion of *frh* allowed isolation of the Δ*vht* mutant in *M. barkeri*.

The Δ*vht* Δ*frh* double mutant is still capable of some H_2 production. The source of this H_2 is most likely Ech, as it is the only functional hydrogenase encoded by the mutant cell. Fre and Vhx are non-functional in the Δ*vht* Δ*frh* double mutant because they are unable to substitute for the role of Frh and Vht, respectively, on any methanogenic substrate tested (16, 22). During methylotrophic growth, Ech has been proposed to transfer electrons from Fd_{red}, produced during the methyl oxidative pathway, to H_2 (30, 31). The H_2 can then be fed into the H_2:heterodisulfide oxidoreductase system for reduction of the CoM-S-S-CoB heterodisulfide (11). In other words, Ech and Vht may also engage in H_2-cycling because the active site of Ech is located in cytoplasm (23), whereas that of Vht is in the periplasm (Figure 3.1). In the absence of Vht and Frh, H_2 produced by Ech accumulates. Although this causes a slight reduction in CH_4 production (*ca*. 4 kPa), growth inhibition does not occur. This is because *M. barkeri* also contains an as yet unidentified Fd_{red} oxidoreductase that can transfer reducing equivalents from Fd_{red} via a H_2-independent pathway (31). Our data

indicate that this Fd_{red} oxidoreductase is efficient enough to prevent a complete loss of electrons from Fd_{red} as H_2. Unlike Δ*vht* Δ*frh* double mutant, the single Δ*frh* mutant accumulates only negligible quantities of H_2. This implies that Vht present in the single mutant consumes H_2 produced by Ech. Although it is uncertain which Fd_{red} oxidation pathway is used preferentially, our evidence suggests involvement of Ech in H_2-cycling. This is significant because, Ech and Vht are also believed to conserve energy via H_2-cycling during acetate metabolism (30, 31).

M. barkeri probably evolved branched electron transport chains for energy conservation to adapt to different environmental conditions. In the environment, methanogens have to compete for H_2 with other micro-organisms, like denitrifiers, sulfate-reducing bacteria, iron-reducing bacteria and manganese-reducers. This is because, these organisms have a higher affinity for H_2 than methanogens. *M. barkeri* occurs as large multi-cellular aggregates in its freshwater habitat (26). Therefore, existence of dual electron transport system might confer it the flexibility of using the faster H_2-dependent pathways when present within the aggregates, where H_2 gas would not be lost to competing H_2-consumers in its environment (17). However, cells at the periphery of the aggregate might employ H_2-independent pathways to prevent such losses. *M. barkeri* has been shown to lose H_2 to its environment under low *in situ* H_2 concentrations or during syntrophic associations with sulfate-reducing bacteria, (15, 41, 48). In such cases, H_2-independent pathways would be undoubtedly beneficial, as H_2 production via the methyl oxidative pathway is not known to

conserve energy (11). A recent model in the sulfate reducer, *Desulfovibrio vulgaris*, proposes similar dual electron transport system for rapid adaptation to availability of various electron acceptors and donors in the environment (35).

M. barkeri might also utilize H_2-independent pathways under certain environmental conditions, when hydrogenases are inactive. For example, Ni-deprivation might result in hydrogenase-deficiency and subsequent use of H_2-independent pathways. Such Ni-dependent regulation is seen in a methanogen that belongs to the order *Methanobacteriales*, *Methanobacterium thermoautotophicum*. This regulation involves [NiFe] hydrogenase Frh and Ni-free enzymes Hmd (H_2-forming methylene-tetrahydromethanopterin dehydrogenase and Mtd (F_{420}-dependent methylene-tetrahydromethanopterin dehydrogenase) (1).

Unlike *M. barkeri* that preferably uses H_2-cycling, other methylotrophic species like *M. acetivorans* (16, 17), *Methanolobus tindarius* (19, 45) and *Methanococcoides burtonii* (44), probably employ H_2-independent oxidoreductase systems for energy conservation, because they do not encode functional hydrogenases. This might be advantageous to these marine species that exist as single cells in their habitat (46) and are therefore more prone to lose H_2 gas to competing micro-organisms in their environment. Also, this could be the reason why these species forego H_2-dependent electron transport pathways. In contrast, the fresh-water *M. mazei* might be able to use H_2-cycling within its cell aggregates, as it has functional Frh, Vht, Ech and Fpo enzymes (14).

Although several studies in the past have proposed the occurrence of H_2-cycling in methanogens (22, 24, 25), this study has provided direct experimental observation in *M. barkeri*. This is significant because, several anaerobic organisms possess the potential to use H_2-cycling for energy conservation. For instance, after its initial proposal in sulfate-reducing bacteria (36), H_2-cycling was also suggested to occur in the acetogen *Acetobacterium woodii* (37) and in the Fe (III) respiring *Geobacter sulfurreducens* (8, 29). Thus, H_2-cycling could be a general phenomenon in an anaerobic microbial community.

The deletion analysis of *vht* provides insight into the metabolism of various methanogenic substrates by *M. barkeri*. In the CO_2 reduction pathway, Vht is proposed to provide MPH_2 for methyl group reduction (47). Consistent with this role, the P_{tet}*vht* and Δ*vht* Δ*frh* mutants are not able to grow using H_2/CO_2. During aceticlastic growth, Vht consumes H_2 produced by Ech, in a presumed H_2-cycling mechanism (30, 31). This is supported by the inability of P_{tet}*vht* mutant to grow using acetate. Furthermore, unlike the single Δ*frh* mutant, Δ*vht* Δ*frh* double mutant fails to grow using this substrate, suggesting involvement of Vht in aceticlastic growth. In the methyl respiration pathway (21), methyl group of methanol is reduced to CH_4 using electrons derived from the oxidation of H_2 by Vht. However, the Δ*vht* Δ*frh* double mutant can grow via this pathway, presumably using Ech. This is because, Ech is the only functional hydrogenase present in this double mutant. Therefore, it must be responsible for oxidizing H_2 to provide Fd_{red} for methyl group reduction. Surprisingly, the conditional P_{tet}*vht* mutant is unable to grow using methanol plus H_2/CO_2. It is unclear why this

mutant fails to utilize the Ech-dependent pathway for growth via the methyl respiration pathway. It is apparent that presence of Frh, prevents Fd_{red}-dependent respiration in the P_{tet}*vht* mutant, however, this needs to be tested.

Finally, Vhx is not able to substitute for the role of Vht on any methanogenic substrate. This may be due to low expression of *vhx*, absence of post-translational processing, mutations in structural or catalytic residues, or some combination of these (16). Thus, the role of Vhx, which is conserved in all the three *Methanosarcina* species, is still unclear.

3.6 LITERATURE CITED

1. **Afting, C., A. Hochheimer, and R. K. Thauer.** 1998. Function of H_2-forming methylenetetrahydromethanopterin dehydrogenase from *Methanobacterium thermoautotrophicum* in coenzyme F_{420} reduction with H_2. Arch Microbiol **169:**206-10.

2. **Ausubel, F. M., R. Brent, R. E. Kingston, D. D. Moore, J. G. Seidman, J. A. Smith, and K. Strhul.** 1992. Current protocols in molecular biology. John Wiley & Sons, New York.

3. **Baumer, S., T. Ide, C. Jacobi, A. Johann, G. Gottschalk, and U. Deppenmeier.** 2000. The $F_{420}H_2$ dehydrogenase from *Methanosarcina mazei* is a redox-driven proton pump closely related to NADH dehydrogenases. J Biol Chem **275:**17968-73.

4. **Baumer, S., E. Murakami, J. Brodersen, G. Gottschalk, S. W. Ragsdale, and U. Deppenmeier.** 1998. The $F_{420}H_2$:heterodisulfide oxidoreductase system from *Methanosarcina* species. 2-Hydroxyphenazine mediates electron transfer from $F_{420}H_2$ dehydrogenase to heterodisulfide reductase. FEBS Lett **428:**295-8.

5. **Beifuss, U., M. Tietze, S. Baumer, and U. Deppenmeier.** 2000. Methanophenazine: Structure, Total Synthesis, and Function of a New Cofactor from Methanogenic Archaea. Angew Chem Int Ed Engl **39:**2470-2472.

6. **Boccazzi, P., J. K. Zhang, and W. W. Metcalf.** 2000. Generation of dominant selectable markers for resistance to pseudomonic acid by cloning and mutagenesis of the *ileS* gene from the archaeon *Methanosarcina barkeri* Fusaro. J Bacteriol **182:**2611-8.

7. **Bradford, M. M.** 1976. A rapid and sensitive method for the quantitation of microgram quantities of protein utilizing the principle of protein-dye binding. Anal Biochem **72:**248-54.

8. **Coppi, M. V.** 2005. The hydrogenases of *Geobacter sulfurreducens*: a comparative genomic perspective. Microbiology **151:**1239-54.

9. **Deppenmeier, U.** 1995. Different structure and expression of the operons encoding the membrane-bound hydrogenases from *Methanosarcina mazei* Gö1. Arch Microbiol **164:**370-6.

10. **Deppenmeier, U.** 2002. Redox-driven proton translocation in methanogenic Archaea. Cell Mol Life Sci **59:**1513-33.

11. **Deppenmeier, U.** 2004. The membrane-bound electron transport system of *Methanosarcina* species. J Bioenerg Biomembr **36:**55-64.

12. **Deppenmeier, U., M. Blaut, S. Lentes, C. Herzberg, and G. Gottschalk.** 1995. Analysis of the *vhoGAC* and *vhtGAC* operons from *Methanosarcina mazei* strain Gö1, both encoding a membrane-bound hydrogenase and a cytochrome b. Eur J Biochem **227:**261-9.

13. **Deppenmeier, U., M. Blaut, A. Mahlmann, and G. Gottschalk.** 1990. Reduced coenzyme F_{420}: heterodisulfide oxidoreductase, a proton-translocating redox system in methanogenic bacteria. Proc Natl Acad Sci U S A **87:**9449-53.

14. **Deppenmeier, U., A. Johann, T. Hartsch, R. Merkl, R. A. Schmitz, R. Martinez-Arias, A. Henne, A. Wiezer, S. Baumer, C. Jacobi, H. Bruggemann, T. Lienard, A. Christmann, M. Bomeke, S. Steckel, A. Bhattacharyya, A. Lykidis, R. Overbeek, H. P. Klenk, R. P. Gunsalus, H. J. Fritz, and G. Gottschalk.** 2002. The genome of *Methanosarcina mazei*: evidence for lateral gene transfer between bacteria and archaea. J Mol Microbiol Biotechnol **4:**453-61.

15. **Finke, N., T. M. Hoehler, and B. B. Jorgensen.** 2007. Hydrogen 'leakage' during methanogenesis from methanol and methylamine: implications for anaerobic carbon degradation pathways in aquatic sediments. Environ Microbiol **9:**1060-71.

16. **Guss, A. M., G. Kulkarni, and W. W. Metcalf.** 2009. Differences in hydrogenase gene expression between *Methanosarcina acetivorans* and *Methanosarcina barkeri*. J Bacteriol **191:**2826-33.

17. **Guss, A. M., B. Mukhopadhyay, J. K. Zhang, and W. W. Metcalf.** 2005. Genetic analysis of *mch* mutants in two *Methanosarcina* species demonstrates multiple roles for the methanopterin-dependent C-1 oxidation/reduction pathway and differences in H(2) metabolism between closely related species. Mol Microbiol **55:**1671-80.

18. **Guss, A. M., M. Rother, J. K. Zhang, G. Kulkarni, and W. W. Metcalf.** 2008. New methods for tightly regulated gene expression and highly efficient chromosomal integration of cloned genes for *Methanosarcina* species. Archaea **2:**193-203.

19. **Haase, P., U. Deppenmeier, M. Blaut, and G. Gottschalk.** 1992. Purification and characterization of $F_{420}H_2$-dehydrogenase from *Methanolobus tindarius*. Eur J Biochem **203:**527-31.

20. **Ide, T., S. Baumer, and U. Deppenmeier.** 1999. Energy conservation by the H_2:heterodisulfide oxidoreductase from *Methanosarcina mazei* Gö1: identification of two proton-translocating segments. J Bacteriol **181:**4076-80.

21. **Keltjens, J. T., and G. D. Vogels.** 1993. Methanogenesis. Chapman & Hall, New York.

22. **Kulkarni, G., D. M. Kriedelbaugh, A. M. Guss, and W. W. Metcalf.** 2009. H_2 is a preferred intermediate in the energy conserving electron transport chain of *Methanosarcina barkeri*. Proc Natl Acad Sci U S A **106:**15915-20.

23. **Kunkel, A., J. A. Vorholt, R. K. Thauer, and R. Hedderich.** 1998. An *Escherichia coli* hydrogenase-3-type hydrogenase in methanogenic Archaea. Eur J Biochem **252:**467-76.

24. **Lovley, D. R., and J. G. Ferry.** 1985. Production and Consumption of H(2) during Growth of *Methanosarcina* spp. on Acetate. Appl Environ Microbiol **49:**247-249.

25. **Lupa, B., E. L. Hendrickson, J. A. Leigh, and W. B. Whitman.** 2008. Formate-dependent H_2 production by the mesophilic methanogen *Methanococcus maripaludis*. Appl Environ Microbiol **74:**6584-90.

26. **Maeder, D. L., I. Anderson, T. S. Brettin, D. C. Bruce, P. Gilna, C. S. Han, A. Lapidus, W. W. Metcalf, E. Saunders, R. Tapia, and K. R. Sowers.** 2006. The *Methanosarcina barkeri* genome: comparative analysis with *Methanosarcina acetivorans* and *Methanosarcina mazei* reveals extensive rearrangement within methanosarcinal genomes. J Bacteriol **188:**7922-31.

27. **Metcalf, W. W., J. K. Zhang, E. Apolinario, K. R. Sowers, and R. S. Wolfe.** 1997. A genetic system for Archaea of the genus *Methanosarcina*: liposome-mediated transformation and construction of shuttle vectors. Proc Natl Acad Sci U S A **94:**2626-31.

28. **Metcalf, W. W., J. K. Zhang, X. Shi, and R. S. Wolfe.** 1996. Molecular, genetic, and biochemical characterization of the *serC* gene of *Methanosarcina barkeri* Fusaro. J Bacteriol **178:**5797-802.

29. **Methe, B. A., K. E. Nelson, J. A. Eisen, I. T. Paulsen, W. Nelson, J. F. Heidelberg, D. Wu, M. Wu, N. Ward, M. J. Beanan, R. J. Dodson, R. Madupu, L. M. Brinkac, S. C. Daugherty, R. T. DeBoy, A. S. Durkin, M. Gwinn, J. F. Kolonay, S. A. Sullivan, D. H. Haft, J. Selengut, T. M. Davidsen, N. Zafar, O. White, B. Tran, C. Romero, H. A. Forberger, J. Weidman, H. Khouri, T. V. Feldblyum, T. R. Utterback, S. E. Van Aken, D. R. Lovley, and C. M. Fraser.** 2003. Genome of *Geobacter sulfurreducens*: metal reduction in subsurface environments. Science **302:**1967-9.

30. **Meuer, J., S. Bartoschek, J. Koch, A. Kunkel, and R. Hedderich.** 1999. Purification and catalytic properties of Ech hydrogenase from *Methanosarcina barkeri*. Eur J Biochem **265:**325-35.

31. **Meuer, J., H. C. Kuettner, J. K. Zhang, R. Hedderich, and W. W. Metcalf.** 2002. Genetic analysis of the archaeon *Methanosarcina barkeri* Fusaro reveals a central role for Ech hydrogenase and ferredoxin in methanogenesis and carbon fixation. Proc Natl Acad Sci U S A **99:**5632-7.

32. **Michel, R., C. Massanz, S. Kostka, M. Richter, and K. Fiebig.** 1995. Biochemical characterization of the 8-hydroxy-5-deazaflavin-reactive hydrogenase from *Methanosarcina barkeri* Fusaro. Eur J Biochem **233:**727-35.

33. **Miller, V. L., and J. J. Mekalanos.** 1988. A novel suicide vector and its use in construction of insertion mutations: osmoregulation of outer membrane proteins and virulence determinants in Vibrio cholerae requires toxR. J Bacteriol **170:**2575-83.

34. **Muller, V.** 2004. An exceptional variability in the motor of archael A_1A_O ATPases: from multimeric to monomeric rotors comprising 6-13 ion binding sites. J Bioenerg Biomembr **36:**115-25.

35. **Noguera, D. R., G. A. Brusseau, B. E. Rittmann, and D. A. Stahl.** 1998. A unified model describing the role of hydrogen in the growth of *Desulfovibrio vulgaris* under different environmental conditions. Biotechnol Bioeng **59:**732-46.

36. **Odom, J. M., and H. D. Peck, Jr.** 1981. Hydrogen cycling as a general mechanism for energy coupling in the sulfate-reducing bacteria, *Desulfovibrio* sp. FEMS Microbiology Letters **12:**47-50.

37. **Odom, J. M., and H. D. Peck, Jr.** 1984. Hydrogenase, electron-transfer proteins, and energy coupling in the sulfate-reducing bacteria *Desulfovibrio*. Annu Rev Microbiol **38:**551-92.

38. **Odom, J. M., and J. D. Wall.** 1987. Properties of a hydrogen-inhibited mutant of *Desulfovibrio desulfuricans* ATCC 27774. J Bacteriol **169:**1335-7.

39. **Pankhania, I. P., L. A. Gow, and W. A. Hamilton.** 1986. The effect of hydrogen on the growth of *Desulfovibrio vulgaris* (Hildenborough) on lactate. Journal of General Microbiology **132:**3349-3356.

40. **Peck, Jr., H. D, J. LeGall, P. A. Lespinat, Y. Berlier, and G. Fauque.** 1987. A direct demonstration of hydrogen cycling by *Desulfovibrio vulgaris* employing membrane-inlet mass spectrometry. FEMS Microbiol Lett **40:**295-299.

41. **Phelps, T. J., R. Conrad, and J. G. Zeikus.** 1985. Sulfate-Dependent Interspecies H(2) Transfer between *Methanosarcina barkeri* and *Desulfovibrio vulgaris* during Coculture Metabolism of Acetate or Methanol. Appl Environ Microbiol **50:**589-594.

42. **Pritchett, M. A., J. K. Zhang, and W. W. Metcalf.** 2004. Development of a markerless genetic exchange method for *Methanosarcina acetivorans* C2A and its use in construction of new genetic tools for methanogenic archaea. Appl Environ Microbiol **70:**1425-33.

43. **Rother, M., P. Boccazzi, A. Bose, M. A. Pritchett, and W. W. Metcalf.** 2005. Methanol-dependent gene expression demonstrates that methyl-coenzyme M reductase is essential in *Methanosarcina acetivorans* C2A and allows isolation of mutants with defects in regulation of the methanol utilization pathway. J Bacteriol **187:**5552-9.

44. **Saunders, N. F., T. Thomas, P. M. Curmi, J. S. Mattick, E. Kuczek, R. Slade, J. Davis, P. D. Franzmann, D. Boone, K. Rusterholtz, R. Feldman, C. Gates, S. Bench, K. Sowers, K. Kadner, A. Aerts, P. Dehal, C. Detter, T. Glavina, S. Lucas, P. Richardson, F. Larimer, L. Hauser, M. Land, and R. Cavicchioli.** 2003. Mechanisms of thermal adaptation revealed from the genomes of the Antarctic Archaea *Methanogenium frigidum* and *Methanococcoides burtonii*. Genome Res **13:**1580-8.

45. **Scheel, E., and G. Schafer.** 1990. Chemiosmotic energy conversion and the membrane ATPase of *Methanolobus tindarius*. Eur J Biochem **187:**727-35.

46. **Sowers, K. R., J. E. Boone, and R. P. Gunsalus.** 1993. Disaggregation of *Methanosarcina* spp. and Growth as Single Cells at Elevated Osmolarity. Appl Environ Microbiol **59:**3832-3839.

47. **Thauer, R. K., A. K. Kaster, H. Seedorf, W. Buckel, and R. Hedderich.** 2008. Methanogenic Archaea: ecologically relevant differences in energy conservation. Nat Rev Microbiol **6:**579-91.

48. **Valentine, D. L., D. C. Blanton, and W. S. Reeburgh.** 2000. Hydrogen production by methanogens under low-hydrogen conditions. Arch Microbiol **174:**415-21.

49. **van den Berg, W. A., W. M. van Dongen, and C. Veeger.** 1991. Reduction of the amount of periplasmic hydrogenase in *Desulfovibrio vulgaris* (Hildenborough) with antisense RNA: direct evidence for an important role of this hydrogenase in lactate metabolism. J Bacteriol **173:**3688-94.

50. **Wanner, B. L.** 1986. Novel regulatory mutants of the phosphate regulon in *Escherichia coli* K-12. J Mol Biol **191:**39-58.

51. **White, D.** 2000. The Physiology and Biochemistry of Prokaryotes, Second ed. pp 165-179. Oxford University Press, Oxford, New York.

52. **White, D.** 2000. The Physiology and Biochemistry of Prokaryotes, Second ed. pp 103-131 Oxford University Press, Oxford, New York.

53. **Zhang, J. K., A. K. White, H. C. Kuettner, P. Boccazzi, and W. W. Metcalf.** 2002. Directed mutagenesis and plasmid-based complementation in the methanogenic archaeon *Methanosarcina acetivorans* C2A demonstrated by genetic analysis of proline biosynthesis. J Bacteriol **184:**1449-54.

CHAPTER 4

CONVERSION OF *METHANOSARCINA BARKERI* INTO A NON-HYDROGENOTROPHIC *METHANOSARCINA ACETIVORANS*-LIKE SPECIES REVEALS FEATURES OF ITS BRANCHED HYDROGEN-DEPENDENT AND -INDEPENDENT ELECTRON TRANSPORT PATHWAYS

4.1 ABSTRACT

The methanogen *Methanosarcina barkeri* encodes three kinds of [NiFe] hydrogenases; ferredoxin (Fd_{ox})-dependent Ech, F_{420}-dependent Frh and methanophenazine (MP)-dependent Vht. Although these hydrogenases are directly involved in H_2 metabolism when the organism is grown using H_2/CO_2 or methanol plus H_2/CO_2, they also play an important role in the methylotrophic and aceticlastic pathways, in which H_2 is produced as an intermediate, in a presumed "H_2-cycling" pathway for energy conservation. To further dissect the roles of these hydrogenases in *M. barkeri* physiology, we constructed a series of hydrogenase deletion mutants in various permutations and combinations, including a mutant that is devoid of all three types of hydrogenases. Our data show that each of the three types of hydrogenases is needed for growth via the CO_2 reduction pathway. In contrast, none of the hydrogenases is essential during methylotrophic growth, indicating the presence of H_2-independent electron transport chains, which are able to support wild-type growth yields. While the reduced F_{420} ($F_{420}H_2$):heterodisulfide pathway has been identified in a previous study to involve Fpo, the components of the reduced Fd_{ox} (Fd_{red}):heterodisulfide pathway remain unknown. However, our study demonstrates that this unidentified pathway is as efficient as H_2-cycling in supporting methylotrophic

growth. Additionally, it allows growth via the methyl respiration pathway when Fd_{red} is made available by the action of Ech. Surprisingly, the Fd_{red}:heterodisulfide pathway is insufficient for aceticlastic growth for unknown reasons. The data presented here also suggest that Ech and/or Frh exert inhibitory effects on the methyl oxidative pathway by catalyzing conversion of H_2 to Fd_{red} and $F_{420}H_2$, respectively. Finally, this study provides evidence for involvement of Hyp proteins in maturation of at least one of the [NiFe] hydrogenases, Ech. This work highlights the similarities and differences between H_2-independent electron transport chains of the hydrogenotroph *M. barkeri* and the non-hydrogenotroph *Methanosarcina acetivorans.*

4.2 INTRODUCTION

Hydrogenases play an important role in microbial metabolism by virtue of their ability to catalyze the reversible oxidation of molecular hydrogen (H_2) (48). In methanogenic Archaea, H_2 is primarily used to reduce CO_2 to methane (CH_4) (46). However, some methanogens like *Methanosphaera* (29, 38) and *Methanosarcina barkeri* (20), can also utilize H_2 for reduction of methylated C-1 compounds like methanol to CH_4. *M. barkeri* also produces H_2, when grown using methanol alone via the methylotrophic pathway (25, 30). It is postulated that aceticlastic growth involves the obligate production of H_2 as well, in *M. barkeri* (25, 30, 36) and *Methanosarcina mazei* (51) *.* Thus, hydrogenases seem to be important for growth of methanogenic species like *M. barkeri* on a range of substrates. *M. barkeri* encodes three types of [NiFe] hydrogenases that differ

with respect to their electron carriers, which is either Fd_{ox} (Ech), coenzyme F_{420} (Frh) or membrane-bound electron carrier MP (Vht) (19).

The Fd_{ox}-dependent hydrogenase, Ech, of *M. barkeri* has been purified and characterized (35). It is a membrane-bound hydrogenase that catalyzes the endergonic transfer of electrons from H_2 to a soluble 2[4Fe-4S] Fd_{ox}, by coupling this reaction to the consumption of an electrochemical ion gradient (Figure 4.1).

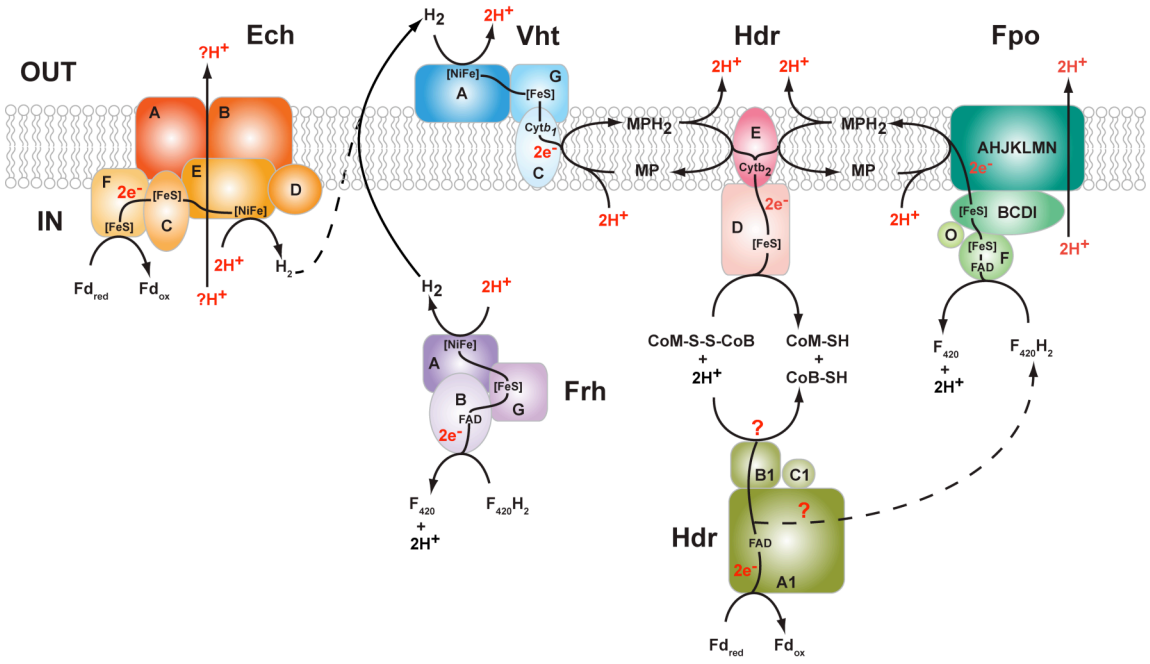

Figure 4.1 The electron transport chain of *Methanosarcina barkeri* (adapted from (25)) has been proposed to comprise two energy-conservation systems, the $F_{420}H_2$:heterodisulfide oxidoreductase and the H_2:heterodisulfide oxidoreductase. In the former, $F_{420}H_2$ is oxidized by FpoF releasing two electrons that are transferred through FpoBCDI and then FpoAHJKLMN to membrane-soluble MP. This reaction is coupled to pumping of two protons outside the cell. Reduction of MP consumes two protons from the cytoplasm, which are subsequently released outside the cell upon oxidation of MPH_2. The electrons are then transferred through HdrED to reduce CoM-S-S-CoB with two protons from the cytoplasm. Alternatively, in the H_2:heterodisulfide oxidoreductase, H_2 is oxidized by Vht to produce two protons outside the cell and two electrons that are transferred to MP, which is then used to reduce CoM-S-S-CoB. The Frh/Vht arrow represents a third energy-conservation mechanism. In this pathway, $F_{420}H_2$ is oxidized by the cytoplasmic hydrogenase Frh to generate H_2. The H_2 then diffuses outside the cell to the active site of membrane-bound hydrogenase Vht, where it is oxidized, resulting in the translocation of two protons via the H_2-cycling mechanism. The electrons are passed through MP to CoM-S-S-CoB as in the other two systems. In all three systems, the entire electron transport process leads to the net translocation of four protons outside the cell per two electrons transferred from $F_{420}H_2$

Figure 4.1 (cont.)

or H_2 to CoM-S-S-CoB. The electrochemical gradient generated is coupled to ATP synthesis via an A-type ATPase. There is evidence to suggest that Ech/Vht may also conserve energy via the H_2-cycling mechanism. In this, Ech presumably couples the exergonic oxidation of Fd_{red} to H_2 formation, concomitantly pumping an unknown number of protons outside the cell. The proton-motive force is likely used for the transfer of methyl group from methyl-CoM to tetrahydrosarcinapterin. However, the H_2 may diffuse out to Vht and enter the H_2:heterodisulfide oxidoreductase system for energy conservation. The organism also contains a soluble Hdr, HdrA1B1C1, which has been proposed to transfer electrons from Fd_{red} to CoM-S-S-CoB in *Methanosarcina acetivorans*. This transfer is mediated in a one-step reaction or using an electron bifurcation mechanism, where for every CoM-S-S-CoB reduced, a molecule of coenzyme F_{420} also undergoes reduction. Scalar or vectorial protons translocated across the cell membrane are highlighted in red. Abbreviations; Ech, Fd-dependent hydrogenase; Frh, F_{420}-reducing hydrogenase; Fpo, $F_{420}H_2$:phenazine oxidoreductase; Vht, methanophenazine-dependent hydrogenase; Hdr, heterodisulfide reductase; CoM-SH, coenzyme M; CoB-SH, coenzyme B; CoM-S-S-CoB, mixed disulfide of CoM-SH and CoB-SH; MP/MPH_2, oxidized and reduced methanophenazine; Fd_{ox}/Fd_{red}, oxidized and reduced ferredoxin; F_{420}/$F_{420}H_2$, oxidized and reduced Factor 420; FAD, flavin adenine dinucleotide; [FeS], iron-sulfur cluster; [NiFe], bimetallic catalytic center; Cytb_2, cytochrome b_2.

Three distinct physiological roles of this hydrogenase were revealed in *M. barkeri* by mutational analysis of the Ech-encoding operon, *echABCDEF* (Figure 4.2) (36). Firstly, in the CO_2 reduction pathway, Fd_{red} generated by Ech acts as an electron donor for reduction of CO_2 to the formyl level. Secondly, Fd_{red} is also needed for biosynthesis in the CO_2 reduction and methyl-respiration pathways. Thirdly, Ech is required during aceticlastic growth as well. Here, it most likely transfers electrons from Fd_{red}, which is produced from oxidation of carbonyl group of acetate to CO_2, to H_2 in an energy-conserving reaction. Subsequently, this cytoplasmically produced H_2 can diffuse out of the cell to the active site of the MP-dependent hydrogenase Vht, where it is oxidized to generate electrons and protons (35, 36). The electrons are fed into the electron transport chain, H_2:heterodisulfide oxidoreductase system (12), that terminates with the reduction of the heterodisulfide (CoM-S-S-CoB) of coenzyme M (CoM-SH) and coenzyme B (CoB-SH). However, the consumption and production of protons by Ech and

Vht in the cytoplasm and periplasm, respectively, creates an energy-conserving proton gradient via the H_2-cycling mechanism (Figure 4.1) (41). A similar role of Ech has also been proposed in the methylotrophic pathway (25, 35, 36), in which Fd_{red} produced by formyl group oxidation might be converted into H_2 by this

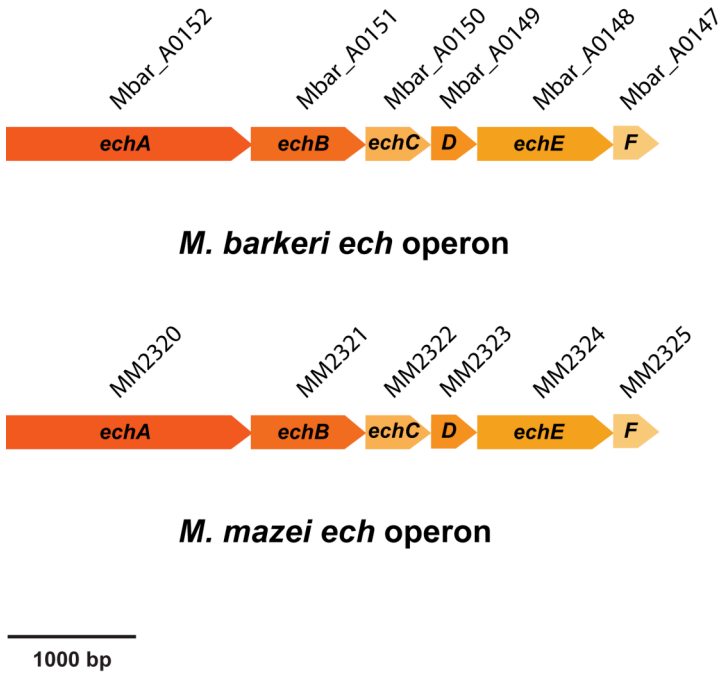

Figure 4.2 Genomic organization of operons encoding ferredoxin-dependent hydrogenase (Ech) in *Methanosarcina* species. Ech is encoded by the 6-gene operon (*echABCDEF*) in *M. barkeri* and *M. mazei*. *M. acetivorans*, however, is missing the *ech* operon.

hydrogenase. However, the Δ*ech* mutant of *M. barkeri* is capable of transferring electrons from Fd_{red} to the heterodisulfide in an Ech-independent manner, suggesting the presence of an alternate H_2-independent pathway involving an unidentified Fd_{red} oxidoreductase (36). Deletion analysis of *ech* operon (Figure 4.2) in the closely related *M. mazei* species, supports the proposed function of Ech in the aceticlastic and methylotrophic pathways (51). In addition, this study

provides biochemical evidence for the presence of a Fd_{red} oxidoreductase in *M. mazei*, which is capable of mediating electron transfer from Fd_{red} to the heterodisulfide in an Ech-independent manner. This is in support of the presence of such an enzyme in *M. barkeri* as well. Interestingly, *M. acetivorans* lacks the *ech* operon (18). Thus, it relies exclusively on H_2-independent putative Fd_{red} oxidoreductases, including the Na^+-pumping Fd_{red}:MP oxidoreductase (Rnf) (28) and/or the soluble heterodisulfide reductase (HdrA1B1C1) (9), while growing on acetate and methanol as substrates. Although Rnf is not present in *M. barkeri* (31) and *M. mazei* (14), both species contain operons encoding HdrA1B1C1 in their genomes. In conclusion, Fd_{red}-dependent H_2-independent pathways seem to be a common feature of all *Methanosarcina* species.

The F_{420}-dependent hydrogenase (Frh) has also been purified from *M. barkeri* (16, 37). It catalyzes the reversible reduction of coenzyme F_{420} with H_2 (Figure 4.1). Reduced F_{420} ($F_{420}H_2$) serves as an electron donor for reduction of methenyl and methylene groups in the CO_2 reduction pathway (37, 46). Consistent with this function, the deletion mutant of the operon encoding Frh, *frhADGB*, in *M. barkeri* is unable to grow on H_2/CO_2 as a substrate (24). The Δ*frh* mutant also shows a severe growth defect on methanol. Therefore, Frh was proposed to transfer electrons from $F_{420}H_2$, produced from methyl and methylene group oxidation, to H_2 in the methylotrophic pathway (37). As shown in chapter 3 (25), the H_2 enters the H_2:heterodisulfide oxidoreductase system via the action of Vht (Figure 4.1). Because Frh is located within the cytoplasm, whereas Vht is periplasmic, the production and subsequent oxidation of H_2 by these two

hydrogenases conserves energy via the H_2-cycling mechanism (25). Although H_2-cycling is the preferential (faster) mode of electron transfer from $F_{420}H_2$ to the heterodisulfide, the $F_{420}H_2$ dehydrogenase (Fpo) is able to perform this transfer in a H_2-independent way by employing the $F_{420}H_2$:heterodisulfide oxidoreductase system (Figure 4.1) (24). In this system (12), electrons are initially channeled from $F_{420}H_2$ to MP via Fpo. Subsequently, as in the H_2:heterodisulfide system, reduced MP (MPH_2) is used by the membrane-bound heterodisulfide reductase (HdrED) to reduce the CoM-S-S-CoB heterodisulfide. *M. mazei* (14) and *M. acetivorans* (18) also contain operons encoding Frh, Vht and Fpo. While *M. mazei* might be able to employ both the Frh/Vht and Fpo pathways for $F_{420}H_2$ oxidation, *M. acetivorans* can only utilize Fpo, because it does not express its *frh* and *vht* operons (19, 20).

M. barkeri also contains a second F_{420}-reducing hydrogenase-encoding operon, *freAEGB*, which lacks the gene *D* present in the *frhADGB* operon (47). Subunit E does not show homology to subunit D that encodes a putative hydrogenase maturation protease or any other protein in the database. Nonetheless, the *fre* operon encodes a hydrogenase that is 85-87% identical to Frh. Also, all the important structural and catalytic residues of Frh are conserved in Fre. Thus, it has been proposed that Fre might be functional if it undergoes processing by FrhD (19). However, deletion of *fre* from *M. barkeri* does not have any effect on its growth. Moreover, Fre is also not able to substitute for the role of Frh in the Δ*frh* mutant (24). Therefore, Fre is not functional under the conditions tested.

The third type of hydrogenase, Vht, catalyzes the reversible reduction of the membrane-soluble electron carrier MP with H_2 (Figure 4.1) (4, 13, 19). MPH_2 acts as an electron donor for reduction of the CoM-S-S-CoB heterodisulfide using HdrED (12). Subsequently, CoM-SH and CoB-SH are used to reduce methyl group in the terminal methanogenic step. Not only have each of the individual reactions in this H_2:heterodisulfide oxidoreductase system been demonstrated using purified *M. mazei* enzymes and chemically synthesized MP (4, 11, 13, 22), the entire electron transport chain has also been reconstituted *in vitro* with *M. mazei* membrane preparations (22). Biochemical and genetic investigations in *M. mazei* and *M. barkeri* (24, 25, 36), have implicated necessity of this oxidoreductase system in each of the four methanogenic pathways (12). The source of H_2 in the CO_2 reduction and methyl-respiration pathways is external (12, 20, 38), whereas in the aceticlastic (35, 36) and methylotrophic (24, 25) pathways, H_2 is presumably produced from Fd_{red} and $F_{420}H_2$ by Ech and Frh hydrogenases, respectively (Figure 4.1). This proposal is consistent with the phenotype of an *M. barkeri* tetracycline (Tc)-regulated conditional *vht* mutant (P_{tet}*vht*) that is unable to grow on any of the methanogenic substrates tested under non-permissive conditions. However, Vht is not required for growth on methanol in the Δ*frh* mutant background. This is probably because, in the double Δ*vht frh* mutant, the Frh/Vht H_2-cycling is disrupted, thereby allowing use of Fpo for electron transfer from $F_{420}H_2$ to the heterodisulfide. In contrast, when Vht is deleted in the presence of Frh in the cell, the faster Frh enzyme out competes Fpo and disposes off electrons from $F_{420}H_2$ on to H_2 gas, which escapes from the

cell (25). Thus, despite its importance, Vht is not essential for growth of *M. barkeri* when Frh is absent from the cell.

While all three *Methanosarcina* species possess two operons, *vhtGACD* and *vhxGAC*, encoding the two MP-dependent hydrogenases, Vht and Vhx, *M. mazei* contains a third *vhoGAC* operon as well (14, 18, 31). The Vho and Vht enzymes are *ca.* 95% identical, however, Vhx displays only *ca*. 50% amino acid sequence identity to the other two hydrogenases. The deduced sequences of the Vht/Vhx/Vho enzymes from the three species possess all the important structural and catalytic residues. Thus, it has been proposed that in spite of missing the maturation protease-encoding gene D, *vhx* and *vho* operons might encode functional hydrogenases if the VhtD protein can process them by acting in *trans* (19). However, a deletion mutant of *vhx* in *M. barkeri* does not exhibit any growth defect. Moreover, in the P_{tet}*vht* mutant, Vhx is not able to substitute for the role of Vht (25). Thus, Vhx is not functional under the conditions tested.

All [NiFe] hydrogenases require posttranslational modification to become enzymatically active (5). Although this modification has not been examined in *Methanosarcina*, it has been extensively studied in *Escherichia coli*, where the gene products of *hypABCDE* and *hypF* are responsible for maturation of hydrogenases by assembly of their bimetallic catalytic center. Homologs of these genes are found in each of the sequenced *Methanosarcina* genomes (14, 18, 31), suggesting that posttranslational activation might occur by similar mechanisms in these organisms.

It is evident from the aforementioned data that hydrogenases play an important role in *M. barkeri* physiology in each of the four methanogenic pathways. However, these data also highlight the dichotomy of the electron transport chains of *M. barkeri*, which comprise of both H_2-dependent and -independent branches. Because little is known about the latter pathways, we constructed and characterized hydrogenase deletion mutants in various combinations, including a hydrogenase minus quintuple mutant of *M. barkeri* that is able to grow methylotrophically.

4.3 MATERIALS AND METHODS

4.3.1 Media and growth conditions

Methanosarcina strains were grown as single cells (45) at 37^{o} C in high salt (HS) broth medium (34) or on agar-solidified medium as described (6). Growth substrates provided were methanol (125 mM in broth medium and 50 mM in agar-solidified medium) or sodium acetate (120 mM) under a headspace of either N_2/CO_2 (80/20%) mix at 50 kPa over ambient pressure or H_2/CO_2 (80/20%) mix at 300 kPa over ambient pressure. Cultures were supplemented as indicated with 0.1% yeast extract (YE), 0.1% casamino acids (CAA), 10 mM sodium acetate, 10 mM pyruvate or 100 mM pyruvate. Puromycin (CalBioChem, San Diego, CA) was added at 2 μg/ml for selection of the puromycin transacetylase (*pac*) gene (42). 8-Aza-2,6-diaminopurine (8-ADP) (Sigma, St Louis, MO) was added at 20 μg/ml for selection against the presence of *hpt* (42). Tetracycline (Tc) was added at 100 μg/ml to induce the tetracycline-regulated

P*mcrB*(*tet*O) promoter (21). Standard conditions were used for growth of *Escherichia coli* strains (49) DH5α/λ-*pir* (39) and DH10B (Stratagene, La Jolla, CA), which were used as hosts for plasmid constructions.

4.3.2 DNA methods and plasmid constructions

Standard methods were used for plasmid DNA isolation and manipulation in *E. coli* (3). Liposome mediated transformation was used for *Methanosarcina* as described (33). Genomic DNA isolation and DNA hybridization were as described (6, 34, 52). DNA sequences were determined from double-stranded templates by the W.M. Keck Center for comparative and functional genomics, University of Illinois. Plasmid constructions are described in tables 4.1 and 4.2.

4.3.3 Construction of hydrogenase deletion mutants

The construction and genotype of all *Methanosarcina* strains is presented in table 4.3. Carl G. Radosevich constructed the Δ*echABCDEF* (Figure 4.2) single mutant in the Δ*hpt* (WWM85) (21) background of *M. barkeri* Fusaro by the markerless genetic exchange method using pCGR10 (42). The mutant was isolated using methanol as the growth substrate and was confirmed by PCR. The Δ*frh fre* double mutant was isolated by deletion of *freAEGB* in the Δ*frhADGB* mutant (25) using pGK6 (24) by the markerless method of genetic exchange (42). The mutant was isolated using methanol plus H_2/CO_2 as the growth substrate. The *M. barkeri* locus containing *vhtGACD*, *Mbar_A1843*, *Mbar_A1842*

Table 4.1 Plasmids used in this study

Plasmid	Description and/or construction	Reference
pJK301	Vector, containing a *pac*-*hpt* cassette, used to delete genes from *M*. *barkeri* Fusaro chromosome using double homologous recombination-mediated gene replacement method	(50)
pMR55	Non-replicating plasmid that contains the Flp recombinase gene under control of the *mcrB* promoter	(44)
pGK61A	Plasmid, containing a *pac*-*hpt* cassette flanked by FRT5 sites and P*mcrB*-*tetR*, used to express *vht* from the tetracycline-regulated promoter P*mcrB*(*tet*O3) in *M*. *barkeri* Fusaro	(25)
pGK6	Plasmid, containing a *pac*-*hpt* cassette, used to delete *fre* from *M*. *barkeri* Fusaro chromosome using the markerless exchange method	(24)
pAMG77	Plasmid containing a *pac*-*hpt* cassette and *ech* downstream region	(17)
pAMG80	*ech* downstream region from PstI/SpeI-digested pAMG77 ligated to NsiI/AvrII-digested pMP44	This study
pCGR10	AscI/NotI-digested *ech* upstream region amplified using primers echupfor and echuprev and ligated to MluI/NotI-digested pAMG80	This study

Table 4.1 (cont.)

Plasmid	Description and/or construction	Reference
pGK82B	Plasmid, containing a *pac-hpt* cassette, used to delete *vht* from *M. barkeri* Fusaro chromosome using the double homologous recombination-mediated gene replacement method	(25)
pGK11	SpeI/NotI-digested *vhx* downstream region amplified using primers vhxdnfor1 and vh3dnrev and ligated to 6.7 kb fragment of SpeI/NotI-digested pGK82B	This study
pGK83A	XhoI/ApaI-digested *hyp* upstream region amplified using primers hypdoubleupfor and hypdoubleuprev and ligated to XhoI/ApaI-digested pJK301	This study
pGK83B	SpeI/NotI-digested *hyp* downstream region amplified using primers hypdoublednfor and hypdoublednrev and ligated to SpeI/NotI-digested pGK83A	This study
pGK12	XhoI/ApaI-digested *vhx* downstream region amplified using primers vhxdnfor2 and vhxdnrev1 and ligated to 7 kb fragment of XhoI/ApaI-digested pGK83B	This study
pGK8	NotI/BamHI-digested *ech* upstream region amplified using primers echdoubleupfor and echdoubleuprev and ligated to NotI/BamHI-digested pJK301	This study

Table 4.1 (cont.)

Plasmid	Description and/or construction	Reference
pGK9	XhoI/ApaI-digested *ech* downstream region amplified using primers echdoublednfor and echdoublednrev and ligated to XhoI/ApaI-digested pJK301	This study

Table 4.2 Primers used in this study

Primer	Sequence (added sites are underlined)	Added sites
echupfor	GGCGCGCCTCAATGGATTGCAGACCAAA	AscI
echuprev	GGCGCGCCGCGGCCGCCCCGGGTATCCTCCGATCTATTAATCC	AscI/NotI/SmaI
vhxdnfor1	GGCGCGCCACTAGTTGATAACAAGCGCAGATATTATTTA	AscI/SpeI
vh3dnrev	GGCGCGCCGCGGCCGCGCTTGGAAGCTGTTTTGGAG	AscI/NotI
hypdoubleupfor	GGCGCGCCGGGCCCCAGGGTAAGAAGGACCCAAT	AscI/ApaI
hypdoubleuprev	GGCGCGCCCTCGAGACACATTCCTCGAACTCTTTTT	AscI/XhoI
hypdoublednfor	GGCGCGCCACTAGTTAAAGATCAGCACTAGCTGAGATTG	AscI/SpeI
hypdoublednrev	GGCGCGCCGCGGCCGCTTCTCGCAATCCGAAGTACC	AscI/NotI
vhxdnfor2	GGCGCGCCCTCGAGTGATAACAAGCGCAGATATTATTTA	AscI/XhoI
vhxdnrev1	GGCGCGCCGGGCCCGCTTGGAAGCTGTTTTGGAG	AscI/ApaI
echdoubleupfor	GGCGCGCCGCGGCCGCGTGTTCATCCGTTCCGATTT	AscI/NotI
echdoubleuprev	GGCGCGCCGGATCCACAGCGTATCCTCCGATCTA	AscI/BamHI
echdoublednfor	GGCGCGCCCTCGAGAGACAAGCCAAAAGCTCCAA	AscI/XhoI

Table 4.2 (cont.)

Primer	Sequence (added sites are underlined)	Added sites
echdoublednrev	GGCGCGCCGGGCCCACATACTCTGCCGCATACCC	AscI/ApaI
frhfor5	AAATTCGGGAGGAGATGTTAGAG	None
frhrev6	CAGAACCCTGCTTTCTAAGAATG	None

[a]The added restriction sites are underlined.

Table 4.3 *M. barkeri* Fusaro strains used in this study

Strain	Genotype	Source or construction
WWM85	Δ*hpt*::P*mcrB*-ϕ*C31int-attP*	(21)
WWM115	Δ*frh* Δ*hpt*::P*mcrB*-ϕ*C31int-attB*	(25)
WWM116	Δ*fre* Δ*hpt*::P*mcrB*-ϕ*C31int-attP*	(24)
WWM237	Δ*vhx* Δ*hpt*::P*mcrB*-ϕ*C31int-attP*	(25)
WWM351	Δ*vht*::FRT Δ*frh* Δ*hpt*::P*mcrB*-ϕ*C31int-attB*	(25)
WWM133	Δ*ech* Δ*hpt*::P*mcrB*-ϕ*C31int-attP*	Deletion of *ech* in WWM85 with pCGR10
WWM234	Δ*fre* Δ*frh* Δ*hpt*::P*mcrB*-ϕ*C31int-attB*	Deletion of *fre* in WWM116 with pGK6
WWM327	Δ*vht* Δ*vhx* ΔMbar_A1842 ΔMbar_A1843 Δ*fre* Δ*frh* Δ*hpt*::P*mcrB*-ϕ*C31int-attB*	Deletion of *vht*, *vhx*, Mbar_A1842 and Mbar_A1843 in WWM234 with XhoI/NotI-digested 5.6 kb pGK11 and removal of *pac-hpt* cassette using pMR55
WWM352	Δ*hyp* Δ*vht* Δ*vhx* ΔMbar_A1842 ΔMbar_A1843::*pac-hpt* Δ*fre* Δ*frh* Δ*hpt*::P*mcrB*-ϕ*C31int-attB*	Deletion of *hyp*, *vht*, *vhx*, Mbar_A1842 and Mbar_A1843 in WWM234 with ApaI/NotI-digested 6 kb pGK12

Table 4.3 (cont.)

Strain	Genotype	Source or construction
WWM370	Δ*ech*::*pac-hpt* Δ*frh* Δ*hpt*::P*mcrB*-ϕ*C31int-attB*	Deletion of *ech* in WWM115 with ApaI/NotI-digested 5.6 kb pGK9
WWM366	Δ*ech*::*pac-hpt* Δ*vht*::FRT Δ*frh* Δ*hpt*::P*mcrB*-ϕ*C31int-attB*	Deletion of *ech* in WWM351 with ApaI/NotI-digested 5.6 kb pGK9
WWM388	Δ*ech*::*pac-hpt* Δ*vht* Δ*vhx* ΔMbar_A1842 ΔMbar_A1843 Δ*fre* Δ*frh* Δ*hpt*::P*mcrB*-ϕ*C31int-attB*	Deletion of *ech* in WWM327 with ApaI/NotI-digested 5.6 kb pGK9
WWM157	*vht*ΩP*mcrB-tetR pac-hpt* P*mcrB*(*tet*O3) Δ*hpt*::P*mcrB-tetR*-ϕ*C31int-attB*	(25)
WWM363	*vht*ΩP*mcrB-tetR pac-hpt* P*mcrB*(*tet*O3) Δ*ech* Δ*hpt*::P*mcrB*-ϕ*C31int-attP*	Expression of *vht* from P*mcrB*(*tet*O3) in WWM133 using NcoI/SpeI-digested 7.0 kb pGK61A

and *vhxGAC*; or *hypCDABE*, *vhtGACD*, *Mbar_A1843*, *Mbar_A1842* and *vhxGAC*, was deleted from the Δ*frh fre* double mutant using XhoI/NotI-digested 5.6 kb pGK11 or ApaI/NotI-digested 6 kb pGK12, respectively, by the homologous gene replacement method (52) in the presence of methanol (Figure 4.3). This gave rise to the two mutants, Δ*frh fre vht vhx Mbar_A1842 Mbar_A1843* and Δ*hyp frh fre vht vhx Mbar_A1842 Mbar_A1843*. The

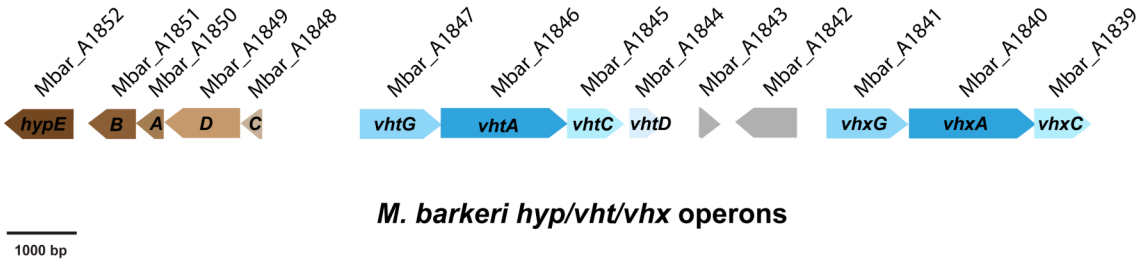

Figure 4.3 Genomic organization of operons encoding methanophenazine-dependent hydrogenases (Vht/Vhx) and hydrogenase maturation proteins (Hyp) in *Methanosarcina barkeri* (adapted from (25))**.** There are two operons, *vhtGACD* and *vhxGAC*, encoding the two hydrogenases, Vht and Vhx, respectively, that are *ca*. 50% identical. The *vhx* operon lacks gene D that encodes a putative hydrogenase maturation protein presumed to be essential for post-translational modification of the *cis*-encoded hydrogenase. The intergenic region between *vht* and *vhx* contains two genes, *Mbar_A1842* and *Mbar_A1843*. While *Mbar_A1842* encodes a peptidoglycan-binding domain containing protein, *Mbar_A1843* encoded protein shows *ca.* 38% amino acid identity to the activator of Hsp90 ATPase 1 family protein of some organisms. *M. barkeri* also contains a *hypCDABE* operon that encodes proteins presumed to be required for synthesis and insertion of the [NiFe] bimetallic catalytic center in its hydrogenases. Other open reading frames (ORFs) are shown as gray arrows.

echABCDEF operon was deleted in Δ*frh*, Δ*vht frh* (25) and Δ*frh fre vht vhx Mbar_A1842 Mbar_A1843* mutant backgrounds to obtain Δ*ech frh*, Δ*ech vht frh* and Δ*ech frh fre vht vhx Mbar_A1842 Mbar_A1843* mutants, respectively, using the homologous recombination-mediated gene replacement method (52). In this method, ApaI/NotI cut 5.6 kb region of pGK9 was transformed into the mutant backgrounds and the transformants were selected using methanol with

supplementation (YE, CAA, acetate and/or pyruvate) and puromycin. All the mutants were confirmed by DNA hybridization (Figures 4.4, 4.5, 4.6 and 4.7). *vht* operon was rendered Tc-dependent in the Δ*ech* background by replacing its native promoter with the Tc-regulated P*mcrB*(*tetO*3) promoter (21). For this, NcoI/SpeI-digested 7.0 kb fragment of pGK61A (25) was transformed into Δ*ech* and the transformants were selected in presence of methanol, Tc and puromycin. The Δ*ech* P_{tet}*vht* strain was confirmed by PCR.

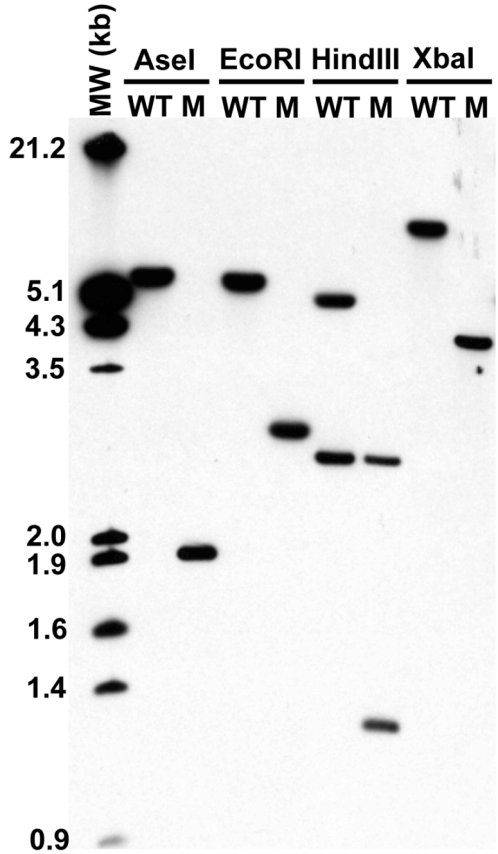

Figure 4.4 Verification of Δ*frh* in Δ*frh fre* by Southern hybridization. Predicted bands (kb): **AseI**: WT (WWM85) = 5.6, mutant (M) = 1.9; **EcoRI**: WT = 5.4**,** mutant = 2.8; **HindIII**: WT = 4.9 and 2.6, mutant = 2.6 and 1.3; **XbaI**: WT = 7.8, mutant = 4.1. MW: DIG-labeled DNA molecular weight marker III (Roche, Indianapolis, IN). 600 bp PCR product of *frh* deletion plasmid pGK4 (25) amplified with frhfor5 and frhrev6 (Table 4.2) was used as probe.

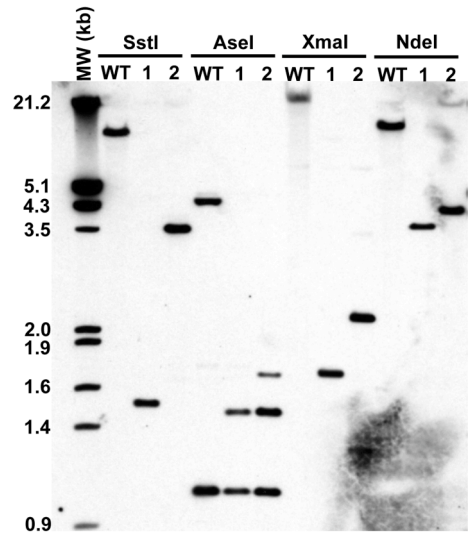

Figure 4.5 Verification of Δ*vht vhx* in Δ*frh fre vht vhx* Mbar_A1842 Mbar_A1843 (1 and 2) and Δ*hyp vht vhx* in Δ*hyp frh fre vht vhx* Mbar_A1842 Mbar_A1843 (3 and 4) by Southern hybridization. Predicted bands (kb): **SstI**: WT (WWM85) = 9.2, mutant A (1 and 2) = 1.5, mutant B (3 and 4) = 3.5; **AseI**: WT = 4.5 and 1, mutant A = 1.4 and 1, mutant B = 1.7, 1.5 and 1.1; **XmaI**: WT = 20.9, mutant A = 1.7, mutant B = 2.2; **NdeI**: WT = 10.8, mutant A = 3.8, mutant B = 4.3. MW: DIG-labeled DNA molecular weight marker III (Roche, Indianapolis, IN). 639 bp and 754 bp fragments of EcoRI-digested pGK12 (Table 4.1) were used as probe.

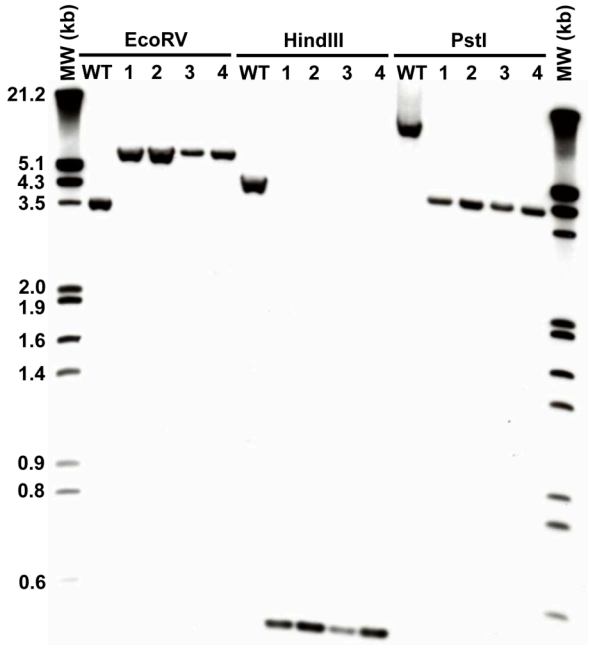

Figure 4.6 Verification of Δ*ech* in Δ*ech frh* (1 and 2) and Δ*ech frh vht* (3 and 4) by Southern hybridization. Predicted bands (kb): **EcoRV**: WT (WWM85) = 3.6, mutants (1, 2, 3 and 4) = 5.9; **HindIII**: WT = 4.5, mutants = 0.5; **PstI**: WT = 9.2, mutants = 4.2. MW: DIG-labeled DNA molecular weight marker III (Roche, Indianapolis, IN). 450 bp fragment of HindIII-digested *ech* deletion plasmid pGK9 (Table 4.1) was used as probe.

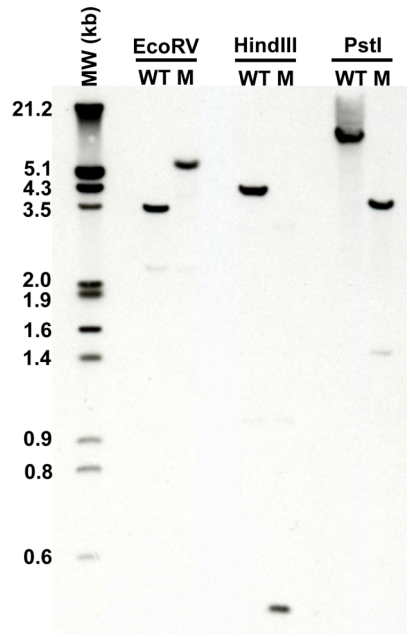

Figure 4.7 Verification of Δ*ech* in Δ*ech frh fre vht vhx* Mbar_A1842 Mbar_A1843 by Southern hybridization. Predicted bands (kb): **EcoRV**: WT (WWM85) = 3.6, mutant (M) = 5.9; **HindIII**: WT = 4.5**,** mutant = 0.5; **PstI**: WT = 9.2, mutant = 4.2. MW: DIG-labeled DNA molecular weight marker III (Roche, Indianapolis, IN). 450 bp fragment of HindIII-digested *ech* deletion plasmid pGK9 (Table 4.1) was used as probe.

4.3.4 Determination of growth characteristics

For growth rate determinations, cultures were grown on methanol or methanol plus H_2/CO_2 (Δ*frh* and Δ*frh fre*) to mid-log phase (optical density at 600 nm [OD_{600}] *ca.* 0.5). Approximately 3% inoculum of the culture (or 10%, in case of acetate) was then transferred to fresh medium in four replicates and incubated at 37^{o} C. Growth was quantified by measuring OD_{600}. Generation times were calculated during exponential growth phase and lag phase was defined as the time required to achieve half-maximal OD_{600}.

Due to the ability of *Methanosarcina* strains to grow on endogenous substrates found in agar (43), growth of Tc-regulated strains was tested on nylon membranes using the spot-plate method. In this, each of the strains was first

adapted for at least 15 generations to the substrate of interest. Once grown to saturation, 10 ml cultures of all strains were washed three times with plain-HS medium and then resuspended in 5 ml final volume. Subsequently, they were serially diluted 10-fold from 10^{-1} to 10^{-7}. The spotting plate was then prepared by placing three layers of GB004 paper (Whatman, NJ), two layers of GB002 paper (Schleicher & Schuell BioScience, NH) and 1 layer of 3MM paper (Whatman, NJ). Subsequently, this stack of papers was soaked in 43 ml of HS-medium containing the substrate of interest with and without Tc. A 0.22 μM nylon membrane (GE Water and Process Technologies, PA) was then placed on top of the paper stack. Finally, 10 μl of the undiluted culture and each of the serial dilutions was spotted on the plate using a multi-channel pipettor. The plate was then sealed with parafilm and incubated for at least two weeks to check growth.

4.3.5 Cell suspension experiments

Cells grown on methanol or methanol plus H_2/CO_2 (Δ*frh* and Δ*frh fre*) were collected in late exponential phase (OD_{600}= 0.6-0.7) by centrifugation at 5,000 x g for 15 minutes at 4^{o}C. They were then washed once with anaerobic HS PIPES buffer, 50 mM PIPES (pH 6.8), 400 mM NaCl, 13 mM KCl, 54 mM $MgCl_2$, 2 mM $CaCl_2$, 2.8 mM cysteine, 0.4 mM Na_2S and resuspended in the same buffer to a final concentration of 10^9 cells/ml. Cells were counted visually using the Petroff-Hausser counting chamber (Hausser Scientific, PA). All assay mixtures contained 2 ml of the suspension and were conducted under strictly anaerobic conditions in 25 ml Balch tubes sealed with butyl rubber stoppers. Puromycin (20

μg/ml) was added to prevent protein synthesis and as indicated the assay mixture contained 250 mM methanol under a headspace of N_2, H_2 or H_2/CO_2 (80/20%) at 250 kPa over the ambient pressure. Cells were held on ice until use and assays were started by transferring tubes to 37°C. For rate determination, gas phase samples were withdrawn at various time points and assayed for methane (CH_4) by gas chromatography at 225°C in a Hewlett Packard gas chromatograph (5890 Series II) equipped with a flame ionization detector. The column used was of stainless steel filled with 80/120 Carbopack™ B/3% SP™-1500 (Supelco, Bellefonte, PA) with helium as the carrier gas. For total CH_4 and CO_2 production, assays were incubated at 37°C for 36 hours and then gas phase samples were withdrawn. These samples were analyzed by GC at 225°C in a Hewlett Packard gas chromatograph (5890 Series II) equipped with a thermal conductivity detector. A stainless steel 60/80 Carboxen-1000 column (Supelco, Bellefonte, PA) with helium as the carrier gas was used. Total cell protein was determined using the Bradford method (8) after 1 ml of the cells was lysed by resuspending it in ddH_20 with 1 μg/ml RNase and DNase.

4.4 RESULTS

4.4.1 Isolation of a series of *M. barkeri* hydrogenase deletion mutants

The hydrogenases of *M. barkeri* Fusaro were deleted sequentially in a specific order, which is depicted in figure 4.8. This is because, certain hydrogenase deletion mutants are only viable, in other hydrogenase mutant backgrounds (25). In addition, to simplify isolation of the hydrogenase mutant

that lacks both the operons encoding MP-dependent hydrogenases, *vhxGAC* and *vhtGACD*, we also deleted the genes present between these operons in the mutant, *Mbar_A1842* and *Mbar_A1843* (Figure 4.3). The growth characteristics of all hydrogenase mutants were then determined on various methanogenic substrates.

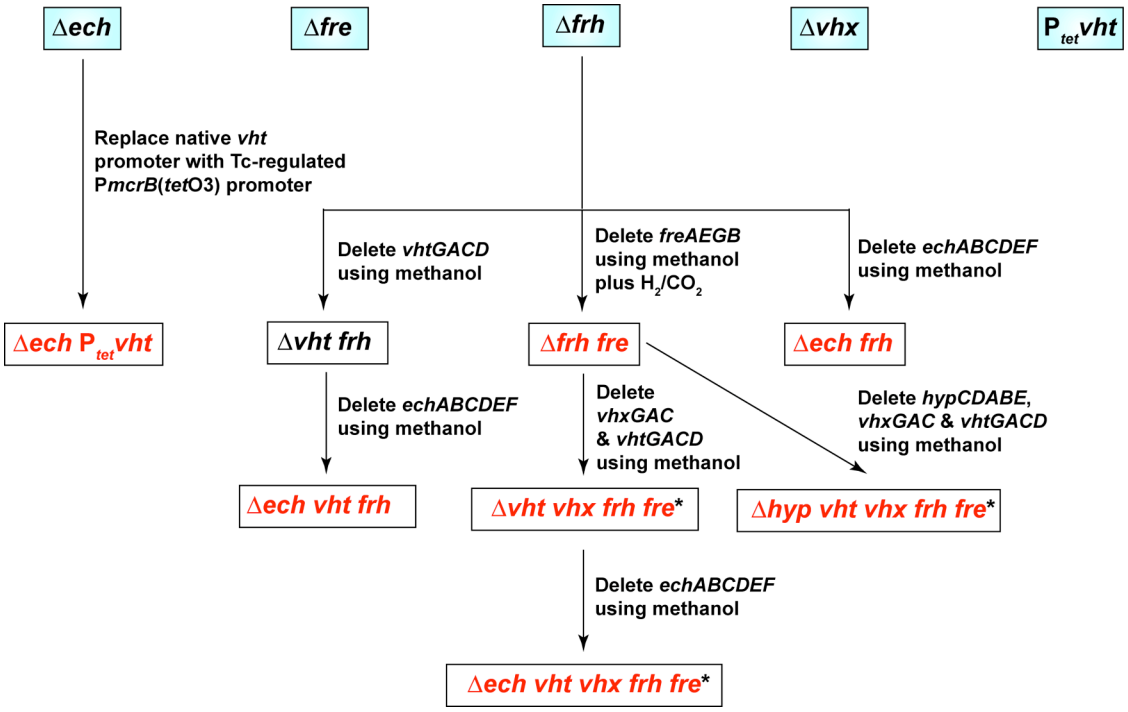

Figure 4.8 Flowchart depicting isolation of a series of *M. barkeri* hydrogenase deletion mutants. The first row represents single hydrogenase deletion mutants (blue boxes). These were used as backgrounds for deletion of other hydrogense encoding operons; *echABCDEF*, *freAEGB*, *vhxGAC*, *vhtGACD* or *hypCDABE*, using different growth substrates, as indicated. The mutants in red were isolated in this study, whereas, other mutants were constructed in previous studies. * mutants were also deleted of genes present in between *vhx* and *vht* operons, *Mbar_A1842* and *Mbar_A1843*. The tetracycline (Tc)-regulated conditional *vht* mutant is denoted as P_{tet}*vht*.

4.4.2 All three types of hydrogenases are needed for growth of *M. barkeri* via the CO_2 reduction pathway

In this pathway, CO_2 is reduced to CH_4 in a step-wise manner using H_2 gas as the electron donor (46). Thus, at every reduction step, a hydrogenase is

needed to harvest electrons from H_2 and funnel them into the pathway. Ech hydrogenase is required to provide Fd_{red} for reduction of CO_2 to the formyl level (36), whereas, $F_{420}H_2$ produced by Frh hydrogenase is needed to reduce methenyl and methylene groups (24). Vht hydrogenase generates MPH_2 for methyl group reduction (25). Consistent with the role of each of these hydrogenases, none of the hydrogenase deletion mutants that lack Ech, Frh and/or Vht (all except Δ*fre* and Δ*vhx* mutants) are able to grow using this substrate (Table 4.4). Also, they are unable to produce CH_4 from H_2/CO_2 in resting cell suspensions (Table 4.5). However, the Δ*frh* mutant converts a very small amount of the substrate to CH_4 in cell suspensions, suggesting an alternate source of $F_{420}H_2$ in *M. barkeri* that is unable to support its growth. It is important to note that as observed in previous studies (24, 25), our data also show that Fre and Vhx hydrogenases are not able to substitute for the role of Frh and Vht hydrogenases in the single Δ*frh* and P_{tet}*vht* mutants, respectively. Thus, they are not functional under the conditions tested.

4.4.3 *M. barkeri* hydrogenases are dispensable during its methylotrophic growth

With the exception of P_{tet}*vht* and Δ*ech* P_{tet}*vht*, all other hydrogenase mutants are able to grow on methanol (Table 4.6). Furthermore, they are capable of converting methanol to CH_4 and CO_2 in a 3:1 ratio in resting cell suspensions (Table 4.5). This suggests that in all these mutants, including the quintuple hydrogenase mutant, all 6 electrons derived from the oxidation of 1 methanol

methyl group to CO_2 are channeled to the terminal step for reduction of 3 methanol methyl groups to CH_4, via H_2-independent pathways. These pathways

Table 4.4 Growth[a] of *M. barkeri* Fusaro strains[b] on H_2/CO_2

Strain	Growth rate (h)	Maximum OD_{600}	Lag phase (h)
Δ***hpt***[c]	10.4±0.7	0.42±0.04	49±11
Δ***ech***	NG	NA	NA
Δ***frh***	NG	NA	NA
Δ***fre***	10.3±0.6	0.35±0.03	59±1
Δ***vhx***	10.7±0.5	0.45±0.02	60±3
P*tet*vht[d]	NG	NA	NA
Δ***ech frh***	NG	NA	NA
Δ***vht frh***	NG	NA	NA
Δ***frh fre***	NG	NA	NA
Δ***ech* P*tet*vht**[d]	NG	NA	NA
Δ***ech frh vht***	NG	NA	NA
Δ***frh fre vht vhx***[e]	NG	NA	NA
Δ***ech frh fre vht vhx***[e]	NG	NA	NA
Δ***hyp frh fre vht vhx***[e]	NG	NA	NA

[a]Growth was measured as indicated in Materials and Methods; lag time represents the time required to reach one half of the maximum optical density at 600 nm (OD_{600}). Values represent the average and standard deviation of at least triplicate measurements.
[b]Strains used are listed in table 4.3.
[c]*M. barkeri* Fusaro parent strain in which all deletions were constructed.
[d]Growth in absence of tetracycline.
[e]Two additional genes, *Mbar_A1842* and *Mbar_A1843*, are absent in these mutants.
NG, no growth for at least 6 months of incubation. NA, not applicable.

Table 4.5 Methane (μmol) and carbon dioxide (μmol) production by resting cell suspensions[a] of *M. barkeri* Fusaro strains[b]

Strain	N_2		Methanol		Methanol + H_2		H_2/CO_2	
	CH_4	CO_2	CH_4	CO_2	CH_4	CO_2	CH_4	CO_2
Δ***hpt***[c]	<1	1±0.1	339±6	118±2	458±6	<1	307±24	NA
Δ***ech***	<1	3±1	331±6	109±2	460±12	<1	5±1	NA
Δ***frh***	<1	1±0.1	310±8	96±2	442±4	<1	34±1	NA
Δ***fre***	<1	<1	339±7	117±2	442±24	<1	316±16	NA
Δ***vhx***	<1	1±0.1	329±7	113±3	453±6	<1	328±21	NA
Δ***ech frh***	<1	3±1	328±7	107±2	440±14	4±1	3±0.1	NA
Δ***vht frh***	<1	2±1	311±5	92±1	225±16	20±1	6±1	NA
Δ***frh fre***	<1	4±0.9	298±13	98±4	436±8	<1	10±2	NA
Δ***ech frh vht***	<1	1±0.2	315±5	93±1	313±5	92±2	1±0	NA
Δ***frh fre vht vhx***[d]	<1	3±1	309±6	92±2	300±8	19±1	5±0.4	NA
Δ***ech frh fre vht vhx***[d]	<1	1±0.3	314±2	94±1	315±8	93±3	1±0.1	NA
Δ***hyp frh fre vhtvhx***[d]	<1	2±0.8	332±10	99±3	325±11	103±3	1±0.1	NA

Table 4.5 (cont.)

[a]Assays were conducted as described in Materials and Methods. Values are the average and standard deviation of at least three trials.
[b]Strains used are listed in table 4.3.
[c]*M. barkeri* Fusaro parent strain in which all deletions were constructed.
[d]Two additional genes, *Mbar_A1842* and *Mbar_A1843*, are absent in these mutants.
NA, not applicable (CO_2 produced could not be measured because it was added to headspace).

Table 4.6 Growth[a] of *M. barkeri* Fusaro strains[b] on methanol

Strain	Growth rate (h)	Maximum OD_{600}	Lag phase (h)
Δ***hpt***[c]	8.9±0.3	0.85±0.05	36±1
Δ***ech***	12.2±0.9	0.69±0.05	46±1
Δ***frh***	19.5±1	0.69±0.05	122±6
Δ***fre***	8.8±0.4	0.78±0.04	37±1
Δ***vhx***	8.5±0.2	0.78±0.08	36±2
P_{tet}*vht*[d]	NG	NA	NA
Δ***ech frh***	12.1±0.7	0.8±0.05	54±2
Δ***vht frh***	11.7±0.7	0.89±0.01	54±2
Δ***frh fre***	16.5±0.8	0.8±0	89±2
Δ***ech*** **P_{tet}*vht***[d]	NG	NA	NA
Δ***ech frh vht***	10.8±0.2	0.71±0.06	48±0.3
Δ***frh fre vht vhx***[e]	12.3±0.6	0.84±0.07	58±2
Δ***ech frh fre vht vhx***[e]	12.1±0.2	0.84±0.06	54±2
Δ***hyp frh fre vht vhx***[e]	14±0.4	0.86±0.03	62±2

[a]Growth was measured as indicated in Materials and Methods; lag time represents the time required to reach one half of the maximum optical density at 600 nm (OD_{600}). Values represent the average and standard deviation of at least triplicate measurements.
[b]Strains used are listed in table 4.3.
[c]*M. barkeri* Fusaro parent strain in which all deletions were constructed.
[d]Growth in absence of tetracycline.
[e]Two additional genes, *Mbar_A1842* and *Mbar_A1843*, are absent in these mutants.
NG, no growth for at least 6 months of incubation.
NA, not applicable.

allow the hydrogenase mutants to achieve growth yields that are comparable to the isogenic parental strain (Table 4.6). However, the mutants exhibit variable rates of growth and CH_4 production in resting cell suspensions (Table 4.7). Consistent with previous observations (24), our results here show that the Δ*frh*

Table 4.7 Rate (nmol min^{-1} mg^{-1}) of methane production from resting cell suspensions[a] of *M. barkeri* Fusaro strains[b]

	Substrate	
Strain	**Methanol**	**Methanol/H_2**
Δ***hpt***[c]	86±7	132±18
Δ***ech***	57±5	122±7
Δ***frh***	23±1	136±9
Δ***fre***	84±1	123±16
Δ***vhx***	71±2	74±12
Δ***ech frh***	20±1	27±3
Δ***vht frh***	38±8	36±4
Δ***frh fre***	14±1	87±3
Δ***ech frh vht***	31±2	30±3
Δ***frh fre vht vhx A1842 A1843***	32±10	34±13
Δ***ech frh fre vht vhx A1842 A1843***	19±2	19±2
Δ***hyp frh fre vhtvhx A1842 A1843***	30±2	28±2

[a]Assays were conducted as described in Materials and Methods. Values are the average and standard deviation of at least three trials.
[b]Strains used are listed in table 4.3.
[c]*M. barkeri* Fusaro parent strain in which all deletions were constructed.

mutant grows twice as slow as the isogenic parental strain. The Δ*frh fre* double mutant exhibits similar growth characterisitics as the single Δ*frh* mutant. Other hydrogenase mutants, except Δ*fre* and Δ*vhx*, grow slightly slower than the parental strain. All hydrogenase mutants lacking Frh exhibit lower rates of CH_4 production than the isogenic parental strain in resting cell suspensions (Table 4.7). This suggests that the H_2-independent $F_{420}H_2$:heterodisulfide pathway is less efficient than the Frh-involving pathway. In contrast, the Δ*ech* mutant has a comparable rate of CH_4 production to the parental strain, implying that the H_2-independent Fd_{red}:heterodisulfide pathway is as efficient as the pathway involving Ech.

To test growth of Tc-regulated conditional *vht* mutants with and without Tc (Figure 4.9), 10-fold dilutions of cultures of these mutants and the wild-type strain (WWM85, Table 4.3) were spotted on a nylon membrane in the presence of

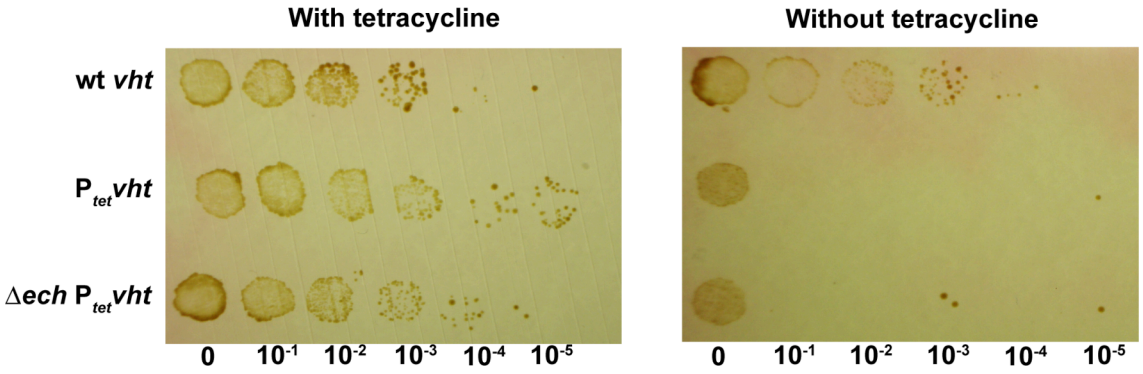

Figure 4.9 Growth of tetracycline-regulated *vht* (P_{tet}*vht*) mutants of *M. barkeri* on plates containing methanol. 10-fold serial dilutions of WWM85 (wt *vht*, Table 4.3), P_{tet}*vht* and Δ*ech* P_{tet}*vht* strains were spotted on methanol plates with and without tetracycline (Tc), as described in Materials and Methods. The dilution factors are indicated at the bottom of each plate. Unlike wt *vht*, which was able to grow in the presence and absence of Tc, P_{tet}*vht* and Δ*ech* P_{tet}*vht* strains could only grow in the presence of Tc at higher dilutions. Growth of these strains at 0 dilution factor (undiluted) without Tc could be due to presence of residual Vht protein within the cell. Suppressors were detected for both P_{tet}*vht* strains in the absence of Tc at higher dilutions.

methanol as the growth substrate. Unlike the wild-type strain that grew up with and without Tc, the P_{tet}*vht* and Δ*ech* P_{tet}*vht* strains were only able to grow in the presence of Tc, when *vht* is expressed. However, in the absence of Tc, the P_{tet}*vht* strains grew up at the lowest dilution. This growth could be attributed to residual Vht protein in the cells at this dilution. Also, a few P_{tet}*vht* mutant colonies were seen at higher dilutions. These could be suppressors with mutation in the Tc-regulated P*mcrB*(*tet*O3) promoter and/or the *tetR* gene, as previously seen for Tc-regulated mutant of *hdrED* operon that encodes the essential HdrED enzyme (9). Thus, our data suggest that Vht is essential for methylotrophic growth of *M. barkeri* in the wild-type and Δ*ech* mutant background. Also, Vhx present in P_{tet}*vht* strains is not able to substitute for the role of Vht, indicating its non-functionality.

4.4.4 Hydrogenase activity is essential for methanol utilization via the methyl respiration pathway

In this pathway, methyl group of methanol is reduced to CH_4 using electrons derived from the oxidation of H_2 by the MP-dependent hydrogenase Vht (20, 38). Thus, unlike in the methylotrophic pathway, 25% methanol methyl groups do not need to be oxidized to CO_2 to obtain reducing equivalents for reduction of the rest of methyl groups to CH_4.

All the hydrogenase deletion mutants containing the Vht hydrogenase are able to convert methanol plus H_2 to CH_4 in resting cell suspensions without detectable CO_2 production or, in other words, via the methyl respiration pathway (Δ*ech*, Δ*frh*, Δ*fre*, Δ*vhx*, Δ*ech frh* and Δ*frh fre*, Table 4.5). Also, all these mutants,

except the Δ*ech* mutant, can grow using methanol plus H_2/CO_2 as the substrate (Table 4.8). As reported in a previous study (36), we were able to restore growth

Table 4.8 Growth[a] of *M. barkeri* Fusaro strains[b] on methanol plus H_2/CO_2

Strain	Growth rate (h)	Maximum OD_{600}	Lag phase (h)
Δ***hpt***[c]	6.2±0.5	0.77±0.03	33±1
Δ***ech***	NG	NA	NA
Δ***frh***	7.4±0.6	0.64±0.14	45±3
Δ***fre***	7.0±0.4	0.68±0.01	38±4
Δ***vhx***	7.5±0.5	0.69±0.04	51±3
P*tet*vht[d]	NG	NA	NA
Δ***ech frh***	13±2	0.54±0.03	248±17
Δ***vht frh***	35±3	0.33±0.03	151±4
Δ***frh fre***	7.7±0.2	0.74±0.01	48±1
Δ***ech* P*tet*vht**[d]	NG	NA	NA
Δ***ech frh vht***	9.0±0.4	0.61±0.02	48±2
Δ***frh fre vht vhx***[e]	29±2	0.43±0.03	116±3
Δ***ech frh fre vht vhx***[e]	9.3±0.1	0.68±0.03	45±1
Δ***hyp frh fre vht vhx***[e]	9.9±0.2	0.72±0.06	54±1

[a]Growth was measured as indicated in Materials and Methods; lag time represents the time required to reach one half of the maximum optical density at 600 nm (OD_{600}). Values represent the average and standard deviation of at least triplicate measurements.
[b]Strains used are listed in table 4.3.
[c]*M. barkeri* Fusaro parent strain in which all deletions were constructed.
[d]Growth in absence of tetracycline.
[e]Two additional genes, *Mbar_A1842* and *Mbar_A1843*, are absent in these mutants.
NG, no growth for at least 6 months of incubation. NA, not applicable.

of the Δ*ech* mutant by supplementation of HS-methanol plus H_2/CO_2 medium with 100 mM pyruvate. On the basis of this observation, it was postulated that Ech produces Fd_{red} required for pyruvate biosynthesis in the methyl respiration pathway. Therefore, it is surprising that the Δ*ech frh* double mutant does not display this biosynthetic defect. The double mutant grows using methanol plus H_2/CO_2, albeit, twice as slow as the isogenic parental strain. Also, it exhibits a *ca*. 7-fold longer lag phase and a lower rate of CH_4 production in resting cell suspensions than the parental strain on this substrate (Table 4.7). Thus, these data suggest that there is an alternate pathway to obtain Fd_{red} for pyruvate biosynthesis, in the Δ*ech frh* double mutant. However, this pathway is not operational in the single Δ*ech* mutant.

To test the role of Vht in the methyl respiration pathway, growth of the conditional *vht* mutant (P_{tet}*vht*) was scored with and without Tc using the spot-plate method described in Materials and Methods (Figure 4.10). The P_{tet}*vht*

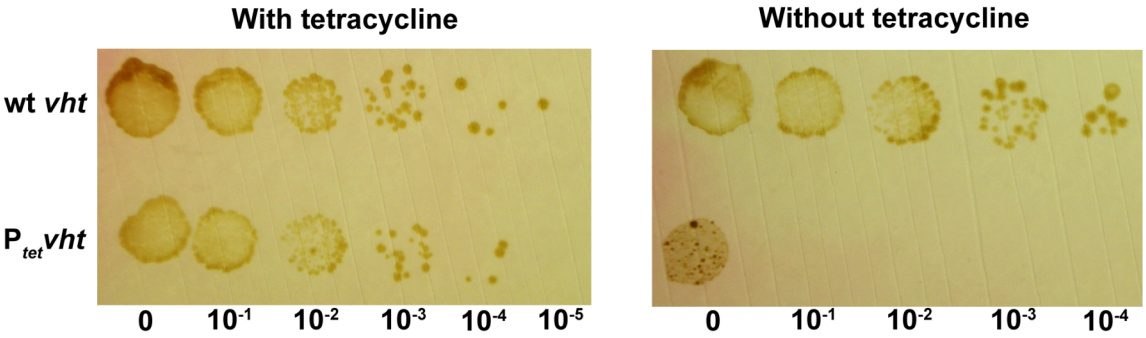

Figure 4.10 Growth of tetracycline-regulated *vht* mutant (P_{tet}*vht*) of *M. barkeri* on plates containing methanol under an atmosphere of H_2/CO_2. 10-fold serial dilutions of WWM85 (wt *vht*, Table 4.3) and P_{tet}*vht* strains were spotted on methanol plus H_2/CO_2 plates with and without tetracycline (Tc), as described in Materials and Methods. The dilution factors are indicated at the bottom of each plate. Unlike wt *vht*, which was able to grow in the presence and absence of Tc, P_{tet}*vht* strain could only grow in the presence of Tc at higher dilutions. Growth of these strains at 0 dilution factor (undiluted) without Tc could be due to presence of residual Vht protein within the cell.

mutant is unable to grow using methanol plus H_2/CO_2 in the absence of Tc, when *vht* is not expressed. Growth of the mutant at lowest dilution without Tc is probably due to residual Vht protein in the cells. Thus, these data suggest that Vht is essential for growth of wild-type *M. barkeri* via the methyl respiration pathway. However, two mutants lacking the Vht and Frh hydrogenases, Δ*vht frh* and Δ*frh fre vht vhx Mbar_A1842 Mbar_A1843*, are able to grow using this pathway. This is because, these mutants convert methanol plus H_2 to CH_4 in resting cell suspensions, with less than 25% CO_2 production. This suggests that another hydrogenase can harvest electrons from H_2 for methyl group reduction, when both Vht and Frh hydrogenases are absent from the cell. This alternate pathway can only support *ca*. 50% growth yield and a nearly four-fold lower growth rate than the isogenic parental strain in the Δ*vht frh* and Δ*frh fre vht vhx Mbar_A1842 Mbar_A1843* mutants (Table 4.8). Also, both these mutants exhibit a *ca.* three-fold longer lag phase than the parental strain. The rate of CH_4 production in resting cell suspensions in these mutants is also lower than the parental strain (Table 4.7). Hence, this alternate pathway seems to be less efficient than the pathway involving Vht.

Mutants that lack all three types of hydrogenases (Ech, Frh and Vht), Δ*ech vht frh* and Δ*ech frh fre vht vhx Mbar_A1842 Mbar_A1843*, convert methanol plus H_2 to CH_4 and CO_2 in a 3:1 ratio in resting cell suspensions. This suggests that they use methanol via the methylotrophic pathway, which is surprising, because the methyl oxidative pathway is known to be repressed in the presence of H_2 (36). The Δ*hyp frh fre vht vhx Mbar_A1842 Mbar_A1843 mutant*, which lacks the

Hyp proteins, also utilizes methanol plus H_2 methylotrophically in resting cell suspensions. Therefore, the Δ*hyp* mutant is functionally equivalent to mutants that lack functional hydrogenases. The growth characteristics exhibited by these mutants on methanol plus H_2/CO_2 are similar to those on methanol alone. They also show similar rates of CH_4 production in resting cell suspensions on both substrates.

4.4.5 Aceticlastic growth requires Fd_{ox}- and MP-dependent hydrogenases

Acetate utilization involves reduction of methyl group of acetate to CH_4 using Fd_{red}, which is derived from oxidation of its carbonyl group (15). It has been proposed that Ech and Vht hydrogenases mediate electron transfer from Fd_{red} to the heterodisulfide, using H_2 as an intermediate (35, 36). Consistent with this proposal, none of the hydrogenase deletion mutants that lack either the Ech or the Vht hydrogenase are able to grow on this substrate (Table 4.9).

4.5 DISCUSSION

In spite of their close evolutionary relatedness (31), the two *Methanosarcina* species, *M. barkeri* and *M. acetivorans*, exhibit basic differences in their energy-conserving electron transport chains. On one hand is the hydrogenotrophic *M. barkeri* species that uses H_2-dependent pathways for electron transfer on every methanogenic substrate examined, including H_2/CO_2 (12), methanol plus H_2/CO_2 (20), methanol (24, 25) and acetate (Figure 4.1) (35, 36). On the other hand, the non-hydrogenotrophic *M. acetivorans* species

employs H_2-independent methylotrophic and aceticlastic electron transport chains (19, 20). To further understand the differences between the electron

Table 4.9 Growth[a] of *M. barkeri* Fusaro strains[b] on acetate

Strain	Growth rate (h)	Maximum OD_{600}	Lag phase (h)
Δ***hpt***[c]	+	ND	ND
Δ***ech***	NG	NA	NA
Δ***frh***	+	ND	ND
Δ***fre***	+	ND	ND
Δ***vhx***	+	ND	ND
P_{tet}***vht***[d]	NG	NA	NA
Δ***ech frh***	NG	NA	NA
Δ***vht frh***	NG	NA	NA
Δ***frh fre***	+	ND	ND
Δ***ech*** P_{tet}***vht***[d]	NG	NA	NA
Δ***ech frh vht***	NG	NA	NA
Δ***frh fre vht vhx***[e]	NG	NA	NA
Δ***ech frh fre vht vhx***[e]	NG	NA	NA
Δ***hyp frh fre vht vhx***[e]	NG	NA	NA

[a]Presence of growth indicated as "+".
[b]Strains used are listed in table 4.3.
[c]*M. barkeri* Fusaro parent strain in which all deletions were constructed.
[d]Growth in absence of tetracycline.
[e]Two additional genes, *Mbar_A1842* and *Mbar_A1843*, are absent in these mutants.
ND, not determined.
NG, no growth for at least 6 months of incubation.
NA, not applicable.

transfer circuits of these two species, we deleted all hydrogenases from *M. barkeri* to convert it into an *M.acetivorans*-like species. This is significant, because hydrogenases have been shown to be intricately involved in each of the methanogenic pathways of *M. barkeri*. Nevertheless, this study proves that they are not essential for growth of *M. barkeri*, thereby implicating presence of unidentified, and perhaps novel, H_2-independent electron transfer pathways. Moreover, we have also been able to construct a useful hydrogenase-minus *M. barkeri* background that can be utilized for complementation studies with *M. acetivorans* electron-transport chain components. While not required for methylotrophic growth, our study shows that hydrogenases are absolutely essential for growth via the CO_2 reduction, methyl-respiration and aceticlastic pathways. The data presented here also suggest that hydrogenases are needed to exert inhibitory effects of H_2 on the methyl oxidative pathway. Furthermore, our results confirm the putative role of Hyp proteins in the maturation of at least one of the [NiFe] hydrogenases of *M. barkeri*, Ech.

In the CO_2 reduction pathway, reduction of CO_2 to CH_4 presumably requires three kinds of electron donors, Fd_{red}, $F_{420}H_2$ and MPH_2 (46). Consistent with this proposal, each of the three kinds of hydrogenases that reduce Fd_{ox} (Ech), F_{420} (Frh) or MP (Vht) is needed for growth on H_2/CO_2. Notably, unlike Frh and Vht, Fre and Vhx are not able to provide sufficient amount of $F_{420}H_2$ and MPH_2, respectively, for hydrogenotrophic growth. This could be due to low expression of *fre* and *vhx* operons, absence of post-translational processing, mutations in structural or catalytic residues or some combination of these (19).

The methylotrophic methanogenic pathway involves two different electron transport chains, one that transfers electrons from Fd_{red} to the heterodisulfide, whereas the other reduces the heterodisulfide using $F_{420}H_2$ as an electron donor (23, 36). In *M. barkeri*, these chains presumably merge, because Ech and Frh hydrogenases oxidize Fd_{red} and $F_{420}H_2$, respectively, to produce a common intermediate, H_2, which enters the energy-conserving H_2:heterodisulfide oxidoreductase system using the Vht hydrogenase (Figure 4.1) (24, 25, 35, 36). This H_2-cycling mechanism is the preferential mode of electron transfer in *M. barkeri*, at least from $F_{420}H_2$. Nevertheless, like *M. acetivorans*, our study shows that *M. barkeri* is capable of methylotrophic growth in the absence of its hydrogenases, implicating presence of H_2-independent electron-transport pathways from Fd_{red} and $F_{420}H_2$ to the heterodisulfide. The well-studied $F_{420}H_2$:heterodisulfide oxidoreductase system (12) involving Fpo has been shown to solely account for electron transfer from $F_{420}H_2$, in the absence of Frh in *M. barkeri* (Figure 4.1) (24). However, Fpo is nearly four-times slower than Frh. Consistent with this fact, all Frh-lacking hydrogenase deletion mutants exhibit lower rates of CH_4 production in resting cell suspensions than the strains containing Frh (Table 4.7). Nevertheless, Δ*frh* deletion mutants attain growth yields that are comparable to those of *frh*$^+$ strains (Table 4.6). This is because, the magnitude of the proton-motive force generated by both Frh- and Fpo-containing pathways is equal ($4H^+/2e^-$) (24). *M. acetivorans* probably uses the $F_{420}H_2$:heterodisulfide oxidoreductase system, because it harbors an *fpo* operon (18) that is expressed (26, 27), but an *frh* operon that is not expressed (19).

Moreover, the *fpo* operon most likely encodes a functional enzyme, because all structural and catalytic amino acid residues that are present in *M. barkeri* Fpo, are conserved in *M. acetivorans* Fpo (24). Interestingly, unlike *M. barkeri* Fpo, *M. acetivorans* Fpo allows high rates of methylotrophic CH_4 production in resting cell suspensions (161 nmol min^{-1} mg^{-1}) (7). This could be attributed to a difference in expression levels, enzymatic properties or both, of the enzyme from the two species.

The H_2-independent Fd_{red}:heterodisulfide oxidoreductase system is a subject of investigation in both species. In *M. acetivorans*, a putative Fd_{red}:MP oxidoreductase, Rnf, has been identified that is essential for growth on acetate (28). However, its deletion does not prevent methylotrophic growth by disproportionation of methanol in a 3:1 CH_4:CO_2 ratio, thus indicating the presence of a second Fd_{red} oxidoreductase. In a recent study, such an enzyme was proposed to be the soluble HdrA1B1C1 heterodisulfide reductase, which mediates direct electron transfer from Fd_{red} to the CoM-S-S-CoB heterodisulfide (9). Although Rnf is absent in *M. barkeri*, the operon encoding HdrA1B1C1 is present in its genome (Figure 4.11) (31). Therefore, HdrA1B1C1 could be responsible for transferring electrons from Fd_{red} to the heterodisulfide in *M. barkeri* (Figure 4.1). However, this cytoplasmically catalyzed exergonic reaction is not involved in direct energy conservation (9). This is in disagreement with our data, which show that the *M. barkeri* H_2-independent route is as efficient as the H_2-cycling pathway in conserving energy. This is because, the Δ*ech* hydrogenase mutant exhibits comparable rates of CH_4 production and growth

yields to the isogenic *ech*$^{+}$ parental strain (Tables 4.6 and 4.7). This suggests that *M. barkeri* may possess another unique Fd_{red} oxidoreductase. Alternatively, as postulated by Buan *et al* (9), HdrA1B1C1 might be involved in energy

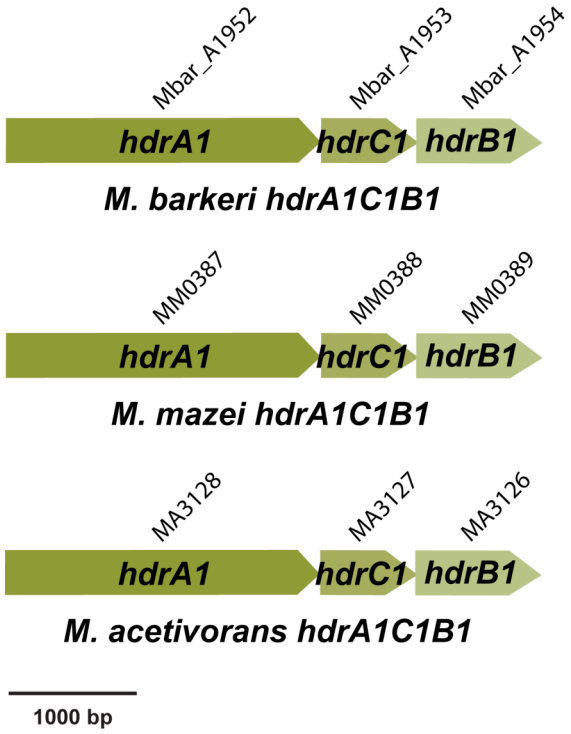

Figure 4.11 Genomic organization of operons encoding soluble heterodisulfide reductase (HdrA1B1C1) in *Methanosarcina* species. All three species contain the HdrA1B1C1-encoding operon (*hdrA1C1B1*).

energy conservation using an electron bifurcation mechanism, wherein, for every CoM-S-S-CoB reduced, a molecule of coenzyme F_{420} also undergoes reduction. Subsequently, electron channeling from $F_{420}H_2$ via the $F_{420}H_2$:heterodisulfide oxidoreductase system (12) would conserve energy. However, the bifurcation pathway would conserve half the amount of energy than the H_2-cycling pathway, because only 50% of Fd_{red} electrons flow through the $F_{420}H_2$:heterodisulfide

oxidoreductase system for energy conservation. Thus, the identity of the Fd_{red} oxidoreductase in *M. barkeri* remains unknown.

In the methyl respiration pathway, energy is conserved via the H_2:heterodisulfide oxidoreductase system, wherein, Vht oxidizes H_2 to release electrons for reduction of the CoM-S-S-CoB heterodisulfide. However, *M. barkeri* Δ*vht frh* and Δ*frh fre vht vhx* mutants probably employ H_2-independent Fd_{red}:heterodisulfide electron transport chain for energy conservation. This is because, Ech is the only functional hydrogenase present in both these mutants. Therefore, it must be responsible for oxidizing H_2 to provide Fd_{red} for CoM-S-S-CoB reduction. However, it is unclear why the conditional *vht* mutant (P_{tet}*vht*) fails to utilize this Ech-dependent pathway for growth via the methyl respiration pathway. It is apparent that presence of Frh, prevents Fd_{red}-dependent respiration in the P_{tet}*vht* mutant, however, this needs to be tested.

Our results suggest that hydrogenases mediate repression of the methyl oxidative pathway by H_2. The fact that Ech is required for biosynthesis on methanol plus H_2/CO_2, but not on methanol alone, suggests that the methyl oxidative pathway is repressed in presence of H_2, precluding the use of CHO-methanofuran dehydrogenase (Fmd)-catalyzed reaction for Fd_{red} synthesis (36). However, H_2 alone is insufficient for this repression, because Δ*ech frh vht* mutants are able to grow methylotrophically in presence of methanol plus H_2/CO_2. In addition, unlike the single Δ*ech* mutant, the Δ*ech frh* double mutant can grow via the methyl-respiration pathway without pyruvate supplementation, thus implying that it probably fulfills its biosynthetic needs of Fd_{red} by oxidizing the

methanol methyl group to CO_2. Hence, H_2 needs to be converted to $F_{420}H_2$ and/or Fd_{red} by Ech and Frh hydrogenases, respectively, to exert an inhibitory effect on the methyl oxidative pathway. The inhibition might occur in two possible ways. Firstly, in the presence of H_2 and the respective hydrogenases, F_{420} and Fd_{ox} pools might get completely reduced, leading to thermodynamic repression of the methyl oxidative pathway. Alternatively, $F_{420}H_2$ and/or Fd_{red} might be involved in direct inhibition of one or more enzymes of the methyl oxidative branch.

Our study also provides experimental evidence for the hypothesis that Hyp proteins are involved in post-translational modification of [NiFe] hydrogenases in *M. barkeri* (5, 19). Unlike *ech*$^+$ Δ*frh fre vht vhx* strain, the *ech*$^+$ Δ*hyp frh fre vht vhx* mutant is unable to grow via the methyl reduction pathway using Ech, suggesting that this hydrogenase is non-functional in the Δ*hyp* mutant. Thus, Hyp proteins are essential for maturation of the [NiFe] Ech hydrogenase.

Deletion of *Mbar_A1842* and *Mbar_A1843* genes might have contributed to the phenotype of Δ*frh fre vht vhx Mbar_A1842 Mbar_A1843*, Δ*hyp frh fre vht vhx Mbar_A1842 Mbar_A1843*, and Δ*ech frh fre vht vhx Mbar_A1842 Mbar_A1843* hydrogenase mutants. *Mbar_A1842* encodes for a peptidoglycan-binding domain containing protein with an unknown function (2, 32, 40). Homologs of this gene are present in the other two *Methanosarcina* species, *M. mazei* (MM2174, 71% amino acid identity (10)) and *M. acetivorans* (MA1145, 55% amino acid identity (10)) at the same genomic location, that is, between the *vhx* and *vht* operons (2, 32). The *Mbar_A1843* homolog present in *M. mazei* (MM2173, 57% amino acid identity (10)) is also located at the same site,

however, the *M. acetivorans* homolog (MA3620, 36% amino acid identity (10)) is present elsewhere in the chromosome (2, 32). Although the function of the protein encoded by this gene is not known, it shows *ca.* 38% amino acid sequence identity (10) to the activator of Hsp90 ATPase 1 family protein from *Nostoc punctiforme* and *Sphingobacterium spiritivorum* (2). Thus, the physiological roles of proteins encoded by *Mbar_A1842* and *Mbar_A1843* are currently unknown. In the future, we plan to complement the aforementioned hydrogenase mutants with these two genes, to test their contribution to the phenotype of the mutants.

Lastly, it is possible that *M. barkeri* and *M. acetivorans* have different physiologies due to a difference in their habitats. Methanogens exist in environments, where they have to compete with other micro-organisms for H_2. These include denitrifiers, sulfate-reducing bacteria, iron-reducing bacteria and manganese-reducers, which have a higher affinity for H_2 than methanogens. In its high-salt marine habitat, *M. acetivorans* exists as disaggregated single cells (45) and is therefore more prone to lose H_2 gas to competing micro-organisms in its environment, especially sulfate reducers, because such habitats are rich in sulfate. This might be the reason why *M. acetivorans* foregoes H_2-dependent electron transport pathways. In contrast, freshwater organisms like *M. barkeri* that exist as large multicellular aggregates (31), have a higher chance of retaining H_2 gas within the aggregates, enabling them to use it as an electron carrier. Nonetheless, these organisms might resort to H_2-independent pathways, when conditions like Ni-limitation prevent synthesis of hydrogenases (1). In

future, we plan to identify components of these electron transport pathways by microarray expression analysis of the quintuple hydrogenase *M. barkeri* mutant.

4.6 LITERATURE CITED

1. **Afting, C., A. Hochheimer, and R. K. Thauer.** 1998. Function of H_2-forming methylenetetrahydromethanopterin dehydrogenase from *Methanobacterium thermoautotrophicum* in coenzyme F_{420} reduction with H_2. Arch Microbiol **169:**206-10.

2. **Altschul, S. F., T. L. Madden, A. A. Schaffer, J. Zhang, Z. Zhang, W. Miller, and D. J. Lipman.** 1997. Gapped BLAST and PSI-BLAST: a new generation of protein database search programs. Nucleic Acids Res **25:**3389-402.

3. **Ausubel, F. M., R. Brent, R. E. Kingston, D. D. Moore, J. G. Seidman, J. A. Smith, and K. Strhul.** 1992. Current protocols in molecular biology. John Wiley & Sons, New York.

4. **Beifuss, U., M. Tietze, S. Baumer, and U. Deppenmeier.** 2000. Methanophenazine: Structure, Total Synthesis, and Function of a New Cofactor from Methanogenic Archaea. Angew Chem Int Ed Engl **39:**2470-2472.

5. **Blokesch, M., A. Paschos, E. Theodoratou, A. Bauer, M. Hube, S. Huth, and A. Bock.** 2002. Metal insertion into NiFe-hydrogenases. Biochem Soc Trans **30:**674-80.

6. **Boccazzi, P., J. K. Zhang, and W. W. Metcalf.** 2000. Generation of dominant selectable markers for resistance to pseudomonic acid by cloning and mutagenesis of the *ileS* gene from the archaeon *Methanosarcina barkeri* Fusaro. J Bacteriol **182:**2611-8.

7. **Bose, A., M. A. Pritchett, and W. W. Metcalf.** 2008. Genetic analysis of the methanol- and methylamine-specific methyltransferase 2 genes of *Methanosarcina acetivorans* C2A. J Bacteriol **190:**4017-26.

8. **Bradford, M. M.** 1976. A rapid and sensitive method for the quantitation of microgram quantities of protein utilizing the principle of protein-dye binding. Anal Biochem **72:**248-54.

9. **Buan, N. R., and W. W. Metcalf.** 2009. Methanogenesis by *Methanosarcina acetivorans* involves two structurally and functionally distinct classes of heterodisulfide reductase. Mol Microbiol.

10. **Chenna, R., H. Sugawara, T. Koike, R. Lopez, T. J. Gibson, D. G. Higgins, and J. D. Thompson.** 2003. Multiple sequence alignment with the Clustal series of programs. Nucleic Acids Res **31:**3497-500.

11. **Deppenmeier, U.** 1995. Different structure and expression of the operons encoding the membrane-bound hydrogenases from *Methanosarcina mazei* Gö1. Arch Microbiol **164:**370-6.

12. **Deppenmeier, U.** 2004. The membrane-bound electron transport system of *Methanosarcina* species. J Bioenerg Biomembr **36:**55-64.

13. **Deppenmeier, U., M. Blaut, S. Lentes, C. Herzberg, and G. Gottschalk.** 1995. Analysis of the *vhoGAC* and *vhtGAC* operons from *Methanosarcina mazei* strain Gö1, both encoding a membrane-bound hydrogenase and a cytochrome b. Eur J Biochem **227:**261-9.

14. **Deppenmeier, U., A. Johann, T. Hartsch, R. Merkl, R. A. Schmitz, R. Martinez-Arias, A. Henne, A. Wiezer, S. Baumer, C. Jacobi, H. Bruggemann, T. Lienard, A. Christmann, M. Bomeke, S. Steckel, A. Bhattacharyya, A. Lykidis, R. Overbeek, H. P. Klenk, R. P. Gunsalus, H. J. Fritz, and G. Gottschalk.** 2002. The genome of *Methanosarcina mazei*: evidence for lateral gene transfer between bacteria and archaea. J Mol Microbiol Biotechnol **4:**453-61.

15. **Ferry, J. G.** 1992. Methane from acetate. J Bacteriol **174:**5489-95.

16. **Fiebig, K., and B. Friedrich.** 1989. Purification of the F_{420}-reducing hydrogenase from *Methanosarcina barkeri* (strain Fusaro). Eur J Biochem **184:**79-88.

17. **Forzi, L., J. Koch, A. M. Guss, C. G. Radosevich, W. W. Metcalf, and R. Hedderich.** 2005. Assignment of the [4Fe-4S] clusters of Ech hydrogenase from *Methanosarcina barkeri* to individual subunits via the characterization of site-directed mutants. Febs J **272:**4741-53.

18. **Galagan, J. E., C. Nusbaum, A. Roy, M. G. Endrizzi, P. Macdonald, W. FitzHugh, S. Calvo, R. Engels, S. Smirnov, D. Atnoor, A. Brown, N. Allen, J. Naylor, N. Stange-Thomann, K. DeArellano, R. Johnson, L. Linton, P. McEwan, K. McKernan, J. Talamas, A. Tirrell, W. Ye, A. Zimmer, R. D. Barber, I. Cann, D. E. Graham, D. A. Grahame, A. M. Guss, R. Hedderich, C. Ingram-Smith, H. C. Kuettner, J. A. Krzycki, J. A. Leigh, W. Li, J. Liu, B. Mukhopadhyay, J. N. Reeve, K. Smith, T. A. Springer, L. A. Umayam, O. White, R. H. White, E. Conway de Macario, J. G. Ferry, K. F. Jarrell, H. Jing, A. J. Macario, I. Paulsen, M. Pritchett, K. R. Sowers, R. V. Swanson, S. H. Zinder, E. Lander, W. W. Metcalf, and B. Birren.** 2002. The genome of *M. acetivorans* reveals extensive metabolic and physiological diversity. Genome Res **12:**532-42.

19. **Guss, A. M., G. Kulkarni, and W. W. Metcalf.** 2009. Differences in hydrogenase gene expression between *Methanosarcina acetivorans* and *Methanosarcina barkeri*. J Bacteriol **191:**2826-33.

20. **Guss, A. M., B. Mukhopadhyay, J. K. Zhang, and W. W. Metcalf.** 2005. Genetic analysis of *mch* mutants in two *Methanosarcina* species demonstrates multiple roles for the methanopterin-dependent C-1 oxidation/reduction pathway and differences in H(2) metabolism between closely related species. Mol Microbiol **55:**1671-80.

21. **Guss, A. M., M. Rother, J. K. Zhang, G. Kulkarni, and W. W. Metcalf.** 2008. New methods for tightly regulated gene expression and highly efficient chromosomal integration of cloned genes for *Methanosarcina* species. Archaea **2:**193-203.

22. **Ide, T., S. Baumer, and U. Deppenmeier.** 1999. Energy conservation by the H_2:heterodisulfide oxidoreductase from *Methanosarcina mazei* Gö1: identification of two proton-translocating segments. J Bacteriol **181:**4076-80.

23. **Keltjens, J. T., and G. D. Vogels.** 1993. Methanogenesis. Chapman & Hall, New York.

24. **Kulkarni, G., D. M. Kridelbaugh, A. M. Guss, and W. W. Metcalf.** 2009. Hydrogen is a preferred intermediate in the energy-conserving electron transport chain of *Methanosarcina barkeri*. Proc Natl Acad Sci U S A **106:**15915-20.

25. **Kulkarni, G., and W. W. Metcalf.** 2010. Demonstration of hydrogen cycling during electron transport in *Methanosarcina barkeri*. Unpublished results.

26. **Li, Q., L. Li, T. Rejtar, B. L. Karger, and J. G. Ferry.** 2005. Proteome of *Methanosarcina acetivorans* Part I: an expanded view of the biology of the cell. J Proteome Res **4:**112-28.

27. **Li, Q., L. Li, T. Rejtar, B. L. Karger, and J. G. Ferry.** 2005. Proteome of *Methanosarcina acetivorans* Part II: comparison of protein levels in acetate- and methanol-grown cells. J Proteome Res **4:**129-35.

28. **Li, Q., L. Li, T. Rejtar, D. J. Lessner, B. L. Karger, and J. G. Ferry.** 2006. Electron transport in the pathway of acetate conversion to methane in the marine archaeon *Methanosarcina acetivorans*. J Bacteriol **188:**702-10.

29. **Liu, Y., and W. B. Whitman.** 2008. Metabolic, phylogenetic, and ecological diversity of the methanogenic archaea. Ann N Y Acad Sci **1125:**171-89.

30. **Lovley, D. R., and J. G. Ferry.** 1985. Production and Consumption of H(2) during Growth of *Methanosarcina* spp. on Acetate. Appl Environ Microbiol **49:**247-249.

31. **Maeder, D. L., I. Anderson, T. S. Brettin, D. C. Bruce, P. Gilna, C. S. Han, A. Lapidus, W. W. Metcalf, E. Saunders, R. Tapia, and K. R. Sowers.** 2006. The *Methanosarcina barkeri* genome: comparative analysis with *Methanosarcina acetivorans* and *Methanosarcina mazei* reveals extensive rearrangement within methanosarcinal genomes. J Bacteriol **188:**7922-31.

32. **Markowitz, V. M., E. Szeto, K. Palaniappan, Y. Grechkin, K. Chu, I. M. Chen, I. Dubchak, I. Anderson, A. Lykidis, K. Mavromatis, N. N. Ivanova, and N. C. Kyrpides.** 2008. The integrated microbial genomes (IMG) system in 2007: data content and analysis tool extensions. Nucleic Acids Res **36:**D528-33.

33. **Metcalf, W. W., J. K. Zhang, E. Apolinario, K. R. Sowers, and R. S. Wolfe.** 1997. A genetic system for Archaea of the genus *Methanosarcina*: liposome-mediated transformation and construction of shuttle vectors. Proc Natl Acad Sci U S A **94:**2626-31.

34. **Metcalf, W. W., J. K. Zhang, X. Shi, and R. S. Wolfe.** 1996. Molecular, genetic, and biochemical characterization of the *serC* gene of *Methanosarcina barkeri* Fusaro. J Bacteriol **178:**5797-802.

35. **Meuer, J., S. Bartoschek, J. Koch, A. Kunkel, and R. Hedderich.** 1999. Purification and catalytic properties of Ech hydrogenase from *Methanosarcina barkeri*. Eur J Biochem **265:**325-35.

36. **Meuer, J., H. C. Kuettner, J. K. Zhang, R. Hedderich, and W. W. Metcalf.** 2002. Genetic analysis of the archaeon *Methanosarcina barkeri* Fusaro reveals a central role for Ech hydrogenase and ferredoxin in methanogenesis and carbon fixation. Proc Natl Acad Sci U S A **99:**5632-7.

37. **Michel, R., C. Massanz, S. Kostka, M. Richter, and K. Fiebig.** 1995. Biochemical characterization of the 8-hydroxy-5-deazaflavin-reactive hydrogenase from *Methanosarcina barkeri* Fusaro. Eur J Biochem **233:**727-35.

38. **Miller, T. L., and M. J. Wolin.** 1985. *Methanosphaera stadtmaniae* gen. nov., sp. nov.: a species that forms methane by reducing methanol with hydrogen. Arch Microbiol **141:**116-22.

39. **Miller, V. L., and J. J. Mekalanos.** 1988. A novel suicide vector and its use in construction of insertion mutations: osmoregulation of outer membrane proteins and virulence determinants in *Vibrio cholerae* requires toxR. J Bacteriol **170:**2575-83.

40. **Mulder, N. J., R. Apweiler, T. K. Attwood, A. Bairoch, A. Bateman, D. Binns, P. Bork, V. Buillard, L. Cerutti, R. Copley, E. Courcelle, U. Das, L. Daugherty, M. Dibley, R. Finn, W. Fleischmann, J. Gough, D. Haft, N. Hulo, S. Hunter, D. Kahn, A. Kanapin, A. Kejariwal, A. Labarga, P. S. Langendijk-Genevaux, D. Lonsdale, R. Lopez, I. Letunic, M. Madera, J. Maslen, C. McAnulla, J. McDowall, J. Mistry, A. Mitchell, A. N. Nikolskaya, S. Orchard, C. Orengo, R. Petryszak, J. D. Selengut, C. J. Sigrist, P. D. Thomas, F. Valentin, D. Wilson, C. H. Wu, and C. Yeats.** 2007. New developments in the InterPro database. Nucleic Acids Res **35:**D224-8.

41. **Odom, J. M., and H. D. Peck, Jr.** 1981. Hydrogen cycling as a general mechanism for energy coupling in the sulfate-reducing bacteria, *Desulfovibrio* sp. FEMS Microbiology Letters **12:**47-50.

42. **Pritchett, M. A., J. K. Zhang, and W. W. Metcalf.** 2004. Development of a markerless genetic exchange method for *Methanosarcina acetivorans* C2A and its use in construction of new genetic tools for methanogenic archaea. Appl Environ Microbiol **70:**1425-33.

43. **Rother, M., P. Boccazzi, A. Bose, M. A. Pritchett, and W. W. Metcalf.** 2005. Methanol-dependent gene expression demonstrates that methyl-coenzyme M reductase is essential in *Methanosarcina acetivorans* C2A and allows isolation of mutants with defects in regulation of the methanol utilization pathway. J Bacteriol **187:**5552-9.

44. **Rother, M., and W. W. Metcalf.** 2005. Genetic technologies for Archaea. Curr Opin Microbiol **8:**745-51.

45. **Sowers, K. R., J. E. Boone, and R. P. Gunsalus.** 1993. Disaggregation of *Methanosarcina* spp. and Growth as Single Cells at Elevated Osmolarity. Appl Environ Microbiol **59:**3832-3839.

46. **Thauer, R. K., R. Hedderich, and R. Fischer.** 1993. Methanogenesis. Chapman and Hall, New York.

47. **Vaupel, M., and R. K. Thauer.** 1998. Two F_{420}-reducing hydrogenases in *Methanosarcina barkeri*. Arch Microbiol **169:**201-5.

48. **Vignais, P. M., B. Billoud, and J. Meyer.** 2001. Classification and phylogeny of hydrogenases. FEMS Microbiol Rev **25:**455-501.

49. **Wanner, B. L.** 1986. Novel regulatory mutants of the phosphate regulon in *Escherichia coli* K-12. J Mol Biol **191:**39-58.

50. **Welander, P. V., and W. W. Metcalf.** 2008. Mutagenesis of the C1 oxidation pathway in *Methanosarcina barkeri*: new insights into the Mtr/Mer bypass pathway. J Bacteriol **190:**1928-36.

51. **Welte, C., V. Kallnik, M. Grapp, G. Bender, S. Ragsdale, and U. Deppenmeier.** Function of Ech hydrogenase in ferredoxin-dependent, membrane-bound electron transport in *Methanosarcina mazei*. J Bacteriol **192:**674-8.

52. **Zhang, J. K., A. K. White, H. C. Kuettner, P. Boccazzi, and W. W. Metcalf.** 2002. Directed mutagenesis and plasmid-based complementation in the methanogenic archaeon *Methanosarcina acetivorans* C2A demonstrated by genetic analysis of proline biosynthesis. J Bacteriol **184:**1449-54.

CHAPTER 5

SUMMARY AND FUTURE DIRECTIONS

5.1 INTRODUCTION

In every methanogenic pathway, methane (CH_4) production is accompanied by formation of a heterodisulfide (CoM-S-S-CoB) of coenzyme M (CoM-SH) and coenzyme B (CoB-SH). The CoM-S-S-CoB heterodisulfide needs to be reduced to regenerate the free coenzymes necessary for sustaining methanogenesis. In *Methanosarcina*, this is accomplished via three energy-conserving electron transport chains that differ in the nature of electron donors, which are H_2, reduced F_{420} ($F_{420}H_2$) or reduced ferredoxin (Fd_{red}) (reviewed in (5, 6)). Although the Fd_{red}:heterodisulfide pathway is not well-understood, the other two electron transport systems have been reconstituted *in vitro* in *Methanosarcina mazei* (1, 11). In the H_2:heterodisulfide system, electrons derived from oxidation of H_2 by the methanophenazine-dependent hydrogenase (Vht) are used to reduce the membrane-soluble electron carrier methanophenazine (MP). Subsequently, oxidation of reduced MP (MPH_2) releases electrons for reduction of CoM-S-S-CoB by the heterodisulfide reductase (HdrED). On the other hand, in the $F_{420}H_2$:heterodisulfide system, the $F_{420}H_2$ dehydrogenase (Fpo) oxidizes $F_{420}H_2$, concomitantly pumping two protons outside the cell and passing electrons to MP. MPH_2 oxidation is then coupled to CoM-S-S-CoB reduction, as in the H_2:heterodisulfide system. In both oxidoreductase systems, four protons are translocated per two electrons

transferred to CoM-S-S-CoB. This proton-motive force can be used for ATP synthesis by an ATP synthase. One or more of these systems is employed by *Methanosarcina* species to conserve energy during growth on a particular methanogenic substrate. For instance, growth using H_2/CO_2 or methanol plus H_2/CO_2 involves utilization of H_2:heterodisulfide system (5). However, Fd_{red}:heterodisulfide and $F_{420}H_2$:heterodisulfide systems are needed to allow growth on methylated C-1 compounds like methanol, because the methyl oxidative pathway produces reducing equivalents in the form of Fd_{red} and $F_{420}H_2$. Hence, Fpo was considered indispensable for methylotrophic methanogenesis (1). Aceticlastic growth involves use of Fd_{red}:heterodisulfide pathway to harvest electrons from Fd_{red}, which is generated from oxidation of carbonyl group of acetate (15, 16). In this study, we employed genetic tools to enhance our understanding of these energy-conserving systems in *Methanosarcina,* using *Methanosarcina barkeri* as our model organism.

5.2 SIGNIFICANT FINDINGS

5.2.1 *M. barkeri* possesses a branched $F_{420}H_2$:heterodisulfide electron transport chain, with a Frh/Vht H_2-cycling branch and another branch involving Fpo

Based on *in vitro* biochemical studies, the Fpo-involving $F_{420}H_2$:heterodisulfide oxidoreductase system was presumed to be required during methylotrophic growth (1). However, in Chapter 2, we found out that deletion of Fpo-encoding operon in *M. barkeri* does not affect growth on methanol or other methanogenic substrates tested. In contrast, loss of the fully

reversible F_{420}-reducing hydrogenase (Frh) (17) from the cell severely affects methylotrophic growth, implicating its involvement in $F_{420}H_2$:heterodisulfide electron transport chain. Nonetheless, our data also showed that Fpo is responsible for slow growth of the Δ*frh* mutant on methanol, because absence of both Frh and Fpo from the cell abolishes growth on this substrate. Thus, *M. barkeri* employs both these enzymes to harvest electrons from $F_{420}H_2$, however, it clearly prefers Frh over Fpo. A plausible reason for this choice could be the ability of Frh to support a higher rate of CH_4 production than Fpo.

H_2 produced by Frh was proposed to feed into the H_2:heterodisulfide oxidoreductase system for energy conservation. To verify this, in Chapter 3, we tried to delete the input module of this system, Vht, without any success, thereby implying that Vht is essential for growth of *M. barkeri*. We proved this assumption correct, by isolating a tetracycline (Tc)-regulated conditional *vht* mutant (P_{tet}*vht*) that is unable to grow on any methanogenic substrate tested under non-permissive conditions, including on methanol. Thus, this result supported the idea that Vht consumes H_2 during methylotrophic growth. This hypothesis was further bolstered by the fact that repression of *vht* expression resulted in a rapid increase in H_2 partial pressure, accompanied with growth inhibition. This suggested that H_2 uptake by Vht is essential for viability of *M. barkeri*. However, Vht is not required in mutants lacking the H_2-producing Frh hydrogenase, which is consistent with functional coupling of Frh and Vht hydrogenases in a "H_2-cycling" mechanism (18). In this mechanism, cytoplasmic Frh hydrogenase couples $F_{420}H_2$ oxidation to reduction of two protons within the cytoplasm to form

H_2 gas. Subsequently, the gas diffuses out of the cell to periplasmic Vht hydrogenase, where it is oxidized to regenerate two protons, thus creating an energy-conserving trans-membrane proton gradient. H_2-cycling has been proposed in various anaerobic micro-organisms (4, 13, 18, 19), however, this is the first study to provide direct experimental evidence for its occurrence.

5.2.2 *M. barkeri* possesses a branched Fd_{red}:heterodisulfide electron transport chain, with an Ech/Vht H_2-cycling branch and another branch involving an unidentified Fd_{red} oxidoreductase

M. barkeri methylotrophic Fd_{red}:heterodisulfide electron transport chain has been proposed to comprise of the ferredoxin (Fd_{ox})-dependent hydrogenase Ech, which couples Fd_{red} oxidation to H_2 production, and the H_2:heterodisulfide oxidoreductase system (15, 16). Thus, this pathway resembles the Frh-dependent $F_{420}H_2$:heterodisulfide system. Also, analogous to Frh and Vht, Ech and Vht can undergo H_2-cycling, because the active site of Ech is cytoplasmic, whereas that of Vht is periplasmic. In Chapter 3, we provided supporting evidence for this hypothesis, because the Ech-containing Δ*vht frh* double mutant produced more H_2 from methanol than the single Δ*frh* mutant, in which Ech/Vht H_2-cycling is not disrupted. Nevertheless, Δ*ech* mutants isolated in Chapter 4 do not display a defect in methylotrophic growth, implying presence of a H_2-independent Fd_{red}:heterodisulfide pathway involving an as yet unidentified Fd_{red} oxidoreductase. Moreover, this pathway is as efficient as Ech/Vht H_2-cycling in supporting growth on methanol. Additionally, it allows growth via the methyl respiration pathway in Δ*vht frh* and Δ*vht vhx frh fre* strains, when Fd_{red} is made

available by the action of Ech. However, the Ech–catalyzed pathway does not allow methanogenesis to proceed at rates as high as the Vht-containing H_2:heterodisulfide system. The H_2-independent Fd_{red}:heterodisulfide pathway is not able to support growth on acetate. Thus, Ech and Vht are absolutely essential for aceticlastic growth.

5.2.3 Fre and Vhx hydrogenases are non-functional under tested conditions

In addition to *frhADGB and vhtGACD* operons, *M. barkeri* contains *freAEGB* and *vhxGAC* operons, which encode putative F_{420}-dependent (Fre) and MP-dependent hydrogenases (Vhx), respectively (14). Both these operons are missing gene D that encodes a putative hydrogenase maturation protease (9). My data suggest that Fre and Vhx are not able to substitute for the role of Frh and Vht in the Δ*frh* and P_{tet}*vht* mutants, respectively. Thus, they are not functional under the conditions tested.

5.2.4 *M. barkeri* hydrogenases are dispensable during methylotrophic growth

The presence of H_2-independent $F_{420}H_2$:heterodisulfide (Fpo) and Fd_{red}:heterodisulfide (unidentified Fd_{red} oxidoreductase) electron transport chains in *M. barkeri* suggested that hydrogenases might be dispensable during growth of this organism using methanol. Thus, in Chapter 4, I attempted deletion of all five hydrogenases in *M. barkeri*, Fd_{ox}-dependent Ech, F_{420}-reducing Frh and Fre, and MP-dependent Vht and Vhx (14). We were able to isolate this quintuple

hydrogenase deletion mutant using methanol as the growth substrate, corroborating the branched nature of *M. barkeri* energy-conservation system.

5.2.5 All three types of hydrogenases are needed for growth of *M. barkeri* via the CO_2 reduction pathway

Deletion of Ech, Frh and/or Vht prevents growth of *M. barkeri* on H_2/CO_2. This is consistent with the proposal that all three electron carriers (Fd_{ox}, F_{420} and MP) reduced by these hydrogenases are needed for CO_2 reduction to CH_4 (20).

5.2.6 Ech and/or Frh hydrogenases mediate repression of methyl oxidative pathway

A previous study had suggested that H_2 represses the methyl oxidative pathway (16). However, the quintuple hydrogenase deletion mutant is able to bypass this repression and grow methylotrophically on methanol plus H_2/CO_2, implicating involvement of hydrogenases in this metabolic regulation. More specifically, Ech and/or Frh hydrogenases might be responsible for this inhibitory effect, because the *vht*$^+$ Δ*ech frh* mutant can oxidize methanol methyl group to CO_2, to obtain reducing equivalents for biosynthetic reactions.

5.2.7 Hyp proteins are essential for maturation of Ech hydrogenase

In Chapter 4, we provide experimental evidence for the hypothesis that Hyp proteins are involved in post-translational modification of [NiFe] hydrogenases in *M. barkeri* (2, 9). Unlike *ech*$^+$ Δ*frh fre vht vhx* strain, the *ech*$^+$ Δ*hyp frh fre vht vhx* mutant is unable to grow via the methyl respiration pathway

using Ech, suggesting that this hydrogenase is non-functional in the Δ*hyp* mutant. Thus, Hyp proteins are essential for maturation of the [NiFe] Ech hydrogenase. *M. barkeri* Ech is functional, when expressed heterologously in the closely related species, *Methanosarcina acetivorans* (10). This implies that *hyp* operon of *M. acetivorans* encodes functional Hyp proteins (9).

5.2.8 Fpo or Frh is needed for aceticlastic growth

Methanogenesis from acetate does not require either Frh or Fpo (7); however, our results in Chapter 2 show that one of the two enzymes, but not both, is needed for growth on this substrate. We previously showed that mutations in the C-1 oxidation pathway prevent growth on acetate, presumably by blocking the production of reducing equivalents needed for biosynthetic reactions (21). The lack of growth of the Δ*frh* Δ*fpo* double mutant on acetate medium suggests that these reducing equivalents must flow through either Frh or Fpo to allow growth.

5.3 FUTURE DIRECTIONS

5.3.1 Identification of H_2-independent branch of the Fd_{red}:heterodisulfide oxidoreductase system

The hydrogenase mutants lacking Ech utilize a H_2-independent Fd_{red}:heterodisulfide electron transport chain during methylotrophic growth. To identify the components of this pathway, we plan to perform microarray expression analysis in various Δ*ech* mutants; Δ*ech*, Δ*ech frh*, Δ*ech frh vht* and Δ*ech frh fre vht vhx*; and the isogenic parental strain. However, our experimental

approach relies on the assumption that this Fd_{red}:heterodisulfide system is up-regulated in the absence of Ech in the cell. Therefore, to overcome this caveat, we could directly target some potential Fd_{red} oxidoreductases in *M. barkeri* for genetic analysis, like the putative Fd_{red}:heteorodisulfide HdrA1B1C1 (3). Also, it has been postulated that the $F_{420}H_2$ dehydrogenase (Fpo) might be involved in this H_2-independent Fd_{red}:heteorodisulfide chain, in case a Fd_{red}:F_{420} oxidoreductase channels electrons from Fd_{red} to F_{420}. To verify this, we could isolate a Δ*fpo ech* double mutant and test its phenotype on methanol as the growth substrate.

5.3.2 Determination of hydrogenase activity exhibited by each of the hydrogenases

Each of the three types of hydrogenases in *M. barkeri* contributes to its overall benzyl-viologen-dependent hydrogenase activity. In this study, we isolated a series of hydrogenase deletion mutants, including single, double, triple, quadruple and quintuple mutants. An estimation of hydrogenase activity of all these mutants would give us an idea of the activity exhibited by each of the hydrogenases individually within the cell.

5.3.3 Determination of functionality of the Fre and Vhx hydrogenases

Hydrogenase activity in the *fre*$^+$ *vhx*$^+$ Δ*ech frh vht* strain can be measured to test if *fre* and *vhx* operons encode functional hydrogenases. If not, we can complement this strain with *frhD* or *vhtD* prior to hydrogenase activity measurements (9). This would tell us if subunit D encoded by *frh* and *vht* operons

can process Fre and Vhx hydrogenases, respectively. In case Fre is a functional hydrogenase, the *vht* mutation in the complemented strain, *frhD*$^+$ *fre*$^+$ *vhx*$^+$ Δ*ech frh vht*, would be lethal to the cell, as has been demonstrated in the P$_{tet}$*vht* and Δ*ech* P$_{tet}$*vht* strains. Thus, an alternative way to test Fre functionality would be to introduce *frhD* in the *fre*$^+$ Δ*frh* single mutant and then test F_{420}-dependent hydrogenase activity.

We also plan to investigate the role of Fre and Vhx as potential regulators of hydrogenases in *M. barkeri*. To this end, *uidA* reporter gene fusions to the promoters of all hydrogenases will be integrated into the chromosome of Δ*fre* and Δ*vhx* mutants. Subsequently, we will determine β-glucuronidase activity in parental and mutant strains to find out differences in expression of hydrogenases between the two strains.

5.3.4 Testing functionality of *M. acetivorans* hydrogenases by complementation with *M. barkeri* hydrogenase deletion mutants

The non-hydrogenotrophic *Methanosarcina* species, *M. acetivorans*, encodes Frh, Vht and Vhx hydrogenases. While previous studies have implicated that these hydrogenases are not expressed within the native host, they contain all the structural and catalytic residues that are present in *M. barkeri* hydrogenases (9, 10). Thus, to test their functionality, we plan to express them in *M. barkeri* quintuple hydrogenase deletion mutant using the tetracycline-regulated P*mcrB*(*tet*O1) promoter and then determine their hydrogenase activity. This strategy might work for Vht, but not for Frh and Vhx. This is because presence of Frh in a Δ*vht* mutant is lethal to the cell and Vhx may not encode a

functional hydrogenase without *vhtD*. Therefore, *M. acetivorans frh* operon can be introduced into *M. barkeri* Δ*frh fre* double mutant, which is unable to grow on H_2/CO_2 due to loss of Frh. If functional, *M. acetivorans* Frh would allow growth on this substrate and the complemented strain would display F_{420}-dependent hydrogenase activity. To test functionality of *M. acetivorans* Vhx, we can introduce *vhx* operon along with *vhtD* in the quintuple *M. barkeri* mutant and then test hydrogenase activity.

5.3.5 Testing aceticlastic Fd_{red}:heterodisulfide electron transport chains of *M. acetivorans* and *M. barkeri*

M. acetivorans Fd_{red}:heterodisulfide aceticlastic chain is postulated to comprise of the Na^+-pumping Fd_{red}:MP oxidoreducatse Rnf (3, 12), whereas, *M. barkeri* is proposed to utilize Ech and Vht hydrogenases to channel electrons from Fd_{red} to MP in this chain (15, 16). These proposals are consistent with the inabilities of *M. acetivorans* Δ*rnf*, *M. barkeri* Δ*ech* and *M. barkeri* Δ*vht* mutants to grow using acetate. However, to conclusively prove these electron transport pathways, we plan to reconstruct the Rnf-containing chain in the *M. barkeri* quintuple hydrogenase mutant by introduction of *rnf* operon into its genome; and the Ech/Vht H_2-cycling pathway in *M. acetivorans* Δ*rnf* mutant by introducing *ech* and *vht* in its chromosome. Subsequently, we can test growth of the complemented strains on acetate. It is important to note that *M. barkeri* is missing the *rnf* operon, whereas, *M. acetivorans* lacks the *ech* operon and does not express its *vht* operon (8, 9, 14).

5.4 LITERATURE CITED

1. **Baumer, S., T. Ide, C. Jacobi, A. Johann, G. Gottschalk, and U. Deppenmeier.** 2000. The $F_{420}H_2$ dehydrogenase from *Methanosarcina mazei* is a Redox-driven proton pump closely related to NADH dehydrogenases. J Biol Chem **275:**17968-73.

2. **Blokesch, M., A. Paschos, E. Theodoratou, A. Bauer, M. Hube, S. Huth, and A. Bock.** 2002. Metal insertion into NiFe-hydrogenases. Biochem Soc Trans **30:**674-80.

3. **Buan, N. R., and W. W. Metcalf.** 2009. Methanogenesis by *Methanosarcina acetivorans* involves two structurally and functionally distinct classes of heterodisulfide reductase. Mol Microbiol.

4. **Coppi, M. V.** 2005. The hydrogenases of *Geobacter sulfurreducens*: a comparative genomic perspective. Microbiology **151:**1239-54.

5. **Deppenmeier, U.** 2002. Redox-driven proton translocation in methanogenic Archaea. Cell Mol Life Sci **59:**1513-33.

6. **Deppenmeier, U.** 2004. The membrane-bound electron transport system of *Methanosarcina* species. J Bioenerg Biomembr **36:**55-64.

7. **Ferry, J. G.** 1992. Methane from acetate. J Bacteriol **174:**5489-95.

8. **Galagan, J. E., C. Nusbaum, A. Roy, M. G. Endrizzi, P. Macdonald, W. FitzHugh, S. Calvo, R. Engels, S. Smirnov, D. Atnoor, A. Brown, N. Allen, J. Naylor, N. Stange-Thomann, K. DeArellano, R. Johnson, L. Linton, P. McEwan, K. McKernan, J. Talamas, A. Tirrell, W. Ye, A. Zimmer, R. D. Barber, I. Cann, D. E. Graham, D. A. Grahame, A. M. Guss, R. Hedderich, C. Ingram-Smith, H. C. Kuettner, J. A. Krzycki, J. A. Leigh, W. Li, J. Liu, B. Mukhopadhyay, J. N. Reeve, K. Smith, T. A. Springer, L. A. Umayam, O. White, R. H. White, E. Conway de Macario, J. G. Ferry, K. F. Jarrell, H. Jing, A. J. Macario, I. Paulsen, M. Pritchett, K. R. Sowers, R. V. Swanson, S. H. Zinder, E. Lander, W. W. Metcalf, and B. Birren.** 2002. The genome of *M. acetivorans* reveals extensive metabolic and physiological diversity. Genome Res **12:**532-42.

9. **Guss, A. M., G. Kulkarni, and W. W. Metcalf.** 2009. Differences in hydrogenase gene expression between *Methanosarcina acetivorans* and *Methanosarcina barkeri*. J Bacteriol **191:**2826-33.

10. **Guss, A. M., B. Mukhopadhyay, J. K. Zhang, and W. W. Metcalf.** 2005. Genetic analysis of *mch* mutants in two *Methanosarcina* species demonstrates multiple roles for the methanopterin-dependent C-1 oxidation/reduction pathway and differences in H(2) metabolism between closely related species. Mol Microbiol **55:**1671-80.

11. **Ide, T., S. Baumer, and U. Deppenmeier.** 1999. Energy conservation by the H_2:heterodisulfide oxidoreductase from *Methanosarcina mazei* Gö1: identification of two proton-translocating segments. J Bacteriol **181:**4076-80.

12. **Li, Q., L. Li, T. Rejtar, D. J. Lessner, B. L. Karger, and J. G. Ferry.** 2006. Electron transport in the pathway of acetate conversion to methane in the marine archaeon *Methanosarcina acetivorans*. J Bacteriol **188:**702-10.

13. **Lovley, D. R., and J. G. Ferry.** 1985. Production and Consumption of H(2) during Growth of *Methanosarcina* spp. on Acetate. Appl Environ Microbiol **49:**247-249.

14. **Maeder, D. L., I. Anderson, T. S. Brettin, D. C. Bruce, P. Gilna, C. S. Han, A. Lapidus, W. W. Metcalf, E. Saunders, R. Tapia, and K. R. Sowers.** 2006. The *Methanosarcina barkeri* genome: comparative analysis with *Methanosarcina acetivorans* and *Methanosarcina mazei* reveals extensive rearrangement within methanosarcinal genomes. J Bacteriol **188:**7922-31.

15. **Meuer, J., S. Bartoschek, J. Koch, A. Kunkel, and R. Hedderich.** 1999. Purification and catalytic properties of Ech hydrogenase from *Methanosarcina barkeri*. Eur J Biochem **265:**325-35.

16. **Meuer, J., H. C. Kuettner, J. K. Zhang, R. Hedderich, and W. W. Metcalf.** 2002. Genetic analysis of the archaeon *Methanosarcina barkeri* Fusaro reveals a central role for Ech hydrogenase and ferredoxin in methanogenesis and carbon fixation. Proc Natl Acad Sci U S A **99:**5632-7.

17. **Michel, R., C. Massanz, S. Kostka, M. Richter, and K. Fiebig.** 1995. Biochemical characterization of the 8-hydroxy-5-deazaflavin-reactive hydrogenase from *Methanosarcina barkeri* Fusaro. Eur J Biochem **233:**727-35.

18. **Odom, J. M., and H. D. Peck, Jr.** 1981. Hydrogen cycling as a general mechanism for energy coupling in the sulfate-reducing bacteria, *Desulfovibrio* sp. FEMS Microbiology Letters **12:**47-50.

19. **Odom, J. M., and H. D. Peck, Jr.** 1984. Hydrogenase, electron-transfer proteins, and energy coupling in the sulfate-reducing bacteria *Desulfovibrio*. Annu Rev Microbiol **38:**551-92.

20. **Thauer, R. K., R. Hedderich, and R. Fischer.** 1993. Methanogenesis. Chapman and Hall, New York.

21. **Welander, P. V., and W. W. Metcalf.** 2008. Mutagenesis of the C1 oxidation pathway in *Methanosarcina barkeri*: new insights into the Mtr/Mer bypass pathway. J Bacteriol **190:**1928-36.

CURRICULUM VITAE

GARGI KULKARNI

University of Illinois at Urbana-Champaign, Department of Microbiology
B420 Chemical and Life Sciences Laboratory, Urbana, IL 61801
Email: gargik@gmail.com
Cell: (217) 721-8408

EDUCATION

PhD in Microbiology, University of Illinois at Urbana-Champaign — May 2010
Thesis Advisor: Prof. William W. Metcalf
GPA: 3.88/4

MS in Microbiology, University of Illinois at Urbana-Champaign — May 2006
Thesis Advisor: Prof. William W. Metcalf
GPA: 3.85/4

MSc in Biotechnology, Indian Institute of Technology Bombay, India — May 2004
Thesis Advisor: Prof. Narayan S. Punekar
GPA: 9.37/10 (Second rank in department)

BSc in Microbiology, University of Delhi, India — May 2002
GPA: 7.32/10 (Second rank in department)

RESEARCH EXPERIENCE

Graduate Research Assistant, UIUC — 2004 - 2010

- *Energy conservation in methanogenic Archaea*: Employed genetic and biochemical techniques in the strict anaerobe *Methanosarcina barkeri* to unravel a different mode of energy conservation, called H_2-cycling, during methylotrophic growth of the organism. Our study provided the first direct experimental evidence for the occurrence of H_2-cycling, since its proposal in sulfate-reducing bacteria in 1981.
- *Analysis of hydrogenases in Methanosarcina species*: Isolated single, double, triple, quadruple and quintuple *M. barkeri* hydrogenase deletion mutants in various combinations. Currently, I am characterizing the mutants in terms of growth characteristics, methane production, hydrogenase activity and expression of various genes. The quintuple mutant will also be used for complementation studies with *M. acetivorans* hydrogenases to determine their functionality.

Masters student, IITB, India — 2003 - 2004

- *Inhibition of Aspergillus niger Glutamine synthetase (GS) by phosphinothricin (PTT)*: Employed biochemical techniques and assays to determine kinetic parameters for *in vitro* inhibition of partially purified GS by PTT. These efforts were directed to enable usage of PTT resistance as a selectable marker in *A. niger*.

PUBLICATIONS

1. **Kulkarni G**, Metcalf WW (2010). Demonstration of hydrogen cycling in *Methanosarcina barkeri*. In preparation.
2. Bose A, **Kulkarni G**, Metcalf WW (2009). Regulation of putative methyl-sulfide methyltransferases in *Methanosarcina acetivorans* C2A. *Mol Microbiol*. 74(1):227-238.
3. **Kulkarni G**, Kriedelbaugh D, Guss AM and Metcalf WW (2009). Hydrogen is a preferred intermediate in the energy conserving electron transport chain of *Methanosarcina barkeri. Proc Natl Acad Sci U S A*. 106(37):15915-15920.
4. Guss AM, **Kulkarni G**, Metcalf WW (2009). Differences in hydrogenase gene expression between *Methanosarcina acetivorans* and *Methanosarcina barkeri*. *J Bacteriol*. 191(8):2826-33.
5. Guss AM, Rother M, Jhang JK, **Kulkarni G**, Metcalf WW (2008). New methods for tightly regulated gene expression and highly efficient chromosomal integration of cloned genes for *Methanosarcina* species. *Archaea*. 2(3):193-203.

AWARDS AND HONORS

- Outstanding Teaching Assistant, UIUC — Fall 2006
- Junior Research Fellowship
  Council of Scientific and Industrial Research, India (offer declined) — Jun 2004
- National Eligibility Test (Eligibility for Lectureship)
  Council of Scientific and Industrial Research, India (offer declined) — Jun 2004
- MSc in Biotechnology, Second rank, IITB, India — May 2004
- BSc (Honors) in Microbiology, Highest Aggregate
  Gargi College, University of Delhi, India — May 2002, May 2001, May 2000
- BSc (Honors) in Microbiology, Second rank
  University of Delhi, India — May 2002, May 2001
- Best Student of Science
  Gargi College, University of Delhi, India — May 2001
- BSc (Honors) in Microbiology, First rank
  University of Delhi, India — May 2000
- AMI (Assocaiation of Microbiologists of India) Quiz Winner — Mar 2000
- 87% in First Level National Mathematics Olympiad Contest — 1995-1996

TEACHING EXPERIENCE

- *MCB 301, Experimental Microbiology* — Fall 2006, Fall 2005
  The course emphasized on fundamentals of microbiology. Experiments involved growth, isolation and identification of bacteria as well as application of genetic and molecular biology techniques. I was in charge of managing and conducting two lab sections of 24 students each. Other duties included holding office hours, grading lab reports & homeworks and proctoring exams.
- *MCB 150, Molecular and Cellular Basis of Life* — Spring 2005
  This course focused on molecular and cellular biology of prokaryotes and eukaryotes. I was in charge of managing discussion sessions for three sections of 24 students each. Other duties included holding office hours, grading project reports & homeworks and proctoring exams.

POSTERS & PRESENTATIONS

Presented Doctoral thesis research entitled "Analysis of Hydrogen Metabolism in *Methanosarcina barkeri* Fusaro" at following conferences and seminars:

Gordon Research Conference

- Poster Presentation — Aug 2007

Allerton Research Conference

- Oral Presentation — Oct 2007
- Poster Presentation — Sep 2009, Sep 2008, Oct 2006, Oct 2005

Student Seminar, UIUC

- Oral Presentation — Oct 2008, Mar 2007

REFERENCES

- Prof. William W. Metcalf,
  Dept. of Microbiology, UIUC
  metcalf@life.illinois.edu
  (217) 244-1943

- Prof. John E. Cronan, Jr.
  Dept. of Microbiology, UIUC
  j-cronan@life.illinois.edu
  (217) 333-7919

- Prof. Andrei Kuzminov,
  Dept. of Microbiology, UIUC
  kuzminov@life.illinois.edu
  (217) 265-0329